Development and Implementation of a Multi-disciplinary Optimisation Framework to Aid Cost Reduction for Floating Offshore Wind Support Structures

EngD Thesis

Victoria Sykes

Naval Architecture Ocean and Marine Engineering Department

University of Strathclyde, Glasgow

January 3, 2026

This thesis is the result of the author's original research. It has been composed by the author and has not been previously submitted for examination which has led to the award of a degree.

Abstract

In order to tackle climate change, a huge shift is required from several industries, namely the energy sector. The decarbonisation of the grid has become essential to adhere to government targets and legally binding treaties. One of the most prominent solutions is harnessing wind energy, having proven itself viable onshore and offshore prior to the new millennium. The development into the offshore environment allowed developers to benefiting from a stronger, more consistent resource. Since the first developments, the UK has grown its offshore capacity to just under 15 GW, with a strong pipeline and government support aiming for 43 to 50 GW by 2030 to meet the clean power plan. However, as build out has progressed, nearshore sites have become utilised, pushing developers into deeper waters where current fixed bottom solutions are no longer either technically or economically feasible. Floating wind is expected to be a solution for deeper water sites, overcoming the limitations linked with fixed offshore wind. However, with new technology and a harsher operating environment comes risks, lack of supply chain and an associated cost, which is expected to be around double the cost of its fixed counterpart in shallower waters.

This research is centred on the exploration of potential cost reductions for floating offshore wind support structures to aid the needed CapEx minimisation, which is in alignment with the Industrial Growth Plan (IGP) published in 2024. The current study plays a crucial role in cost reduction of floating offshore wind to try and determine a more standardised but optimised set of geometries to bring down the cost. By standardising designs, it will allow supply chains to develop and mature, which also leads to a cost benefit and potential economic growth within the UK. The opportunity to manufacture and build locally is exceptionally strong for floating offshore wind

platforms and the UK, given their large size, which not only makes them increasingly difficult to transport but also creates a larger carbon footprint, which is not desirable. Ultimately, cost reductions will allow floating to become more competitive with other energy sources to deliver green, secure, affordable energy.

Few studies have carried out optimisations for current geometries in literature to seek cost-benefits, exploring non-traditional geometries, with an expected mass reduction and therefore cost. However, cost models utilised within these works often use a mass based pricing approach where only the materials consumed are considered or assumptions are made to increase density to reflect secondary steel cost. These presented approaches neglect all manufacturing costs or attempt to capture them through vague assumptions. This work presents a multi-disciplinary optimisation framework, which finds the optimal geometry for a range of different platform typologies, with appropriately sized mooring lines and anchors within a defined design space. This design space is controlled by bounds for each design variable to ensure sensible combinations are considered. The optimal solutions meet a number of constraints on the geometry, manufacturability, intact stability, floatability, and structural integrity. The overall objective seeks to minimise cost, to do so a structural model combined with detailed cost estimates of both material and manufacturing costs such as forming, welding, and painting are considered. This allowed the author to find the defining qualities of optimal solutions and whether there were any true benefits in exploring non-traditional geometries, other than the expected reduction in material mass. The optimisation technique used in this work was a pattern search combined with a multi-start approach to ensure the global minimum had been found. The framework quickly found optimal solutions which minimised cost while being constrained by the previously mentioned parameters, ensuring performance was not impacted and a realistic design was found. The solutions were then considered in frequency domain analysis, further assessing their stability capabilities.

One of the difficulties of optimisation is the length of time required to carry out the task. An approach which was considered within this work is the Technique for Order of Preference by Similarity to Ideal Solutions (TOPSIS). This technique was used as a

concept selection tool to rank different platform typologies at specific sites. This allowed a number of different criteria regarding site parameters such as soil condition, tidal range, water depth, and wave height compatibility to be considered. The remaining criteria were linked to the different substructure typologies, capital, operational and decommissioning costs, size and Technology Readiness Level. This step allowed the author to rule out platforms which were not suitable and, therefore, reduce the number of platforms which had to be optimised for specific sites.

Implementing the presented techniques, this study demonstrated that firstly, the semi-submersible platform is highly flexible for a number of different sites, reinforcing its prominence within industry. The case studies for the optimisation found the TLP to be the cheapest, best-performing platform for Scotwind site NE8, noted as Site 8 in this work. Whereas site 14, otherwise known as N2 Scotwind, finds the Semi-submersible to be cheaper than the Spar, both have a dynamic response within the allowable limits. In terms of exploring non-traditional geometries, there was no benefit for Spar, however, there was a cost benefit for the TLP, but more so Semi-submersible, since they have a greater number of 'parts' which can benefit from having reduced size, allowing both material and manufacturing cost to be reduced while keeping the desired stability. Overall, this work highlighted that the manufacturing cost should be considered when assessing different platform geometries, given that the material cost alone is expected to represent 40% of the total platform cost. Finally, setting a constraint on the static pitch angle of the platform resulted in the optimal platforms having good dynamic performance, and the exclusion of dynamics from the optimisation itself was justified.

Looking ahead, the key insight from future work indicates that building upon the detailed model is essential. Including installation and Operations and Maintenance (O&M) specifically to capture the nuanced behaviours of each platform, allowing all of the benefits and drawbacks to be captured for each platform.

Contents

Abstract **ii**

List of Figures **ix**

List of Tables **xiv**

List of Symbols **xvii**

Acknowledgements **xxviii**

1 Introduction **2**

1.1 Technology Review 6

1.2 Aim and Objectives 11

1.2.1 Work Package One 12

1.2.2 Work Package Two 13

1.2.3 Work Package Three 14

1.2.4 Work Package Four 16

1.2.5 Work Package Five 17

1.2.6 Contributions to Knowledge 17

2 Literature Review: Floating Offshore Wind Cost Modelling **19**

2.1 Introduction 19

2.2 Literature Review Approach 20

2.3 Cost Modelling Review 23

2.3.1 Development Cost 26

2.3.2 Manufacturing 28
2.3.3 Installation 33
2.3.4 Operations and Maintenance 36
2.3.5 Decommissioning 39
2.3.6 General Assumptions 42
2.4 Data Review 46
2.4.1 Capital Expenditure 48
2.4.2 Operation and Maintenance Expenditure 59
2.4.3 Decommissioning Expenditure 63
2.4.4 Levelised Cost of Energy 66
2.5 Cost Modelling Research Gaps 67
2.6 Conclusion 71

3 Literature Review: Floating Offshore Wind Substructure Optimisation Frameworks 72

3.1 Introduction 72
3.2 Literature Review Approach 73
3.3 Optimisation Review 75
3.3.1 Optimisation Problem Methodology 75
3.3.2 Overview 76
3.3.3 Objective Function 81
3.3.4 Constraints 85
3.3.5 Design Variables and Platform Modelling 93
3.3.6 Optimisation Algorithms 98
3.3.7 Modelling Software Utilised 102
3.3.8 Cost Modelling 106
3.4 Optimisation Framework Discussion 117
3.4.1 Optimisation Framework 117
3.4.2 Literature Findings 120
3.5 Optimisation Framework Research Gaps 126
3.6 Conclusion 137

4 Model Development **140**

4.1 Geometrical Model . . . 140

4.2 Structural Model . . . 143

4.2.1 Manufacturing Considerations . . . 143

4.2.2 Shell Considerations . . . 146

4.2.3 Stiffener Sizing . . . 148

4.3 Cost Model . . . 150

4.3.1 Material Cost . . . 153

4.3.2 Forming Cost . . . 153

4.3.3 Welding Cost . . . 153

4.3.4 Paint Cost . . . 155

4.4 Hydrostatics . . . 155

4.5 Mooring line and Anchor System . . . 157

4.5.1 Catenary Mooring Line Sizing . . . 157

4.5.2 Taut Mooring Line Sizing . . . 159

4.5.3 Mooring Stiffness . . . 160

4.5.4 Anchor sizing . . . 162

4.5.5 Complete Cost . . . 165

4.6 Hydrodynamics . . . 165

4.7 Aerodynamic model . . . 169

4.8 Design Load Case . . . 170

5 Methodology Validation **174**

5.1 Cost Model . . . 174

5.1.1 Spar . . . 174

5.1.2 Semi-submersible and TLP . . . 177

5.2 Structural Model . . . 180

5.3 Hydrodynamic Model . . . 181

5.3.1 OC3 Spar . . . 181

6 Floating Sub-structure Concept Preliminary Selection 185

6.1 Platform Typology Classification Review 186

6.1.1 Seabed Characteristics 186

6.1.2 Water Depth Characteristics 188

6.1.3 Wave Height Characteristics 189

6.1.4 Tidal Range Characteristics 190

6.1.5 Cost Breakdown 190

6.1.6 Technology Readiness Level 196

6.1.7 Platform Size 201

6.2 Methodology 201

6.2.1 TOPSIS Methodology 202

6.2.2 Marking criteria and attributes 204

6.3 Case Study: Scotwind 206

6.4 Discussion 212

6.5 Conclusion 219

7 Optimisation Problem 221

7.1 Optimisation Definition 221

7.2 Objective 222

7.3 Design Variables 222

7.3.1 Spar 222

7.3.2 TLP 223

7.3.3 Semi-submersible 224

7.4 Bounds 224

7.5 Constraints 226

7.6 Optimisation Technique 228

8 Case Studies 230

8.1 Inputs 230

8.2 Site 14: SS Spar vs TC Spar 231

8.2.1 Static Stability 231

8.2.2 Cost Comparison . . . 235
8.2.3 Dynamics . . . 245
8.3 SS Semi-submersible vs TC Semi-submersible . . . 251
8.3.1 Site 14 . . . 253
8.3.2 Site 8 . . . 266
8.4 SS TLP vs TC TLP . . . 268
8.5 Site 8 . . . 268
8.5.1 Cost . . . 270
8.5.2 Dynamics . . . 271
8.5.3 Varying Number of Legs . . . 275
8.5.4 TLP vs Semi-submersible . . . 276
8.6 Findings Summary . . . 277
8.6.1 Spar . . . 277
8.6.2 Semi-submersible . . . 279
8.6.3 TLP . . . 281

9 Conclusions **284**

10 Future work **289**

Bibliography **292**

A Appendix **322**
A.1 Wave scatter diagram . . . 323
A.2 Design Variables for Spar platforms . . . 324
A.3 Cost breakdown for Spar platforms . . . 326
A.4 Design Variables for Semi-submersible platforms . . . 327
A.5 Cost breakdown for Semi-submersible platforms site 14 . . . 329
A.6 Cost breakdown for Semi-submersible site 8 . . . 331
A.7 Design Variables for TLPs . . . 332
A.8 Cost breakdown of the optimised TLPs. . . . 334

List of Figures

1.1 Growth in turbine size and power (1). 3
1.2 Installed and predicted installations across Europe in the coming years (2). 4
1.3 Main platform types from the left: a) Monopile, b) Jacket, c) TLP, d) Spar, e) Semi-submersible (3). 7
1.4 Main platform concepts found in literature and test sites (4). 10
1.5 Work packages for this research. 11

2.1 The literature published per year relevant to the research area. 21
2.2 Most relevant papers. 23
2.3 Cost category breakdown. 26
2.4 Complete cost details for the development cost. 27
2.5 All costs related to the manufacturing cost. 29
2.6 All costs related to the installation cost. 37
2.7 All costs related to the Operations and Maintenance cost. 40
2.8 All costs related to the decommissioning of the wind farm. 43
2.9 Impact of WACC on LCOE (5). 44
2.10 Varying wind farm capacity, water depth and distance to shore for the literature. 47
2.11 Preliminary costs, turbine and transmission costs found within literature represented in MEuro(2025)/MW. 49
2.12 Platform costs for each typology found within literature represented in Million Euro (2025)/MW. 52

2.13 Mooring and anchors costs for each typology found within literature represented in Million Euro (2025)/m (water depth). 53
2.14 Combined manufacturing cost for each typology found within literature represented in Million Euro/MW (smallest numbers on the graph represent the minimum values). 55
2.15 Variation in manufacturing costs found within literature represented in MEuro(2025)/MW 56
2.16 The installation costs found within literature represented in MEuro(2025)/MW/km. 57
2.17 The installation costs variation found within literature represented in MEuro (2025)/MW/km (value on the graphs for each platform is the minimum found in literature). 59
2.18 The O&M costs found within literature represented in Million Euro(2025)/MW/km. 61
2.19 The O&M costs variation found within literature represented in Million Euro(2025)/MW/km. 62
2.20 The decommissioning costs found within literature represented in Million Euro(2025)/MW/km. 64
2.21 The decommissioning costs variation found within literature represented in MEuro(2025)/MW/km (Additional values for each platform highlight the minimum cost found in the literature). 65
2.22 The variation in the LCoE for each platform in the literature. 66

3.1 Process for finding appropriate literature. 74
3.2 Number of publications per year. 75
3.3 Universal Buoyancy Body from (6). 80
3.4 Platforms optimised within literature. 80
3.5 Wind turbine power capacity used in the existing literature. 82
3.6 Type of objectives used in the literature. 82
3.7 Spar support structure proposed in (7). 97
3.8 Space-frame concept utilised in (8). 98
3.9 Optimisation algorithms used within the literature. 99
3.10 Additional software used within the optimisation frameworks. 103

3.11 Cost breakdown found in Myhr et al. (9). 122

4.1 Model flow chart. 141
4.2 Column geometry example, where L_o is overall length, R_i is The segments radius, t_i is shell thickness and L_i is the length of individual segments 142
4.3 Bracing geometry example, where L_o is overall length, R_i is The segments radius, t_i is shell thickness and L_i is the length of individual segments 142
4.4 Different stiffener geometries in this work, where width is w_{si}, height is h_{si}, thickness is t_{si}, and y_{Ei} is the centre of mass. 145
4.5 Cross section of the bracing. 147
4.6 Cost breakdown of the tapered column presented in (10). 151
4.7 Fabrication process: 1) Forming 2) Welding formed plates to create a segment 3) Creating the stiffener from parts 4) Welding the stiffener into the shell 5) Assembling all segments 6) Welding segments together. 152
4.8 Stability triangle, this triangle can become destabilised or have a negative contribution to the restoring capabilities due to the Centre of Gravity position (11; 12) 157
4.9 Mooring line diameter vs MBL for grade 3 steel (13). 158
4.10 Soil classification (14). 164
4.11 The Cumulative Probability Density Function on log scale for Scotwind site 14. 172
4.12 IEA 15MW turbine power curve. 173

5.1 Cost Breakdown (15). 177
5.2 a) Pelastar TLP b) WindFloat Semi-submersible. 177
5.3 RAO for 5 MW NREL Turbine and OC3 Spar (16). 182
5.4 RAO for 5 MW NREL Turbine and OC3 Spar, with exact same mass as literature (16). 182

5.5 Comparison between excitation force found in literature and the current model for OC3 Spar (16). 183
5.6 Comparison between added mass found in literature and the current model for OC3 Spar (16). 184
5.7 Comparison between damping found in literature and the current model for OC3 Spar (16). 184

6.1 Anchor types (17). 187
6.2 TOPSIS Methodology. 202
6.3 Recent Scotwind sites up for leasing (18). 206

7.1 The Spar platform geometry 223
7.2 The TLP geometry. 224
7.3 The Semi-submersible platform geometry. 225

8.1 Comparison between the optimised solutions for SS1 Spar and TC1 Spar geometry and cost breakdown. 232
8.2 Optimisation results for TC varying maximum angle of inclination. . . . 234
8.3 Optimisation results for Spar. 237
8.4 Weighted cost difference between SS1 and TC1.[1] 240
8.5 Difference in percentage of each cost between SS1 and TC1.[1] 242
8.6 Further optimisations. 243
8.7 Further optimisations. 244
8.8 Added mass of the optimised Spar results. 248
8.9 Damping of the optimised Spar results. 248
8.10 Damping coefficient normalised with the critical damping of the optimised Spar results. 248
8.11 Displacement RAOs of the optimised Spar results. 249
8.12 Mooring stiffness sensitivity a) Fairlead b) Radius 251
8.13 Design variables from all of the optimisations carried out from most optimal (right hand side, to the least left hand side) for the SS semi-submersible. 252

8.14 Design variables from all of the optimisations carried out from most optimal (right hand side, to the least left hand side) for the TC semi-submersible. 252
8.15 The most optimal Semi-submersible solutions for site 14. 253
8.16 Sub-optimal Semi-submersible solutions for site 14. 254
8.17 Sub-optimal Semi-submersible solutions for site 14. 255
8.18 The cost breakdown of the optimal solutions for site 14. 256
8.19 The optimal solutions costs for varying number of outer columns. 261
8.20 The cost of the platform, mooring and anchor cost when varying the number of outer columns. 262
8.21 The most optimal TC and SS Semi-submersible geometries for site 8. . . 266
8.22 Geometry dimension ratio between SS and TC Semi-submersible for each site. 267
8.23 Cost ratio between SS and TC Semi-submersible for each site. 268
8.24 Optimised TC TLPs for site 8. 269
8.25 Optimised SS TLPs for site 8. 269
8.26 Most optimal TC and SS TLPs for site 8. 270
8.27 Added mass and damping for TC and SS TLP at site 8. 274
8.28 Excitation force for TC and SS TLP at site 8. 275
8.29 Cost for different number of bracings for a TLP. 276
8.30 Cost per kg for each platform type at the specific sites. 283

A.1 Wave scatter diagrams for scotwind site 14 323

List of Tables

2.1 Journals and their given performance indicators for 2020. 23
2.2 Losses and methods to find AEP as reported in the literature, INC. means it is included but no explicit value was stated. 46

3.1 The nacelle acceleration constraints applied within the current literature and newly published DNV stantards 86
3.2 Serviceability limit state load cases for tower tilt. 89
3.3 Number of design variables used in each work and the shape considered. 95
3.4 Summary of the reviewed works in Section 6.1.5, describing the support structure, tower structure, mooring line, anchor, cable, AEP, additional costs, optimisation related costs, LCoE, and relevant notes (N/A indicates it was not included in the work) 116
3.5 Percentage of the literature reviewed considering a specific floating wind turbine subsystem or aspect in the design variables, objectives, and constraints. 120
3.6 Complexity factors used in (15) 121
3.7 LCoE found in cost model literature. 123
3.8 Details of the platforms ranked in literature from best (left) to worst (right). 126
3.9 Optimisation overview. 136

4.1 Plate sizes (19; 20). 144
4.2 Stiffener sizes (21; 22). 145

4.3 Yield stress of S355 for different thicknesses (23). 148
4.4 Constant value for to determine taut mooring diameters and mass (24). 160
4.5 Anchor and mooring line details. 163
4.6 Price per ton of each anchor used in the current works model. 163
4.7 Details on anchor suitability for seabed types, adapted from (25). 164
4.8 Details of the equations used to calculate anchor mass for each considered typology for soft clay. 164

5.1 Optimised geometries found in the literature. 175
5.2 Cost estimated by model presented in this work. 175
5.3 The estimated dimensions of Principle Power and Pelastar Platform (15; 26; 27). 178
5.4 The cost of Principle Power and Pelastar Platform. 178
5.5 Comparison of the dimensions of the mooring line from literature and current model. 180

6.1 Details on anchor suitability for seabed types (17; 28; 29; 30). 188
6.2 Cost breakdown for each geometry, highlighting minimum, means and maximum values found across the literature (4; 9; 29; 31; 32; 33; 34; 35; 36; 37; 38; 39; 40; 41; 42; 43; 44; 45; 46). 192
6.3 TRL from 2015 updated for 2023. 200
6.4 TRL Average and maximum values. 201
6.5 Attributed and potential support structure options. 205
6.6 Details of Scotwind sites. 208
6.7 Inputs for the criteria limits and the weighting vector 210
6.8 The most platforms ranked in order of best to worst for each site. 211
6.9 The platforms ranked in order of best to worst for each site, with a CapEx importance ranking of three rather than five. 215
6.10 The percentage of each platform which ranked best for the weighting matrices with each attribute doubled. 218

6.11 The percentage of each platform which ranked best for the weighting matrices with each attribute halved. 218

7.1 Design variable bounds. 226

8.1 Inputs for the optimisations. 231
8.2 Design variable comparison between 5° and 9° constrained platform. . . 234
8.3 Spar cost comparison for different cost inclusions within the optimisation. 245
8.4 Spar Dynamics comparison in percentage between SS1 and TC1 fo DLC 6.1 (negative % highlights SS being worse.) 246
8.5 Semi-submersible Dynamics comparison in percentage between SS1-14 and TC1-14. 259
8.6 Difference between the cost for 4 and 6 mooring lines for the 6 columns Semi-submersible (the percentage is calculated as $(4_{lines} - 6_{lines})/6_{lines}$). 262
8.7 Cost comparison between the Semi-submersible and Spar TC and SS (calculated (semisubmersible-spar)/spar, where negative shows the spar is more expensive). 264
8.8 TC and SS Spar vs Semi-submersible (calculated (semisubmersible-spar)/spar, where negative shows the spar is worse). 265
8.9 TLP dynamics comparison in percentage between SS and TC. 273
8.10 Cost difference between 3, 4 and 6 compared to 5 bracing TLP 276
8.11 Cost difference reasons and drivers for the Spar platforms. 278

A.1 Spar optimisation design variables. 324
A.2 Design variables of optimised Semi-submersible platforms. 327
A.3 Optimised TLP design variables for site 8. 332
]

Nomenclature

α	The taper angle of the segment (°)
α_i	Angle the mooring line has with the centre of the platform (°)
η_a	Amplitude of exciting body (m)
γ_b	Safety factor ()
$\hat{x}$	Design variables vector ()
λ_i	Slenderness factor ()
μ	Coefficient ()
ω	Frequency matrix (rad/s)
ρ	Material density (kg/m^3)
ρ_{air}	Density of air (kg/m^3)
ρ_{moor}	Mooring line material density (kg/m^3)
ρ_{sw}	Sea water density (kg/m^3)
σ_{crit}	Critical stress on the shell (Pa)
σ_{Ei}	Equivalent stress (Pa)
σ_i	Stress acting on each segment (Pa)
σ_i	Zeroth moment ()

Nomenclature

σ_{yy}	Stress in the yy plane on the bracing (Pa)
θ	Angle of inclination (°)
Θ_f	Complexity factor ()
	Universal Buoyancy Body
ξ_i	Coefficient ()
A	Added mass matrix ()
A	Area of the rotor (m^2)
A^+	Positive Ideal Solution ()
A^-	Negative Ideal Solutio ()
A_{i-th}	Marking criterion vector ()
A_i	Area of the individual segment (m)
A_{rad}	Anchor radius (m)
A_{rotor}	Area of rotor ()
A_{tot}	Total surface area including the stiffeners, and inside and outside of the shell (m^2)
a_{wi}	The fillet weld size (mm)
A_z	Area at each point of the platform (m^2)
AEP	Annual Energy Production
AHV	Anchor Handling Vessel
B	Damping matrix ()
b	Breadth of the bracing (m)
b_d	Bracing depth (m)

b_l Bracing length (m)

B_v Viscous damping (kg/s)

b_w Bracing width (m)

BM_y Distance from the CoB to the metacentre (m)

$BOBYQA$ Bound Optimisation BY Quadratic Approximation

C Stiffness matrix ()

C_{55moor} Stiffness provided by the mooring lines ()

c_D Drag coefficient ()

c_{ii} Mooring line static stiffness ()

C_i Closeness vector()

C_i Reduced buckling coefficient ()

C_{j-th} Support structure vector ()

C_{moor} Mooring stiffness ()

c_T Thrust coefficient ()

$CapEx$ Capital Expenditure

CMN Cumulative Multi-Niching

CoB Centre of Buoyancy

CoG Centre of Gravity

$COST_{Overall}$ Total cost ($)

d Depth of the bracing (m)

d_i Distance from the centroid to the neutral axis (m)

D_{moor} Mooring line diameter (m)

D_{tower} Diameter of tower (m)

$DecEx$ Decommissioning Expenditure

DLC Desgin Load Case

DoF Degree of Freedom

E Young's modulus of the material (Pa)

EA_{moor} Mooring line Youngs modulus (Pa)

F_B Buoyancy force (N)

F_D Total drag of tower and RNA (N)

F_e Excitation force matrix ()

F_T Total thrust (N)

f_y Material yield (Pa)

$FOWT$ Floating Offshore Wind Turbine

g Acceleration due to gravity(m/s^2)

g_i Inequality constraints ()

GA Genetic Algorithm

GM_y Metacentric height (m)

$GMAW - C$ Gas Metal Arc Welding with CO_2

h Vertical distance between fairlead and seabed (m)

h_i Equality constraints ()

h_{si} Stiffener height (mm)

Nomenclature

$HVAC$ High Voltage Alternating Current

$HVDC$ High Voltage Direct Current

i	Segment number ()
I_{byy}	Second moment in the yy plane of the bracing (m^4)
I_i	Moment of inertia of the (m^4)
I_{reqi}	Required second moment in the yy plane of the stiffener(m^4)
I_{yy}	Second moment in the yy plane (m^4)
$INC.$	Included
IRR	Internal Rate of Return
J	Objective function (n/a)
K_1	Total cost of welding formed plates to create a segment ($)
K_2	Total cost of creating the stiffener from parts ($)
K_3	Total cost of Welding the stiffener into the shell ($)
K_4	Total assembly cost ($)
K_A	Anchor Cost ($)
k_a	Anchor Cost per tonne ($/ton)
K_b	Ballast material cost($)
k_b	Price of ballast material ($/kg)
K_{F0}	Total forming cost ($)
k_f	Fabrication cost ($/$Min$)
k_{ml}	Cost of mooring line per unit of mass ($/kg)

K_M Total material cost ($)

k_m Cost of material per kg ($/kg)

K_P Total paint cost ($)

k_p Cost of painting per unit area ($/m^2)

KB Distance from the keel to the CoB (m)

KG Distance from the keel to the CoG (m)

L_{efi} Distance between stiffeners which can be used to calculate the number of stiffeners required (m)

L_{ei} Equivalent length of the segment (m)

L_i Length of each segment (m)

L_{moor} Mooring line length (m)

L_o Overall length (m)

$LCoE$ Levelised Cost of Energy

LCS Life Cycle System

$M\&A$ Mooring and Anchoring

M Mass matrix ()

m_a Mass of anchor (ton)

m_b Mass of ballast material required (kg)

m_{ml} Total mooring line mass (kg)

m_{total} Total mass of the structure including shell and stiffeners (kg)

M_{yy} Moment acting in the yy plane on the bracing (N)

$MCDA$ Multi-Criteria Decision Analysis

$MDAO$ Multidisciplinary Design Analysis and Optimisation

$MOEA$ Multi-Objective Evolutionary Algorithm

n_{ps} Number of parts which make up the stiffener ()

n_p Number of plates required to make up one segment ()

n_w Number of welds ()

$Nacelle_{acc}$ Nacelle acceleration (m/s^2)

NIS Negative Ideal Solution

$NLPQL$ Non-Linear Programming technique, Quadratic Lagrangian

No_{stiff} Number of stiffeners in each segment ()

no_s Number of segments ()

NPV Net Present Value

$NREL$ National Renewable Energy Laboratory

$NSGA$ Non-dominated Sorting Genetic Algorithm

$O\&G$ Oil and Gas

$O\&M$ Operations and Maintenance

$OpEx$ Operational Expenditure

p Maximum hydrostatic pressure (Pa)

p_h Plate height (m)

p_w Plate width (m)

PDF Probability Density Function

PIS Positive Ideal Solution

$QuLaF$ Quick Load Analysis of floating offshore wind turbines model

R Normalised decision matrix ()

R_1 Inner column radius (m)

R_2 Outer column radius (m)

R_{Ei} Distance from the centre of the column to the COG of the stiffener (m)

R_{ei} Equivalent radius of the truncated cone (m)

R_i Radius of the section with respect to i (m)

R_{moor} Radius of the platform at the fairlead coordinate (m)

RAO Response Amplitude Operator

$RINS$ Relaxation-Induced Neighbourhood Search

RMS Root Mean Square

RNA Rotor Nacelle Assembly

S_η Wave spectrum ($m^2/(rad/s)$)

$SLOW$ Simplified Low Other Wind Turbine Model

SQP Sequential Quadratic Programming

SS Straight Sided

SWL Sea Water Level

T Draft (m)

t_{ei} Equivalent thickness of the shell (mm)

T_h Mooring line horizontal tension(N)

t_i Thickness of the segment shell (mm)

T_{pre} Mooring line pretension (N)

t_{si} Thickness of the stiffener (mm)

T_v Mooring line vertical tension(N)

t_{wi} Thickness of the plate being welded (this is used to consider the thickness when two welds are required) (mm)

TC Truncated Cone

TLB Tension Leg Buoy

TLP Tension Leg Platform

$TOPSIS$ Technique for Order of Preference by Similarity to Ideal Solutions

TRL Technology Readiness Level

U Wind speed (m/s)

UHC Ultimate Holding Capacity

V Weighted normalised decision matrix ()

v Possions ratio of the material

V_i Volume of each segment (m^3)

V_{si} Volume of each stiffener (m^3)

V_{Total} Total volume of the structure (m^3)

W Weight of the platform (kg)

w_j Weighting vector ()

w_{moor} Mass of the mooring line per meter of length (kg/m)

w_{si} Stiffener width (mm)

WPA Water Plane Area

X_d	Decision matrix ()
x_j	The x coordinate of the mooring line connection on the waterplane section (m)
x_{lower}	Design variables vector lower bounds ()
x_{upper}	Design variables vector upper bounds ()
y_{Ei}	Distance from shell to Centre of mass of the stiffener (mm)
y_{Ei}	Distance from the shell to the centre of mass of the stiffener(m)
y_j	The y coordinate of the mooring line connection on the waterplane section (m)
z	Vertical centre specific to each area (m)
z_B	Centre of Buoyancy (m)
z_B	The centre of buoyancy (m)
z_G	Centre of Gravity (m)
z_g	The centre of gravity (m)
Z_i	Curvature parameter ()
z_M	Fairlead coordinate (m)

Acknowledgements

I would like to express my deepest appreciation to both of my supervisors, Prof. Maurizio Collu and Dr. Andrea Coraddu. They have been instrumental throughout my journey at Strathclyde, both as an undergraduate and a postgraduate. Their expert advice, insightful opinions, and unwavering support have been invaluable. Beyond their professional guidance, their friendship and encouragement have meant the world to me.

I am also grateful to my fellow PhD students and cohort members, particularly my best friend, Jade, for her editing help, late-night feedback sessions, and dinner dates. Thanks, should also go to the lecturers, research assistants, and study participants from the university, who impacted and inspired me.

I would like to acknowledge the EPSRC for funding the work completed within this thesis, through the Wind and Marine Energy Systems Centre for Doctoral Training (EP/S023801/1). A special mention to Lynn O'Brien and Drew Smith for all their help navigating the past four years.

My family for their unwavering love, support and encouragement, which is ultimately the reason I am fortunate enough to be in the position I am today. I would like to thank my best friend and fiancé, for all of the hours of reasoning, engineering judgement, practising of presentations, cups of coffee and moral support. For being my biggest cheerleader and support through my PhD journey – he could probably have a PhD in offshore renewables himself!

Finally, I'd like to acknowledge myself for persevering, and being patient when the PhD journey got tough.

Chapter 0. Acknowledgements

Chapter 1

Introduction

The first wind turbine used to create electricity was built in 1887 in Marykirk, Kincardineshire, by Professor James Blyth (47). Since then, wind turbines have evolved to the most commonly known configuration today: horizontal axis, three-bladed, variable speed, pitch-controlled turbines. The story started firstly onshore, where the turbines could be engineered in the most efficient manner to maximise electrical production from the wind, which allowed learning, standardisation of parts and more importantly, a decline in cost. However, there are a few issues with onshore sites, particularly visual impacts, noise and transportation. To avoid such friction with wind energy, a solution was to install them offshore and they have been since 1991 (48). Since then, developments in engineering capabilities have allowed wind turbines to quickly increase in size, in terms of rotor diameter and power production. Figure 1.1 shows this increase and future predictions, it can, however, be noted that the industry is already at the 22 MW stage, a lot earlier than this Figure predicts.

Since the world's first offshore wind power project was installed 30 years ago in Vindeby, Denmark, the industry has come a long way with a global installed capacity of 64.3 GW in 2022 (49). The main driver behind the offshore wind industry has been to move away from fossil fuels and adopt a more sustainable lifestyle, utilising natural, renewable sources such as wind. To ensure decarbonisation, legally binding international agreements have been signed: the 2008 Paris Agreement (COP21) was signed by 192 parties to keep the world's average temperature within 2 degrees of what

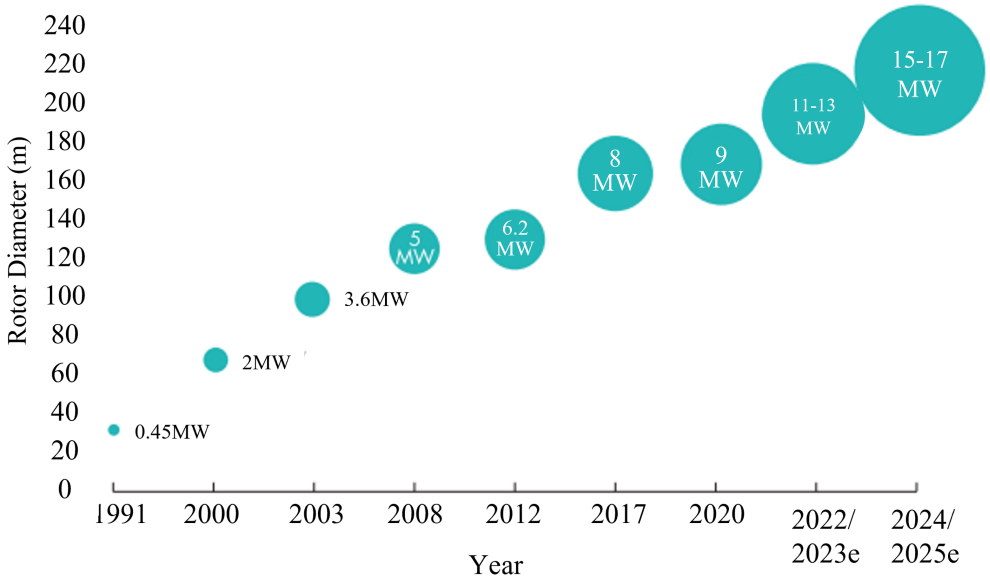

Figure 1.1: Growth in turbine size and power (1).

had been experienced before the industrial revolution (50) - which has prompted these governments to accelerate the rate of deployment of renewable energy devices. The UK is already a world leader in the offshore wind sector, with one of the largest offshore capacity, totalling 15 GW (51; 52). The government has pledged that all homes in the UK will be powered by offshore wind by 2030, creating a target of 42 to 50 GW of installed capacity in the clean power plan (53). The end goal for the UK is to be net zero by 2050, with Scotland aiming to achieve the same goal by 2045 (54).

In order to install capacity at such a rapid rate, there is a considerable demand to explore all sites available. As expected, nearshore sites were the first to be explored, with around 77% of current installations in Europe utilising monopile foundations, which current technology is limited to depths of around 40 m (55). However, it has been expressed that the feasible upper limit of water depth is 70 m for fixed platforms (56). The seas around China, similar to installations around Europe, also utilise monopile and jacket structures due to their shallow water characteristics, applying to both near and further distances to shore (55). There are, however, also conditions where near-shore sites are only deep water, where there is a small Continental shelf. Examples of this are Japan and the western coasts of North and South America (57). As more

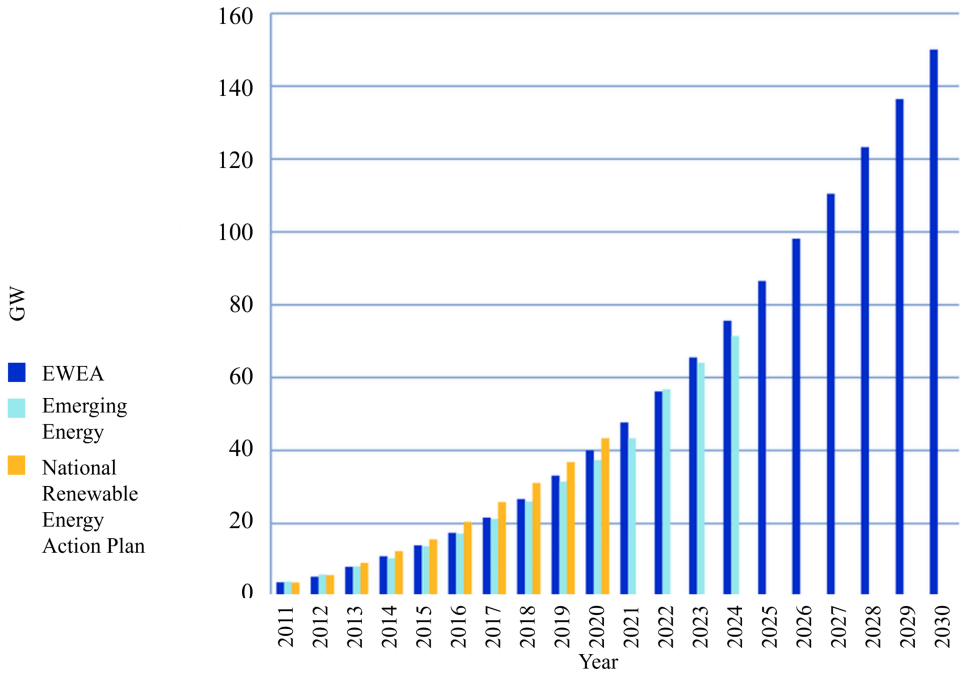

Figure 1.2: Installed and predicted installations across Europe in the coming years (2).

and more nearshore sites with shallow water depths are exploited, the only option is to move to deeper, and potentially further field sites.

It was estimated by the Scottish Government that around 80% of Europe's wind resource is in waters deeper than 60m, further highlighting the great potential the wind sector has to provide green energy (58). As the water depth increases, traditional fixed foundations become much more difficult to design and install, and they may become economically unfeasible or at least very challenging (3; 59; 60; 61; 62; 63). Compared to fixed foundations, floating options provide flexibility. The main advantage of a floating foundation is the ability to operate in deeper water where the resource is stronger and more consistent, with little to no visual impacts. The possibility of transporting the fully assembled wind turbine on its platform via a tug arises, with the hope of reducing installation costs. The same concept can be echoed in the maintenance strategy, where it is expected that tow to port will become an option as well as innovative in-situ installations and repair, such as wind spider, recently used at Kincardine offshore wind farm. The former will allow major repairs to be carried out at the port, which, depend-

ing on the Operations and Maintenance (O&M) port location, could be cheaper and safer. Unlike fixed platforms, floating only requires anchors which have a less negative effect on marine life (3). Decommissioning of wind farms is more than ever becoming a predominant topic of conversation as the first farms approach the end of their life span. Due to the ease of removal, it is expected that specialised vessels will no longer be required and it will be a much cheaper clean-up process for floating (59).

With advantages, there are always disadvantages. the main drawback is the harsh environment, which makes it difficult to install and operate in, leading to a high likelihood of increased failure rates (3; 64). The cost and difficulty of carrying out O&M are also expected to be greater with a reduced number of available weather windows due to the harsher environment. The CapEx of the offshore wind turbine is also expected to be around double that of the same turbine in shallower waters (17; 41). Increasing the distance offshore increases the length of export cable to transport energy. This has cost implications as well as increased losses, making traditional high-voltage AC (HVAC) no longer the most feasible option. At around 50 km offshore, it is predicted that High Voltage DC (HVDC) is more cost-effective due to its higher efficiency (3; 65). Using greater wind resources creates the possibility of installing larger turbines, however, this can cause issues at port due to handling capabilities. The floating structures can also pose an issue for port handlers due to their large size and sometimes awkward shape (3). These challenges are, however, expected to be rewarded with a better capacity factor and, therefore, energy yield.

An important parameter of any technology is cost. By quantifying the cost in generic terms such as Levelised Cost of Energy (LCoE), different energy types can be easily compared and proven feasible. The first step of finding the LCoE is being able to quantify the cost accurately. This is key in identifying the cheapest technology, allowing it to be competitive or better than existing energy resources. However, cost modelling is something which has been sparsely explored in terms of floating offshore wind. Since new technologies come with inherent risks and generally higher costs (9; 17; 41; 66), this is particularly relevant given that the industry has not yet found an "optimum configuration" suitable for every situation. It is therefore predicted that

there will be no such universal solution due to variations in site characteristics and lack of maturity in the floating offshore wind industry, the latter being one of the driving factors of increased cost (67; 68). It is for this reason that cost reduction is of the utmost importance, ensuring green, secure electricity is still affordable to the user (69). The Capital Expenditure (CapEx) makes up around $65 - 75\%$ (41; 70) of the total cost, making it a key area for cost reduction. For floating wind, the two highest costs that form the CapEx are the rotor-nacelle assembly and the floating support structure, each around 35% (41). This research focuses on the floating support structure, due to its large contribution to the CapEx and lack of standardisation (71). At present, few studies have addressed the concept of an optimal support structure. Instead, the focus has been on determining an optimal rotor nacelle assembly design (72; 73; 74; 75; 76; 77; 78; 79; 80; 81; 82; 83).

Optimisation is a technique which has been highly utilised in the automotive and aerospace industry to find an optimal design (84). This process covers a large design space in a much shorter time frame compared to traditional, iterative design methods, making it appealing for a less mature industry (84). Given the similarities to the aerospace industry and the lack of experience, it is expected that optimisation will be a useful tool in determining the best floating offshore support structure for a given application (85). By applying an optimisation approach and several design constraints, the best overall solution can be found by removing unfeasible options, even when there are conflicting objectives such as cost and performance (86; 87).

1.1 Technology Review

Floating platforms have been used in the last 60-70 years for offshore oil and gas (O&G) platforms, meaning the technology is already proven, with lessons learnt over the years (88). It is for this reason that a number of floating platform typologies have been adopted from O&G to floating offshore wind. There are three main categories of floating offshore platforms: Spar, Semi-submersible, and Tension Leg Platform (TLP). Figure 1.3 provides a graphical representation of those categories.

Semi-submersibles have a large waterplane area, which helps provide the necessary

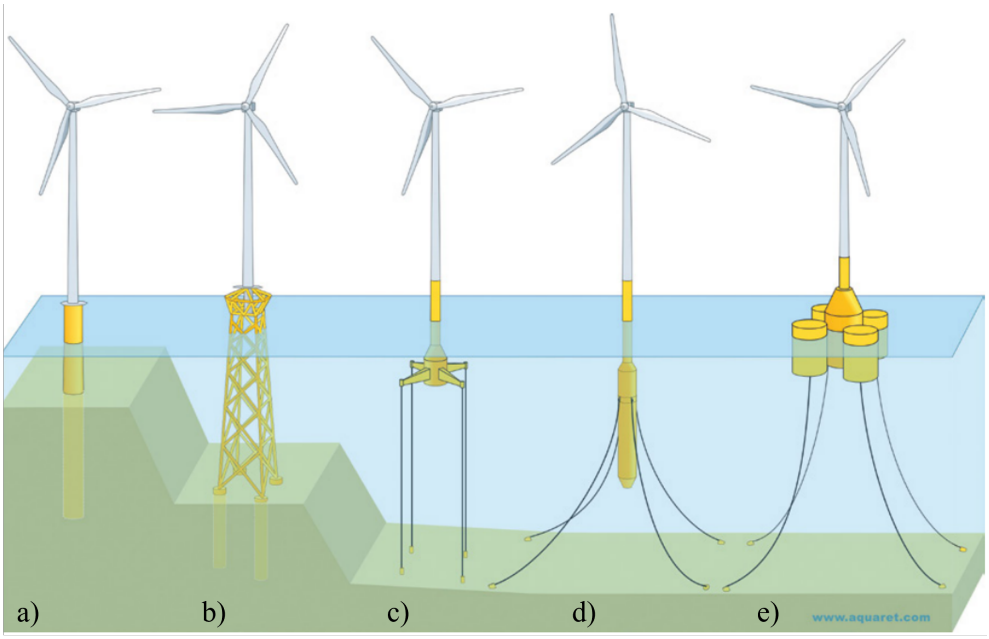

Figure 1.3: Main platform types from the left: a) Monopile, b) Jacket, c) TLP, d) Spar, e) Semi-submersible (3).

stability to counteract the large inclining moment imposed by the aerodynamic forces acting on the rotor.

The main stability contributor for a semi-submersible is its large waterplane area, which influences the second moment of area about the roll and pitch axis. Where the platform experiences external factors such as wind and wave causing it to tilt, the large second moment is critical in providing the large shift in the CoB relative to the CoG, creating a large righting arm (GZ) and, therefore, restoring the moment. This can, however, also be further aided by adding ballast to the lower segments of the column overall lower CoG, providing stability. Due to this, these structures may afford to have a shallow draft (3; 89). The configuration of the Semi-submersible in Figure 1.3, highlights a number of columns joined together. This typology does not need a solid water plane area, it can in fact be built based on a number of columns joined together by bracings, so long as they are spread out in a manner which creates a large enough second moment of waterplane area, to provide the restoring force. Heave plates are typically used at the bottom of the columns to augment the added mass and therefore reduce vertical motions (89). Due to its sometimes complex geometry, it

has a higher level of difficulty and complexity to fabricate, which will be reflected in terms of cost. Cost benefits are predicted considering the structure should have a lower overall structural mass (3). Improved stabilisation can be achieved using active ballast to counteract the inclining moment created by the wind (89). Due to the stability of the platform, it can be built onshore and then towed to the site using tugs, making it fairly easy and inexpensive to do, reducing installation, O&M, and decommissioning costs (89).

Once at the site, three to six catenary mooring lines are used to prevent the platform from drifting, which is the cheapest and most simple mooring system (89). The platform is not sensitive to water depth, allowing it to be installed in a wide range of locations. This will, however, have an impact on the mooring line costs since this is directly linked to water depth. Catenary mooring lines use a combination of their weight and a large footprint on the sea bed to keep the platform stable and in its desired location (17). One main advantage of a catenary mooring system is that the forces acting on the anchors are horizontal, allowing cheaper anchors to be used and a greater range of seabed explored (17). This mooring system does pose the issue of larger oscillations when exposed to waves, creating an issue for turbine operation and the export cable (3; 89).

The Spar typology consists of a longer, slender, cylindrical body constructed from steel or concrete, typically utilising a catenary mooring system, similar to a Semi-submersible. Unlike the Semi-submersible, the Spar has a very small water plane area (WPA) and relies on the vertical distance between the centre of gravity and the centre of buoyancy for stability. This works by the combination of the buoyancy force acting on the centre of buoyancy and the weight force acting on the centre of gravity, forming a restoring moment which counteracts the inclining moment acting on the platform (3; 89). The small WPA makes the support structure suitable to operate in high sea states (89). As previously mentioned, it has been proven feasible in the O&G industry and has been installed in depths up to 2000 m (3). This has many advantages, particularly in locations where there is a small continental shelf close to shore. The shelf region can use traditional methods or potentially TLPs and Semi-submersibles but the Spar will allow such areas outwith the shelf to be utilised for offshore wind energy.

It does have limitations, it is suggested that this configuration cannot be installed in a water depth below 100 m (for 5 MW turbines), as wind turbines become larger it is expected the Spar size will also have to increase, increasing the minimum water depth it can be installed in (90). However, it can be noted that Hywind Scotland Pilot Park installed five 6 MW turbines in water depths ranging from 90-120 m. This demonstrates there is clearly a constraint on depth but maybe not as strict as the literature suggests. The deep draft also requires, in some instances, the floating substructure to be towed in a horizontal manner, requiring a specialised vessel to position the Spar at a site and install the tower and the Rotor Nacelle Assembly (RNA), increasing installation costs. However, due to the lack of complexity of the structure, the structural and maintenance costs should be less (3; 89).

A Tension Leg Platform has large buoyancy which is restrained by a taut mooring system. The mooring system is slightly different from the catenary arrangement, where the length of the mooring lines is essentially equal to the water depth, holding the platform in position and creating a restoring moment when inclined (3; 89). For such systems, anchors which can bear vertical and horizontal loading are required; this is inherently more expensive, and the overall mooring system is more complex with higher loading. Since specialised anchors are required for this platform, the design is then limited to certain seabeds (17). The taut mooring system is more expensive, but it is more stable, resulting in very low motions, which is seen positively by RNA manufacturers. Compared to the catenary system, the footprint is smaller, requiring a lot less mooring line length and consideration for other platforms' mooring lines. Due to the high loading on the tendons, they are at higher risk of breaking and the anchors are at higher risk of becoming dislodged, therefore it is argued the system requires a higher redundancy. In locations where there is a higher probability for storm surges or large tidal variations, currently, this platform is inappropriate due to risks of overloading the mooring system, which could cause drifting and potential capsizing. TLP's can be installed in intermediate water depths making them relatively flexible (89). Since the stability of the TLP is provided by the mooring system during the installation process, specialised vessels may be required depending on the platform's own stability (3). There

are also additional requirements for specialised vessels to install the mooring system due to its complexity. These platforms typically have a smaller draught than a Spar but larger than a Semi-submersible. The manufacturing difficulty also lies between a Spar and a Semi-submersible, with a small, simple structure comprised of a central column and a number of 'arms'.

It is evident that there is no clear consensus on which platform is the best, however, it is very likely that there will be no 'winner' as they are all good for different sites and operational conditions (17). A few concepts found within the literature and on test sites are shown below in Figure 1.4. Both the Spar and Semi-submersible have been used in commercial sites. Semi-submersibles have, however, been highlighted as the most popular solution due to their many advantages.

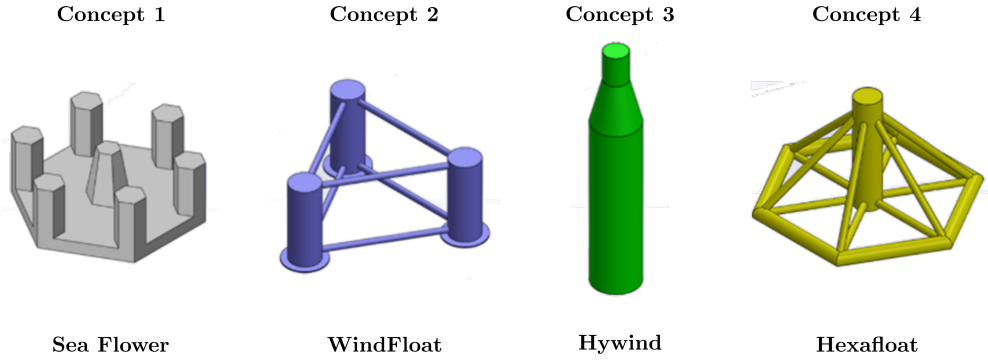

Figure 1.4: Main platform concepts found in literature and test sites (4).

It is clear that there is a large amount of diversity in platform configurations, most notably two of these platforms shown in Figure 1.4 are being used in operational farms around Scotland. Concept three is being used at the Hywind Pilot site in Scotland installed in 2017, further details can be found here (91). It has been operational for the past seven years, and concept two was adopted more recently in 2021 at the Kincardine site off the coast of Aberdeen (92; 93).

This work is split into a number of chapters. Firstly, Chapters 2 and 3 explore the current literature for cost modelling and optimisation frameworks for floating offshore wind, respectively. Chapter 4 details the methodology for model development, and Chapter 5 validates this model. Chapter 6 presents a preliminary concept selection tool, which is then followed by the optimisation problem and the proposed framework.

Finally, tying all of this work together, Chapter 8 provides a number of case studies and the optimal solutions found by the optimisation framework. The conclusions of this work are summed up in Chapter 9, and finally, potential improvements and future work are presented in Chapter 10. The remainder of this Chapter focuses on presenting the aims and objectives, along with the main contributions to knowledge.

1.2 Aim and Objectives

To define the overall aim and objectives of this work, the identified knowledge gaps in this area of research were carefully considered. These gaps include limited considerations of turbine size, simplified manufacturing cost estimates (relying solely on £/kg for substructures), a lack of diversity in substructure types, and the use of generic sites or the failure to account for platform applicability to specific sites. These shortcomings result in unnecessary optimisations and increased development time.

The overall aim of this research is to develop a quick yet flexible multi-disciplinary optimisation framework which can consider traditional and non-traditional geometry typologies to accurately compare costs and explore potential benefits. To help define the objectives, the research can be split into five work packages, which are shown in Figure 1.5 and are discussed further in the following sections.

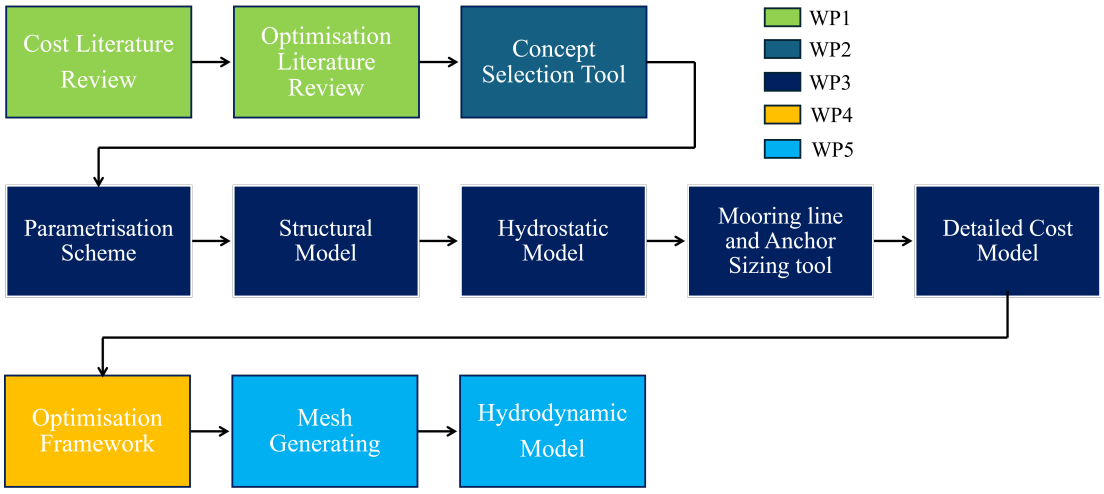

Figure 1.5: Work packages for this research.

1.2.1 Work Package One

This package focuses on the existing literature related to cost modelling and platform optimisation frameworks for floating offshore wind.

Aim(s):	To identify any shortfalls in the literature or potential improvements from which key research aims and objectives can be found, allowing a new contribution to be made to the field.
Objective(s):	Using a filtering technique go through all of the literature available which is related to both cost modelling and optimisation to find appropriate literature. Collate all of the cost data found within the literature to create a database, from which trends, uncertainty and variation across the literature can be found and the potential causes can be identified. Collect the design variables, constraints, objectives, modelling techniques, and algorithms used in the optimisation literature and draw a comparison on their outputs, identifying why the results are different, looking for potential causes related to the methodology used.
Output(s):	Journal Paper: Floating offshore wind cost model literature review (Published 2023). Journal Paper: Floating offshore wind support structure optimisation literature review (Published 2023).
Contribution(s) to Knowledge:	Collection of cost data from the literature to create a database and highlighting the level of uncertainty within literature. Comparison of current literature highlighting gaps and weaknesses in optimisation and cost literature for floating offshore wind.

1.2.2 Work Package Two

This package focuses on creating a preliminary concept selection tool, which will allow the user to rank and rule out the main platform typologies in terms of suitability for a given site.

Aim(s): To create a method of ranking the different platform types highlighting the best typology based on a number of criteria and information regarding the different platforms for specific sites which considers the user's preferences.
This allows to identify which platforms are not applicable or not appropriate considering the user's preferences, allowing fewer platforms to be used in the optimisation technique reducing computational time.

Objective(s): The relevant literature will be assessed in order to determine criteria to find differences in platforms and how the site affects the choice.
In order to rank the platforms giving the user's opinion, a TOPSIS methodology will be used.

Output(s): A universal code which will act as a prefilter to any optimisation framework, reducing the number of platforms optimised and improving computational time.
Journal paper: TOPSIS Methodology Applied to Floating Offshore Wind to Rank Platform Designs for the Scotwind Sites (published 2024).

Contribution(s) to Knowledge: Understand the effects of site and different platform characteristics to determine which are most compatible. Which of these parameters are the main drivers in selecting a particular platform for a site and if there is a particular platform which performs well in most cases.
A review of the literature, which details important parameters which affect platform choice for different sites.

1.2.3 Work Package Three

This work package focuses on the gaps and findings of the literature review, creating a multi-disciplinary model which includes the main floating typologies, Spar, Semi-submersible and TLP.

Aim(s): To create a multi-disciplinary model, where the main floating typologies are expressed by one parameterisation scheme.

Objective(s): Create a parameterisation scheme which will describe the platform geometries.

A structural model which uses DNV rules, to find the minimum required shell size and stiffener size, to more accurately predict manufacturing costs.

Create a hydrostatic model to determine system stiffness and inclination angle.

Create a quick and effective quasi-static model for initial mooring line and anchor sizing and costing.

Develop a detailed cost model which can help to determine the manufacturing cost such as forming, welding, painting and material cost to understand the relationships and benefits of non-traditional geometries, as well as determining if using £/kg value is acceptable.

Within this model, considerations for manufacturing such as standardising plate sizes, thicknesses and stiffness are used within the model.

Finally, validate this model by comparing outputs to the existing literature.

Output(s): A model which is multi-disciplinary considering structural design, station keeping, hydrostatics, and cost.

Contribution(s) to Knowledge:	Present the true impact and importance of including manufacturing costs and, therefore, the limitations of using a £/kg estimate. Provide costs for the substructure of 15 MW turbines, which are more in line with current technology sizes.

1.2.4 Work Package Four

With the model in place, an optimisation framework can be developed to try and find the optimal platform while considering a number of constraints and bounds.

Aim(s):	To create a robust, flexible and quick optimisation framework.
Objective(s):	Create an optimisation framework which aims to minimise cost and maintain the desired performance prescribed by the constraints for traditional and non-traditional platform geometries. Determine which constraints are required to find realistic geometries. Find the best optimisation algorithm based on the nature and the constraints of the problem and tune the optimisation parameters to ensure the trade-off between depth and time for the optimisation. Find optimal geometries for specific sites and understand why they are best and where the cost benefits come from.
Output(s):	Journal Paper (in preparation).
Contribution(s) to Knowledge:	Identification of which platform typologies are most suitable for a range of generic sites, with understanding of which elements of the platforms drive cost reductions in certain cases. A better understanding of manufacturing cost for floating offshore wind platforms and which parameters affect this the most since this can be a driving parameter in determining the optimum configuration. Determine the benefit and drawbacks of non-traditional geometries due to a mass reduction as expressed in current literature the inclusion of the detailed cost model will allow a more realistic, accurate representation and conclusion.

1.2.5 Work Package Five

Work Package 5 addresses the next steps in the typical design phase, progressing from initial hydrostatic analysis carried out in work package 3 to hydrodynamic analysis. Evaluating hydrodynamic performance enables the author to assess whether the most optimal platforms for each site exhibit favourable dynamic stability characteristics to pass DNV standards. This work package comes after work package 4 because you would not carry out hydrodynamic analysis on a hydrostatically unstable platform.

Aim(s):	Develop a tool to assess the hydrodynamic performance of the optimal platforms, to compare them and determine if there is a benefit in certain designs, particularly non-traditional platforms.
Objective(s):	Create an automated mesh generator which can be used for any platform typology. Utilise NEMOH to calculate hydrodynamics coefficients, which can be used to solve equations of motion, to find displacements and accelerations. Validate this model compared to the existing literature.
Output(s):	Journal Paper (in preparation).
Contribution(s) to Knowledge:	Present the performance benefits or failings of non-traditional geometries compared to traditional geometries. Explore the reasons behind these findings and determine if their is a trade of between higher cost and performance.

1.2.6 Contributions to Knowledge

The contributions to knowledge from this EngD have been stated in the prior sections. However, collating prior work into the presented research is a contribution in itself. Combining an improved cost model with the optimisation framework, currently, models only include £/kg models, which have been highlighted in multiple papers as a weakness and potential improvement. Taking a different approach to other papers by considering the site before the optimisation is carried out, implementing a pre-filtering criterion

allows platforms which are not applicable to be discarded, reducing computational time. The result of the optimisation will provide an accurate cost of the platforms which have been optimised, accompanied by full cost details of related costs, allowing platforms to be ranked from highest to lowest in terms of price, TRL and performance. It is hoped that this will make it easier for users to determine which platform to select. As mentioned, combining all of these considerations into a complete framework itself will be a contribution to knowledge since the literature lacks accurate cost models and structural considerations. Assessing the hydrodynamic performance of optimal solutions will allow the author to determine if there is a benefit in considering non-traditional shapes. By excluding the hydrodynamic analysis from the optimisation, it will also help the author to determine if it is required, or if hydrostatic analysis is enough at this point. Combining this work will create an overall improved optimisation framework for all platform typologies, integrating a number of separate things from the existing literature into one. Considering the optimisation tool in a more real-life scenario, trying to bridge the gap between this area of research and industry is at the core of this work.

Chapter 2

Literature Review: Floating Offshore Wind Cost Modelling

This chapter reviews current literature related to cost modelling for floating offshore wind farms. The work in this chapter is based on the published review paper in the Journal Renewable and Sustainable Energy, 'A review and analysis of the uncertainty within cost models for floating offshore wind farms' (94).

2.1 Introduction

As the water depth increases, traditional fixed foundations become much more difficult to design and install, and they may become economically unfeasible or at least very challenging (59). It is, however, estimated that, due to harsher environments, increased turbine size and more complex structures, the CapEx could be doubled in comparison to fixed turbines (17; 41). The increased distance from shore, fewer weather windows, and requirement for larger vessel capacity are also predicted to have an impact on O&M and installation costs (95). It is, however, due to such harsh operating environments that a stronger and more consistent wind resource can be found, allowing the Annual Energy Production (AEP) and the load factor to be increased, making Floating Offshore Wind Turbines (FOWTs) potentially competitive in terms of LCoE (39; 46; 96).

An important parameter of any technology is cost. By quantifying the cost in

generic terms such as LCoE, different energy types can be easily compared and proven feasible. The first step of finding the LCoE is being able to quantify the cost accurately. This is key in identifying the cheapest technology, allowing it to be competitive or better than existing energy resources. However, cost modelling is something which has been sparsely explored in terms of FOWTs. Thus, this chapter aims firstly in Section 2.2 to define the methodology used to collect the relevant literature. Section 2.3 will review existing analytical cost models found within the literature, comparing the assumptions and accuracy of each model. For ease of understanding trends, this section was further broken down into subsections detailing preliminary works, manufacturing, installation, O&M, decommissioning and general assumptions. Leading on from this review, Section 2.4 consists of a collection of all data found in the reviewed literature, which leads to a data analysis that determines the variation across literature and the potential causes. Assessing this literature shows a wide range of model considerations, often leading to assumptions with little or no data to be validated against. Hence, high levels of variation and a lack of consensus on the cheapest floating platform were noted. A summary of the gaps found within the review is presented in Section 2.5, and finally, the conclusion is presented in Section 2.6.

2.2 Literature Review Approach

In order to carry out a comprehensive literature review, works related to cost modelling for offshore wind turbines were found and assessed.

A range of keywords was used to find this literature, including cost model, floating offshore wind, offshore wind turbine, LCoE of floating offshore wind, wind turbine cost model, and offshore wind turbine cost model. Once the related literature was identified, the author started highlighting more papers found within the references, thus discovering the main authors in this area of work. From this research, it has been made clear that this area is relatively new, with the majority of papers being published in the last 10 years and an increasing number of publications over time, as reported in Figure 2.1 which highlights this trend.

A total of 76 papers were collected for the literature review. Inherently, not all of

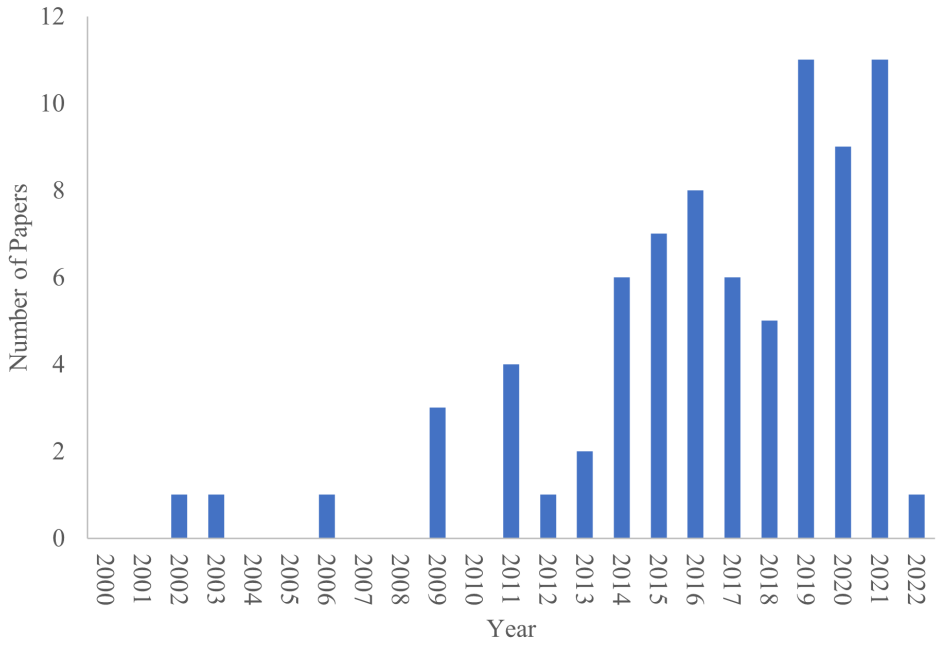

Figure 2.1: The literature published per year relevant to the research area.

these papers would be appropriate, hence filtering criteria were set to select the most relevant papers. These criteria were: appropriate content, number of citations and year published, journal, impact factor, and citescore.

The main aim of this research was to review cost models for floating offshore wind turbines. Therefore, the first step was to remove any papers which did not have a cost model. During the literature review, it was observed that there are three types of cost models used: i) analytical, ii) probabilistic, and iii) audited data models. The analytical method is the most popular, using formulae to find the cost of each system/process related to the offshore wind farm, considering a bottom-up approach. The focus of the review will be on the analytical cost modelling. The probabilistic approach fits a probability curve to historical data related to wind farm cost, allowing the cost to be determined. Papers which use this approach can be found here (97; 98; 99). This was not considered in the current work because the papers are based on fixed offshore wind, not floating, and the cost information is very high-level, considering CapEx, OpEx and DecEx as a whole, with no further breakdown. Using an audited cost

model technique to determine the cost relies heavily on existing data similar to the probabilistic method. However, the available data used in these pieces of research are all for fixed offshore turbines due to the lack of maturity and, therefore, data in the floating wind industry. For instance, Aldersey et al. (100) utilise this technique for cost modelling, using audited accounts to try and better determine the LCoE of different energy resources. This led to three sub-filters. Firstly, papers without cost models, secondly, if they used a probabilistic approach to find the cost and lastly, if they used an audited data method to predict costs.

The following criterion analyses the citation number, where a higher citation number indicates better visibility and impact. However, it is acknowledged that there are instances where papers can still be relevant, timely, and of good quality despite having lower citation counts. Therefore, the year of publication was also taken into consideration. Newer papers are expected to have fewer citations due to their recent publication. To account for this, the average citations per year were used as an indicator. Additionally, the author considered the journals in which the works were published by examining their impact factor, citescore, and the author's opinion on the paper's usefulness. This evaluation involved reading the paper and comparing the cost models to those in journals with high-impact factors and citescores. If the author felt they were comparable, then they were also included in the review. Table 2.1 highlights the most common journals in which the research was published, along with their relevant scores accurate for 2020.

Journal	Papers' Number	Impact Factor	CiteScore
Renewable and Sustainable Energy Reviews	2	14.982	30.5
Applied Energy	1	9.746	17.6
Energy Conversion and Management	1	9.709	15.9
Journal of Cleaner Production	1	9.297	13.1
Renewable Energy	6	8.001	10.8
Energy	1	7.147	11.5
Sustainable Energy Technologies and Assessments	2	5.353	5.9
Energy Sources, Part B: Economics, Planning and Policy	1	3.205	5.2
Energies	1	3.004	4.7
Marine Science and Engineering	2	2.458	2

Energy Procedia	2	N/A	4.4
Other (e.g., Technical Report, Thesis)	5	N/A	N/A
Total	25		

Table 2.1: Journals and their given performance indicators for 2020.

Applying this methodology, 25 papers were selected for review. Figure 2.1 highlights the years in which these papers were published, showing the growth in research within this area over the last decade.

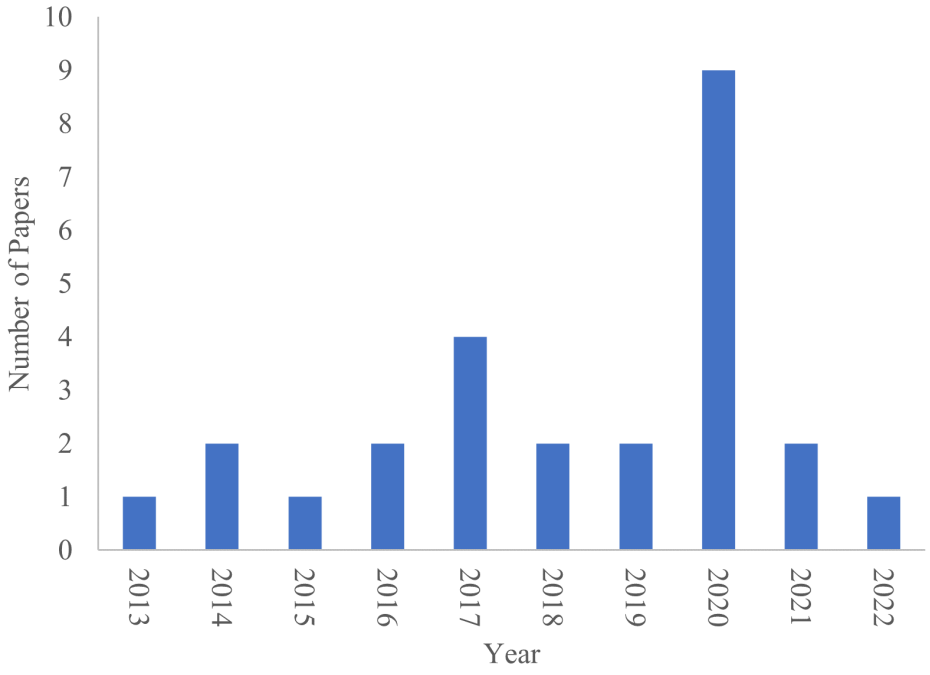

Figure 2.2: Most relevant papers.

2.3 Cost Modelling Review

There has been little work done to develop cost models for floating offshore wind thus far, with only a small number of papers found in the literature. Castro et al. (39; 40; 101; 102; 103; 104) have contributed the greatest number of papers in this research area, with six publications since 2014. These papers created by Castro et al. built

upon their initial cost model presented in 2014 (40). The authors of (40) created a life-cycle model which was used over an area in the North West of Spain allowing the Life Cycle Cost System (LCS) to be determined over this space for the three different platform types. Expanding this model, in 2016, the researchers (39) added a wave energy converter, developing a cost model for renewable energy farms. In this work, only a Semi-submersible platform was considered for the two proposed sites. In the same year, the authors (101) followed the same procedure as (39). However, the paper is made more concise by removing a lot of equations. Reducing the equations provides a more general methodology, only stating the dependent variables for each section. In (102), they give a detailed cost model for the installation of three different platforms. Finally, two papers written in 2020 by Castro et al. (103; 104) utilise the previously defined cost models in their work to map the LCoE, the Internal Rate of Return (IRR), and Net Present Value (NPV). This allows the user to determine over a selected region which platform is the cheapest and which areas in the region are cheapest. Considerations for bathymetry, distance to shore, wave height and period, and port are included in this work. The only difference between these two papers is the location considered.

Martinez et al. (43; 44), in 2021 and 2022, created a map of LCoE over two different regions, for Semi-submersibles which is comparable to Castro et al. (39). Similarly to Castro et al., Maienza et al. (41) created a cost model which can be used for any of the three generic platform types at a given site. In 2016, a flexible tool was created for the Life50+ project (105), which only has three inputs: water depth, turbine capacity, and distance to shore, resulting in an output of LCoE for each foundation type (106).

Mhyr et al. (9), built upon the work by (45), and created an LCoE cost model which allows both floating and fixed platforms to be compared. Bosch et al., (107) utilised some of the same methodology present in the cost models in (9; 45), but is limited to Tension Leg Buoy (TLB).

Sarker et al. (108) focused on creating a model specifically for the installation cost, providing a higher level of detail than other complete cost models. Judge et al. (109) created a spreadsheet-based cost model, which includes a database of information for installation, O&M, and decommissioning to reduce the required number of inputs for

the user. The most comprehensive decommissioning model within the literature is found in (110), considering both fixed and floating platforms. Although their case study focuses on a jacket foundation they highlighted the main differences in cost and how to calculate these for fixed and floating platforms. A decommissioning cost model for offshore wind was also presented by Milne et al. (111), utilising existing wind farm data. For this reason, it is suggested that this model would be most appropriate for fixed platforms, given all of the data for existing wind farms is for fixed platforms.

Focusing on HVDC and HVAC transmission systems, Gil et al. (65) presented cost data for individual components and empirical formulas, allowing the cost and losses of each transmission system to be compared.

Unlike all other papers reviewed, Ghigo et al. (4) presented an optimisation framework for floating offshore wind platforms with cost analysis. This work optimised the platform's geometry to minimise cost.

A simplistic cost model based on material mass was used in (112) to compare the three main platform typologies. Similarly, Heidari et al. (29) created a basic cost model, with most of the data based on GBP/MW, GBP/ton for structures, GBP/MW/year for OpEx costs, fixed values and trends within the wind industry. Comparable in simplicity, a number of models have been created basing all costs on a GBP/MW value (42; 97; 113; 114).

A general overview of the literature in this area highlights a large amount of variation from cost model to cost model. In order to get a better understanding of the differences in each model, the following sections will break down the overall cost into five main categories, for more detailed analysis: preliminary works, manufacturing, installation, operations and maintenance, and decommissioning. Nearly every paper examined considered a similar breakdown in cost percentage with CapEx 70%, Operational Expenditure (OpEx) 20-30% and Decommissioning Expenditure (DecEx) 5% (41). This breakdown can be seen in Figure 2.3, where the circled numbers highlight the number of related costs to this topic.

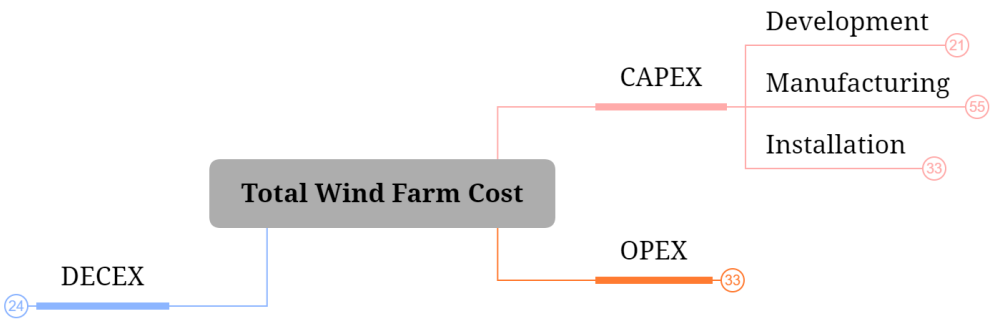

Figure 2.3: Cost category breakdown.

2.3.1 Development Cost

The most simplistic way to model the full CapEx of an offshore wind farm is using a GBP/MW value found within the literature or from published wind farm data, an example of this approach is shown in (114). The issue with this approach for floating offshore wind is the lack of data, the large number of potential support structures and site variation.

Maienza et al. (41) created one of the best models within the literature with a high level of detail. However, the model does lack the inclusion of costs related to concept definition, engineering, and project management. Similarly, Judge et al. (109) also neglected this cost. Generally, preliminary costs make up for around 4% of the total cost (113). Ensuring that appropriate preliminary work is carried out is essential to ensure the project runs smoothly, and no other costs are incurred at a later stage.

In (29; 39; 40; 42; 97; 113) the preliminary costs such as market study, legislative factors, farm design, management and engineering were included. These costs are the same for all three platform typologies and are calculated based on the wind farm power capacity. Rather than using the wind farm capacity, another method which has been used is a percentage of the CapEx, as in Lerch et al. (46). A number of papers used data from fixed offshore wind farms, including environmental, met station and seabed station surveys, project management and development services GBP/MW values (9; 43; 44). The reason fixed wind farm site data is used is that there is no real data for floating platforms as of yet, due to the lack of operational sites, and the potential similarity between fixed and floating platforms for the development cost. The

cost models presented in (9; 45) have similar categories to those listed above, but also include GBP/MW values for human impact studies, insurance and contingency. A general GBP/MW value was used in Bosch et al. (107) for general preliminary works, with no detail of what is included.

An improvement on a GBP/MW estimate would be to include cost information on the surveys carried out. It would be relatively simple to implement, considering installation cost models already including a variety of vessels and their related costs (39; 41; 102). It is estimated by (9) that survey costs account for around 34% of the developmental cost phase.

A mind map detailing all costs which should be included in an offshore wind farm according to the literature can be seen in Figure 2.4.

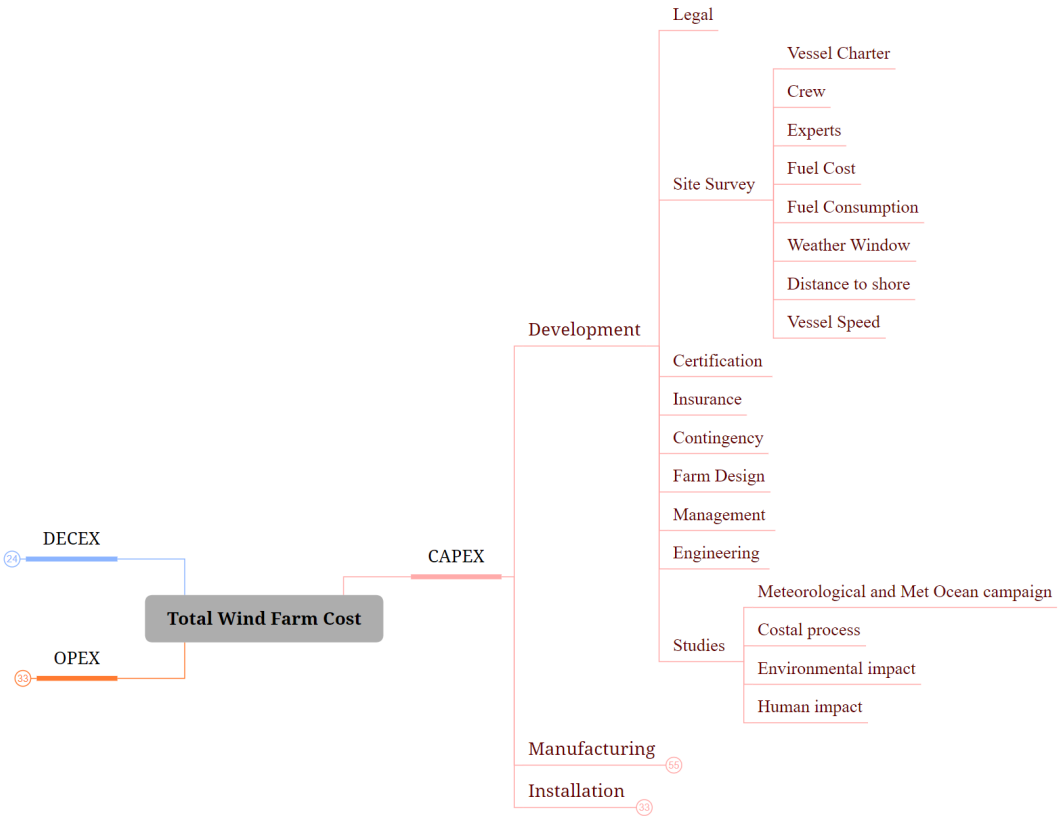

Figure 2.4: Complete cost details for the development cost.

2.3.2 Manufacturing

Generally, the manufacturing costs calculated are broken down into four main categories in a range of different research papers: wind turbine, platform, transmission system, and mooring and anchors (4; 9; 29; 39; 40; 41; 45; 46; 103; 104). These areas are reviewed in subsequent sections. Figure 2.5 shows all of the costs related to the manufacturing costs.

Wind Turbine Cost

Wind turbine costs have previously been estimated using a linear regression approach, fitting a line to 2-10MW wind turbine cost information from a dataset (41). The most common approach to find the wind turbine cost was to use a GBP/MW value (4; 29; 39; 40; 43; 44; 46; 107). In (9; 45), the authors used a set value for the 5 MW NREL wind turbine based on the available literature. Gil et al. (65) considered that there is variation in the cost of wind turbines, depending on whether they use HVAC or HVDC. The Alternating Current (AC) turbine cost was calculated using a formula related to wind turbine power, while the Direct Current (DC) turbine cost was calculated as a percentage of the AC turbine because it does not require a back-to-back power converter.

Platform Cost

Few basic cost models available used a generic GBP/MW value to cover all floating platform types (29; 42; 97; 113). Similarly, Martinez et al. (43; 44) assumed a cost per platform of eight Million Euros, because their work utilises the WindFloat platform. A simplistic method utilising linear regression to derive a line of best fit from available data, to find the platform cost considering water depth, is presented in (107). Ioannou (2020) et al. (112) calculated different platform costs based on material mass and a complexity factor, which accounts for the fabrication process and complexity of each support structure.

Such models can create a good benchmark value, however, it is important to consider platform variation and more detailed cost estimates, particularly as wind farm

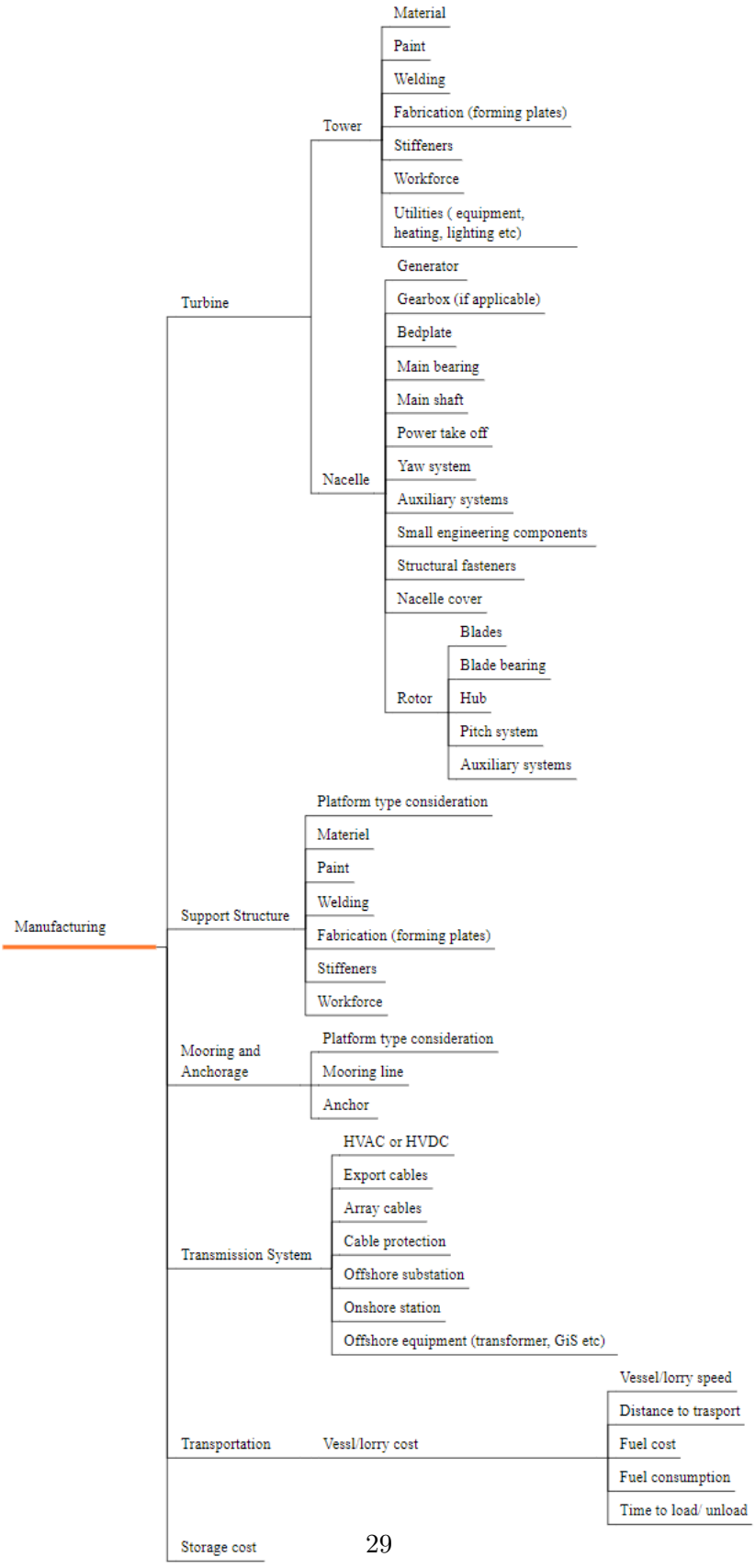

Figure 2.5: All costs related to the manufacturing cost.

owners proceed further into the project design. Platform cost was expressed simply as material cost in terms of steel, concrete, and ballast used for the different platforms in (4). Their research does not include additional costs related to the fabrication of the platform. Maienza et al. (41) produced a fair estimate of the floating platform cost, detailing its dependency on platform type. They calculated the platform cost, including material cost based on the platform mass, painting, corrosion protection, salaries, and engineering equipment. The latter is taken as 5% of the sum of the other manufacturing costs. Castro (2014) et al. (40) found the cost for the same categories; however, the relationship and any level of detail between these terms were excluded, therefore it is unclear how the above was calculated. A more detailed explanation was provided in (39) on how these costs are found. The cost is related to the generator cost which is a function of material, direct labour, and activity cost. These costs are all a function of the platform mass, live, dead and interior surface of the platform, cost per hour, and the cost of steel. It is unknown what the live and dead surfaces of the platform are since the author does not explain this. In Lerch et al. (46) the substructure cost considered material, labour, overheads, shipyard hire and transport to port. Myhr et al. and Bjerkseter et al. (9; 45) found the cost of the material consumed based on a GBP/kg and the manufacturing cost, including: rolling, cutting, painting, corrosion treatment of steel plates, welding and miscellaneous assembly of materials into complete structures. This is accounted for based on the complexity of the platform, which changes with different concepts (9; 45).

Transmission System Cost

Ghigo et al. and Lerch et al. (4; 46) used a simple, yet effective way to find cable cost using the price per meter of array and export cable. The transmission system in (40; 41) defines export and array cable costs for the given distance and water depth, considering the voltage rating and whether HVAC or HVDC is used. There is a general rule that around 50 km offshore, HVAC losses become high, so switching to HVDC is more cost effective due to lower losses (65). Bosch et al. (107) considered the HVAC and HVDC possibility drawing upon the literature to give a set value for the transmission cost with

a power of 500-1000 MW. In 2016, Castro et al. (39) decided to remove the inclusion of the HVDC link, probably due to the site selected for the case study being relatively close to shore. A general cable cost was found using the water depth, distance to shore, and relative distance from the platform to the substation. The found length is then multiplied by GBP/m of cable (39). This work did not include the difference in cost for export and array cables, which is an oversimplification. A less complex approach was considered in (43; 44), neglecting the variation of voltage rating. The transmission system in (9; 45) included export and array cables, considering GBP/m, with additional thought for the cable diameter and voltage. Similar to the other papers listed in their research only HVDC is considered.

The most detailed transmission cost for HVDC is presented in Gil et al. (65). This work presented four different collection grids, highlighting the parallel HVDC configuration to be the most comparable to the traditional radial layout used for HVAC. Rather than using the GBP/m value to find the cost of cables, Gil et al. implemented two different formulae for both AC and DC cables which consider: length, current, and coefficients related to voltage rating. Unlike the majority of papers, (65; 101) included the cost for transformers, but both studies use different methods. Gil et al. (65) used a formula related to rated power and Castro (2016) et al. (101) used a set value. Other components considered in (65) are AC/DC & DC/DC power converters, and switch gear. The cost relative to the AC/DC converter is derived as a function of the rated power, while DC/DC is a set value depending on the layout and power capacity of the farm. Switch gear costs were modelled as a function of the nominal voltage. Substation platform costs vary rapidly depending on whether AC or DC is used. To represent this cost, Gil et al. (65) used a simplistic formula for the AC platform, and a more complex formula for the DC case, including feeder and collector platforms.

In (41), the offshore platform for the electrical station cost was expressed as 11% of the installed power. Using the wind farm power in MW and providing the cost in Millions of Euros. The onshore platform was expressed as half of the price of the offshore platform. Both platforms necessary for energy transmission, onshore and offshore, are considered as a fixed value in (9; 45). (44; 44) uses a fixed value for onshore and offshore

transmission platforms, considering the number of each platform required, depending on whether HVAC or DC is used. Lerch et al. (46) decided to exclude the cost of an onshore substation because it was assumed that there should already be one existing. The offshore substation considers the number of transformers used (46). Ghigo et al. (4) represented both onshore and offshore platforms with a set price. Heidari et al. (29) used data from existing wind farms in order to fit a linear function dependent on distance to shore to find the total cost of the transmission system.

Mooring and Anchors Cost

The station keeping costs were expressed in (41; 46), considering the different platform types and the requirement of different material types for each mooring line configuration. Maienza et al. (41) used a GBP/kg estimate for the anchors. It is fairly straightforward to find the cost of different anchor types for each configuration, however, two set values were used here for catenary and taut mooring. Compared to (40), this work considered wind, wave, and current forces in order to determine the required mass of the mooring line and anchor, where similar to (41) the cost was calculated in terms of GBP/kg. (29) used a similar approach considering the minimum breaking load of the mooring line within empirical formulae to find the cost for both mooring and anchors. An additional consideration by (40) was the use of a chain in waters less than 40 m and synthetic rope for deeper waters. (39) calculated mooring and anchors based on a GBP/m and GBP/kg value, respectively, neglecting different mooring line types. Lerch et al. (46) found the cost of anchors in terms of the number of anchors. Martinez et al. (43; 44) utilised a formula to determine the cost of the mooring system, considering the number of anchors, length of mooring lines and chain, the cost of each, and the water depth at the selected site. A range of different anchor and mooring line types are considered in (9; 45). This allows different platforms to have a more accurate cost, as some require different mooring configurations. The cost is represented as the price per anchor and the price per meter of mooring line. Mooring line types considered are chain, wire, fibre rope, and pipe. The stiffness of the mooring line and the appropriate diameter are also selected for the upper and lower sections of the line to

ensure it does not exceed the minimum breaking load. The most simplistic account for mooring and anchors cost is presented in (4) using a set value for each, not considering water depth, or different requirements for different platforms. All of these subsystem costs are considered as 'dry CapEx' in (109), where details of how each is calculated have not been provided.

Notably, Lerch et al. (46) were the only researchers to include transportation costs within the manufacturing stage, considering parts and materials have the requirement to be moved from a different site to the port. Such costs include offshore costs, vessel hire, number of vessels, fuel rate, fuel cost, and time required to perform a task, as well as port costs including equipment hire (cranes), number of equipment used, time for the task, and storage hire (46).

2.3.3 Installation

Maienza et al. (41) developed an installation model discussing a range of different vessels within the text, it has however been noted that for the calculation of time to transport from port to farm, only two vessel speeds are available: tug and crane speed. Similarly, (39; 40) also considered the use of different vessels for installation. An issue surrounding the installation is the lack of clarity on the vessel charter type in all papers expressed within this review. This is an important factor to consider as this determines whether the client must provide their own crew and pay fuel costs. (39; 40; 41) did not explicitly state if such costs are included within the hire rate. It is important to account for fuel costs due to its volatility and since there are limitations on which fuels can be used due to the sulphur cap in place, pushing consumers to use more expensive marine diesel oil compared to traditional heavy fuel oil (115). Work by Lerch et al. (46) did not state the charter type but it does include fuel cost and fuel consumption. It is, however, unclear if this is fixed or varies for each vessel type.

In the following work (39; 40; 41; 46) the installation cost was broken down into turbine, platform, mooring, anchors, and transmission systems. This captures all of the turbines' major systems. A range of different installation methods has been well explained within (41; 46), highlighting that a single lift is generally the best for a

floating platform. The installation was, however, varied to suit each platform, making it more accurate. Work carried out by Castro (2018) et al. (102) focused purely on the installation cost, similarly to (41; 46), this research included six potential lifting methods. Consideration of the shipyard capabilities is also considered in (41) and (102), related parameters were given in the latter, these parameters are: storage area and shipyard draft. When the shipyard is insufficient, the closest port was utilised, also considering the transportation cost from the port to the yard (102). Castro (2018) et al. (102) considered different methods for installation of each system, i.e mooring and anchors installed via a tug and barge or specialised anchor handling vessel, and a similar procedure is carried out for the other systems. This research is probably the most detailed account of installation costs, with the inclusion of a very high level of detail, including vessel type, speed, range of installation methods for each system, range of lifting methods, time to carry out all tasks and comprehensive equations and tables of data used within the calculation. However, similar to all other papers, there is no charter type, fuel cost, or fuel consumption of any vessel included. On top of this, there is no account of crew or technicians, without which no work would be carried out.

The cost model within (29) included the installation of Spar and Semi-submersible utilising an empirical formula depending on the distance to shore and port cost only. Another method which utilised a formula for turbine installation is (43; 44), this cost depended on vessel hire, speed, number of turbines, turbine capacity of the vessel, and installation speed. This model did, however, only consider a jack-up crane as the vessel used, limiting the installation site to a water depth of about 50-60 m, as this is the typical maximum operational range of such a vessel (43; 44).

Myhr et al. (9) calculated the installation cost of the turbine and platform considering a range of methods, allowing the cheapest for each platform to be highlighted. This model considers the requirement for different vessels but does not explicitly state if it is considered within the cost model. Similarly, the only time considered is that of the installation at the site. It does not include travelling to and from the site, or the number of crew/technicians to do such tasks. Installing the cables was based on a GBP/m value, and station keeping installation cost is based on deck capacity to store

the system, transition time, installation time, and operational window to carry out the installation (9; 45).

Relatively simple models for installation costs were included in (42; 97; 113), using a GBP/MW value for all installations, with no variation for different platforms or distance to shore. Similarly, Bosch takes information from (9; 45) and considers the installation cost to be GBP/MW, they did, however, consider the platform type (107). Ghigo et al. (4) also considered a GBP/MW value for the Hexafloat and Spar platforms.

Sarker et al. (108) sought to minimise the cost of installation and hence reduce the LCoE. The installation process highlighted the use of a jack-up vessel, which is not appropriate for substantial water depths, and hence is not deemed applicable to floating platforms. The type of platforms this installation model used is not stated, but it is expected to be suitable for fixed wind turbines only. It did, however, include a learning rate parameter, which could be useful for all areas of floating offshore wind as the number of operational sites increases, which would be useful for all costs (108).

Judge et al. (109) includes a range of different installation techniques for the different systems, such as different methods for cables: plough burial or separated trenches, turbines can be fully assembled or partially, and the support structure can be floated out or crane lifted. The hire, fuel cost, and the number of turbines or foundations each vessel can transport with the selected installation method, transport distances from manufacturing centre to port by road and sea for all project assets (e.g. turbines, foundations, export cable etc.) as well as the distance from port to offshore site are all considered in this work. Additional project costs such as project management, port costs, and survey and monitoring costs were included in the installation phase, which in general would be in the first section of preliminary works. A highlight of this work is the use of meta-ocean data to determine weather windows to carry out any activities offshore such as installation, O&M and decommissioning (109).

Fatigue and stability during installation present significant challenges for floating offshore wind turbines, especially during the assembly, transport, and pre-commissioning stages. These phases subject the structure to dynamic and unpredictable conditions—fluctuating buoyancy, mooring tension, and environmental loads from wind and waves. Floating

systems must maintain equilibrium throughout, ensuring that the righting moment always exceeds the overturning moment to prevent excessive tilting or capsizing (116). In terms of fatigue, the temporary phases can be particularly demanding. Repeated load cycles induced by wave motion, crane lifts, and towing adjustments—even though transient—can generate high stress concentrations in critical areas such as joints and welds. Overlooking these transient loads can accelerate fatigue damage, compromising the long-term integrity of the structure (116). Collu et al. emphasise the importance of rigorous dynamic analysis during these stages, recommending time-domain simulations to replicate real-world load histories and verify compliance with stability criteria [1]. They propose a systematic framework for identifying critical scenarios, applying standards-based requirements, and validating designs through semi-submersible case studies. These techniques are essential for mitigating risks and ensuring that floating wind turbines remain safe and reliable during their most vulnerable phases.

2.3.4 Operations and Maintenance

O&M captured within Maienza et al. (41) included insurance and seabed rental, along with preventative and corrective maintenance. Both maintenance types include the probability failure rates of each component and the related downtime to carry out the repair. Indirect costs such as port storage, vessel hire, and maintenance planning were also included. One parameter which is not included is availability, which is a considerable factor which can affect the length of downtime and therefore revenue. This is, however, not a simple task to include and would require a model in itself (41).

The operational cost found in (39; 40) included tax, assurance and management costs, all related to the GBP/MW value. Maintenance costs are also included considering the failure rates of components. One main difference between (40) and (39) is the assumption made in (40) that all maintenance is carried out via a helicopter. This is a very specific assumption, based on a number of different works, it has been stated that helicopters can only operate below 1.4 m significant wave height and 18 m/s wind speed due to survivability requirements under a ditching scenario (117), heavily limiting the availability and reducing flexibility.

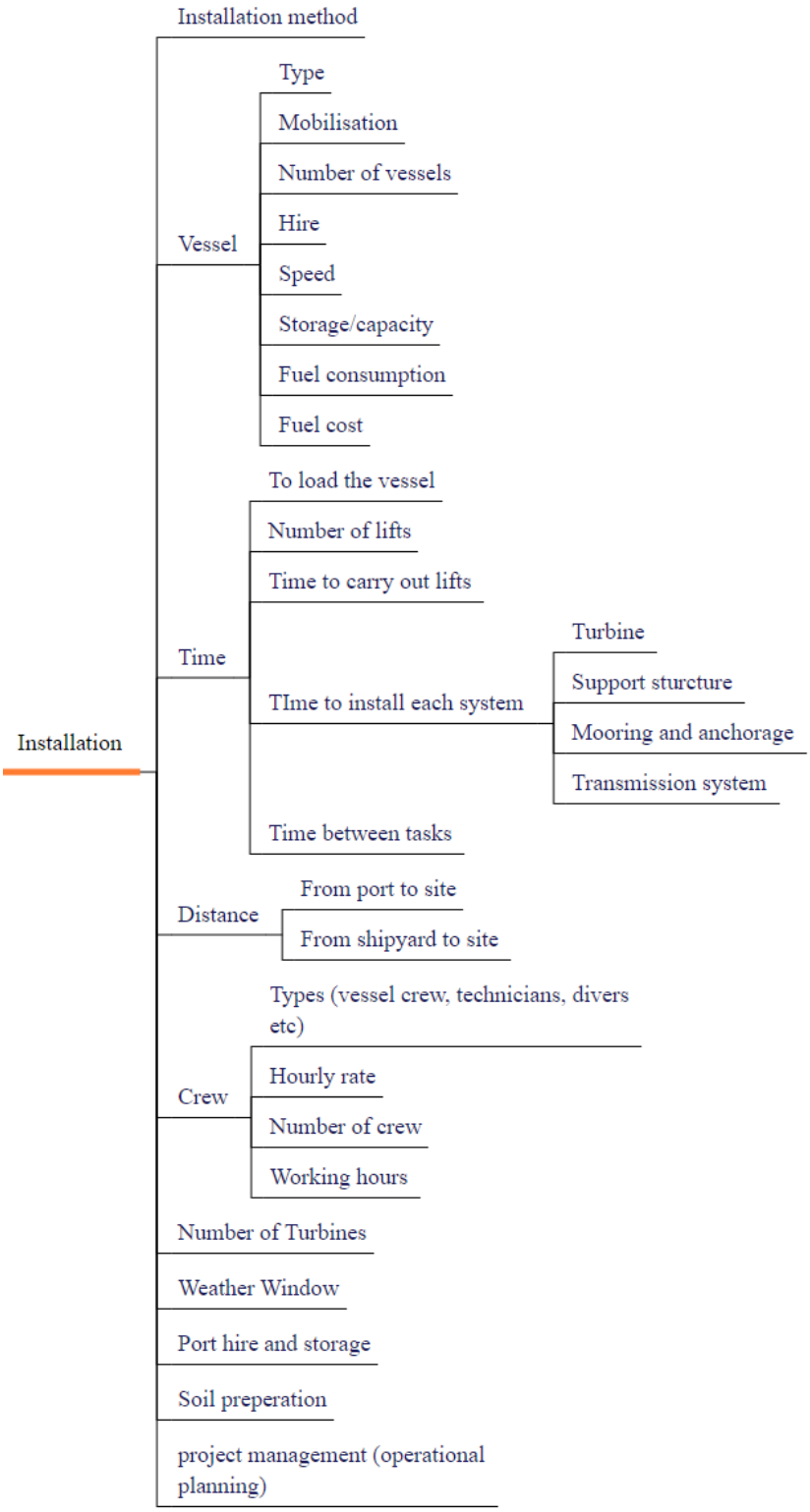

Figure 2.6: All costs related to the installation cost.

Lerch et al. (46) opted to incur general insurance, contingency and operation costs within their model which was related to a GBP/MW value. The maintenance, similarly to the previously explained paper is split into corrective and predictive maintenance. The latter depends on the frequency of maintenance, vessel hire, fuel cost, fuel consumption, materials needed, and cost of divers (46). Cost related to 'divers' includes all personnel costs and time. Corrective maintenance follows a very similar calculation, but it also includes annual failure rates for each component (46).

(9; 45) utilised a pre-existing cost model for O&M called OMCE-Calculator. This is generic and does not use wind farm data, it is based on past experience and engineering judgment. Unplanned, condition and calendar-based maintenance is considered for floating and fixed, detailing the number of maintenance events for each. Downtime, time to repair, number of crew, vessel hire, port fees, inspections each year, and spare parts are all considered in this work (9; 45). Alongside the maintenance, insurance costs were also considered GBP/MW. One main parameter which has been neglected is the distance to shore, hence there is no consideration of the additional time to hire the vessels to get to the site. It is, however, expressed that the maintenance strategy will have a mother ship at the wind farm site, with daughter crafts to carry out any work. These vessels will still have to come to the port to change, crew, refuel, etc., which is neglected. Fuel costs are also not considered for any vessel (9; 45). (107) re-used the methodology laid out in (9; 45). Judge et al. (109) similar to other models, their research included preventive, corrective, and condition-based maintenance. There are no formulas to highlight relationships or how costs are found, but the main parameters were: vessel hire, type, personnel, spare parts, time to complete a task, vessel mobilisation, downtime and most importantly weather windows to carry out the O&M (109).

A simplified assumption for the O&M cost was presented in (4; 42; 97; 113; 114) based only on GBP/MW. A slight improvement on using a GBP/MW value is to consider the distance (43; 44), use data from other research, and modify the GBP/MW value to consider the distance to shore for their own site. Similar to installation cost the O&M model within Heirdari et al. (29) only considered distance to shore to determine

O&M, and insurance (using GBP/MW). The most simplified assumption seen for both O&M and decommissioning was presented by Ioannou (2020) et al. (97) neglecting both costs because they are assumed similar for each platform. Mhyr and Bjerkseter et al. (9; 45) also considered O&M to be the same for each platform. Based on all other literature which analyses the three different platforms stated above, this is not true. A mind map is presented below in Figure 2.7 highlighting all costs related to the Operations and Maintenance of a wind farm.

2.3.5 Decommissioning

In (4; 41; 107), the decommissioning costs were expressed as a percentage of the installation cost, which leads the author to determine that any uncertainty is carried over from the installation cost to the decommissioning cost. Maienza et al. (41) also included the cost related to site clearance represented as a cost per area. Castro (2014) et al. (40) had a slightly more comprehensive decommissioning cost, including distance to port and shipyard, vessels required, hire rate, and vessel speed. This model also included the reselling of scrap metal, which brings down the overall decommissioning cost. Castro (2016) et al. (39) employed the same method as their previous work but presented more detailed formulae. A more in-depth model was presented in (46), where the decommissioning cost was split into main subsystems, and for each subsystem, the disassembly cost, transport, and port fees were calculated. The first two considered vessel hire, number of vessels, crew, and the time this takes to be completed. The port fees were related to the cost of hire, storage space, and the use of vehicles. Site clearance was also considered to ensure the wind farm site is restored to its original state, this cost was based on the area. Finally, disposal and selling of all materials, including material cost and transportation costs, were included (46).

An opposing opinion on most papers is that of (29): this work considered the DecEx to be negligible because they expected scrap costs will cover any removal and clearance costs. In (43; 44) it was assumed that the decommissioning of a wind farm would only create revenue due to the scrap material, considering a return of 250 kEuro per MW. This paper highlights the large amount of uncertainty when predicting this cost, due

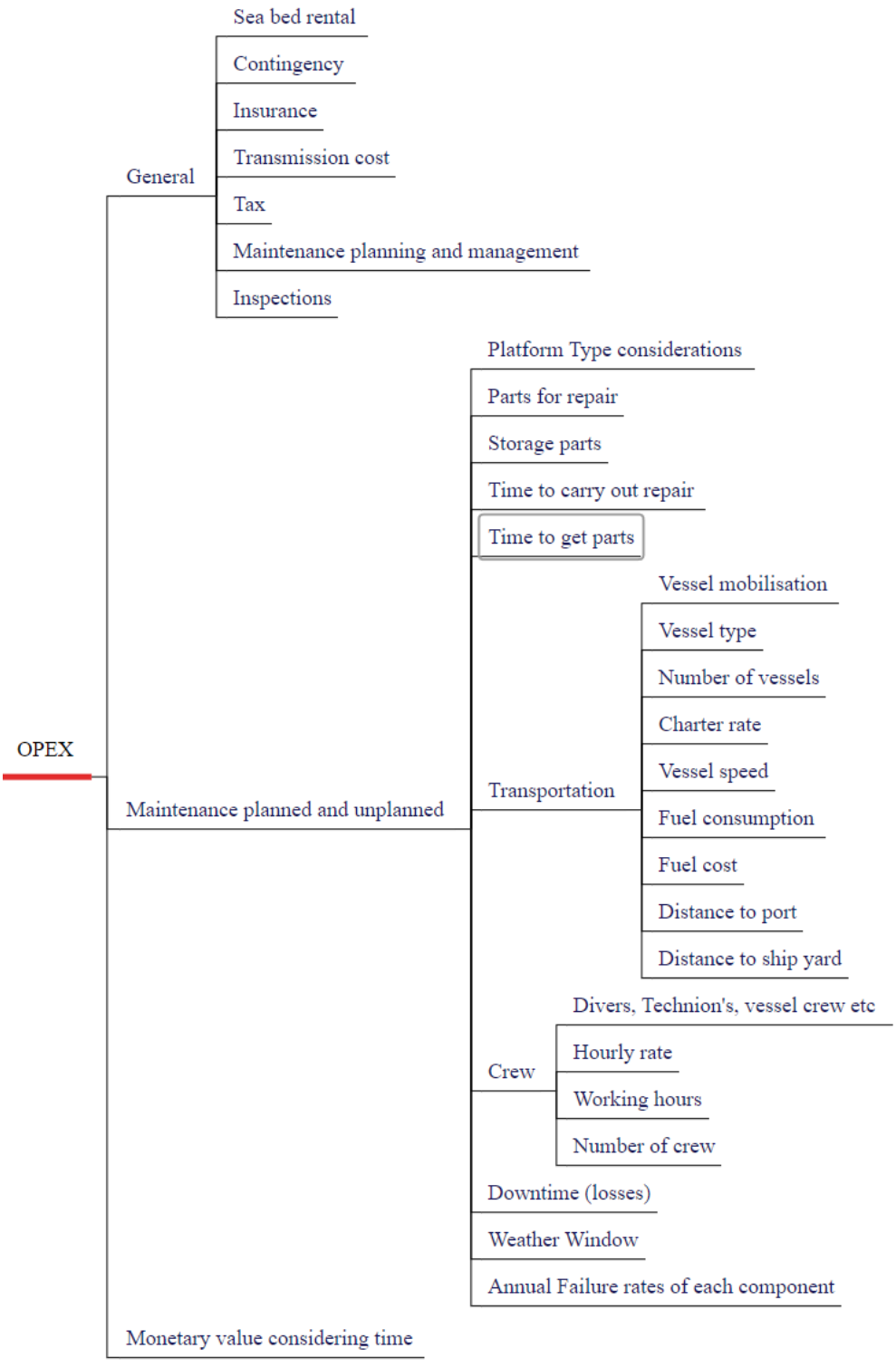

Figure 2.7: All costs related to the Operations and Maintenance cost.

to uncertainties about the time that decommissioning activities are anticipated to take place, the duration of the decommissioning process, the weather window for execution, options available for decommissioning, etc. Another factor not considered in (43; 44), but considered in (9; 45), is the fluctuation in the price of steel for scrap cost.

Adedipe et al. (110) broke the DecEx into four main categories: planning and regulatory approval, execution, logistics and waste management, and post-decommissioning. This is the only work to have considered regulatory approval, the cost was based on approval needed for oil and gas projects. Engineering and management costs, contingency, and insurance were considered within this subcategory as a percentage of total decommissioning. (109) is the only other paper to have considered these costs within the DecEx model. The execution phases within both (109; 110) included: disconnection of wind turbines from the grid, cost of wind turbine preparation for removal, cost of lifting and removal of wind turbines, tower, foundations and scour protection, cost of decommissioning of offshore substations, and cost of decommissioning of all cables. Within each section, considerations for the time to carry out all tasks, vessel hire, type of vessels, number of vessels, crew costs, distance to port and number of journeys required (110). The cost related to logistics which considers how the decommissioning will take place and the organisation of transport and recycling/scrapping is calculated in (110) and includes the same parameters as the execution phase which was previously described. Both Judge et al. (109) and Adedipe et al. (110) include waste management costs, detailing: port fees, landfill cost, salvageable materials, waste processing for non-recyclables, transportation costs to the landfill/recycling centre, capacity, number of trips, and how far the truck needs to drive (109; 110). The post-decommissioning cost in (109; 110) includes: site survey, site clearance, site monitoring, site remediation, and miscellaneous costs, but the details on the calculation are not given. The main difference between (110) and (109) is the level of detail presented. Judge et al. (109) did not include any formulations on how the cost is calculated, unlike Adedipe et al. (110).

In (9; 45) the decommissioning costs were expressed in GBP/MW with the scrap cost in terms of mass highlighting that some platforms actually create revenue from decommissioning. Stehly et al. (42) excluded decommissioning costs, but included a

decommissioning bond: this is a financial agreement to ensure proper removal and site clearance. In the references (97; 113; 114) decommissioning cost was not considered.

Everything related to the decommissioning cost can be seen in Figure 2.8.

2.3.6 General Assumptions

The approaches presented in (29; 40; 41; 107) used a formula to calculate LCoE that did not contain a discount rate, but this is important to include as over time the value of money varies, particularly when it is over a wind turbine life (20-25years). Castro (2014) et al. (40) had what seems to be a quite comprehensive cost model, however, it does not state any formulas used to find the end results. Then in 2016, the authors (39) provided more details on the formulations used, although it is both for wave energy converters and offshore wind turbines. The work which considers the discount rate in the LCoE calculation are (4; 9; 29; 39; 42; 43; 44; 45; 46; 97; 103; 104; 107; 114). The following authors also decided to separate the cost into CapEx, OpEx, and DecEx because the only values which should be heavily affected by discount rate are OpEx and DecEx, since CapEx is typically paid at the start of the project (4; 39; 43; 44; 103; 104; 106). Duan et al. (114) applied a discount rate to both CapEx and OpEx, with CapEx distributed over the first four years of the project and OpEx starting only after the initial four years of operation, which better reflects real project conditions. The choice of discount rate is critical: Figure 2.9 illustrates how variations in the discount rate or Weighted Average Cost of Capital (WACC) influence the LCOE, showing that at a 10% WACC, the cost of capital accounts for more than 50% of the LCOE. Conceptually, the discount rate and WACC are equivalent, as both represent the required rate of return used to discount future cash flows to present value in valuation models. For early floating wind projects, WACC is expected to be high due to unproven technology and associated risk premiums, making it essential to deploy demonstrators to reduce risk, validate technology, and ultimately lower LCOE to achieve competitiveness.

A common method to find the AEP is the use of the Weibull Probability Density Function (PDF) shown in (9; 39; 40; 41). Castro (2016) et al. (39) however considered the efficiency of the transmission and the overall availability of the wind farm, making

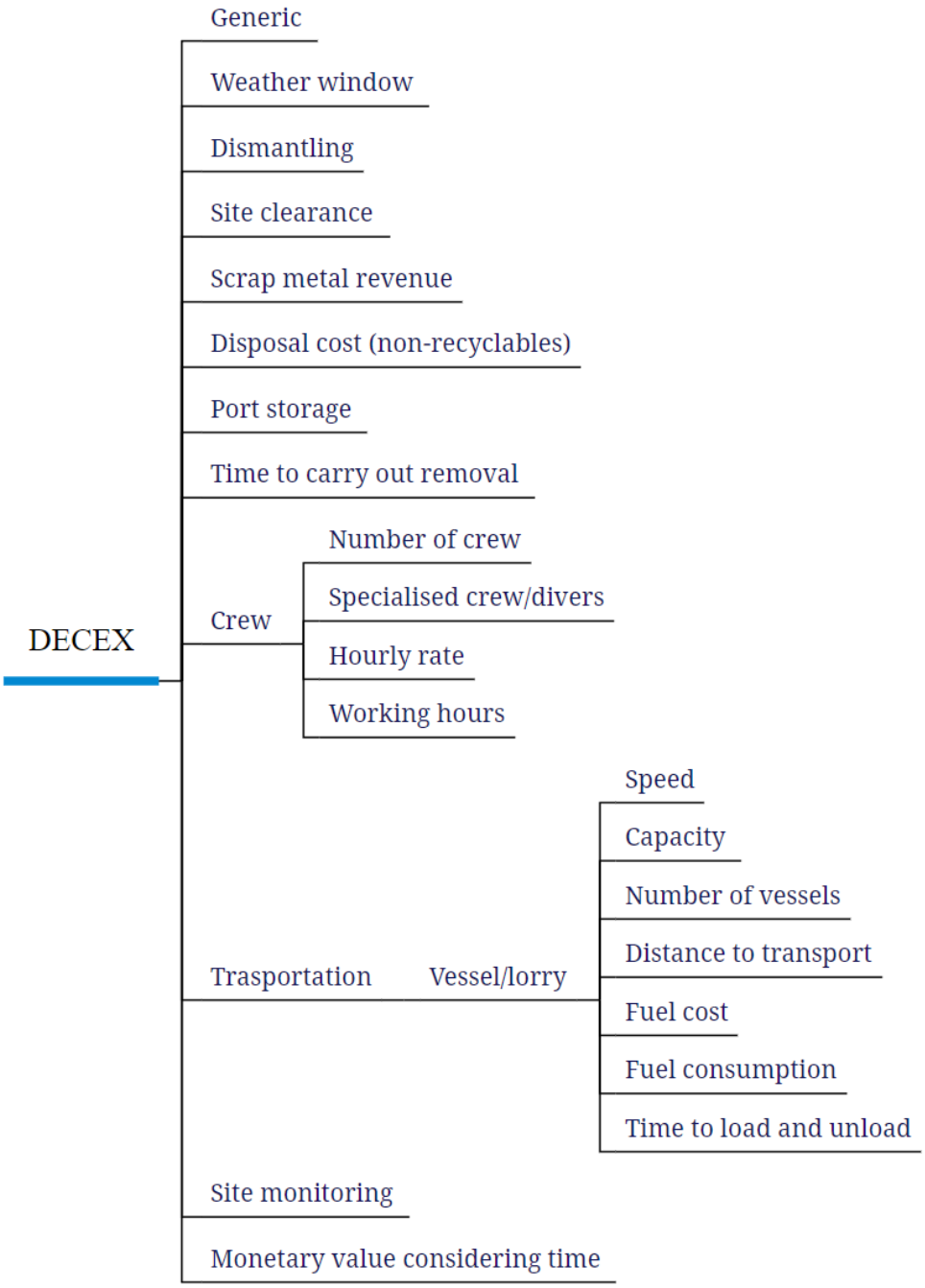

Figure 2.8: All costs related to the decommissioning of the wind farm.

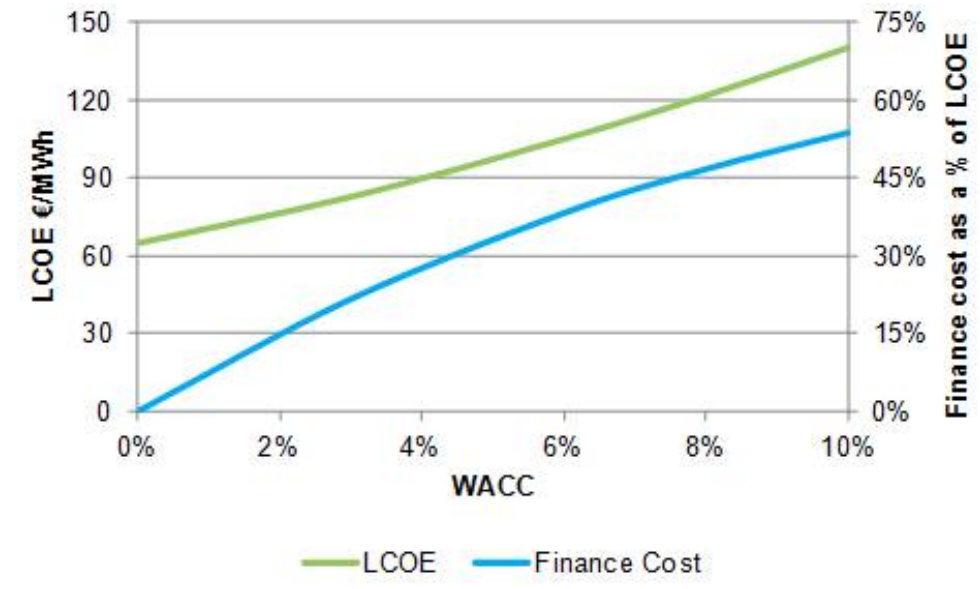

Figure 2.9: Impact of WACC on LCOE (5).

it more accurate. The layout of a wind farm is generally considered in a grid format within cost models. (41) ensured the wind turbines were spaced seven diameters apart, whereas (103; 104) considered intra-Row and inter-Row spacing of four and seven diameters, respectively. The life 50+ LCoE modelling tool was used within (46), with further details found in (106). When calculating the LCoE, (46; 106) the AEP is required, unlike other papers it did not include considerations for losses. The losses were listed as turbine, wake, availability, collection and transmission losses (46). Similarly, Heidari et al. (29) included losses in this calculation, but also considered the capacity factor. Losses such as availability, electrical, aerodynamic, and others were considered in (9; 43; 44; 109). Electrical losses are converted into a cost metric in (65), by considering the energy price of the given year and the losses related to the transmission system.

Another consideration made by (29; 45) was the year the data used was found. Rather than using it straight from literature, which could potentially be years old, each cost value was translated with a discount rate to today money. Table 2.2 highlights the assumptions made within the literature for losses and methods to find AEP. The capacity factor in some cases was assumed and in others was calculated based on the

AEP calculation. The INC. abbreviation is included to show that it was considered in the work, but an explicit value was not expressed. Using a Gaussian distribution with a confidence of 95% the maximum and minimum values for each value were found.

Reference	Capacity Factor (%)	Electrical Losses(%)	Aerodynamic/ Wake Losses (%)	Other Losses (%)	Availability (%)	Discount Rate (%)	AEP Method
(41)			5.26				Weibull
(39)		INC.			INC.	INC.	Weibull
(104)						8	Weibull
(103)						INC.	Weibull
(46)	Calculated	INC.	INC.		INC.	INC.	Weibull
(29)	42	1	7	3	95	9	Capacity factor
(42)	38				98	5.8	Weibull
(97)	52.1	1	9	4.6	95.4	8.9	N/A
(114)	INC.					INC.	Capacity factor
(43; 44)	Calculated	1.8	7	3	94	10	Weibull
(9; 45)	Calculated	1.8	7	3	93.8	INC.	Weibull
(107)	Calculated	3	INC.		97	INC.	Probability method
(4)	Calculated	3.6	10			INC.	Weibull
Average	44.03	2.03	7.54	3.4	95.53	8.43	
Maximum	56.28	2.91	8.93	4.34	96.9	10.57	
Minimum	31.78	1.16	6.15	2.46	94.16	6.28	

Table 2.2: Losses and methods to find AEP as reported in the literature, INC. means it is included but no explicit value was stated.

This work covered in Section 2.3 is summarised in a table found in the supplementary document 'offshore wind cost'. This table highlights what existing research includes and does not include in their work.

2.4 Data Review

The aim of this review is to analyse the data presented in the literature, identifying what the causes are for the large variations in cost estimates.

There is a general trend for the sites expressed in the literature, as wind farm capacity increases the distance from shore increases. This pattern can be seen in Figure 2.10

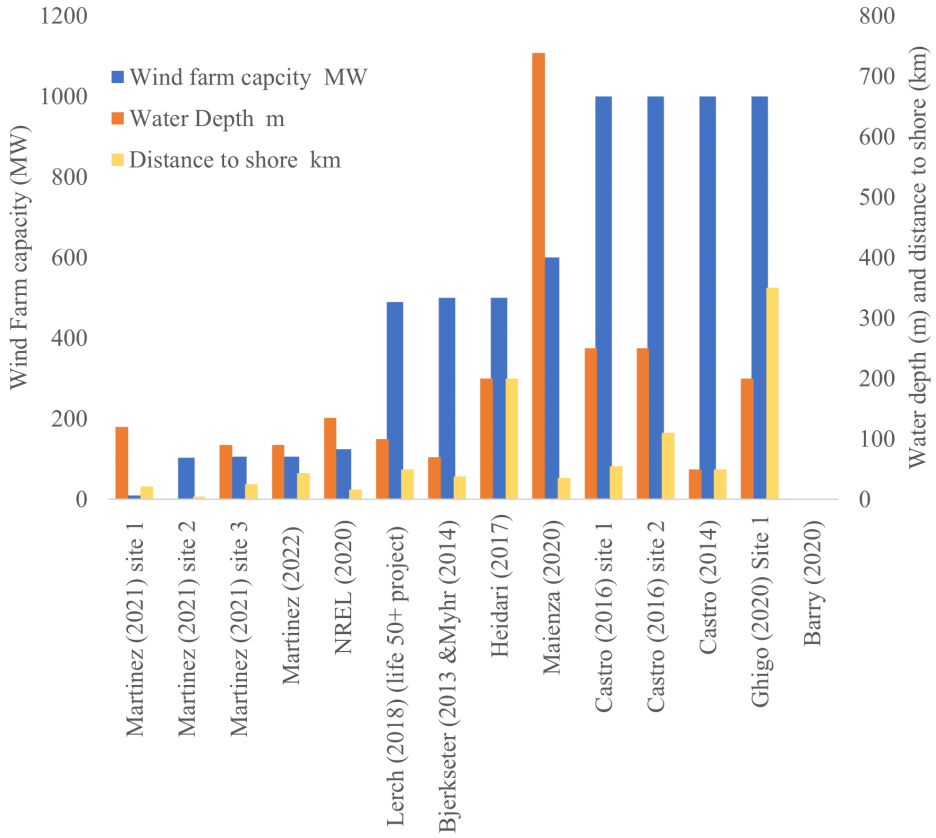

Figure 2.10: Varying wind farm capacity, water depth and distance to shore for the literature.

One major issue with comparing literature is the huge variation in sites used. In order to consider this in the comparison, some of the values have been made dimensionless with respect to capacity and distance to shore, removing the limitation of units, and allowing each paper to be compared in a fair and consistent manner. The preliminary concepts and manufacturing costs for the majority of the sub-system were presented in a MEuro/MW value, as these are not expected to vary heavily with distance or water depth. The mooring cost was presented in MEuro/m to consider the depth of each site. The installation, O&M, and DecEx costs were all presented in MEuro/MW/km to remove the power and distance to the shore element.

All costs considered were converted to 2025 prices, using the Consumer Price Index (CPI), it can however be noted that converting the costs made no differences in the trends seen, which is likely due to research using cost value without considering the time value of money in there use.

2.4.1 Capital Expenditure

The capital cost is split into generic, manufacturing, and installation costs to analyse each section better.

Generic Costs

This section includes development, turbine, and transmission system cost estimates found within the literature, see Figure 2.11.

The Euro/MW value for both preliminary and turbine costs is relatively similar for each paper, which is to be expected considering that these costs should not vary with parameters such as water depth or distance to shore.

The transmission cost (MEuro/km), on the other hand, is generally increasing with the distance to shore, which makes sense as the technology used will typically switch at 50 km from HVAC to DC which is more expensive. The expected trend was taken from Maienza et al. (41) since this work has a very detailed cost model for transmission cost including all details relevant, hence this was used as a rough guide when looking at the trend in literature.

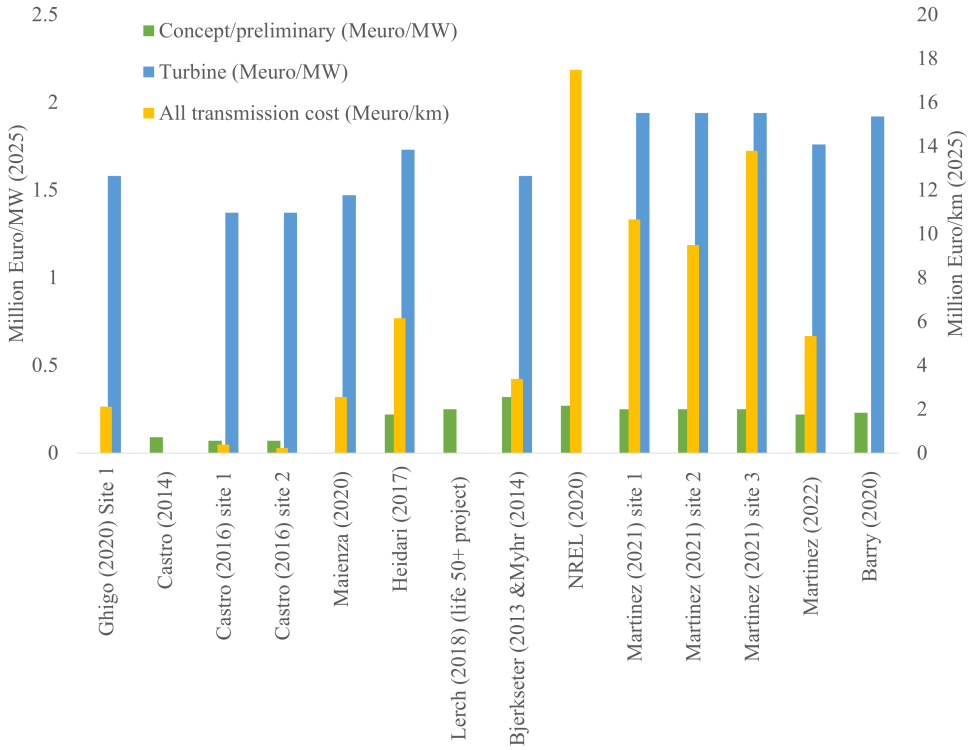

Figure 2.11: Preliminary costs, turbine and transmission costs found within literature represented in MEuro(2025)/MW.

Castro et al. (39) has an extremely small value for transmission cost. However, the cost model is relatively detailed considering both water depth and distance to shore in the cable cost calculation. The expected reason is the lower installed power compared to other sites, requiring lower capacity cables, this is shown in Figure 2.10 which highlights that overall, other sites have a capacity five to ten times greater.

Myhr et al. (9) and Bjerkseter et al. (45) present a relatively low value, this is potentially due to only including a Euro/km value for cable cost. This is a set value for both export and array cables, therefore it is assumed the export cable cost has been underestimated. Both onshore and offshore substations were considered fixed costs. Ghigo et al. (4) has a lower value than expected, but this research does not include HVDC, which would explain the lower cost estimate since HVAC is cheaper than HVDC. This model only uses set values for the on and offshore substations, these costs in other literature have been shown to vary with wind farm capacity.

Stehly et al. (42) utilises a Euro/MW value, Heidari et al. (29) also express the transmission cost in the same way. Both completely disregard the length of the cable and the water depth at the site. This is expected to be the reason for the substantial overestimation in (42).

Martinez et al. (43; 44) shows a decreasing trend with increasing distance to shore, which in general may be considered as inaccurate as generally the distance to the shore is increasing along with the water depth. The method used to calculate this cost is based on the length of the cable required and hence the distance. This cannot even be considered as a benefit from increased wind farm capacity because each site presented in (43; 44) has the same wind farm capacity. The break-even for HVDC technology is expected to be roughly 56 km (44) , hence it would be expected that Martinez et al. (44) site three would be cheaper than sites one and two. Since site one is 5 km further offshore than site three and site two, it would be considered for HVDC technology.

Manufacturing Costs

Platform manufacturing costs can be seen in Figure 2.12. It can be highlighted that there is no strong trend present. This could be potentially due to the different configu-

rations of the three main platform typologies. With this in mind, it would be expected that the Spar would have a slightly similar value for each piece of research, given that it has a relatively standard geometry. Comparing the literature it can be seen that the MEuro/MW value is decreasing with installed capacity, with TLPs following a similar trend. This could be due to the benefit of a higher amount of power produced or potential cost reductions due to mass production. On the other hand, Semi-submersible costs appear to be relatively similar with some outliers. A potential reason for more consistency is the higher amount of research done on the platform, drawing from similar assumptions and approaches.

In (9; 45) the manufacturing cost is well presented, considering material cost and a complexity factor for each platform. The Semi-submersible has the highest complexity factor, while the TLP has the lowest. The Semi-submersible is also expected to have the highest mass, followed by the Spar and the TLP. It is mainly for these reasons that the Semi-submersible is the most expensive. Considering the size of the Spar, it would be expected that it would have a higher mass, as shown in the work by Maienza et al. (41). The formula to find manufacturing cost in (41) relies mainly on platform mass and direct labour, explaining why the Spar is the most expensive. This confirms the author's suspicions that the mass of the Semi-submersible would potentially be a lot less than the Spar. The Semi-submersible is 293 tonnes less in (41).

Heidari et al. (29) follow a similar trend to Myhr et al. (9). The main difference is that the Spar is expected to be more expensive than the TLP. This is reasonable when considering the mass of each platform and the generally low complexity of each. The methodology to find the platform cost in Heidari et al. (29) uses the cost per tonne of: columns, stiffened columns, truss members, heave plates, and outfitting. This considers the mass of each platform and additional components and hence the increased complexity of the Semi-submersible.

The work by NREL (42) has a higher value than other papers, but it is hard to determine the cause since the paper does not explain what is included in the platform manufacturing cost, only a simple GBP/MW value is given. Similarly, Johnston et al. (113) considers a set Euro/MW value for all floating platforms, considering previous

explanations, it is an over simplified assumption. Considering it is a generic value for all platforms, it has a very similar value to (9; 29; 41; 45) if they were averaged out as one cost for all platforms. Martinez et al. (43; 44) have very average values, but this model uses a set value for the platform cost found within other literature for the WindFloat platform. This cost considers the labour cost, etc., making it a good benchmark for a Semi-submersible cost comparison. Ghigo et al. (4) have predicted relatively high platform costs, the model uses only the mass of the platform, explaining why the Spar is expected to be more expensive than a TLP.

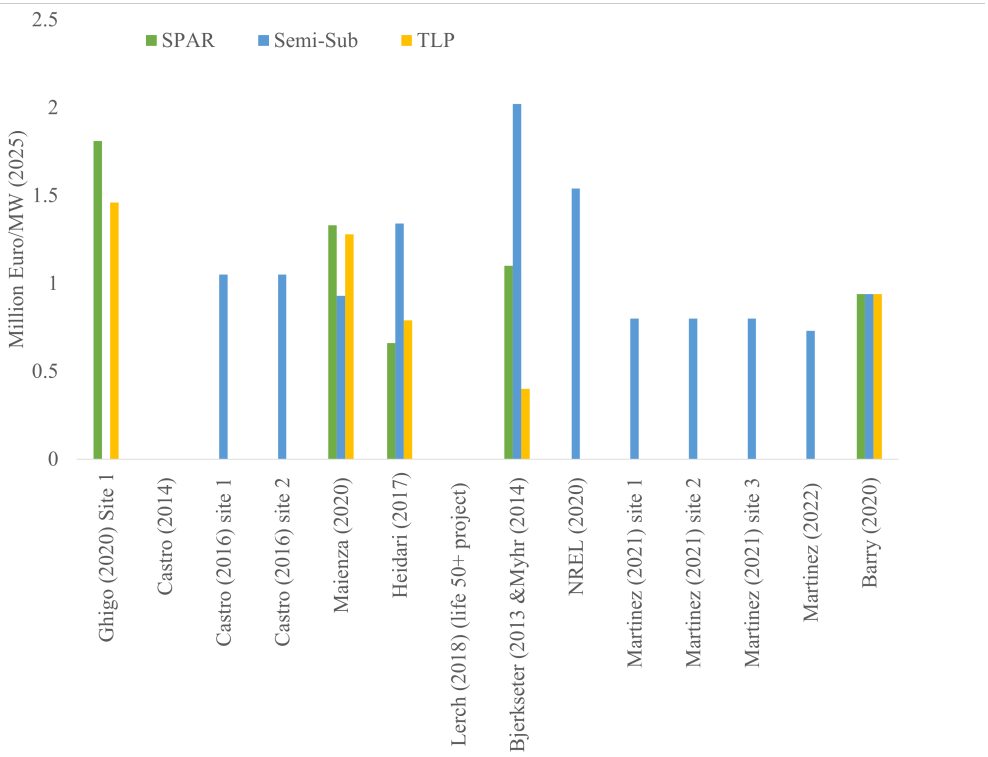

Figure 2.12: Platform costs for each typology found within literature represented in Million Euro (2025)/MW.

The mooring and anchors (M&A) costs are presented in Figure 2.13. M&A given Euro/m is increasing with water depth, which highlights that the deeper the water, the more expensive the mooring becomes, which is in line with the fact that the footprint and potentially the diameter of the mooring line will also have to increase.

Martinez et al. (44) site three has a large Euro/m value for mooring and anchors.

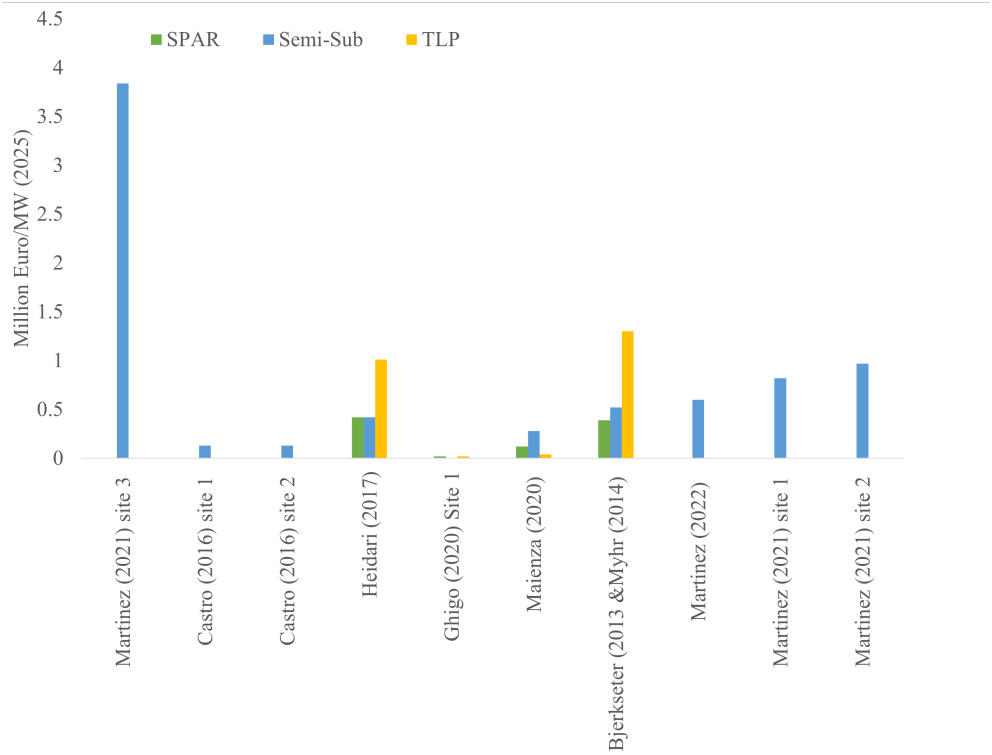

Figure 2.13: Mooring and anchors costs for each typology found within literature represented in Million Euro (2025)/m (water depth).

The reason for this is the way their model calculates this value. It considers the mooring line length to be 560 m for 100 m depth, and an additional 150 m of mooring line is added for every 100 m of increased water depth. In comparison to work by Ma et al. (118), the line length is not considered to be linearly varying with water depth. Instead, this work considers that with increasing water depth, there is an exponential decay, which makes sense given that at shallower water depths, there is potential for greater interactions between the surface and the sea bed. Ghigo et al. (4) uses a set cost for M&A with no variation depending on platform type. Considering other literature and that there are different types of mooring configurations, this is a very simplified approach. This could explain the very low GBP/m value presented. The other papers, shown in Figure 2.13, (9; 29; 39; 41; 45) all follow the expected increasing trend with water depth.

Heidari et al. (29) consider the price of M&A for the Spar and Semi-submersible to be the same, which makes sense since they both utilise catenary systems. Although TLPs have shorter mooring lines overall they are more complex, which could explain their higher cost in (9; 29; 45). Maienza et al. (41) consider TLP to be the cheapest, this could be potentially due to the model using length to determine the mooring cost and fixed anchor costs. Semi-submersibles were determined as more expensive than Spar in (9; 41; 45), this is expected to be due to Semi-submersibles having a larger waterplane area and second moment of waterplane area, leading to higher wave load. Greater wave loads cause the platform to experience higher motions, and hence greater loading on the station keeping, requiring anchors with a higher capacity.

Combining all manufacturing costs to a Euro/MW shows an expected trend of increasing cost with distance to shore. This is due to the transmission cost increasing with distance to shore and generally the depth increasing with distance, hence mooring costs should also have a larger contribution. See Figure 2.14.

The variation in the cost data is presented in Figure 2.15. The average value for each cost is presented as a red point, then using the maximum and minimum from literature, the range was plotted on the graph with the lower and an upper point represented by yellow and blue points respectively. It can be noted that in some of

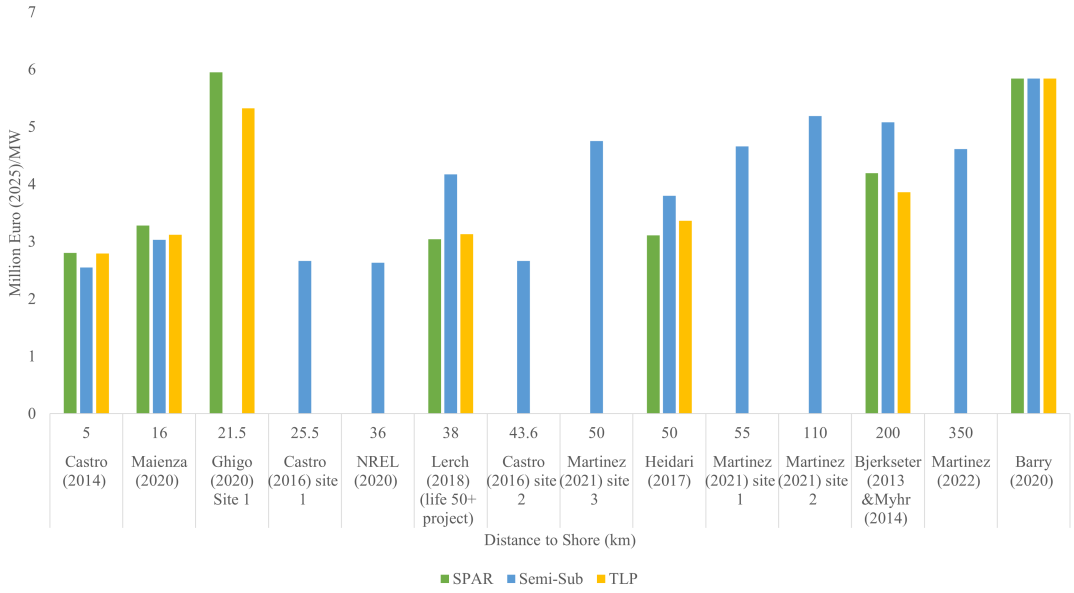

Figure 2.14: Combined manufacturing cost for each typology found within literature represented in Million Euro/MW (smallest numbers on the graph represent the minimum values).

these cases the cost comes close to zero. Clearly, these costs will not be zero in real life. It is purely to highlight the low and high cost assumptions in the data, and therefore the huge variation across the literature. The average from the literature is represented as a red point, and the standard deviation for each cost is provided on the graph. The greatest uncertainty lies in the transmission system cost, which is expected, given that some literature includes HVAC and not HVDC and substation costs within their work. Overall, the platform cost is relatively similar throughout the literature for each platform. The mooring and anchors have the least variation for the Spar, which could be due to the Hywind site being already installed and operational for the past eight years.

Installation Costs

Overall, looking at Figure 2.16, a clear decreasing trend is noted with increasing farm size and distance to shore. A few of the papers within the literature do not fit this trend, however, potential reasons for this are explained below.

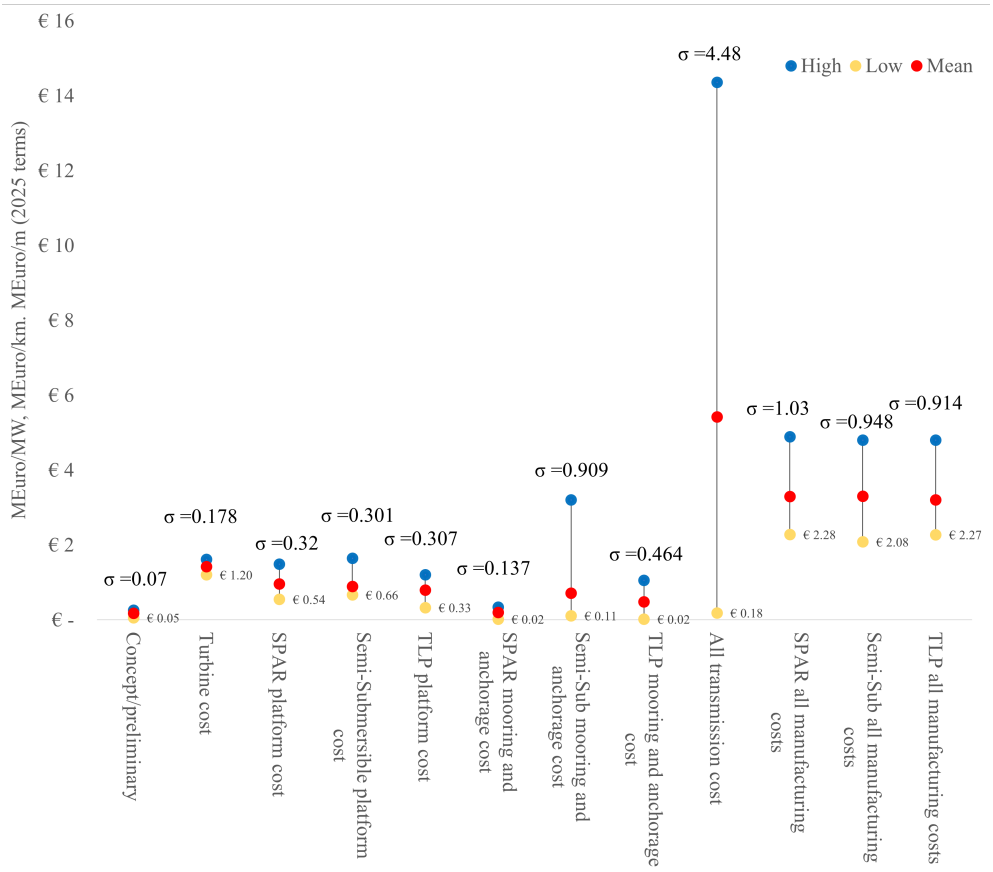

Figure 2.15: Variation in manufacturing costs found within literature represented in MEuro(2025)/MW

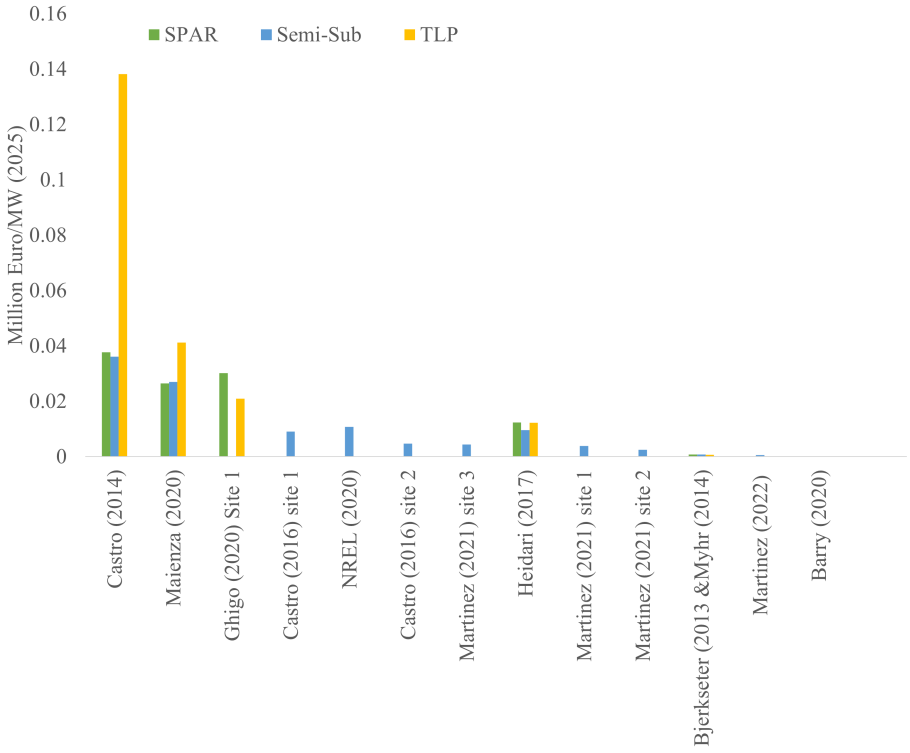

Figure 2.16: The installation costs found within literature represented in MEuro(2025)/MW/km.

Castro et al. (39; 40) and Maienza et al. (41) follow a very similar trend given the sites selected for each paper. Both papers have a very detailed process, making them among the more accurate papers within the literature.

Stehly et al. (42) and Ghigo et al. (4) use a GBP/MW value, and Heidari et al. (29) use a formula related to the distance to shore, which has been fitted to the data from other literature. Both (42) and (29) have slightly higher values than expected. Both methods may provide inaccurate results since they do not include vessel cost, speed, fuel cost, fuel consumption or installation methodology.

Martinez et al. (43; 44) utilise a set value for the installation cost of the platform, a Euro/km value for anchor and moorings, Euro/km for the transmission system, and finally a formula including time to carry out the work and vessel details. This is a simplistic method to find the installation cost. The output of these papers seems rather small when compared to other literature, causing the author to question the accuracy of the assumptions made rather than calculating vessel cost and considering installation time. Similarly, Lerch et al. (46) and Bjerkseter et al. (45) present a small estimate for installation cost.

Figure 2.16 shows there is no consensus on which platform has the cheapest or the most expensive installation cost. (40; 41) state that TLPs will be the most expensive platform, and this seems to be in line with the fact that the TLP will require specialised vessels for the more complex mooring system. Conversely, Ghigo et al. (4) expected the Spar to be more expensive than the TLP, and this could be due to the higher difficulty related to handling the Spar. Heidari et al. (29) found the Spar to be the most expensive and the Semi-submersible to be the cheapest, in terms of installation costs: this is potentially due to the difficulty of handling related to the Spar and the ease of handling of the Semi-submersible.

Myhr et al. (9) and Bjerkseter et al. (45) both assume that the cost would be the same for all platform types. Given the difference in the geometry, this seems a substantial approximation, since each platform will require different installation techniques, of which some are unproven for flaoting wind.

Figure 2.17 shows the average installation cost for each platform found in the liter-

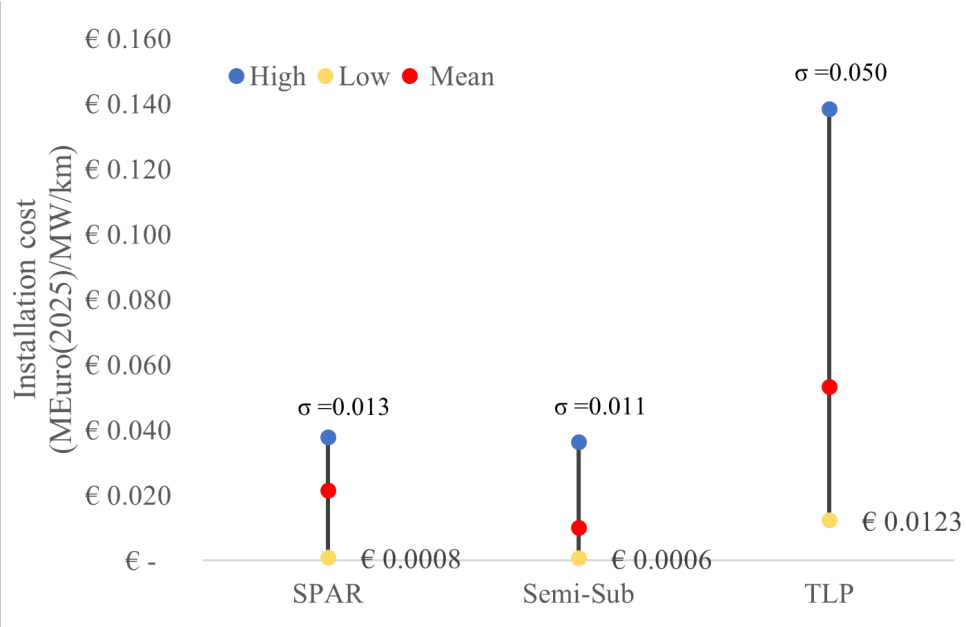

Figure 2.17: The installation costs variation found within literature represented in MEuro (2025)/MW/km (value on the graphs for each platform is the minimum found in literature).

ature. Overall, the TLP is the most expensive, which is expected because of its more complex mooring system, which will take longer to install and require specialised vessels. It also has the largest range, which is potentially due to there being only one TLP installed as of yet. This leads to greater uncertainty in the installation process. Semi-submersibles are the cheapest, they have easier to handle geometries and simple mooring arrangements. This platform is currently being used at the Kincardine site, combining this with the large amount of literature around Semi-submersibles, this is expected to be the reason for the relatively small variation in cost.

2.4.2 Operation and Maintenance Expenditure

Operation and Maintenance is a highly complex cost to determine. A general decreasing trend has been identified as the wind farm capacity and distance to shore increase, highlighting the benefit of cost savings for a larger farm, see Figure 2.18. One argument against this general trend is that the further offshore the farm, the more difficult it is to get a weather window and the greater amount of time to get to the farm, resulting

in higher vessel and personnel costs. There is, however, a slight variation in the mid-section, which does not support the statement of a decreasing trend, which needs further explanation. Castro (2014) and (2016) et al. (39; 40) have the same methodology which shows the decreasing trend in cost for the increased wind farm capacity and distance to shore. This model includes vessel hire and failure rates but it neglects the consideration of weather windows which would have a dramatic effect on downtime and revenue. This seems to be a very common assumption in all papers (40; 41; 101). Maienza et al. (41) also have a relatively similar method, but the cost is substantially smaller for a wind farm which is not much larger. A reason for this could be assumptions of component failure rates, which is difficult to determine as the inputs are not given to compare. Lerch et al. (46) generally follow the trend of the data. This is expected to be because it follows a similar methodology to (39; 40; 41), however, they do not consider sea bed rental, insurance or transmission costs, which could be the reason for (46) being lower than anticipated. Heidari et al. (29) do not consider weather windows, component failure rates, or vessel hire. It is based on a function of distance, which has been fitted to the data found in the literature. This model presents one of the lowest predicted values, which is potentially due to the fact that it does not use failure rates, vessel hire, labour, etc. (9; 45) provide a relatively small value for O&M, this model uses the OMCE-calculator. This calculator uses data, which would be accurate for fixed platforms, but the accuracy of this for floating platforms is uncertain. Since there are only two operational sites, there is no real data available for floating O&M as of yet.

Ghigo et al. (4) predict a very small O&M cost compared to other literature with similar wind farm sizes. The assumption in this work is based on a Euro/MW value. Stehly et al. (42), similarly to the work carried out in (4), use a Euro/MW value for O&M. This is a relatively simple method to estimate O&M costs. Since O&M is heavily dependent on vessel costs, hire times, time to carry out work, weather windows, vessel availability, and component failure rates, assuming a cost/MW value is an oversimplification of the problem. This oversimplification is expected to be why values found in (4; 42) are so different from other wind farms with similar power capacities. Finally, the sites within Martinez et al. (43; 44) do not follow the trend and create

the 'bump' seen in Figure 2.18. This model has a fixed yearly rate and a variable Euro/MW/km/year value to account for travel expenses. It should be noted that the calculation does not consider failure rates, among other things. Based on the other data, this seems to be an overestimate.

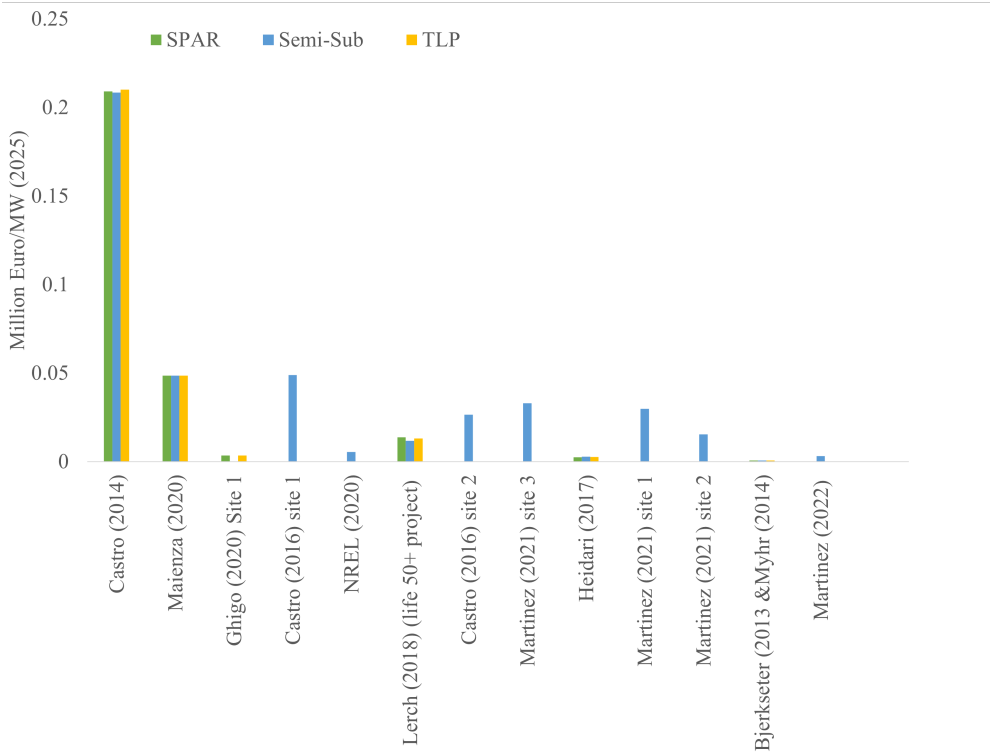

Figure 2.18: The O&M costs found within literature represented in Million Euro(2025)/MW/km.

A number of papers include more than one platform. It is unclear from this analysis which platform would have the most expensive and cheapest O&M. Castro (2014) et al. (40) highlight that the O&M for a TLP is the most expensive and the Semi-submersible is the cheapest. This seems fair given TLPs have the most complex mooring system which is under high loading, exposing it to a higher likelihood of failure. Heidari et al. (29) claim that the Semi-submersible is the most expensive and the Spar is the cheapest, potentially due to its simplicity. Lerch et al. (46) state that the Spar is the most expensive and the Semi-submersible is the cheapest, which, in general, compared to the other papers, goes against the general trend seen in Figure 2.19. On the other

hand (9; 41; 45) detailed that the O&M cost, regardless of platform type, would be the same. Similarly, Ghigo et al. (4) assumed the TLP and Spar would also have the same O&M cost. It is clear from other literature and authors' knowledge that this cost should be different for each platform (29; 40; 46).

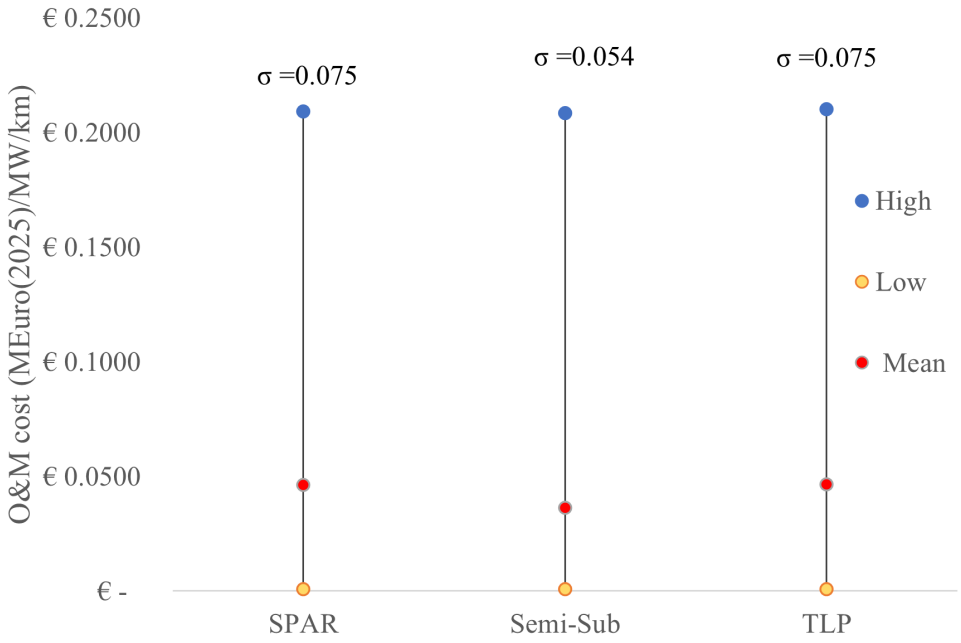

Figure 2.19: The O&M costs variation found within literature represented in Million Euro(2025)/MW/km.

The variation in data found in the literature is expressed in Figure 2.19. This Figure highlights that, on average, the Semi-submersible has the cheapest O&M, and Spar and TLP are the same. The variation is expected to be larger as explained, no two models are the same, and the level of detail varies heavily, causing the O&M cost outputs to vary heavily from paper to paper. Since the Semi-submersible has been more heavily researched, there is potentially more consensus on how to accurately model the Semi-submersible O&M cost, causing the variation to be slightly less than the other two platform types.

2.4.3 Decommissioning Expenditure

The cost of decommissioning more regularly than not is dismissed and not considered. Only 30% of the papers found in the literature included a decommissioning cost model. A general trend found is that increasing the distance to shore and increasing the wind farm capacity causes a decline in decommissioning cost to negative values, see Figure 2.20. A reason for this negative value seen in the literature is the revenue created from scrap materials. As wind farms expand in capacity, the mass of re-saleable material also increases. This is estimated to be more than the cost of hiring vessels and removing the farm.

This highlights that the assumptions made, such as neglecting decommissioning or assuming it as a fixed percentage of CapEx, may be inaccurate, as the cost values associated with decommissioning are significant and sometimes negative.

Another reason for the decreasing trend in cost could be the cost-benefit of installing larger capacities, driving down the MEuro/MW/km. As previously analysed in the literature section, Castro (2014) et al. (40) have a cost model which is the same as their work presented in 2016 (39). The work in 2014 and 2016 for the two sites is included in Figure 2.20. Considering their work utilises the same model, this trend of increased power and the general relationship of increased distance to shore with power. This solidifies the findings of decreasing DecEx cost with wind farm size.

Adedipe et al. (110) presents one of the best models of decommissioning, however, the case study used is for a fixed platform. The author expects that this cost could be less for a floating platform, as removal of the platform itself would be much easier. The mooring system and power export cable are disconnected, and then the platform is towed back to shore. Whereas fixed platforms, such as monopiles or jackets have to be cut, which requires vessels with such capabilities and more time to carry out the task.

Maienza et al. (41) considers the DecEx as a percentage of the installation cost, which, given that there is potential for revenue made from the re-saleable materials, may be considered inaccurate. (4) utilises a set 2% value of the CapEx to determine DecEx, explaining the substantial cost. The decommissioning cost in Lerch et al. (46)

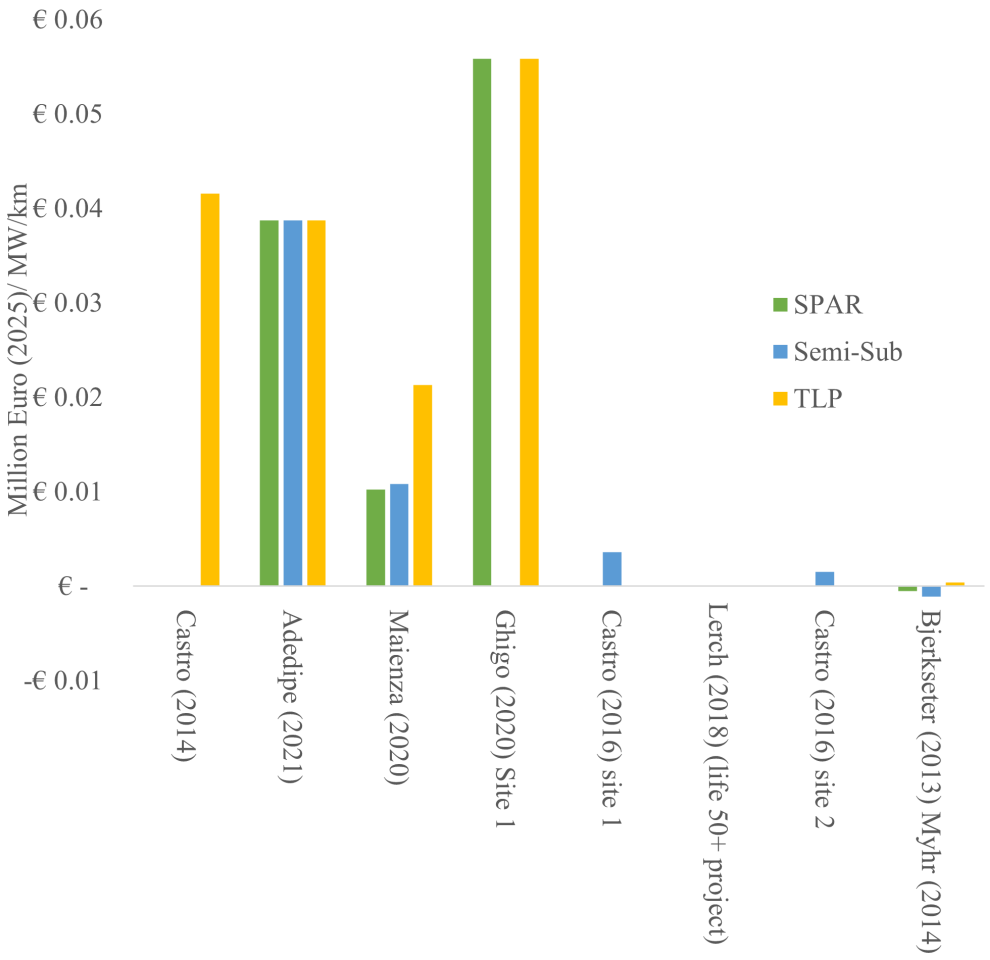

Figure 2.20: The decommissioning costs found within literature represented in Million Euro(2025)/MW/km.

is so small that it was considered negligible, hence it is not shown in the Figure 2.21 or 2.20.

(9; 40; 41; 45) consider that each platform would have a different decommissioning cost, which is expected as each platform has a different geometry and hence there is potential for different vessel sizes required. The difference in the mooring system will also have an impact, as shown in Figure 2.20: TLPs are expected to be the most expensive, which is logical considering their more complex mooring system. The Semi-submersible is expected to be the cheapest in the work presented by Myhr et al. (9) and Bjerkseter et al. (45). The expected reason for this is in comparison to a Spar, the Semi-submersible is easier to handle. However, it could be argued that the Spar has a larger mass and hence greater revenue from recycled materials, explaining the work within (41). More research on this area is crucial to understand this.

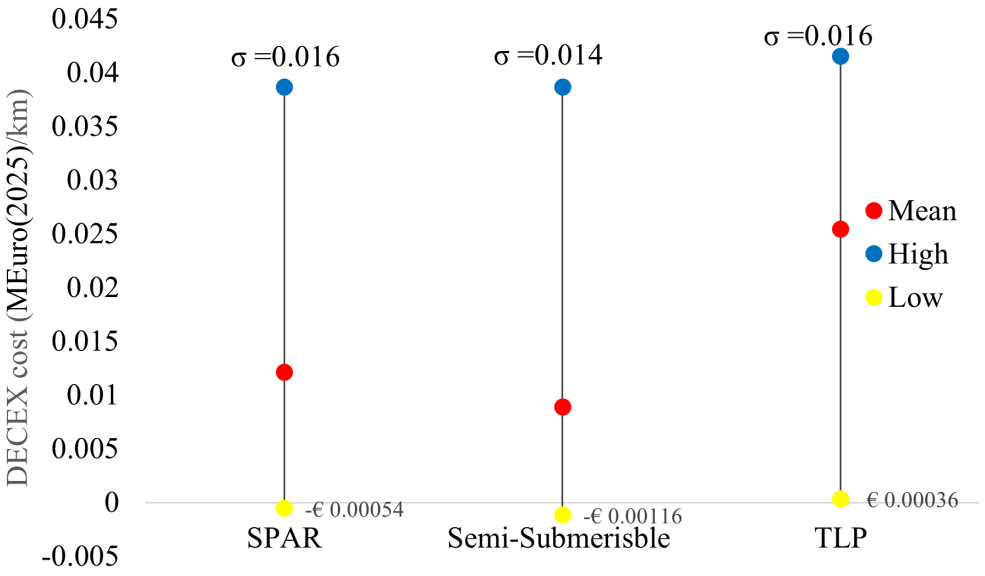

Figure 2.21: The decommissioning costs variation found within literature represented in MEuro(2025)/MW/km (Additional values for each platform highlight the minimum cost found in the literature).

One of the main issues with predicting decommissioning cost is the lack of available data, and this data is expected to be available around 2040 when the first sites which have been installed come to the end of their design life. The advantage of this is that it would allow the models to be benchmarked with real-life data. This is likely to be the

reason for the huge variation in cost estimations presented within the literature. This can be seen in Figure 2.21.

2.4.4 Levelised Cost of Energy

The LCoE is one of the main outputs from most papers in this research area. In the present work it was highlighted that this substantially varies throughout the literature, as shown in Figure 2.22, mainly due to the different assumptions and models adopted.

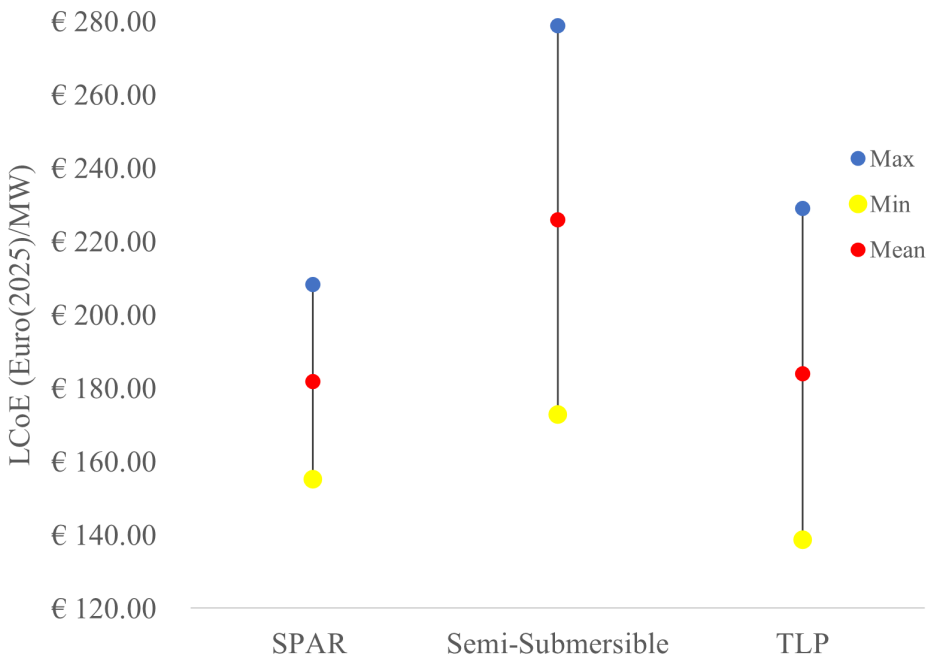

Figure 2.22: The variation in the LCoE for each platform in the literature.

There is currently only one TLP being used in operational offshore sites, off the coast of France. This is expected to be a main contributor to the large variation in costs related to TLPs. Since there is one operational site, current cost models cannot be benchmarked against them to improve the accuracy in predicting cost

Both the Spar and the Semi-submersible have been utilised for longer periods at different sites hence these are expected to have smaller variations. This is true for the

Spar, Figure 2.22 detailing this. The Semi-submersible has a slightly larger variation than the TLP. This is expected to be due to the fact that Semi-submersibles have been covered the most in the literature, with a huge variation in assumptions for cost throughout, as presented in prior sections of this work. As highlighted previously, a varying degree of detail is presented across all literature, causing the LCoE to be very different depending on which paper is considered. Another factor which leads to variation in LCoE is the fact that no two papers considered in this review have the exact same site, hence there will be differences in the resource and hence AEP, distance to shore, water depth and wind farm capacity.

2.5 Cost Modelling Research Gaps

This review has highlighted some clear areas of improvement in each section of the cost model. The shortfalls are summarised below, followed by a more detailed explanation.

- Survey cost estimations are limited to £/MW value;
- Limited turbine size considerations;
- Simplified manufacturing cost estimates, considering only £/kg or £/MW for substructures;
- Lack of HVDC consideration;
- Assuming fabrication yard and assembly port are at the same location, neglecting transportation cost;
- The charter type is not considered;
- O&M cost models are vague, with little weather considerations;
- Decommissioning is often over simplified or neglected;
- Few models consider AEP.
- Lack of real world data to assess uncertainty.

The most common estimation of preliminary works is based on a GBP/MW value, which seems sufficient given that the majority of the literature uses a very similar value. However, there are some elements within the preliminary cost, such as surveys, which could be better expressed in a GBP/km or GBP/km^2 value to better capture the distance to the site and the area surveyed in the cost. Another way in which this could be further improved is to consider the cost of vessel hire, fuel cost, distance to shore and the vessel specifications along with the required crew and surveyors, giving a more accurate cost representation.

Manufacturing cost is a large area, some costs are relatively well defined such as the wind turbine. It can be seen from the literature that the majority of the turbines used are 5 MW. However, since turbine growth has been rapidly increasing over the past years, a 5 MW turbine assumption is relatively outdated. This is particularly with Dongfang Electric Corporation (DEC) unveiling their 26 MW turbine this year (119). By creating a cost model which can include larger wind turbines, the cost information could be combined with the AEP model, and it will help to determine if economies of scale are present or if there is a maximum size of turbine where it no longer becomes economically feasible, creating investor confidence for port upgrades and vessel investment. To best determine the cost of the platform moving away from assumptions related to mass only, will improve the accuracy. Considering the mass, welding, painting and forming of the structures along with structural members would be a much more accurate way to determine the cost of each platform typology and allow optimisation of the geometry to reduce the cost. For the transmission system, the inclusion of an HVDC transmission system in the work presented in (65) in all cost models will be essential for floating offshore wind since the distance to shore can increase rapidly, making conventional HVAC no longer feasible. In general, the mooring and anchors model could be improved by considering the appropriate mooring and anchor sizing based on the site characteristics.

In general, there is very little inclusion in the literature on transporting the platform and other sub-systems to the port where they are stored and eventually taken from the port to the site. It has been seen with other projects, such as Seagreen, that

the platforms were built in a Chinese shipyard and then transported to Scotland to be installed (120). This suggests there was a cost-benefit in building the platforms in China perhaps this was due to the lower price of steel or workforce, however, the transportation cost would have been significant and the risk of potential delay is high, including such information in the cost model is important. Another issue linked to this is the lack of capability of current ports in the UK to build these large structures. This issue is, however, expected to be removed as the IGP aims to have local manufacturing capabilities, and the Floating Offshore Wind Manufacturing Investment Scheme (FLOWMIS) announced up to £160 million in grant funding, from which 2 ports were successful.

To refine the installation, O&M and decommissioning model considering the charter type is key. Having discussed with industry experts from Farra Marine in 2020 it is clear that in general, the charter type is a time charter, which does not include fuel costs. All vessel costs could then be more accurately presented. An accurate database representing how long it takes to install each sub-system would be useful, currently, it is vague and sometimes hard to determine how long the installation of each system would take.

In order to make a comprehensive O&M cost model combining the indirect costs such as sea bed rent, insurance, port storage and planning with the corrective and preventative maintenance considerations with failure rates for each individual platform type and sub-systems of the wind farm considered would create this improved model. A factor which is often neglected but should be included is available weather windows and potential downtime and loss of revenue due to lack of accessibility. This is a complex problem but one which should be addressed in order to better determine the overall O&M cost and LCoE.

Decommissioning cost is very often neglected, and the accuracy of the current models is difficult to determine since the first floating offshore wind farms have only been in operation for a maximum of a eight years, however, more work could be done to improve the accuracy.

The inclusion of an AEP model is essential to determine the performance and cost-

effectiveness of a wind turbine, with only very few models actually considering this. A future step could be to consider the platforms motions and wind turbine controller within the AEP model allowing a more accurate representation of LCoE to be calculated. Another factor which is linked to energy production is the losses experienced by the turbine, there are a few papers which include all of the losses, however, this is something that could potentially be more accurately expressed since there is quite a large variation in the literature in percentage for each loss.

Finally, the lack of real-world data makes it challenging to fully address the uncertainty in the assumptions and costs presented. This could be improved through engagement with industry to obtain input; however, this is often difficult and involves sensitive information that cannot be publicly disclosed.

Overall, work done to create a complete model which considers all elements of the wind farm in detail would be very beneficial and allow the user to determine the potential wind farms cost. However, based on this research a modified LCoE could also be useful to best determine which platform is cheapest, this could be expressed as an equivalent LCoE. By removing costs which are not affected by the platform type, such as preliminary, electrical transmission system and the wind turbine. This could allow the user to determine which platform is the cheapest based only on costs which can carry depending on the platform choice such as manufacturing of the platform and mooring system, installation, operations and maintenance, and decommissioning. When determining the cheapest platform the cost of full-life operation is important, particularly considering the variation in monetary cost over the years of operation, which could be an improvement to some of the existing models. By considering the cost over the life of the project, better-informed decisions can be made on whether to have a higher capital, but a lower OpEx or vice-versa throughout the life of the project. This would be an interesting comparison to see the three main platform types on where the trade-off point is between the CapEx and OpEx. By doing so this might highlight a different ranking in terms of cost for the platforms, which is important given the requirement to reduce cost and make floating offshore wind competitive with other renewable energy sources.

2.6 Conclusion

The aim of this chapter was to determine the variation in the cost models found within the existing literature allowing the author to identify potential areas and assumptions which have led to these uncertainties. In order to compare the literature, data from each paper was collected and made adimensional. The mean value and standard deviation across the literature were found which could be easily compared.

From this work, it is clear that there is space to improve current cost models. The data review shows the differences in cost estimates in the literature due to the variation of assumptions and exclusions in each model. A number of things highlighted which could potentially improve the accuracy of the cost model are: including the charter type, fuel costs, weather windows, losses due to downtime, improved AEP models and the manufacturing costs for the platform removing the bias to higher mass platforms being more expensive.

In general, combining some of the current models to create a complete comprehensive model would be useful. The benefit of more accurate cost models is the potential to discover areas which could have potential cost savings, helping to drive down the cost. An example could be alternative geometries to reduce material and hence cost. However, when it comes to determining the cheapest platform, perhaps using an equivalent LCoE, which only considers costs which vary with platform type, would be more appropriate and less work.

Overall, this review chapter was successful in identifying a number of areas which could be worked on to improve the accuracy in predicting the cost of floating offshore wind farms.

Chapter 3

Literature Review: Floating Offshore Wind Substructure Optimisation Frameworks

This Chapter focuses on the review of current literature surrounding the optimisation of the floating sub-structure for offshore wind. The following chapter is based on the published work in the Journal of Ocean Engineering, 'A review and analysis of optimisation techniques applied to floating offshore wind platforms' (121).

3.1 Introduction

In an attempt to address climate targets, the development of floating wind is imperative to produce clean energy, however, new technologies come with inherent risks and generally higher costs (9; 17; 41; 66). This is particularly relevant given that the industry has not yet found an "optimum configuration" suitable for every situation. It is predicted that there will be no such universal solution due to variations in site characteristics and lack of maturity in the floating offshore wind industry, the latter being one of the driving factors of increased cost (67; 68). It is for this reason that cost reduction is of the utmost importance, ensuring green, secure electricity is still affordable to the user (69). The CapEx makes up around 75% (41; 70) of the total

cost, making it a key area for cost reduction. For floating wind, the two largest contributors to the CapEx are the RNA and the floating support structure, each around 35% (41). For this reason, this review chapter focuses on the floating support structure (71). At present, few studies have addressed the concept of an optimal support structure. Instead, the focus has been on determining an optimal rotor nacelle assembly design (72; 73; 74; 75; 76; 77; 78; 79; 80; 81; 82; 83). Optimisation is a technique which has been highly utilised in the automotive and aerospace industry to find an optimal design (84). This process covers a large design space in a much shorter time frame compared to traditional, iterative design methods, making it appealing for a less mature industry (84). Given the similarities to the aerospace industry and the lack of experience, it is expected that optimisation will be a useful tool in determining the best floating offshore support structure for a given application (85). Due to the high complexity and dependency of floating offshore wind systems, it is expected that a multi-objective approach will be necessary. By applying a multi-objective approach and a number of design constraints, the best overall solution can be found by removing unfeasible options, even when there are conflicting objectives such as cost and performance (86; 87). This chapter aims to review the current literature, determining the shortfalls and the potential improvements to such optimisation approaches.

Following this introductory section, Section 3.2 details the approach adopted to find the analysed literature, and in Section 3.3, optimisation-related works will be reviewed, looking at the considered design variables, constraints, objective functions, solvers, and numerical approaches implemented. Section 3.4 will provide a critical discussion with proposed gaps in the current literature, while Section 3.6 will conclude with a summary of the work's findings.

3.2 Literature Review Approach

In order to conduct an extensive, yet relevant, review, a wide range of keywords were used in a range of different search engines; these keywords include optimisation, floating offshore wind, and floating platform. This allowed a large number of papers to be collected. The most appropriate research from these papers was found by applying a

number of criteria. The first criterion was to ensure the paper included the platform in the optimisation process, and this was not only restricted to floating offshore wind research, optimisation for O&G support structures were also considered. The second filter was based on the publication format of the research, i.e. firstly, if it was published in a conference proceeding, and if so, what was the highest h-index of the authors. If the index was above a set value the paper was used in the review. If the research was published in a scientific journal, the impact factor was reviewed, and if it was above the acceptable threshold, it was included. In the event that the journal's impact or h-index was low, the author used their judgment to determine whether the article would be appropriate or not. Finally, if the research was published elsewhere, the relevance and usefulness of the work were assessed by the authors.

The explained methodology can be seen in Figure 3.1.

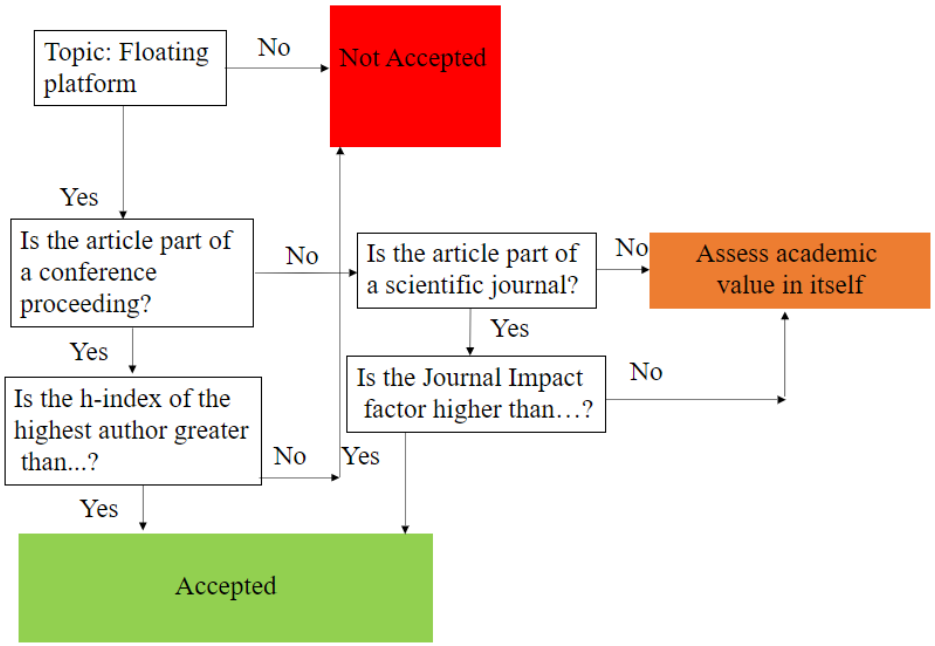

Figure 3.1: Process for finding appropriate literature.

The year of publication of each paper is reported in Figure 3.2, this figure highlights that in recent years the topic has been increasingly growing in popularity.

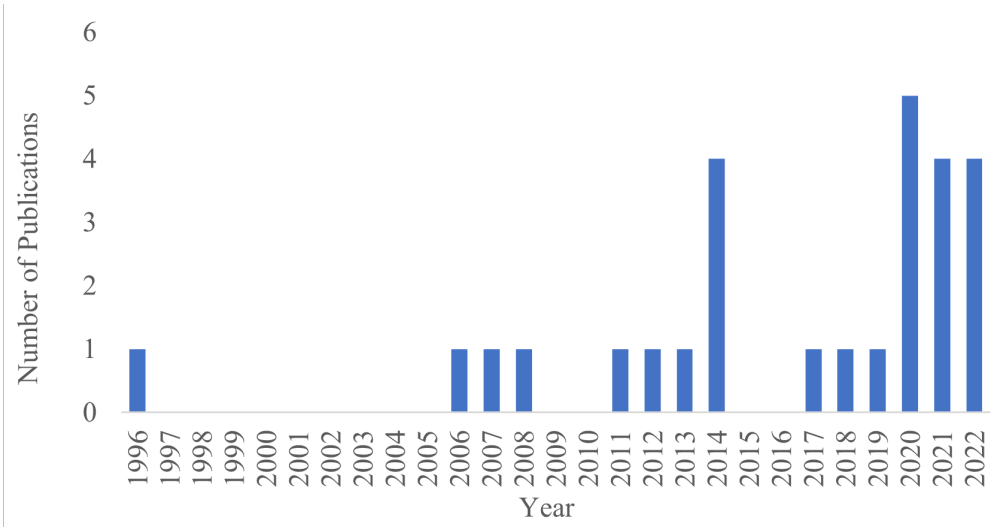

Figure 3.2: Number of publications per year.

3.3 Optimisation Review

The outline of the subsequent Sections is as follows: Section 3.3.1 firstly details the generic multi-objective optimisation problem. The remaining sections detail a review of the overall optimisation, objective functions, constraints, design variables and platform modelling, optimisation algorithms, modelling and additional software required, cost models used, and the overall outcome of each paper.

3.3.1 Optimisation Problem Methodology

The formulation, which details a general objective design optimisation, can be expressed in Eq. 3.1.

$$\min_{\hat{x}\in\mathbb{R}} \quad \boldsymbol{J}(\hat{x}) \tag{3.1}$$

$$\text{subject to} \quad \begin{cases} \hat{x}_{lower} \leq \hat{x} \leq \hat{x}_{upper} \\ h_i(\hat{x}) = 0; \quad i = 1, \cdots, m \\ g_j(\hat{x}) \geq 0; \quad j = 1, \cdots, p \end{cases} .$$

where $\hat{x} = [x_1, x_2, ..., x_k]$ defines the design vector, which contains the design vari-

ables which are varied through the optimisation, and $\boldsymbol{J}(\hat{x}) = [J_1(\hat{x}), J_2(\hat{x}), ..., J_n(\hat{x})]$ is an n-dimensional vector of objective functions. The design vector has upper and lower bounds, $\hat{x}_{lower}$ and $\hat{x}_{upper}$ respectively, which help to not only reduce the design space and computational time but consider more realistic design variables. In this notation, m and p are the numbers of equality and inequality constraints, respectively. In the situation where $\boldsymbol{J}(\hat{x})$ has competing components, there is no unique solution, and therefore the multi-objective solution will be found on the Pareto optimal set (86; 122). The frontier presents a set of optimal solutions, moving along the front to another optimal solution, will improve one objective but worsen another, all points on this frontier can be considered as solutions to the multi-objective optimisation problem (86; 122). This can then introduce preference from the user, selecting the overall best solution for their needs.

3.3.2 Overview

An overview of the relevant literature considered within this work can be found in Table 3.9. This contains a breakdown of the support structure, wind turbine and systems considered. Details of the domain analysis technique, objectives, constraints, design variables and optimisation algorithms are also provided as well as details of the software utilised in each of the works.

Literature Overview

The paper by Clauss et al. (123) was one of the first which explored the optimisation of offshore O&G platform geometries. The main aim of this work was to create an optimisation tool which could handle any platform geometry in order to reduce cost and maintain good seakeeping performance. The methodology was not described in detail in this work, making it difficult to compare some aspects of their model. Birk et al. (7) follow on from (123) however, in this work, experimental validation was carried out to prove that the hydrodynamic analysis carried out in WAMIT was accurate for the non-traditional hull shapes. A major focus in this work was the automated shape generation of the hull, which was modified to include a moonpool. Since the early work

of (7; 123) was for offshore O&G platforms, no considerations for the wind turbine were included in either optimisation. Similarly, mooring lines were also neglected. Unlike (7; 123), Wayman et al. (124) produced the first work to perform an optimisation of the Spar, TLP, and barge platform geometry for a 5 MW wind turbine. This work also considered the optimisation of the mooring lines, however, this was carried out in a separate optimisation. Sclavounos et al. (125) focused on the performance of the turbine, the weight, and the mooring line tension to find the optimal of the three platform stability classes for varying water depth.

Fylling et al. (126) was the first to create an optimisation tool (WINDOPT) for Spar platforms, including the mooring and power cable within the optimisation, determining how these aspects affect the overall shape of the platform when minimising cost and maintaining performance. Nordstrom et al. (127) in 2013 created a similar tool but for the PelaStar TLP. This tool returns a set of optimal particulars and scantlings that represent the platform with the lowest cost of energy. The platform is then verified against standards. Similarly, Myhr et al. (8) focus on optimising the layout of the Tension Leg Buoy (TLB) and its mooring lines to reduce costs while considering the loads acting on the structure, which can cause excessive loading on the anchors. (8) approached the TLB in a different manner, considering a space frame to try and reduce loads, rather than other works which consider a tubular floater. Like (124), (8) perform optimisations of the platform and mooring lines separately in the time domain and the frequency domain, respectively. Similar to (8; 126), Ferri (2021) et al. (128) focus on only the Semi-submersible platform, while the work carried out in 2022 by Ferri et al. (129) improve on their previous work by including a detailed cost model and an AEP model. Ghigo et al. (4) presents six concepts. However, the optimisation result is only provided for the Spar and Hexafloat platforms. Similarly (129), (4) also have a detailed cost and AEP model presenting an end output value for the LCoE for each platform. Sandner et al. (130) and, more recently, Hegseth et al. (131) also integrate multiple systems, with a strong focus on optimising the control system for three different Spar platforms. Sander et al. (130) carry out the optimisation of three different Spar geometries finding the most optimal controller gains to maximise power

and reduce tower bending moment and inherently the nacelle acceleration, like a large percentage of other works seen in Section 3.3.3.

Hall (2013) et al. (132) is one of the leading authors in this field, having published multiple articles. The work carried out in 2013 details an optimisation framework that includes the three main platform typologies, which can consider a wide range of existing and feasible non-existent platforms. Karimi et al. (122) follows a very similar process to (132) considering the three main platform stability classes, Spar, TLP, and Semi-submersible for a 5 MW wind turbine. This work resembles that of Hall et al. (132) focuses on the trade-off between cost and performance. Hall (2014) et al. (133) took a different approach to all other papers considering the hydrodynamic properties to express the support structure rather than making prior assumptions about the geometry with traditional geometrical design variables. This method removes the geometrical constraints and widens the design space. This work uses six generic support structure designs, which allows the hydrodynamic coefficient calculated to be compared to each support structure to determine their similarity.

Gilloteaux et al. (134) do not carry out an optimisation as such, but it is the beginning of an optimisation process, a cylindrical body is modelled, and the hydrodynamics are assessed. From this assessment, four changes are made to the platform by adding one heave plate, two heave plates with different aspect ratio, and finally, three heave plates and active ballast. In essence, this is an optimisation that is not automated and over a smaller design space. Lemmer et al. (135) also do not carry out an optimisation, it does however explore three Semi-submersible designs with varying drafts to find the best solution.

Initial work carried out by Leimeister et al. (136) uses an optimisation approach to determine a Spar geometry for a 7.5 MW turbine based on the 5 MW turbine rather than using traditional up scaling methods, ensuring the platform is still stable. (137; 138) focus on implementing the optimisation of Spar platforms into the Modelica library for Wind Turbines (MoWiT) model for a wide range of design load cases, (138) including considerations for the blade shape to optimise power generation without increasing thrust and load on the structure.

In 2020, Hegseth et al. (131) was one of the very few groups of researchers to consider not only the platform, but the combined platform, tower, mooring, and control system in the optimisation process. This allows the coupling effects between the tower and the platform to be considered. Dou et al. (139) and Lemmer et al. (135) also consider the control system, the work by (139) add an extension to the optimal control parameters of the work by (131). The work by Hegseth et al. (131) and Dou et al. (139) draw focus on optimising the Spar platform whereas Lemmer et al. (135) focus on a Semi-submersible with heave plates.

In later work by (140) the tower and Spar were optimised to host a 10 MW wind turbine considering environmental effects, as well as the trade-off between CapEx and OpEx based on fracture mechanics and updating reliability through inspection. Similarly, Leimeister et al. (141) use a reliability approach for platform optimisation; by doing so, this addresses the issues of lack of standardisation, design standards, and over-engineered platform shapes. Bracco et al. (15) also addresses design standards but instead focuses on optimising four main platform prototypes, considering the hydrostatics of each meet DNV design standards.

Benifla et al. (6) present a different platform typology, called Universal Buoyancy Body (UBB). Rather than using traditional stiffening methods, this platform has an inner and outer 'pipe' to strengthen the structure. Figure 3.3 shows the structures' geometry. It is predicted that this design will help reduce costs, by avoiding longer manufacturing times and complexities related to stiffeners. It is also expected that it could work in place of any cylindrical body in any of the three main platform typologies.

Figure 3.4 highlights the platforms that have been worked on the most and how many papers include the three stability classes in their work. The majority of the research carried out has only considered a Spar substructure. The reason for this is expected to be due to their simplicity for modelling purposes and the utilisation of a Spar support structure at the Hywind site for a number of years. However, a large number of papers also considered all three platforms in their optimisation.

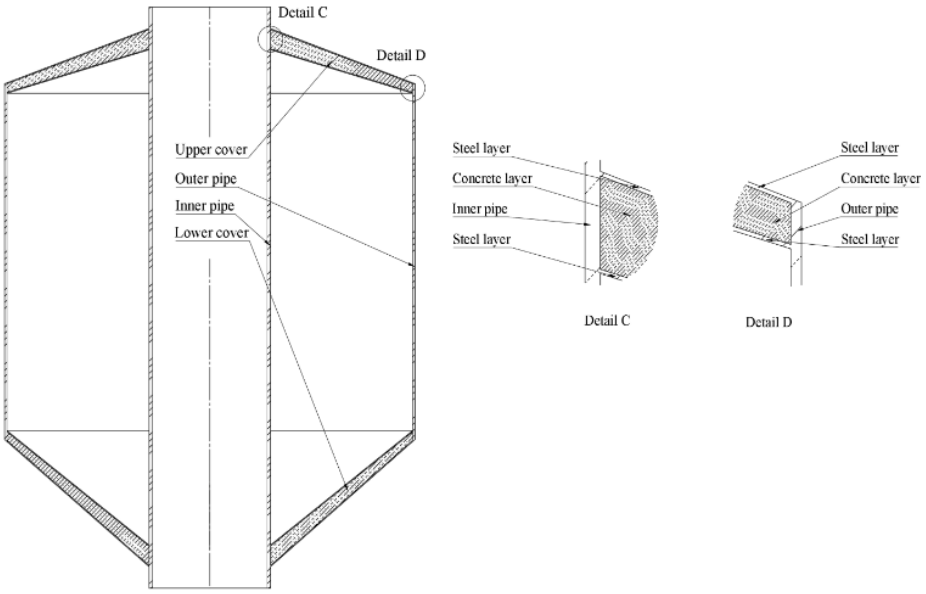

Figure 3.3: Universal Buoyancy Body from (6).

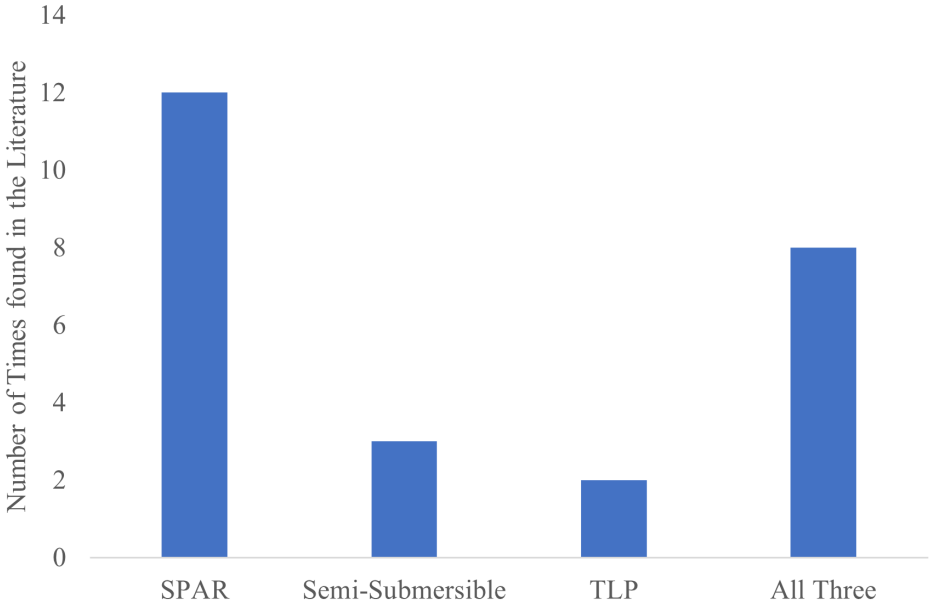

Figure 3.4: Platforms optimised within literature.

Turbine Size

An improvement in (131) compared to other work was the use of the 10 MW DTU wind turbine, compared to other work that only used the 5 MW NREL turbine (15; 122; 125; 126; 132; 133; 137; 138; 141). Some of these papers, particularly (15; 137; 138; 141) were published in the last two years and still only use the smaller 5 MW wind turbine, making it difficult to compare with current industry turbines, and even more difficult for future floating wind farms with an expected turbine capacity of upwards of 15 MW (1). Similarly to (131; 139), Ghigo et al. (4) carry out an optimisation for the 10 MW as well the 5 MW and wind turbines for six floating platform concepts allowing for a comparison between technologies. Dou et al. (139), Lemmer et al. (135) and Ferri et al. (128) also recognised the need to use a larger turbine by optimising the Spar platform and the Semi-submersible platform, respectively, for the 10 MW DTU turbine, while both consider the mooring system. Pollini et al. (142) are the only researchers who use the 15 MW wind turbine in their optimisation with a focus on the optimisation of the mooring system and the support structure of a Spar in a very fast process that takes only a few minutes. This is a key tool for quickly analysing and comparing future sites given the drive in the industry to draw out the maximum power, using bigger turbines (1). Pollini et al. (142) are the most relevant in terms of turbine size since the industry is expanding so rapidly. Figure 3.5 shows visually how little work has been done on any turbine greater than 5 MW.

3.3.3 Objective Function

An overall summary of the type of objectives used in the literature can be seen in Figure 3.6.

Figure 3.6 highlights that overall cost is the most predominant objective followed by the response. Cost is expected to be the main objective in the majority of engineering work and floating offshore wind is no different. The ability to find the cheapest yet feasible design option is crucial to help drive down the cost and, maintain high energy yield allowing FOWTs to be more competitive with other energy sources. In a lot of cases, there are conflicting objectives within the literature such as cost and performance,

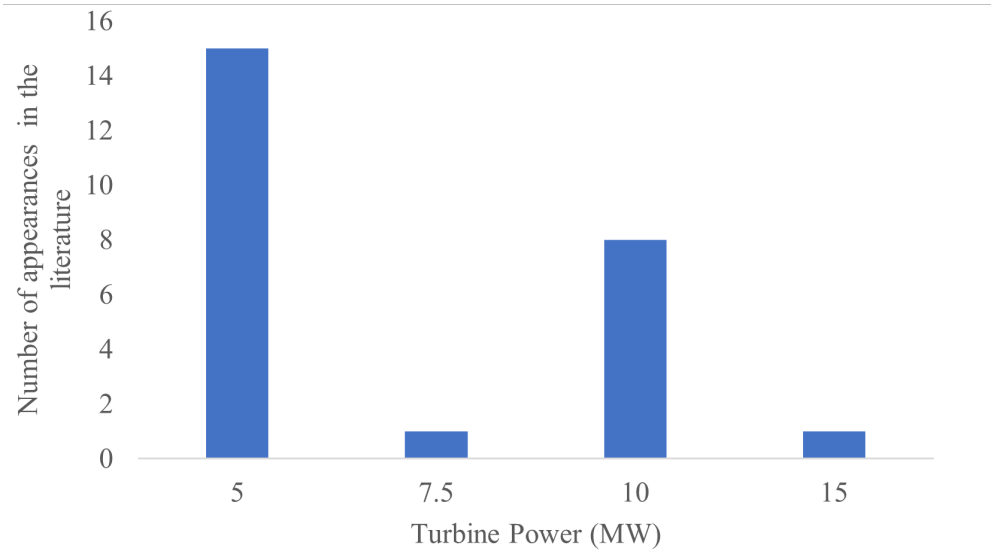

Figure 3.5: Wind turbine power capacity used in the existing literature.

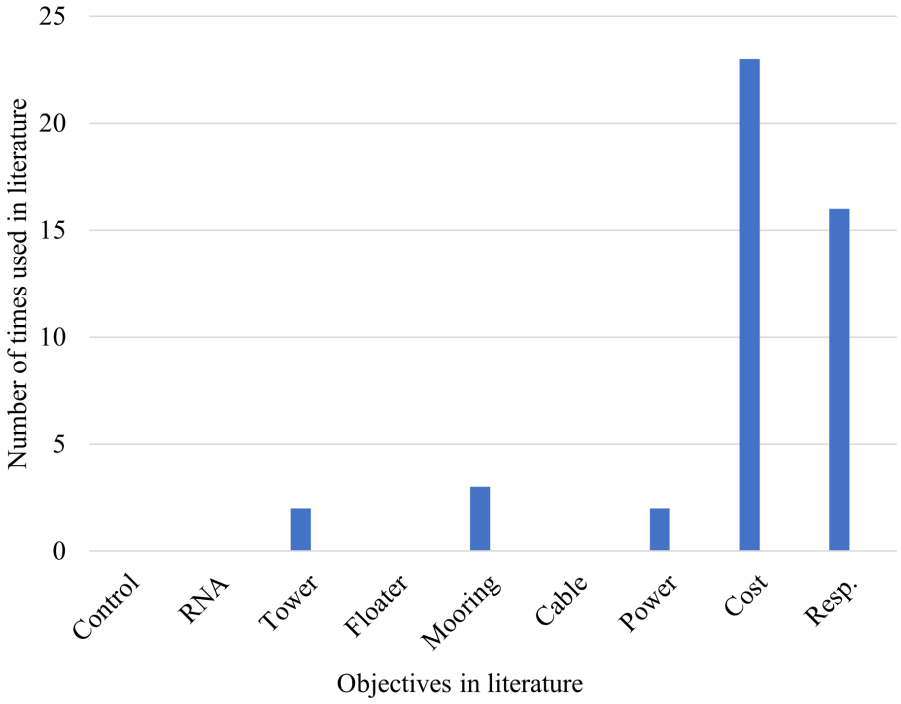

Figure 3.6: Type of objectives used in the literature.

whereby improving one you negatively impact the other. The cost as objective is used in work by (4; 7; 8; 106; 122; 124; 125; 126; 129; 131; 132; 133; 135; 137; 138; 139; 140; 141; 142; 143; 144; 145). The platform response was used as the objective in (4; 7; 122; 123; 124; 125; 128; 129; 130; 132; 133; 134; 136; 137; 138; 138; 144). The power production (130; 131), mooring (8; 125; 146) and tower systems (106; 143) were considered less frequently in the objective function.

Cost Objective

Fylling et al. (126) has one of the most adopted objectives, aiming to minimise the cost of the platform, the mooring lines, and the power cable. Similarly, in (122) the objective is to minimise the cost of the platform and the mooring system. The main objective in (8) is to try and reduce the loading on the structure, which in turn will help reduce structural and station keeping system maintenance costs.

Bracco et al. (15) and Ghigo et al. (4) focus purely on minimising the material cost of the different platforms. Dou et al. (139), (6) and (142) use platform mass and mooring line minimisation as the objective. Hegseth et al. (140) share the same objective as the above articles to minimise cost, in their case for the platform and tower. Wayman et al. (124) set the objective to minimise the surface area of the cylinder, by doing so the volume and therefore the mass of steel required will be reduced, leading to a reduction in material cost. Scalavonous et al. (125) consider the weight of the platform and the dynamic tension of the mooring line to find the optimal platform. This paper highlights that a reduction in weight will lead to a reduction in platform cost. This is consistent within all of the literature considered. Like in many other papers presented, Hegseth et al. (131) consider the reduction in cost as a sub-objective along with the power quality of the turbine expressed as the rotor speed standard deviation. Both parameters are combined into one main objective function. Each sub-objective is given a weighting, which combined will equal one. The weighting of each is varied to determine the importance of each sub-objective. Hall et al. (132) and (122), share the same multi-objectives: to minimise cost and nacelle acceleration, similarly to (131) weightings are added to each sub-objective.

Motion Objective

The nacelle acceleration is the other competing objective in (122; 132) with the goal to minimise this parameter due to the platform's pitch and surge motions. The purpose of this is to avoid excessive loads or higher fatigue damages on the blades and the drive train, leading to a decreased system life span.

Both (122; 132) Scalavonous et al. (125) and Hall (2014) et al. (133) only consider the nacelle acceleration in the objective function. It is assumed that Hall (2014) et al. (133) focus on this single objective function due to the use of hydrodynamic properties to determine the geometry. The rationale given is that it would be difficult to set cost as the objective when geometric values such as length, thickness, and diameter are not available in the optimisation process.

Leimeister et al. (136; 141) have as objectives to minimise the horizontal displacements (i.e., surge, sway, and yaw) of the system, due to restrictions on the power cable motion. The overall goal of the work carried out by Leimeister (2021) et al. (141) is to find the most reliable structure design. This has been done by considering the limit state of the bending stress at the tower base and the tensional stress of each mooring line, which are linked to the platform dynamic response to the metocean conditions, and hence also linked in turn to the platform geometry. Leimeister et al. (137; 138) objectives were to minimise the angle of inclination, reduce nacelle acceleration, and minimise translational motion, with the overall objective of reducing mass and cost. The reason for these objectives was based on the fact that the OC3 Spar considered in their work has very high safety factors.

Work by Clauss et al. (123) for O&G platforms aimed to minimise the double amplitude of various forces and motions to stop disruption of platform operations. Similarly, Birk et al. (7) had the objective to reduce the double amplitude of the heave motion along with the heave resonance. This can be done by increasing the draft of the platform and reducing the waterplane area, the motions will also be decreased. However, this is expected to also have a knock-on effect increasing the cost of construction and installation, along with difficulty in handling this geometry which is not considered in the optimisation process. Both pieces of work by (7; 123) are not for floating off-

shore wind however are still important and valuable when determining which platform is most suitable to meet a specific objective. Ferri et al. (128) had the objective to minimise the amplitudes of the surge, heave, and pitch Response Amplitude Operator (RAO) at their respective eigen frequencies. More recent work by Ferri et al. (129) had slightly different objectives, aiming to reduce the fatigue damage in certain load cases, maximum stress on the tower, and overall cost. These objectives are hoped to extend the service life and reduce the LCoE.

As mentioned earlier, (134; 135) do not carry out optimisations however, similar to most other work, the objective within (134) is to maintain stability. Whereas the objective in (135) is to maximise power, by tuning the controller gains and minimise nacelle acceleration and cost.

3.3.4 Constraints

In order to ensure the optimisation results are within the realms of reality, it is important that constraints are added to the process. The most common constraints added within the literature impose limits on parameters linked to the: nacelle acceleration, platform motion, design variables, stability, mooring and structural design. All of which are discussed in this section.

Cost Constraints

Cost is one of the main drivers within all industries, and it has been made clear that floating offshore wind is no exception; for this reason, Hall et al. (132) adopted a cap of $9 million (2013 USD) on the support structure. This constraint was only seen three times in the literature, and the purpose of the constraint is unknown. It is speculated by the author that its purpose is to remove economically unfeasible design solutions. Karimi et al. (122) has the same constraint on cost but includes additional constraints on performance, and design variables, these can be seen below in Table 3.9. Ferri et al. (129) apply a constraint on the cost of 8.15 m€ and the tower bending moment, the purpose of this constraint is to avoid contradictory results with respect to the ultimate load state optimisation.

Table 3.1: The nacelle acceleration constraints applied within the current literature and newly published DNV stantards

Ref	Nacelle acceleration limit (m/s^2)	Operating condition
(122)	1	Below, at, and above rated wind speed, and normal wave operating conditions.
(137; 138; 141)	1.962	IEC standard 61400-3-1, Design Load Case (DLC) 1.1, 1.3 and 1.6*a*
(136)	1.962	IEC standard 61400-3-1, DLC 1.1, 1.3, 1.6*a* and 1.6*b*
(142)	1.962	IEC standard 61400-3-1, DLC 1.2
(139)	2	IEC standard 61400-3-1, DLC 1.2
(126)	2.6	Operational and survival load cases
(134)	5	normal operating condition and survival condition
(147)	2.943	DLC 1.2 and 1.6
(147)	5.886	DLC 6.1 and 6.2

All other work considered in this review does not include a cost constraint, but (4; 6; 15; 122; 124; 125; 126; 131; 139; 140; 142) consider it as an objective in their work. Ferri et al. (128) is the only study which imposes that the mass of the 10 MW platform and mooring system should not be greater than the upscaled 5 MW basis platforms and mooring system. The purpose of this constraint is to seek a cost reduction and avoid over-engineering.

Nacelle Acceleration Constraints

The nacelle constraints which were applied in the literature can be seen below in Table 3.1. This table also shows the serviceability limit state load cases published by DNV (147). These are slightly more relaxed compared to the assumptions in previous literature.

Design Load Case (DLC) 1.1 is for normal power production at around rated wind speed, DLC 1.3 is for below, at, and above rated wind speed with an extreme turbulent model, and DLC 1.6*a* is also below, at, and above rated wind speed in a severe sea state. Additionally in Leimeister (2019) et al. (136) DLC 6.1*b* was also considered which is

parked operation in the extreme wind model, and extreme sea state model both with 50 year recurrence period. Pollini et al. (142) use DLC 1.2 for a wind turbine operating in normal conditions. Since (136; 137; 138; 141; 142) cover a larger range with more harsh operating conditions, the use of a more relaxed allowance on the maximum nacelle acceleration is understandable. Fylling et al. (126) and Gilloteaux et al. (134) both have a larger acceptable nacelle acceleration this is expected since it considers operational and survival load cases.

A number of papers consider the nacelle acceleration as a constraint since it is expected that it can cause damage to equipment, create large platform motions, is thought to reduce the lifetime, induce higher flap wise bending moments, reduce turbine performance and hence power production. It has however been argued by Nejad et al. (148) that the nacelle acceleration is not correlated to the drive train response and does not affect the power production, so long as the pitch controller remains operational. It was also predicted by Nejad et al. (148) that the main bearing fatigue is also not affected by the nacelle acceleration. These findings cause the author to question the use of this constraint in the optimisation framework. It would be interesting to see if the nacelle acceleration affects other parts of the turbines fatigue life, such as the tower, support structure and mooring lines. The work by Nejad et al. (148) only considers a 5 MW turbine since the tower height increases with turbine since the author wonders if there is still no effect on the drive train and the main bearing due to the acceleration of the nacelle.

Motion Constraints

When considering motion constraints the simplest is to impose a constraint on the inclination angle in the direction of the wind. This can easily be improved by considering both static and dynamic pitch for a number of operational cases. This constraint is important because as the pitch angle increased it leads to a power reduction and therefore reduced revenue. However if an appropriate controller is used this reduction should be minimised, but there are instances where this can break or have to work hard to minimise the losses putting stress on the system. Other constraints on other

degrees of freedom can also be considered to ensure the platform is not moving more than the acceptable limit ensuring the mooring lines and dynamic cable are not under severe loading. The final motion constraint generally considered is the natural period/frequency, which helps avoid resonance and potential failures of the system as a whole. In the extensive work by Leimeister et al. (136; 137; 138; 141) to achieve the required wind turbine performance, the total inclination angle of the floating structure must be less than 10 degrees. Both consider a number of normal operational conditions and extreme events. Karimi et al. (122) and Sclavounos et al. (125) both consider the static pitch angle should be less than 10 degrees, both consider normal operational conditions only. Work completed by (4; 128; 129) impose stricter constraints, requiring the maximum static pitch angle to be less than 5 degrees, for both normal and extreme conditions. This choice is probably due to the fact that the platform dynamic response is neglected in their work. Pollini et al. (142) require the static pitch and surge to be less than 8 degrees and 50m, respectively. Dou et al. (139) also apply a maximum static surge motion of 50m to the platform. When considering only the static pitch having a lower constraint seems like a fair assumption given there is no environmental loading considered.

It is beneficial to consider both dynamic and static pitch as a summation since the static position will be the average equilibrium for the system. Combining the static position with the dynamic displacement helps to simulate the real life event or potential phenomenon more accurately. Gilloteaux et al. (134) consider the summation of static and dynamic pitch should be less than 10 degrees, whereas (139) consider dynamic and static pitch individually, imposing that each should be less than 10 degrees. The work by Gilloteaux et al. (134) deals with extreme and normal operating conditions, whereas Dou et al. (139) only consider normal operating conditions, making their constraints more relaxed in comparison to (134). Hall et al. (132) also include a similar constraint, the static pitch angle in this work has a 10 degree limit and separately the dynamic pitch plus the standard deviation of the pitch must be less than 10 degrees. The DNV-RP-0286 (147) details the maximum allowable tower tilt and since this was published after these pieces of literature they do not consider it. Table 3.2 presents the different

DLC	Description	Value
1.2 and 1.6	Permanent value	5 Degrees
1.2 and 1.6	Mean value in time series	5 Degrees
1.2 and 1.6	Max. value in time series	10 Degrees
6.1 and 6.2	Max. value in time series	15 Degrees

Table 3.2: Serviceability limit state load cases for tower tilt.

values for the load cases mentioned prior.

Hall et al. (132), similar to (139), only examine normal operating conditions, making the consideration of a degree limit seems fair. Fylling et al. (126) apply a constraint on the dynamic pitch of the platform, requiring the inclination of the tower to be less than 9 degrees, for both normal and extreme conditions. Hegseth et al. (131; 140) apply a 15 degree constraint on the combined static and dynamic pitch angle in the 50-year survival condition. Since this is for a survival condition it makes sense for it to be higher than other literature.

A more flexible approach which is considered in the following paragraph, considers the motion as a percentage of water depth, since a displacement may seem largely dependent on how deep or shallow the water depth is. Leimeister et al. (136; 141) constrain the mean translational motion to not exceed 20% of the water depth in normal and extreme conditions, whereas (131) set a maximum constraint of 32m on the offset in the 50-year condition. Applying a similar constraint to (131), Ferri et al. (128; 129) state that the admissible platform offset to water depth ratio must be less than 0.15 (i.e. 15% of the water depth). Both normal and extreme load cases were considered in (128; 129). Considering this constraint as a percentage of water depth is a more flexible approach, making it suitable for multiple different sites.

Both the heave and pitch periods are required to be within a given range in Fylling et al. (126), to avoid resonance with typical wave load periods. Building on the work in (126), Dou et al. (139) also include these constraints along with the maximum surge frequency. It was however noted that Birk et al. (7) only consider the heave period. Hegseth et al. (140) also only consider the heave period applying a lower limit of 25 seconds to avoid resonance with the wave period. Lemmer et al. (135) only considered a constraint on the pitch natural frequency, the reason for this is the strong focus on

the effect of the controller, since it is related to reducing torque and thrust, it will also affect the motion of the platform in the pitch direction. Similarly (142) also apply constraints to the eigenvalues, however in this case three Degrees of Freedom (DoF) are considered.

Design Variable Constraints

It is common practice to include constraints on design variables, Bracco et al. (15) along with (4; 7; 122; 123; 125; 128; 131; 131; 132; 135; 136; 137; 138; 141; 142) include such constraints on the design variables. This removes unrealistic designs and creates a more focused design space. Birk et al. (7) highlight that the purpose of the diameter constraints is to ensure the platform can be transported and removes restrictions during the construction phase. Dou et al. (139) only apply an allowable range for the mooring line length, which would probably need to change for each site investigated since water depth varies. Perhaps taking into account the maximum mooring line length as a percentage of water depth would make the work more universal for different site conditions. This is also the only work to consider the maximum percentage of the suspended line.

The constraints imposed on the design are directly linked to the individual components considered in the work. For example, (140) include the tower in their optimisation and therefore, a constraint is set to ensure that the bottom of the tower and the top of the Spar have the same diameter and thickness. The hull taper angle is also limited to a maximum value of 10 degrees to avoid shapes where the physics is not captured correctly due to the model presented in the work only being strictly valid for hull sections with vertical walls, unlike the conical sections which are considered (140). Since Birk et al. (7) proved with experimentation that WAMIT can correctly capture hydrodynamics of less standard geometries, perhaps this constraint is not required for this purpose but maybe for the manufacturability of the structure.

As discussed, in Section 3.3, Hall et al. (133) takes a different approach than other works reviewed, and therefore also takes a unique approach in terms of variable constraints. As explained before (133) consider hydrodynamic performance coefficients rather than traditional geometrical values to describe the platform geometry. For this

reason, a collection of unique geometrically-defined platforms are used as basis designs, from which the hydrodynamic performance coefficients can be linearly combined to approximate the characteristics of any platform in the design space. Constraints are applied to the performance coefficient to a range between zero and one, and the summation of the variables must equal one. The reason for a range of zero to one is the coefficients of each basic design are scaled and superimposed to find the new coefficients for each design. If the coefficients are summed equal to one then the platform geometry is known, however, if it equals zero then the optimisation tool has no bearing on the platform configuration. This work does not explicitly state the constraints they used, however, it is noted that the constraints are on the hydrodynamic design properties. This suggests that there are bounds on parameters such as stiffness, damping, and added mass matrix etc.

Static Stability Constraints

Bracco et al. (15) differ slightly from other work, as the constraints are related to the DNV design standards DNVGL-ST-0119 for the free-float condition, minimum freeboard, and the DNV-OS-C301 standard for the maximum intact inclination angle under normal and survival conditions. These constraints are good because the designed platform will need to pass this criteria in order to get certification. Sclavounos et al. (125) consider a minimum restoring coefficient to ensure adequate restoring under the towing condition and operation, similar to the free float constraint in (15). Clauss et al. (123) have constraints on floating stability of the O&G platform, but do not explicitly state what they are. Fylling et al. (126) apply a limit on the Spar draft as the only constrained design variable, leaving a much wider design space. Work in (4; 134) also constrains the draft but additionally sets a minimum value on the metacentric height, Birk et al. (7) also constrain the metacentric height. Additionally, (4) place a minimum freeboard requirement which would be something design standards would require like (15) inclusion of DNV standards. In (139; 142) a simple constraint related to hydrostatics was used to ensure that the centre of buoyancy is higher than the centre of mass. Benfila et al. (6) require the buoyancy to be above a particular value, depending

on the type of platform.

It is unclear what constraints were actually set in (124), however from the work it can be seen that for the Spar, Trifloater, and Barge there needs to be a minimum restoring coefficient for the pitch degree of freedom, since both the Spar, Trifloater, and barge should be able to maintain stability without mooring lines. These listed platforms are also required to have a realistic draft in order to remain below the waterline and in the Spars case provide sufficient restoration. Wayman et al. (124) require the TLP to remain below the water line to reduce structural loading.

A slightly different perspective was applied in (125), where a constraint was added to the elevation of the free surface, ensuring that it does not exceed the draft of the cylinder when it is heeled, ensuring the support structures remain submerged. This constraint could also be useful to ensure that the minimum freeboard requirement is met.

Mooring Line Constraints

Mooring line constraints were also considered in Karimi et al. (122) where they require that the tension remains relatively constant for taut mooring lines i.e, the standard deviation of the tension in the mooring line cannot be greater than a third of the overall tension. Hall et al. (132) also use the same constraint for the mooring lines. The mooring constraint in (124) is related to the mooring line tension, they must provide sufficient restoring in the surge, and the tension of the windward tether must never exceed the maximum allowable tension, and the leeward tension cannot fall below the minimum allowable tension. (8) apply mooring line constraints, which are considered by a penalty function on the cost function. Constraints were also applied to the natural periods for the optimisation of the mooring lines, to avoid natural periods of the rotor etc. Within (8), as previously explained, the mooring and structure optimisation are in two separate domains. The constraints for the mooring line optimisation, in the time domain, are the following two: minimum tension required in a storm event, and the maximum axial stress in the space frame. Both (125) and (131) apply similar constraints to the mooring line, stating that the dynamic line tension cannot exceed the breaking

load of the mooring line, with (125) applying a safety factor of two. Pollini et al. (142) set a constraint on the maximum vertical force to which the fairlead is exposed. They also require the mooring line length to fall within a prescribed range. This range will need to change depending on the depth of the water at the site. Fylling et al. (126) have more constraints on the mooring line which are: maximum and minimum tension on the mooring line segment, minimum fatigue life, and maximum slope angle at the anchor. Constraints are also applied to the power cable, maximum tension, minimum cable curvature radius, maximum horizontal offset, and minimum static horizontal pretension limit. (128) apply cable length constraints, to ensure the triangular shape and the minimum amount of cable on the sea bed.

Structural Constraints

The inclusion of structural constraints is limited within the literature, only appearing in the work of Hegesth et al. (131; 140) and Leimeister et al. (141). Hegseth et al. (131) focus on the constraints related to fatigue and the ultimate limit state for the Spar and the tower, Table 3.9 details these constraints applied. Similarly, Hegseth et al. (140) impose that the support structure fatigue damage must be less than a given value for the design fatigue factors. Other work which considers a structural constraint is (6), placing a constraint on the maximum allowable stress over the complete platform structure.

Leimeister et al. (141) have two main constraints related to the bending stress at the base of the tower and the tensional stress of the mooring line. These constraints ensure the tower base and mooring lines do not exceed the ultimate values (141).

3.3.5 Design Variables and Platform Modelling

Platform Design Variables

The design variables and the number used to describe different platforms varies heavily across the literature, this is summarised in Table 3.3, a more detailed breakdown for each piece of work is given in Table 3.9. In Table 3.3, it can clearly be seen that the majority of work only carries out the optimisation of a single platform. However, there are a few which consider multiple platform types only half of the work presents

parametric schemes which can describe all platforms considered. The other half rely on individual design variables to describe the geometry.

There are two approaches which are quite different from the rest. Hall et al. (133) use a slightly different parameterisation scheme: rather than using values to describe the geometry, such as diameter or length, hydrodynamic properties are used. The other differing approach was implemented by Hegseth et al. (131) considering both the tower and the Spar as a number of truncated cones rather than cylindrical segments creating a changable 'smoother' geometry. Additionally, the Spar hull considers the overall length as a variable, unlike the tower, which is kept constant to ensure the correct hub height. Hegseth et al. (131), unlike the approaches in the other works, include variables for the controllers that allow the proportional and integral gain to be optimised to get the maximum energy output.

Platform Geometry

Work by Benifla et al. (6) presents a UBB aimed at reducing production cost by serialising the fabrication procedure using standard components. In Figure 3.3, a visual representation is reported.

It is expected that because it is expressed with cylindrical bodies joined by bracings it can represent many different platform typologies since in general terms most support structures comprised of cylinders. Unlike the work of (131), which considers the scantling, (6) use an inner and outer cylinder which can both be expressed by length, thickness, and radius. It is hoped that this design will reduce the manufacturing cost by reducing the material and production costs since traditional stiffeners are not used. The strength of the structure will be provided by using thicker plates to create the inner and outer cylinders. The author does however wonder if this research has considered that by increasing the thickness of the steel plates, the difficulty to form plates into cylinders increases and often more sections are required to make the cylinder to avoid difficulties in rolling. As the thickness of plates increases the weld size required also increases for the welding process, causing the weld cost to increase. When considering this it would be interesting to draw a comparison of the cost of a traditional stiffening

Table 3.3: Number of design variables used in each work and the shape considered.

Reference	Platform Type	Shapes Considered	Number of Variables
(122)	Barge/Semi-submersible, Spar, and TLP	Cylinder	9
(132)	Barge/Semi-submersible, Spar, and TLP	Cylinder	12
(125)	Barge/Semi-submersible, Spar, and TLP	Cylinder	5
(133)	Barge, Semi-submersible, Spar, ring, sub and TLP	Cylinder	N/A
(123)	Gravity base, TLP, Caisson Semi-submersible, or Semi-submersible	Cylinder	6, 3, 4, 4, respective to the platform types
(7)	Spar	Cylinder	4
(15)	Spar, Windfloat, Pelastar, and Windstar	Cylinder	4, 4, 6, 5 respective to the platform types
(4)	Spar and Hexafloat	Cylinder	4, 5
(131)	Spar	Truncated cones	80
(141)	Spar	Cylinder	4
(124)	Spar, Barge and Tri-floater	Cylinder	3, 3,7
(130)	Spar	Cylinder	2
(136)	Spar	Cylinder	3
(142)	Spar	Cylinder	6
(134)	Cylindrical body	Cylinder	3
(7)	Spar	Cylinder	6
(139)	Spar	Cylinder	6
(137; 138)	Spar	Cylinder	3
(126)	Spar	Cylinder	11
(8)	Tension-Leg-Buoy	Cylinder	7
(140)	Spar	Truncated cones	54
(128)	Semi-submersible	Cylinder	7
(6)	Cylindrical body	Cylinder	9
(135)	Semi-submersible	Cylinder	9
(129)	Semi-submersible	Cylinder	5

structure compared to this new proposed structure.

Authors of (6; 122; 124; 128; 129; 132; 139; 142) present the platforms in their work using right circular (i.e., straight sided) cylinders, therefore not considering any changes in radius along the vertical direction in the single cylinder (although different cylinders may have different radii). Authors of (15; 133) also use multiple cylinders to describe the geometry of the different platforms. Similarly, (4) use a right circular cylinder to describe the Spar hull, and a number of the same elements to describe the Hexafloat platform. The cylinders are not split into a number of smaller cylinder segments, and they can only change the overall diameter and length during the optimisation process. The work presented in (125) only considers singular, straight sided cylindrical bodies and does not include any additional appendages, such as bracing or legs, making the geometry simplified. The work by Leimeister et al. (89; 136; 137) also present the platform in a simplistic manner, only modelling the complete vertical section of the Spar: similarly to (122; 132; 133) it does not consider the cylinders segmented into a number of smaller segments or changes in radius. A more advanced modelling approach was adopted by (126): the Spar is divided into segments, where each segment can have a different radius. In a real scenario, it is more realistic to consider the support structure is constructed from multiple parts, since the platform would be made from a number of segments in order for it to be manufactured. It could, however, be argued in this case that it is less realistic since the radius of each cylinder is different, and it will likely be more difficult to manufacture. Clauss et al. (123) use horizontal cross sections which could be meshed together, allowing the radius to change vertically, giving a curved body unlike the stepped shape in (126). Hegseth et al. (131; 140), differently from the others, but similar to (123), describe the platform and tower geometry with truncated cones rather than right circular cylinders. Birk et al. (7) propose a parameterisation scheme for the Spar, the body consisting of four vertical-sided columns and three truncated cones to join the vertical columns. The radius of each column can have a different value hence the requirement for the truncated cones to join each section. Figure 3.7 shows examples of the proposed Spar support structure.

Myhr et al. (8) utilise a space-frame which differs from other work done in this area,

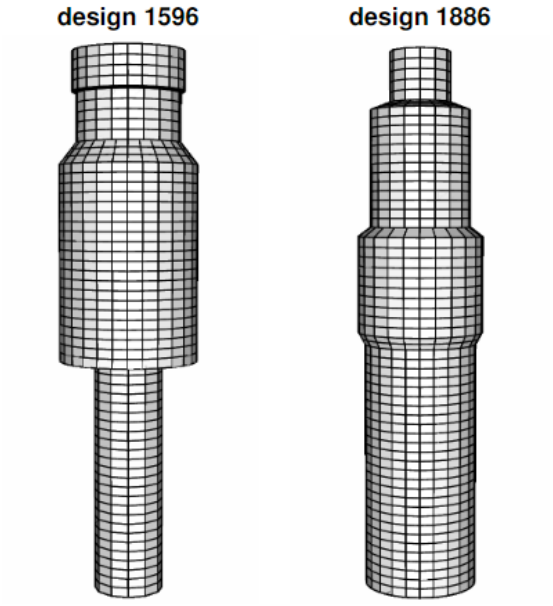

Figure 3.7: Spar support structure proposed in (7).

see Figure 3.8. There are four variables which change the geometry, the outer diameter of the lower cylinder, height of the space-frame, distance between column and turbine centre line and the outer diameter of the vertical column(s) in the space-frame. The purpose of using this geometry is by replacing the cylinders it is expected that the wave forces will be reduced a significant amount as well as reduce the fabrication costs.

Mooring Line Design Variables

Fylling et al. (126) identify the mooring lines and power cables' geometry with the following variables: line direction, pretension, segment length, diameter, and net submerged weight. (125) use three variables to describe the mooring system, considering the angle between the free surface and the anchor, allowing the type of mooring system to be determined, i.e., taut or catenary. Hegseth et al. (131) also model the mooring line, using the diameter of the line, the depth of the fairlead below the waterline, the total length of the line, and the horizontal distance between the fairlead and anchor. Since different platforms may require different mooring configurations, (122; 132) use one of the variables to identify which mooring type arrangement is used such as taut, semi-taut or catenary.

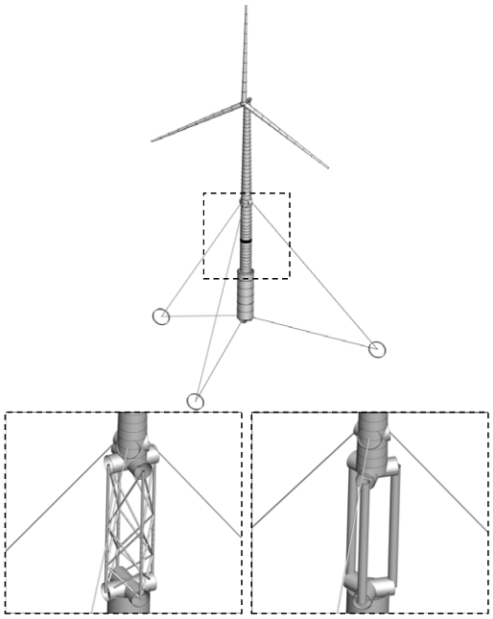

Figure 3.8: Space-frame concept utilised in (8).

3.3.6 Optimisation Algorithms

This section focuses on the optimisation algorithms used within the current literature, these different techniques will be briefly explained, for further details on trends see (149). Figure 3.9 highlights the algorithms used graphically, where it can be easily identified that genetic algorithms (GA) are used the most. Authors of (4; 6; 7; 15; 122; 128; 129; 132; 136; 137; 138) all use GA optimisation techniques. Further information on genetic algorithms can be found here (150). The gradient-based methods used in (8; 123; 126; 131; 133; 139; 140; 142) make use of functions gradients to search for the optimal design, seeking out the 'turning points' of the objective function and constraints in a given design space to find the global maximum or minimum depending on the goal.

Several authors use a multi-objective GA tool to find the optimal platform (4; 6; 15; 122; 128; 129). Hall et al. (132) use a Cumulative Multi-Niching GA (CMN GA). Leimeister et al. (136; 137; 138; 141) use the Non-dominated Sorting GA II (NSGA II) from Platypus. Clauss et al. (123) utilise a nonlinear programming algorithm. Similarly, (126) adopt a Non-Linear Programming technique, Quadratic La-

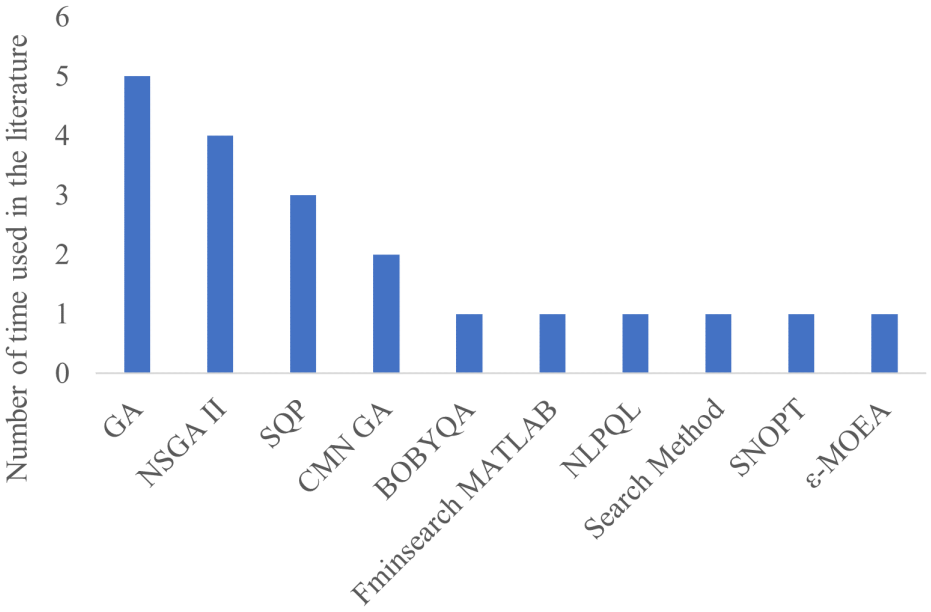

Figure 3.9: Optimisation algorithms used within the literature.

grangian (NLPQL) optimisation. Hall (2014) et al. (133) also use a non-linear optimiser found in the MATLAB toolbox, 'fminsearch'. Myhr et al. (8) apply a Bound Optimisation BY Quadratic Approximation (BOBYQA). (131; 140) use a gradient-based method (SNOPT) that uses Sequential Quadratic Programming. Similar to Hegseth et al. (131), (139) also use a Sequential Quadratic Programming (SQP) method. (7) utilise a Multi-Objective Evolutionary Algorithm (MOEA).

Unlike other works, Pollini et al. (142) use two optimisation techniques, the first for a global solution and the second for a localised optimisation. The first stage of optimisation uses SQP and the latter uses Relaxation-Induced Neighbourhood Search (RINS). Authors of (124; 125) do not state which optimisation algorithm is used.

Optimisation Technique Review

Reviewing the literature it was highlighted in Figure 3.9 that various different GA options were commonly implemented. These were classic GA, NSGA II, CMN GA, and MOEA.

The classic GA is a population-based optimisation technique which utilises the Darwinian theory of evolution. The basic components of a GA consist of a random population containing many chromosomes (particular solution), which are comprised of a number of genes (design variables). The size of the population is typically dependent on the number of design variables, the population size is typically 50 for less than five design variables or 200 if there are more than five. This population is also influenced by the limits of the design variables; a larger design space with broader bounds necessitates a larger population. For the optimisation procedure two chromosomes are selected based on their fitness, they are combined with the cross-over probability to produce an offspring. A mutation operator is applied to this offspring with a mutation probability. This process will be repeated on the current population until a new population is created. This process is iterated over a number of generations until there is no improvement in the fitness and the optimised solution is found (151).

This method is favourable compared to traditional methods since it does not require a derivative approach which utilises the gradient. Gradient-based methods are effective in linear regression-type problems, where there is a singular peak or trough, however in more realistic real-world problems this method suffers from the tendency to get become confined to a local minima or maxima rather than the global solution. Since the GA does not require the gradient of the objective function it can be used to successfully find the global solution where the objective function is discontinuous, non-differentiable, stochastic or highly non-linear. The GA also has the advantage of handling multi-objective problems, whereby there are competing objectives, which is typical for real situations.

One of the main issues with the GA is the high computational time linked to the fitness function being repeatedly calculated. An increasing number of design variables typically lead to an exponentially larger design space further adding to the computational time. Convergence can also be an issue if particular parameters are not tuned appropriately such as rate of mutation, crossover, and the selection criteria. Despite these drawbacks, GA is one of the most widely used optimisation algorithms for non-linear problems (152).

The Non-dominated Sorting GA II (NSGA-II) was created to overcome the issues with traditional evolutionary algorithms, which lacked elitism and used a sharing parameter in order to sustain a diverse Pareto set. The inclusion of elitism ensures the best solution from the previous iteration is kept unchanged, this allows the rate of convergence to increase, helping to combat the issue related to high computational times. Using a fast non-dominated sorting algorithm helps to significantly reduce the complexity, reducing the time further but comes at the penalty of requiring a larger storage space (153; 154). The Cumulative Multi-Niching (CMN) GA implements a different yet similar approach by never discarding individuals from the population, taking advantage and learning from every objective function evaluation as the design space is explored. By considering a population density control over the design space taking into account the fitness of each solution, allows unnecessary evaluations of the objective function to be avoided. This approach allows convergence to multiple local optima (132).

The other approach which has been widely covered in literature is search methods. There are a number of different search methodologies however they all utilise the objective function. This is a much more simplistic approach compared to the GA. The pattern search optimisation is derivative-free, which finds a solution by systematically searching the design space (155). Starting with an initial point, the algorithm uses multiple directions to create a set of potential moves i.e a pattern to cover the domain. As the algorithm iterates through the design space the objective is evaluated at each point, the way in which the algorithm moves through the design space is dependent on whether the new solution is better or worse than the prior. The step size which is taken between each iteration can also change depending on the objective function value. To determine the optimal solution, the convergence criteria are evaluated, typically including step size, constraint satisfaction, and the objective function. The pattern search algorithm is fast and works for a range of different problems which have nonlinear, non-continuous or non-convex objective functions. It is also a useful method where the gradient information is unavailable or is computationally expensive to find (156; 157). Unlike the GA, pattern search typically gets trapped in local solutions rather than finding the global optimal. A method to counteract this is to implement a multi-start

approach. Starting the optimisation from a number of different points within the design space (158). Since this method requires a large number of objective function evaluations, it can become computationally expensive where the design space is large (156).

The function Fminsearch used in MATLAB is a simplex search method which utilises the Nelder Mead algorithm (159). Like other search methods, this is a derivative-free method however it is unconstrained. It starts with an initial set of points (simplex) and iteratively evaluates the function at those points. The algorithm then replaces the worst point with a better one through reflection, expansion, or contraction, reshaping the simplex until it converges to the minimum. (160).

The Sequential Quadratic Programming (SQP) method is effective at solving problems with non-linear objectives and constraints. Firstly, starting with an initial feasible point which satisfies the constraints, the problem is then iterated and for each iteration, a subproblem is created and the optimal solution must be found for this first, i.e where the gradient is equal to zero. This sub-problem can be defined as a quadratic approximation of the scenario based on the Taylors series expansion of the Lagrangian function, this is constructed by combining the objection function and the constraints. To find the optimal solution for the overall problem, the algorithm steps along a search direction, where the current solution is updated by following the direction of improving objective function with consideration for constraint requirements. The optimal solution is found as the problem comes to convergence, ensuring the changes in the constraints and objective function are sufficiently small (161; 162). Both SNOPT and NLPQL use SQP (161; 163). BOBYQA similar to the classic search method does not require derivatives. This is an iterative algorithm which has a "black box" design that returns feasible solutions. Each iteration implements quadratic approximations which satisfy the objective functions provided by the black box (164).

3.3.7 Modelling Software Utilised

A number of papers use frequency domain dynamic models, due to the smaller computational time to carry out the analysis (7; 8; 122; 124; 125; 126; 128; 129; 131; 132; 133; 134; 139; 140; 142). Few other works use a time analysis domain (128; 129; 134;

135; 138; 141). Some work included a time domain to verify the work carried out in the frequency domain (8; 122; 131; 140).

The effectiveness of an optimisation framework, and subsequent results, is dependent on the types of software available which are fit for purpose. Figure 3.10 highlights how dependent this research is on both WAMIT and FAST for hydrodynamic and aerodynamic analysis. For this reason, a large number of the existing literature use non-gradient-based methods for their optimisation. However, authors such as (131) use gradient-based optimisations, since they use formulae from which gradients can be derived.

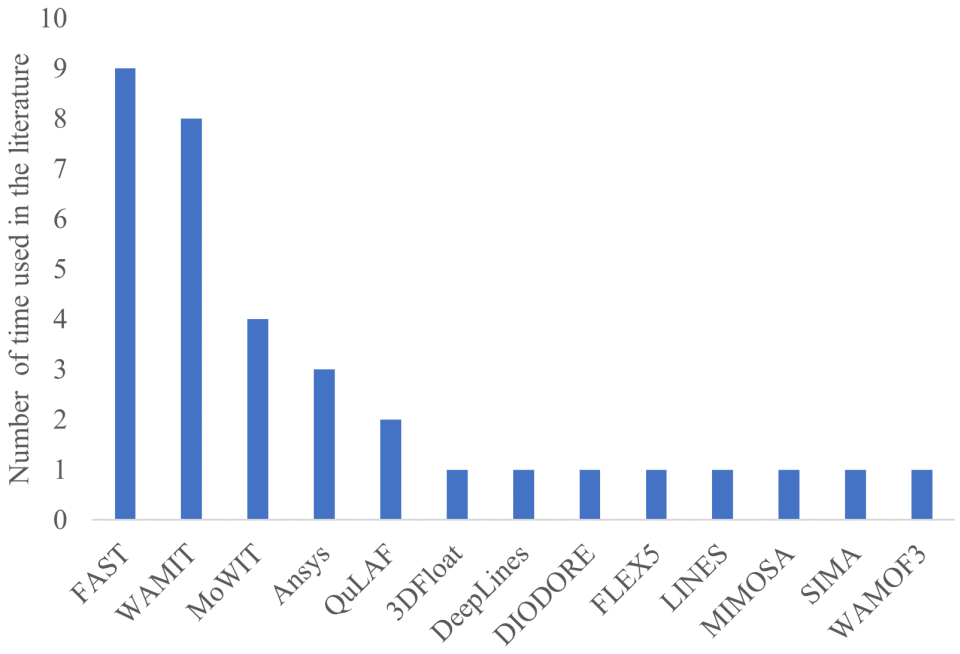

Figure 3.10: Additional software used within the optimisation frameworks.

In the work by Karimi et al. (122) the hydrodynamic properties of the platform was found using WAMIT [1] which can then be combined with the equations of motion. Authors of (7; 123; 124; 125; 132) followed a similar approach for hydrodynamic analysis. Hall (2014) et al. (133) unlike (122; 123; 125; 132) do not use WAMIT to find the hydrodynamic properties of each platform geometry; instead, WAMIT is used

[1] https://www.wamit.com/

to find the hydrodynamic properties of six base designs, which can then be used as a starting point for optimisation. Fylling et al. (126) use WAMOF3 rather than WAMIT to obtain the hydrodynamic coefficients and from these the motion transfer functions. A different technique was proposed in Hegseth et al. (131; 140): rather than using a potential flow code (e.g. WAMIT), they adopt the MacCamy-Fuchs theory to determine hydrodynamic excitation loads, while the added mass was based on analytical 2D coefficients, the radiation damping was neglected, viscous damping was computed using a stochastic linearisation of the drag term in Morison's equation. Since this is a linear model, a time domain verification was carried out using SIMA. [2]

Gilloteaux et al. (134) utilise DIODORE[3] software to find the hydrodynamic properties using the frequency domain, DeepLines[4] is then used to model the platform and mooring lines in the environment in the time domain.

Both Dou and Pollini et al. (139; 142) use the Quick Load Analysis of floating offshore wind turbines model (QuLaF) to determine the hydrodynamics of the platform, a model created by (165). The only works which use ANSYS AQWA to find the hydrodynamic forces were (128; 129; 135), this model was also verified with WAMIT in (128).

Bracco et al. (15) apply an in-house hydrostatic tool, (4; 135) also use basic hydrostatic concepts to determine the stability of the platforms.

Several authors (122; 124; 125; 128; 129; 132; 133; 139; 142) use FAST, this allows the influence of the rotor aerodynamics and the wind turbine mass effect on the FOWT motions to be considered. It can be noted that some of the aerodynamic effects on platform motion can also be considered by utilising a frequency domain approach without using FAST. Karimi et al. (122) utilise FAST as verification in the time domain, which shows the variation in the surge, pitch, and nacelle acceleration of a TLP and a Spar. Lemmer et al. (135) applied a similar approach and used FAST as a verification tool for their Simplified Low Other Wind Turbine Model (SLOW) methodology.

In work by (122; 132; 133) the mooring lines are modelled using a quasi-static

[2] https://www.sintef.no/en/software/sima/
[3] https://www.principia-group.com/blog/product/diodore/
[4] https://www.principia-group.com/blog/product/produit-deeplines/

mooring subroutine of FAST. (126) use MIMOSA to perform extreme conditions for fatigue analysis on the mooring lines. Finally, (125) utilise the LINES software to find the properties of the mooring system. Hegseth et al. (131) utilise a dynamic frequency-domain model to find the tension in the line, considering it only has one DoF (166)

Research carried out by Leimeister et al. (136; 138; 138; 141) use MoWiT (Modelica library for Wind Turbines) to perform aero-hydro-servo-elastic analysis for the wind turbine, in the time domain. Similarly, Myhr et al. (8) also apply an aero-hydro-servo-elastic tool called 3DFLOAT and Hegseth et al. (131; 140) combines structural and control parts to create a full aero-hydro-servo-elastic model.

Bracco et al. (15) did not include any dynamic modelling and focused purely on the hydrostatics of the platform to assess the stability. Benifla et al. (6) also does not include any dynamic modelling; however, it does use Ansys SOLID186 to perform finite element analysis and FLEX5 to determine the loading on the platform.

In general it can be noted that both time and frequency domain have been used throughout the literature, it is key to highlight the advantages and disadvantages of these types of analysis. Time domain analysis solves the equations of motion step by step over time using numerical integration. The key benefit of time domain is the ability to capture non-linearities and effects from mooring dynamics, wave forces, aerodynamic forces, etc. Coupled dynamics can also be considered between the turbine, platform and mooring system to create an accurate representation of the system and its interactions. As always there is a computational price to pay with higher accuracy, requiring long duration simulations. This type of analysis is good when considering a few or one design to gain the best understanding of the full system and its response.

On the other hand frequency domain analysis solves the system response in the frequency domain using spectral methods and assumes linearisation of the governing equations. Frequency analysis is fast and computationally efficient, which is ideal for early-stage design, where there are a number of different options to consider. Another advantage over time domain analysis is the clear insight to the system resonance and dominant frequencies making it easy to high light overlap with blade passing or wave frequencies, being able to identify this easily in early stage design is useful, allowing

the designer to adapt the design to avoid resonance. Unlike the time domain non-linearities are not captured, making the results less accurate where there are strong non-linearities (167).

Overall time-domain analysis is essential for detailed design, considering all non-linear effects. Frequency-domain analysis is useful for early-stage design, resonance identification, and fatigue estimation. A combination of both methods is often used: frequency-domain for initial screening and time-domain for final verification (167).

3.3.8 Cost Modelling

Cost is one of, if not the, most important and utilised objective within this area. For papers which do not include cost as the main objective, the cost can often be linked to the objective implemented. Therefore, the following section is dedicated to this important objective. Table 3.3.8 provides a systematic analysis of the cost aspects considered in each reference cited.

The section is broken down as follows: **Reduced Complexity Model**, highlights the simplistic models used within literature, and **Improved Model** details the more complex cost models used. The mooring line cost models are presented in **Mooring Line Cost**, which is followed by other costs considered in **Other Costs**. Finally, **Indirect Cost Consideration** details objectives which have been used and can be linked indirectly to the costs.

Reduced Complexity Model

Karimi et al. (122) and Hall et al. (132) use the same cost model, including the support structure and mooring lines. The cost of the platform is found using the mass of the platform combined with the cost per unit of mass. It is stated in both works that this includes consideration for material cost, manufacturing, and installation. Bracco et al. (15) determine the cost of the platform in a similar manner to (122; 132), i.e. using a simplistic "bill of material" approach, similar to a number of other papers (4; 6; 8; 125; 135). Additional considerations were added in (124), by expressing the material cost in GBP/kg and the labour cost, expressed in GBP/hour. To determine the cost,

Fylling et al. (126) use a different approach starting with the initial price for the Spar, which was then scaled in proportion to the dimensions of the new optimised Spar.

From this review, it was made very clear that the most common method to find the platform cost was to consider the mass of the platform and multiply it by a value for the price of material per kg. One of the best cost models found within the optimisation literature was presented in (129). This model considers not only the platform mass but the associated labour costs for welding and assembly, in terms of hours and the paint cost in correspondence with the surface area covered. The ballast to meet the required draft is also found and the cost of ballast made in concrete is calculated.

Improved Model

Hegseth et al. (131; 140) recognise that only considering the mass could lead to an underestimation of the costs, as it does not include any other manufacturing costs. For this reason, they model the tower and Spar costs by considering the material cost and the fabrication costs, which include forming, assembly, welding, and painting by using a fabrication constant which is multiplied by the length of time to manufacture the product. No other details have been provided about this work.

Zhou et al. (145) carried out a sensitivity study to determine which parameters affect the cost most for a Semi-submersible. For this work, a detailed cost model was used to determine material, forming, welding and painting using the method found in (168). There was however no structural consideration for stiffeners of the required thickness of the shell. Zhou et al. (145) found the radius of the columns had the largest effect on the overall cost.

Mooring Line Cost

As far as the mooring system costs are concerned, Fylling et al. (126) found the cost of the mooring line by simply multiplying the mass per unit length, the length, and the cost per unit mass. A more advanced method was considered in (122; 132): by finding the cost based on the length of the mooring line and the maximum steady-state tension, considerations for the possible requirement for a thicker line are allowed. Similarly, the

anchor cost is a combination of a fixed installation cost and the anchor itself, which can be derived by multiplying a coefficient of cost per unit load by the maximum steady-state load on the anchor. The coefficient depends on which of the three main anchor types is considered (122; 132). The mooring line cost, unlike in other works, is calculated based on the mass of the line in (131). Ferri et al. (129) is the only research to show how the anchor size is calculated using ABS anchor design document (169), once the required weight was found considering an ultimate holding capacity of 1.5 times the maximum mooring line tension from the weight, the cost can be then found. The mooring line cost considers the diameter required and the unstretched length. The unstretched length was found using the quasi-static approach presented in (131). In later work by (140), the cost of the mooring was discarded and the focus was solely on the tower and support structure. Anchor and mooring costs were derived considering, respectively, a fixed value and a cost per unit length. Wayman et al. (124) also consider the installation cost, based on the time to carry out the installation and the cost to hire the related vessels. From all of the optimisation papers reviewed, 18.5% considered the cost of the mooring line within their optimisation.

Other Costs

Fylling et al. (126) were the only group to consider the cost of the power cable. The power cable cost is related to the cost per unit length of the bare cable, the cost of the buoyancy material per unit mass, the density and the cross-section of the buoyant material, and the length of the power cable segments. The buoyancy material or its purpose is not explicitly stated in this work, however, it is expected to be an elongated segment(s) of buoyant material around the cable used to keep a required length of cable buoyant underwater, reducing the tension at the connection to the wind turbine (170; 171). Anchor, mooring line, and installation costs are briefly discussed in (15), but are not considered in the optimisation. Other authors that also included additional costs outwith the optimisation are (4; 124).

An important additional parameter that can be evaluated by knowing the total cost is the LCoE, if a model to quantify the AEP is available. Both (4; 124; 129) use

a simple method to find the AEP, by combining a Weibull distribution with the wind turbine power curve, which provides the electric power produced as a function of the wind speed. When finding the LCoE, both authors (4; 124) combined the summation of cost and divided it by the AEP, however (124) lacks the inclusion of all associated costs and does not include a discount rate, which is important given the expected life span of around 25 years. The costs neglected were parts of the CapEx related to the complete turbine and electrical system costs, operations and maintenance costs, and decommissioning costs. On the other hand (4) estimate the remaining cost using the following assumptions: cost per MW for the complete wind turbine, operations and maintenance, installation cost, and a set value for mooring lines, anchors, offshore and onshore substation, decommissioning, and cost per unit length for electrical cables and cable ducts. Ghigo et al. (4) include a more detailed cost estimate compared to (124), however, a number of assumptions are made in this work, and the accuracy of these are unknown since there is little data to validate such assumptions. Ghigo et al. (4) also assume a fixed installation cost, which is inaccurate considering that it is heavily related to the type of platform, the site, and the installation techniques used. The operation and maintenance cost was considered as a cost per MW value, however, this is a far more complex problem since it is related to weather windows, failure rates, mobilisation, and downtime, which are key factors affecting the wind farm energy production. These parameters affecting the O&M cost are highly dependant on the site and the platform, hence a generic approach is not accurate. Decommissioning is a relatively new topic, with only a few bottom-fixed offshore wind farms now coming to the end of their operational life, (4) assume decommissioning cost to be 2% of the CapEx. Similar to other costs related to floating offshore wind, DecEx will also be affected by the platform type and cannot be standardised. Other fixed cost, such as mooring and anchors, were expressed as generic values for all platform types (4): these are in general not the same for all platforms, and depend on sites too. Different platforms require different mooring arrangements and anchors, depending on the seabed. The length of the mooring lines will also vary depending on the depth of the water, affecting the cost associated with the mooring lines. Similar to the work in (4), Sclavounos et al. (125) find the optimal

platforms first using only the platform cost which is then followed by an economic assessment, based on cost per kW values with no breakdown of the cost values included.

Indirect Cost Considerations

The following papers (7; 123; 125; 128; 130; 133; 134; 136; 137; 141) do not explicitly include a cost model, but, in their optimisation framework, the objective function can be very easily related to cost. (125; 133; 141) have as their objectives the (minimisation of) the nacelle acceleration, which in turn should reduce fatigue and maintenance costs. A reduction in the platform motion, in general, should improve the power output from the turbine, augmenting the AEP and therefore driving down the LCoE. Another benefit of reducing platform motions is the reduction in ultimate and fatigue loads, overall improving the life span and reducing maintenance costs. The objective of reducing the angle of inclination of the tower would also help to improve power performance and hence the LCoE (136; 137; 141) Similar effects would arise from reducing the forces or motions of the platform (7; 123; 128; 130).

For the sake of completeness, the review's summary is also reported in Table 3.3.8, where **N/A** highlights that this system is excluded from the research.

Ref.	Support Structure	Tower Structure	Mooring Line	Anchor	Cable	AEP	Additional costs	Optimisation Related Costs	LCoE	Notes
(131)	Mass times steel cost factor plus the fabrication factor multiplied by time, considering: material assembly, welding, and painting costs ($2.7EUR/kg$).	Same as support structure	Uses mass ($3.5EUR/kg$)	**N/A**	**N/A**	**N/A**	Cost and standard deviation of the rotor were combined, with weighted factors, then used in optimisation process	Support structure, tower, mooring and rotor standard deviation	**N/A**	Aim to minimise standard deviation of rotor speed
(122; 132)	Mass of platform, including fabrication and installation considerations ($2.5USD/kg$).	**N/A**	Total length and maximum steady state tension ($0.42USD/m - kN$)	Anchor cost is a function of the maximum steady-state load, the installation cost is also included. 100-150 USD/anchor.kN and 5000-11000USD/anchor installation	**N/A**	**N/A**	**N/A**	Support structure and mooring lines	**N/A**	**N/A**
(133)	**N/A**	**N/A**	**N/A**	**N/A**	**N/A**	**N/A**	**N/A**	**N/A**	**N/A**	Minimising nacelle acceleration, which would reduce fatigue and hence maintenance costs

(141)	**N/A**	**N/A**	**N/A**	**N/A**	**N/A**	**N/A**	**N/A**	**N/A**	**N/A**	Minimise nacelle acceleration and total inclination angle
(123) (O&G)	**N/A**	**N/A**	**N/A**	**N/A**	**N/A**	**N/A**	**N/A**	**N/A**	**N/A**	Minimise platform forces and motions
(124)	Mass of platform and labour costs(USD/ton and 40 USD/hour).	**N/A**	**N/A**	Mooring line, anchor and two installation cost options: Barge, tug, labour, pumps and divers, anchor handling vessel. $25000-$50000 per anchor, installation 11285.71 - 18000 USD/per anchor	**N/A**	Uses Weibull and power curve of wind turbine	Installation cost port: hours and workers per installation, labour rate and crane fee. Installation cost at sea: installations per day, labour, crane, barge, tug hire. Total installation = $145280 per turbine	Cost is not included in optimisation	Does not include a discount rate, or the full cost of the system	Aim is to achieve restoring (increased stability)
(130)	**N/A**	**N/A**	**N/A**	**N/A**	**N/A**	**N/A**	**N/A**	**N/A**	**N/A**	Aim too minimises deviations in rotor speed and and platform dynamics

(136)	**N/A**	**N/A**	**N/A**	**N/A**	**N/A**	**N/A**	**N/A**	**N/A**	**N/A**	Aim too minimise nacelle acceleration, translational motion and total inclination angle
(142)	Mass only	**N/A**	**N/A**	**N/A**	**N/A**	**N/A**	**N/A**	Support structure	**N/A**	**N/A**
(134)	**N/A**	**N/A**	**N/A**	**N/A**	**N/A**	**N/A**	**N/A**	**N/A**	**N/A**	Aim is to ensure floating structures maintain stability
(7)	**N/A**	**N/A**	**N/A**	**N/A**	**N/A**	**N/A**	**N/A**	**N/A**	**N/A**	Aim too minimise significant heave double amplitude

(4)	Platform mass, the steel density is increased to consider flanges and welds ($3000 EUR/ton$)	**N/A**	Fixed value ($500 Million$)	Fixed value (80000)	**N/A**	Used historical data to get Weibull distribution, then multiplied by the turbines power curve	**N/A**	Only mass used for optimisation	Array cables $400 EUR/m$, export cables 600EUR/m, offshore and onshore substation 0.431 millionEUR, cable duct 500 EUR/m, installation (2.5 and 1.5 million EUR/MW Spar and Hexafloat respectively), Decommissioning 2% and O&M $0.91 MNOK/MW$	Uses discount rate, and includes all costs
(138)	**N/A**	**N/A**	**N/A**	**N/A**	**N/A**	**N/A**	**N/A**	**N/A**	**N/A**	Aim too minimise the variation in power output
(137)	**N/A**	**N/A**	**N/A**	**N/A**	**N/A**	**N/A**	**N/A**	**N/A**	**N/A**	Aim too minimise nacelle acceleration, translational motion and total inclination angle
(125)	**N/A**	**N/A**	**N/A**	**N/A**	**N/A**	**N/A**	**N/A**	**N/A**	**N/A**	Aim too minimise nacelle acceleration

(126)	Uses and initial cost of a Spar and scales it depending on the Spar dimension (diameter, length and depth), the platform is considered in sections	**N/A**	Cost per unit of mass, length and mass of each segment	**N/A**	Cost per unit bare cable per unit length, cost of buoyancy material per unit mass, density and cross sectional area of material, length of each cable segment	**N/A**	**N/A**	Support structure and mooring lines	**N/A**	**N/A**
(8)	Only Mass	**N/A**	**N/A**	**N/A**	**N/A**	**N/A**	**N/A**	Support structure	**N/A**	**N/A**
(140)	Mass times steel cost factor plus the fabrication factor multiplied by time, considering: material assembly, welding and painting costs ($2.7 EUR/kg$)	Same as support structure	**N/A**	**N/A**	**N/A**	**N/A**	**N/A**	Support structure and tower	**N/A**	**N/A**
(128)	**N/A**	**N/A**	**N/A**	**N/A**	**N/A**	**N/A**	**N/A**	**N/A**	**N/A**	Aim to minimise surge, heave, pitch RAO amplitudes
(15)	Material cost times mass ($3000 EUR/ton$)	**N/A**	**N/A**	**N/A**	**N/A**	**N/A**	**N/A**	Support structure	**N/A**	**N/A**
(6; 135)	Material cost times mass	**N/A**	**N/A**	**N/A**	**N/A**	**N/A**	**N/A**	Support structure	**N/A**	**N/A**

(129)	Material cost (0.5EUR/kg), ballast material (0.1EUR/kg), labour (17.05EUR/hr) and paint cost (12.5EUR/m^2)	**N/A**	Mooring line (1.6 – 2EUR/kg)	Anchor cost(6706 – 10250EUR/kg)	**N/A**	Weibull and turbine power curve	**N/A**	Support structure and mooring line	**N/A**	**N/A**

Table 3.4: Summary of the reviewed works in Section 6.1.5, describing the support structure, tower structure, mooring line, anchor, cable, AEP, additional costs, optimisation related costs, LCoE, and relevant notes (N/A indicates it was not included in the work)

3.4 Optimisation Framework Discussion

The following section is broken into three parts, firstly, a discussion highlighting the shortfalls in the literature for optimisation frameworks, reported in Section 3.4.1. This section is further broken down into design variables, objectives, and constraints. Then a review of the overall output of each paper is provided in Section 3.4.2, followed by potential areas which could help improve the area of research in Section 3.5.

3.4.1 Optimisation Framework

Firstly, focusing on the optimisation frameworks found in the literature, the percentage of each system (i.e floater, mooring, tower etc) to which design variables, objectives and constraints are applied can be found in Table 3.5.

Design Variables

Starting with design variables, roughly 93% of the literature uses design variables to describe the floater - this is expected since the main focus of the present work is on optimisation of floating substructures. In comparison, the next most represented system in the design variable vector is the mooring system, again as expected, although only half of the reviewed literature have included it. The control, cable, and tower systems were rarely included, and no system/subsystem belonging to the RNA has been included. A potential reason for the systems related to the RNA not being included is turbine OEMs design turbines and then typically everything else is designed around this, therefore the this is not a design variable but a fixed input to the models. However, carrying out a more holistic approach, considering the turbine, tower, floater, mooring lined and anchor as one system there is the potential to achieve a globally better solution where the interaction between each system is considered. It is expected that these inclusions will help to find, overall a better platform, considering the complex and interconnected relationships between systems.

Objectives

The majority of literature (83%) has cost as objective of the optimisation, while 58% of them consider the dynamic response of the platform as one of the objectives. Clearly, 83% and 58% come to a total greater than 100%, the reason for this is the fact that the following works considered multi-objective functions: (4; 7; 122; 124; 129; 132; 133; 137; 138; 141; 144). The mooring system is included in approximately 11% of the objective functions, by (8; 125). The mooring line has very few appearances in the objective function but the majority of the research have considerations for it (8; 122; 125; 126; 128; 129; 130; 131; 132; 133; 134; 137; 138; 139; 140; 142; 144; 145). A possible reason is the expected percentage of the cost. The mooring line is predicted to be between 1% to 6.5% of the overall cost depending on platform type (41). Since the cost of the various floating substructures, excluding the mooring cost, lies between 20% and 27%, there is a potential to make a much more significant impact on the overall cost reduction (41). The mooring line might be better considered in the optimisation as a constraint, to ensure the tension remains below the minimum breaking load. By considering the mooring line in this sense, the minimum diameter and length can be found, giving a cheaper design while still considering a safety factor. The tower and the power production are both considered in the objective function in roughly 7% of research. Given that wind turbine towers have been in production and operation for a much longer period of time compared to the support structure, it makes sense for an optimal design to already be known, removing the requirement for the tower to be part of the objective function. However, when considering structural considerations and eigen frequencies, it could be relevant to consider the tower in the optimisation, since floating wind turbines have a dynamic response to the metocean conditions substantially different from onshore and offshore fixed wind turbines (172). This has become particularly important with DNV adding a guidance note to DNVGL-ST-0119 regarding turbine approval and tower eigen frequency for floating wind specifically. This note states that it is often impractical to maintain the same tower stiffness because the type assumes the tower is connected to a rigid or significantly stiffer foundation, unlike the flexible foundation of a floating structure (173). The consideration of the power produced is

relatively low considering that the more energy is produced the higher the revenue, and this is potentially due to only very few works (130; 131; 140) considering the controller, which is associated with improving power output. The power production, similarly to cost, can be improved by improving the platforms response, and hence geometry and mooring system. As mentioned an improved control system would also have a positive impact on the power production. Increased power production will push down the LCoE making offshore wind more competitive. Overall, it is clear that all systems are highly interconnected, with a strong correlation to cost.

Constraints

In terms of design constraints, the most common (92.86%) are related to the platform dynamic response, which includes nacelle acceleration, platform motion, and natural frequencies, all of which are expressed in more detail in Section 3.3.4. The nacelle acceleration in particular has been highlighted in previous section 3.3.4 as an over used constraint, with little benefit of inclusion since the acceleration is expected to have no negative impact on the nacelle. Furthermore, constraints are commonly imposed on the platform geometry (78.57%) to ensure feasibility/manufacturability/transportability are considered within the optimisation. Constraining the design variables also reduces the design space to help improve computational time. Mooring line constraints are applied in 50% of current research, more specifically imposing limits on the maximum tension in the mooring line. Applying constraints which reflect maximum values like that of the mooring line tension is a good way to consider design standards, which eventually each sub-structure will have to comply with. Both cost and tower constraints are represented in 17.86% of research, the latter makes sense since the tower is required to be a certain geometry with the hub height being an important constraint. A cost constraint, however, as expressed in Section 3.3.4 is not expected to be related to finding the best platform but to remove economically unfeasible designs and reduce the design space and therefore computational time. Since the control, RNA, cable and power production are rarely seen in the literature, they are uncommon in the design constraints applied to the optimisation.

Table 3.5: Percentage of the literature reviewed considering a specific floating wind turbine subsystem or aspect in the design variables, objectives, and constraints.

	Control	**RNA**	**Tower**	**Floater**	**Mooring**	**Cable**	**Power**	**Cost**	**Resp.**
Design Variables	10.71%	0.00%	14.29%	92.86%	50.00%	3.57%	0.00%	0.00%	0.00%
Design Objectives	0.00%	0.00%	7.14%	0.00%	10.71%	0.00%	7.14%	82.14%	57.14%
Design Constraints	7.14%	3.57%	17.86%	78.57%	50.00%	10.71%	3.57%	17.86%	92.86%

3.4.2 Literature Findings

A number of articles have performed multiple platform optimisations ranking the platforms from best to worst, see Table 3.8. It can very quickly be noticed there is no clear consensus on which platform is 'best'. Most of these platforms are ranked on the basis of cost, and nearly all of them use slightly different cost models and different site characteristics. The use of cost per unit of mass could easily cause bias in ranking which platform is best, not considering the complexity, manufacturability, transportation, installation, operations and maintenance, and lastly decommissioning. Similarly, the different sites explored by each paper will have a direct impact on cost, further afield and deeper sites are expected to be more expensive making it difficult to compare them directly.

Tension Leg Platform

Karimi et al. (122) found that the TLP is the optimum solution, while the multibody platform optimisation found a Semi-submersible with four columns to be the most cost-effective, yet stable platform. Both Karimi et al. (122) and Hall et al. (132) conducted similar work producing similar results. Their results are presented on graphs with nacelle acceleration vs cost, showing the Pareto frontier, making it very easy to observe the best performing platforms for these optimisations. Similarly, (125; 133) also find that a TLP is optimal with a Semi-submersible also considered a strong platform choice for the given objective in (133). The TLP in (125) is expected to be the best solution due to its low nacelle accelerations and mass. Similarly, the outcome of (124) shows the Spar to be the most expensive and a barge - the cheapest, followed very closely by a TLP. It has been noted that at no point was a Spar the optimal solution (122;

Table 3.6: Complexity factors used in (15)

Platform Type	**Complexity factor**
Hwyind Spar	120%
PelaStar TLP	150%
Wind star TLP	170%
WindFloat Semi-submersible	200%

124; 125; 132; 133). In these studies, however, the manufacturing complexity, which is generally higher for column-stabilised platforms, and its impact on the costs derived, is not taken into account. Taking this aspect into account may have favoured the Spar, thanks to its simpler geometry. The complexity factor of manufacturing for each specific platform was considered in the work by (15), see Table 3.6. Since the work in (15) is for existing prototypes, it is wondered how universal a complexity factor is when considering a design space with non-existent platform types. Since there is a wide range of very different, for example, Semi-submersible platform geometries, the complexity factor is expected to vary. Both the optimisation and cost literature which presents a complexity factor consideration is always fixed to one value for the three main platform classifications.

Similar to (122; 125; 132; 133), Bracco et al. (15) use the same method as (4) and the outcome of each paper is that the TLP is the cheapest option, however, there is no consideration of which platform has the best trade-off between cost and stability, unlike work in (122; 125; 132). Only considering the lowest platform cost has the potential to find not only an infeasible solution in terms of performance but also a platform that may not guarantee the lowest overall cost. The works described above all find the TLP as the best option with the main reasons being linked to potentially good performance and low cost. Since a TLP has been repeatedly presented as the optimal option, there has been additional work done to explore non-traditional TLP geometries. Myhr et al. (8) highlight the traditional TLB without the space frame performs best, with the TLB with a space frame giving very similar results. This work highlights the negative impact on moving away from traditional TLBs by implementing a space-frame. Benifla et al. (6) compare the standard TLP buoy with the UBB and then the optimised UBB.

Both UBB platforms have a higher mass, however, also a lower cost with the optimised UBB having a 30% cost reduction. The above works show a low cost with potential for large cost reduction, making the TLP a favourable option. Since the manufacturability is not fully represented in this work, comparing welding, forming, and paint costs might alter which platform is cheapest. Additionally, when considering the full picture, it is expected that the capital cost and installation cost of the station keeping system for a TLP will be much larger than the Spar and Semi-submersible due to its higher complexity (9; 29; 45) see Figure 3.11.

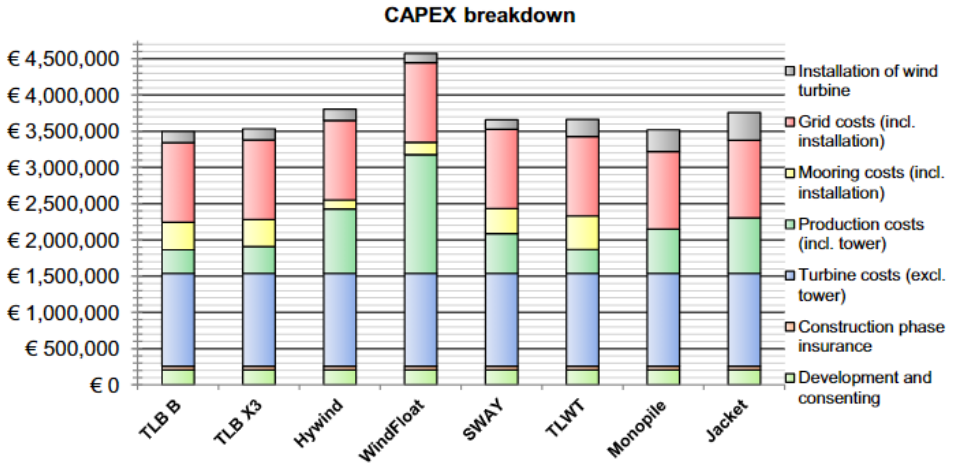

Figure 3.11: Cost breakdown found in Myhr et al. (9).

Since the mooring, installation, O&M, and the decommissioning cost for each platform type is different, the cheapest platform option might not be the overall cheapest design when considering the life span of the platform. Considering the LCoE found in cost model research, it can be identified that the cost and cheapest platform vary from site to site, see Table 3.7. It is notable that since each model and the assumptions made in each differ the LCoE will be effected by this.

Due to the reasons highlighted above, a proposed approach would be to optimise the appropriate platforms for a given site, finding the best platform based on cost and performance. Work by Clauss et al. (123) focuses on a range of O&G platforms, which considers the notion of finding the best geometry for each platform type. It was shown that the downtime of a Semi-submersible can be reduced from 15.5% to 2.5%

Table 3.7: LCoE found in cost model literature.

Reference	Spar [Euro/MWh]	Semi-submersible [Euro/MWh]	TLP [Euro/MWh]	Water Depth [m]	Distance to Shore [km]	Farm Power [MW]
(46)	82	78	N/A	70	38	500
(46)	93	93	83	130	57.8	500
(46)	120	112	108	100	180	500
(41)	94.17	91.97	106.7	135	16	125
(29)	137.8	147.8	141.8	100	50	490
(42)	N/A	132	N/A	36	16	600
(104)	184.52	172.81	187.98	N/A	N/A	106.575
(103)	289.49	303.97	325.6	N/A	N/A	106.575
(101)	N/A	415	N/A	90	25.5	106.57
(101)	N/A	442	N/A	90	43.6	106.57
(43)	N/A	135	N/A	200	350	1000
(9; 45)	133.55	157.2	120.4	200	200	5000
(109)	161	161	161	N/A	30	30

and the sub-submersible once optimised has a decrease in 70% of vertical excitation forces due to changes in shape. The maximum cyclic tendon force is reduced by 40% for the TLP and, finally, the gravity-based structure once optimised has a decreased overturning moment by 78%. Since this work finds the optimal platform geometry for each substructure type, its cost can then be combined with a complete LCoE model which can provide even more insight into which platform is best in a monetary sense, considering the energy produced. Bracco et al. (15) also propose the inclusion of energy performance and a more detailed cost model for each platform in future work, which takes into account manufacturing costs, as well as other related costs.

Semi-submersible

The Semi-submersible has been highlighted as a good option in (122; 128; 129; 132; 133; 135). It has been observed that by adding heave plates, a greater reduction in the acceleration of the nacelle can be observed than by increasing the radius of the platform (122). By adding a heave plate it not only adds mass lowering the centre of gravity but it increases the added mass in the heave and pitch direction. This also reduces the natural frequency in both directions, augmenting the natural frequency,

pushing them away from the most energetic wave periods. This is the reason the motion of the platform and there for acceleration is reduced. This could be a cheaper alternative to achieve the desired response at a lower cost without making the platform larger. Drawing a comparison between platforms which are characterised by the same nacelle acceleration with and without heave plates could also provide useful insight. This consideration could, potentially, make the semi-submersible competitive against the low cost TLP described in previous works. Lemmer et al. (135) focus on optimising Semi-submersibles with heave plates and it was found that the platform with the shallowest draft provides the lowest nacelle acceleration and is the best at rejecting disturbances. Ferri et al. (129) found that for both sites analyses the general trend is for increased overall radius (WPA), and narrow, intermediate draft columns, to obtain the best trade-off between cost and performance.

Spar

In 2018, it was found that the optimised Spar had 80% of the original floater steel mass, and around 44% less ballast (89). It was also found that the optimised Spar had not only reduced mass but improved performance compared to the original design (137; 138). Similarly, in 2019, Leimeister (136) proved that the 7.5 MW turbine would only require a slightly larger Spar than that of the OC3 Spar for the 5 MW turbine, again verifying the OC3 Spar is over-engineered. Comparable to the work done by Leimeister et al. (89; 136; 137; 138; 141), the optimised Spar geometry in (126) also shows a maximum reduction of 23% in cost for extreme weather conditions. When fatigue constraints are added, the shape of the Spar is similar, but slightly larger, but still 18% cheaper than the initial platform. The largest reduction in cost of a Spar (33%) was found in the work by Dou et al. (139) when considering static conditions and 24% when considering dynamics within the model. Unlike any other work on the optimisation of a Spar, (142) finds the fully optimised platform to be more expensive than the initial design. Similar to work by Leimeister et al., Birk et al. (7) only optimises the Spar platform. The results give five different designs that are all optimal but perform better under different conditions. For example, one of the designs gives the smallest area under the RAO,

whereas another has the lowest draft. While both still meet the design constraints, the platform with the lower draft is expected to be cheaper in terms of CapEx. The O&M cost, however, might be cheaper for the design with the smaller response, no work has been done to consider this. The expected reason for this is the CapEx is predicted to lie between $60 - 70\%$ of the overall cost and the OpEx is only $25 - 30\%$, pushing the focus on the CapEx reduction (41). The consideration of different conditions is key in determining the best platform. This is even more relevant when considering each site will have different conditions, changing which platform is best for the site.

Hegseth et al. (131; 140) produce an optimised Spar shape similar to that of the work by (123) presenting an hourglass shape below the waterline with the addition of a traditional tapered tower. In (131) the thickness is considered to vary from Spar to tower, showing that the Spar requires thicker steel than the tower. Hegseth et al. (131) highlight the controller design as highly important to normalise the rotor speed deviation, improving it by 10.9%. In 2021, Hegseth et al. (140) found that by applying fatigue constraints, there was a constant reduction in fatigue damage of roughly 65% and an increase in the reliability index from 1.12 to 2.5. Overall, a cost reduction of $5 - 11\%$ was presented in (140), which is mainly due to improvements in the design of the platform driven by the buckling of the shell and hydrodynamic stability. This is one of the lower reductions found in this review, which is expected to be related to the consideration of structural constraints, ensuring the platform has the correct thickness of steel, which affects its cost. This is directly related to the material cost as well as the forming and welding cost. The lower expected reduction in capital cost presented in this work seems more realistic than 33%. This work has one of the most detailed cost models utilising the work by (10). It is however only limited to a Spar and the level of detail take from Farkas et al. is unknown however it does have considerations for welding, painting and forming. The work by Hegseth et al. (140) however does not predict the reduction in O&M cost which would expect a reduction since the reliability index increases, leading to a greater overall reduction in cost. A potential improvement in the work by (131; 140) would be to add an AEP model, resulting in a possibly improved outcome, since the controller is also optimised,

Table 3.8: Details of the platforms ranked in literature from best (left) to worst (right).

Reference	**Best to worst**			
(125)	Spar	TLP	-	-
(15)	TLP	Spar	Semi-submersible	-
(4)	TLP	Spar	-	-
(124)	Barge	TLP	Spar	Semi-submersible
(132)	Semi-submersible	TLP	Spar	-
(133)	Semi-submersible	TLP	Spar	-
(122)	Semi-submersible	TLP	Spar	-

improving the power output and reducing the LCoE.

Ferri et al. (128) carry out multiple optimisations with an increasing number of design variables, resulting in different values for the platform variables. The platform shape also changes depending on whether it was optimised for surge, heave or pitch. This shows that it is important to consider all motions combined to get the best overall performance.

3.5 Optimisation Framework Research Gaps

This review has highlighted some clear areas of improvement in a number of areas in the optimisation frameworks presented in current literature, in summary the gaps are highlighted below, which is followed by a more detailed explanation.

- Over simplified cost models;
- AEP models are typically not considered;
- Little variation in substructures considered;
- Turbine size considered is limited;
- Optimisation sites are generic and/or, platform applicability for a specific site is not considered. Leading to unnecessary optimisations and increased time.

In the initial research by Wayman et al. (124), areas of suggested future work included: the development of a fully integrated time domain analysis and modelling tool,

detailed design, cost analysis, structural analysis, turbine control mitigation, active or passive inertial control of the platform for motion mitigation, and, finally, careful consideration of the design of a wind turbine suitable for offshore deployment. Since then, in the past 16 years, improvements have been made in the majority of the areas that were highlighted. There are, however, still areas which could be improved. The following paragraphs summarise potential improvements.

The majority of cost models reviewed only consider the cost per unit mass of the materials used, and, therefore, the optimisation is limited to a minimisation of the amount of material used. Typically, the unit value per mass used is higher than just the material (steel/concrete/ballast) cost, in order to include consideration for other costs such as welding, painting, forming, and labour. These approaches adopt the hypothesis that all of the above additional listed costs are linearly proportional to the mass of the material considered. This may be violated, for example, when considering welding costs, since they are also related to the complexity of the structure, i.e. number of joints, the time to carry out the work, the labourer, and then any other overheads. The forming cost of the material is highly related to the thickness of the material, which in turn effects the difficult to roll the plates. When the forming process becomes difficult it requires a greater number of plates rolled at a smaller angle, increasing the number of welds.

In some cases, it would be straightforward to develop a more advanced cost approach considering these factors. For example, in the work of (131), the Spar platform is split into ten segments. This creates an opportunity to include the additional cost related to the joints between each segment. This could easily be expanded to include the cost to weld curved plates together to get the completed segment. The painting cost, rather than being related to the mass, is better described by the surface area covered, which could also include labouring, time and overhead costs. Plate forming is an important process to create the curved shells which make up the cylindrical segments. Since the scale of these parts is large, it would be done by large machinery, which would come at a cost, related to the time, labour, and overheads.

Generally, cost models use the same cost per kg value for all three platform typolo-

gies, which creates a bias based on the mass of the platforms. This is not fully justified since other factors such as forming, welding, and painting are included in the cost as well as the material cost. In fact, the simple Spar design (essentially a cylinder) has often a larger mass than a TLP or Semi-submersible counterpart, but this methodology fails to acknowledge the Spars ease of manufacturability - leading to an unfair comparison. A TLP or a Semi-submersible configuration may be more complex from a manufacturing point of view, considering the large number of main structural elements and bracings. In some instances, the cost model addresses this aspect by adding an additional complexity factor, however, calculating the additional costs would be more accurate and should be relatively easy if the geometry is known.

Based on the authors' knowledge, it would be more effective to independently optimise the platform based on cost. The output would then be combined with an external cost model to determine the total cost of the turbine and its support system. Since there are only two papers which detail other costs after finding the optimal platform, it is very difficult to determine which platform in general is the optimum solution. This is due to the huge difference in platform typologies which make them more or less suitable for a specific offshore site. This consideration must be kept in mind when comparing platforms which are from different pieces of literature. By combining the optimised platform cost with a complete model including installation, operations and maintenance, and decommissioning, the cheapest platform for a given site could be more accurately identified.

The installation cost is often expressed in terms of mass, and this may lead to inaccuracies. In cost modelling literature, the installation is often expressed as a cost per MW value, however, as found in previous work by the author, this cost also depends on vessel hire, vessel speed, fuel cost, fuel consumption, distance to site, time to install, and other parameters not usually considered in the literature. Considering there are only three operational floating offshore sites around the world, having accurate estimates for total installation time is difficult. However, it is even more challenging to determine the accuracy of assuming a cost per MW value with such little available data to validate this assumption. The inclusion of the installation cost in the GBP/kg value

seems irrelevant since, as explained, it is not only related to the geometry of the platform, and the installation technique would be different for each platform. The authors do, however, agree that if the platform is larger then there could potentially be the requirement for larger vessels and large space which need to be hired at the port to store the platform, relating these costs to the mass. Considering the size of the platform for transportation could also improve the optimisation by ruling out platforms that would not be able to be transported due to their large size. The time to complete installation will also depend on the type of platform, as the geometry and mooring arrangements are different.

A number of papers recognise the requirement for a more accurate cost model and highlight this as an important area of further research, for example in (6; 15; 131; 132). As mentioned in Section 6.1.5, not all optimisation frameworks include cost models, however, by improving the performance of the system, the over arching aim is to achieve a positive effect on the cost. A method to quantify the positive impact on cost would be an interesting addition to these pieces of work. For example, the improvement in terms of reliability derived in (141) could be translated to decreased operation and maintenance costs, and potential life extension. Similarly, improving the dynamic response of the platform should improve the AEP, therefore reducing the LCoE. Only two of the papers included in this review consider the AEP, however, the impact of the platform's dynamic responses on power production is neglected. Recent work by Amaral et al. (174) has created an AEP model that can be used in the time or frequency domain, considering platform motions. This could be a potential addition to optimisation frameworks in finding the LCoE value.

An enhancement which could be included in future work would be the platform applicability for each site. For example, a Semi-submersible might be the cheapest option, but it could be inappropriate for the sites characteristics, however, in these same conditions a Spar might be better. Similarly, if the water depth is limited to around 100 m, the Spar is not really an option, considering modern large floating wind turbine rating (15-20 MW). Weighing up the different considerations of the site and introducing this into the determination of the best platform for a specific site would

be highly valuable. Lerch et al. (46) (Table 3.7) show that the cost of the wind farms does change for the three proposed sites, which is in line with the authors' views, and confirms the consideration of each platform's cost at each specific site would be important, rather than predicting which platform is better than another in generic terms.

Another key takeaway is that the majority of work focused on Spar platforms, probably due to their simplicity and early deployment. There have been some studies (4; 15; 122; 123; 124; 125; 132; 133) comparing the three platform typologies. The authors recognise that including all three platform geometries creates a large design space, which is computationally very expensive to explore. A potential solution could be the development of a "preliminary concept selection" process to determine which platform is most appropriate for a given site. The elimination of even one design option would still reduce the optimisation time by around a third.

An important finding in this review was the repeated use of the 5 MW NREL wind turbine. The 15 MW IEA wind turbine was only used once for the Spar geometry. Since there has been such a rapid expansion in the size of wind turbine technology, lessons from the optimisation of the 5 MW turbine can be used to expand all platform typologies to the 15 MW wind turbine. The scaling method used in (136) to expand from 5 MW to 7.5 MW could be a useful addition to optimisation frameworks, allowing a range of different wind turbines to be used in one framework, improving its flexibility.

Similar to the suggestions of Wayman et al. (124) the author expects the future work within this area will produce well-rounded multi-disciplinary models considering cost, energy production, structural, statics and dynamics of the platform together to find the most optimal platform which has been tested in a number of different load cases for six DoF. To reduce the computational expense linked to the expansion of current models using a platform selection tool as a pre-filter step for each specific site should also be considered. A shift to 15 MW and greater turbines is indefinitely the future of this area of research.

Overall, the work described above highlights the huge potential of implementing optimisation techniques within the industry in order to explore a wide range of platform

geometries. An overview of everything discussed in Section 3.3 can be seen in Table 3.9 below. It is clear from this review that optimisation is a very powerful tool which could be used to designers' advantages to explore a wide range of designs, quickly discarding unacceptable designs.

Ref.	**Support Structure**	**Wind Turbine Power (MW)**	**Systems Considered**	**Optimisation tool**	**Domain Analysis**	**Objectives**	**Constraints**	**Design Variables**	**Software Used**
(131)	Spar	10	Platform, Tower, Mooring system and control system	Sparse Nonlinear OPTimizer, SNOPT	Frequency domain with time domain verification	Power quality and system cost	Spar: Fatigue damage (FLS): Shell buckling, Panel ring buckling, Column buckling, limit states(ULS), extreme response. Tower: Fatigue damage (buckling stress). Mooring system: max mooring tension, only horizontal anchor tension. Control system: Closed-loop poles must have negative real parts (ensure stability)	Spar: Section length, diameter, thickness, and T-ring stiffer: distance between stiffeners, thickness, and length of web and flange. Tower: Diameter and wall thickness. Mooring System: diameter, total line length, depth of fairlead below SWL and horizontal distance between anchor and fairlead. Control System: Proportional and integral gain	SIMA
(132)	Spar, Semi-submersible and TLP	5	Platform, mooring	Cumulative Multi-Niching Genetic Algorithm CMN GA	Frequency Domain	Minimise cost and root mean square nacelle accelerations	Minimum and maximum bounds on radii of cylinders, structural cost capped ($\$9 million$), static pitch angle limited to 9 degrees, dynamic pitch angle limit 10 degrees, mooring line slackness variation cannot be greater than 3 times the steady state line tension	Platform: Inner cylinder draft, radius, top taper ratio, number of outer cylinders, outer cylinder radius array, radius, draft, and radius of the heave plate. Truss member radius based on critical buckling load. Mooring System: Number of lines, length, fairlead position, and type of mooring system (catenary or taut). Anchor depends on mooring system variables	WAMIT and FAST
(133)	Spar, Semi-submersible, Cylinder, Barge, Ring and sub.	5	Platform	fminsearch MATLAB	Frequency domain	Minimise root mean square nacelle accelerations	Hydrodynamic properties	Hydrostatic stiffness's and wave excitation coefficients (added mass, damping, stiffness, and wave excitation)	WAMIT and FAST
(122)	Spar, Semi-submersible and TLP	5	Platform, Mooring and Wind Turbine	Multi-objective Genetic Algorithm	Frequency Domain and time Domain Verification	Minimise cost and maximise performance (stability and nacelle acceleration)	Minimum freeboard 5m, minimum and maximum for each design variable, diameter is not less than tower base diameter, truss diameter based on critical buckling load, platform must be less the 9 million, nacelle acceleration limited to $1 m^2/s$, maximum degree of steady-state pitch angle, and constraint of the anchor line.	Inner cylinder draft, the inner cylinder radius, the top tapper ratio of inner cylinder, number of outer cylinders, the radius of outer cylinder array, the outer cylinder draft, the outer cylinder radius,the outer cylinder heave plate radius, Xm which determines which mooring arrangement is used.	WAMIT and FAST

(141)	Spar	5	Support Structure	Non-dominated sorting genetic algorithm II from Platypus	Time domain	Increase reliability, avoid oversized design (reduce cost), horizontal nacelle acceleration, system inclination angle, and dynamic translational motion to be used in the objective function	Design variables constraints, bending stress at the base of the tower, tensional stress of the mooring line, nacelle acceleration, angle of inclination, and translational motion	Spar base diameter, height, ballast density and height	MoWiT
(123) (O&G)	Spar, Semi-submersible and TLP	N/A	Support Structure	Nonlinear programming - Tangent search method	N/A	Minimise double amplitude of forces and motions	Design variable constraints and floating stability variable to determine platform type. Gravity Base: Radius vector for first and last point column, cross-sectional area and its shape, volume, centre of buoyancy.	TLP: Displacement distribution, cross-sectional area of the column and column spacing. Cassion Semi-submersible: Vertical location of the center of buoyancy, the waterplane area, the draft and the bottom area) Semi-submersible: displacement ratio , buoyancy distribution of pontoons, cross section area in the middle of pontoons, diameter of hemispheres at both ends of pontoons	WAMIT
(124)	Spar, Semi-submersible and TLP	5	Support Structure	N/A		Surface area reduction (reduce cost)	draft constraints, sufficient restoring coefficient (in pitch) and TLP mooring line restoring	Spar and Barge: Radius and height structure and ballast height. Additional terms of Trifloater: Number of cylinders, radius from origin to outer columns, height and radius of outer columns	WAMIT and FAST
(130)	Spar	5	Support Structure			Maximise power		Support structure radius and draft	
(136)	Spar	7.5	Support Structure	Non-dominated sorting genetic algorithm II	Time domain	Minimise inclination angle, translational motion and horizontal nacelle acceleration	Design variables bounded, ballast height cannot exceed bottom cylinder height, bounds on the angle of inclination, translational motion, and acceleration of the nacelle	Bottom cylinder diameter and height, ballast density	MoWiT

(142)	Spar	15	Support structure and mooring system	Sequential Quadratic Programming and relaxation induced neighbourhood search	Frequency Domain	Minimise cost of substructure and mooring system in terms of mass	Pitch motion, nacelle acceleration and pitch angle, static pitch and surge, design variable constraints (ensure non deformed shape) - buoyancy centre, mooring line length, vertical force fairlead and Spar body/head diameters and natural frequencies	Length of main cylinder, diameter of Spar body and head, depth of the fairlead, anchor radius and mooring line length	FAST, QuLAF
(134)	Cylindrical body	5	Support structure (heave plates)	N/A	Frequency and Time domain	Maintain stability	Floater radius and draft, heave plate span, metacentric height, maximal tilt angle, maximum pitch angle, maximum acceleration of nacelle		DIODORE, DeepLines
(7)	Spar		Support structure	Multi-objective Evolutionary Algorithm, ϵ-MOEA	Frequency Domain	Minimise double amplitude of heave motion, heave resonance and draft (cost and location consideration)	Design variable constraints, minimum metacentric height, heave response and maximum diameter of cylinder	3 sections: 3 area ratios, length ratios and lengths and draft	WAMIT
(4)	Spar, Semi-submersible and TLP (5 platforms)	5 and 10	Support structure	Genetic Algorithm		Minimise weight (cost) but ensure buoyancy and static stability	Minimum draft, Metacentric height, freeboard and maximum static pitch angle Spar: height, diameter, ballast height, seawater height	TLP: Central column diameter, platform height, hexagon radius, ballast mass and ballast distance above sea level	
(139)	Spar	10	Support structure and mooring system	Sequential Quadratic Programming	Frequency Domain	Minimise mass (therefore cost)	Pitch motion, nacelle acceleration, natural frequencies (related to design variables), pitch angle and surge motion max and min of mooring line length as well as maximum percentage of mooring line suspended on the sea bed and design variable upper and lower bounds	Spar: draft, upper and lower diameter. Mooring system: Length line, fairlead position and anchor radius	QuLAF and FAST
(138)	Spar	5	Support structure	Non-dominated Sorting Genetic Algorithm, NSGA II	N/A	Minimise motions (acceleration, inclination and translation); this in turn reduces size of platform and cost	Design variables limits, inclination angle, acceleration and transitional motion	Spar diameter, height and ballast density	MoWiT

(137)	Spar	5	Support structure	Non-dominated Sorting Genetic Algorithm, NSGA II	N/A	Maintain performance (rotational stability, translational motion and nacelle acceleration) and minimise cost	Top diameter (to ensure tower fits), elevation of top diameter, upper cylinder length, and taper length all fixed, lower and upper bounds for the design variables, minimum draft, maximum inclination angle, static displacement, max nacelle acceleration	Length and diameter of the lower cylinder and ballast density	MoWiT
(125)	Concrete ballasted cylinder (Spar, barge, TLP	5	Support structure, mooring system and tower	N/A	Frequency domain	Minimise nacelle accelerations	Minimum restoring force (avoids pitching more than 10 degrees), heel angle, dynamic displacements (pitch), mooring line tension should not exceed break load but cannot become slack, and cylinder design variables are constrained	cylinder radius and draft, mooring system defined by: Water depth, line tension and angle between free surface and anchor line	LINES, WAMIT, FAST
(126)	Spar	5	Support structure, mooring system and power take off cable	Non-Linear Programming by Quadratic Lagrangian, NLPQL	Frequency domain	Minimise Spar, cable and mooring line costs	Heave and pitch period, mooring line tension, minimum fatigue life, Spar buoy motion and inclination, Spar draft, nacelle acceleration, cable curvature and tension	Spar mass, height and diameter of each segment, thickness of bottom plate and vertical position of fairlead, mooring line and cable: Line direction, pretension, segment length, diameter and net submerged weight	MIMOSA, WAMOF3
(8)	Tension-Leg-Buoy	5	Support structure and mooring system	Bound Optimization BY Quadratic Approximation (BOBYQA)	Frequency Domain and Time Domain	Reduce mooring forces and hence steel mass (cost)	natural frequency (avoid 1P and 3P), minimum mooring line tension, maximum axial stress in the space frame Mooring line: anchor radius , lower and upper mooring line diameter, yaw stiffness	Support structure: outer diameter of the lower floater part, height of the middle section below WL, lower and upper mooring line prestrain, distance between column and turbine centre line, outer diameter of vertical columns in space frame.	3DFloat
(140)	Spar	10	Support structure and tower	Sequential Quadratic Programming (SQP)	Frequency domain	Minimise cost of tower and Spar	Fatigue damage of tower and support structure, global buckling of tower, maximum platform pitch, avoid heave resonance, geometrical constraints to ensure structure is realistic	Platform and tower segment diameters and thickness and the length of the support structure segments	
(128)	Semi-Submersible	10	Support structure, mooring system	Genetic Algorithm	Time and frequency Domain	Minimise RAO (pitch, heave and surge)	Geometrical constraints, avoid natural frequencies, maximum pitch angle, maximum platform offset, minimum length of mooring cable on seabed, total mass maximum	Columns diameter, platform radius, draft, fairlead position and cable length. Anchor radius and unstretched mooring line length	FAST, ANSYS AQWA, WAMIT
(15)	Semi-Submersible, Spar and TLP	5	Support structure	Genetic Algorithm	N/A	Minimise cost	Design variable bounds, metacentric height must be greater than 1 m, draft must be greater than 10 m, freeboard height must be larger than 5 m, maximum pitch angle should be lower than 5°, minimum freeboard, limited intact inclination angle of 6 and 12 for normal and survival conditions.	Spar: Diameter, height, seawater height and ballast height. Windfloat: Diameter, Height, length, and heave plate height. Pelastar: Column height and diameter, hull diameter and depth, arm radius, and concrete volume. Windstar: Column height and diameter, arm radius and depth, and support radius	N/A

(6)	Cylindrical body	Multi-megawatt	Support structure	Cumulative Multi-Niching Genetic Algorithm CMN GA	N/A	Reduce mass	Minimum buoyancy requirement, maximum stress occurring allowed in the structure, maximum cover angle	Cylinder length, inner and outer pipe diameters, inner and outer pipe thickness, the thickness of steel and concrete covers, angle of the covers and expansion coefficient	Ansys SOLID186, FLEX5
(135)	Semi-submersible	10	Support structure and control system	N/A	Time domain	Maximise power, minimise nacelle acceleration and cost	Design variables and pitch natural frequency	Column spacing, heave plate height, column radius, heave plate radius, draft, steel tripod strut width and thickness, mooring line fairlead position and wind turbine controller gains	Validated with FAST, Ansys aqwa-line
(129)	Semi-submersible	10	Support structure	Genetic algorithm	Frequency domain	Minimise tower base bending moment and platform costs	Maximum pitch 5 degrees and maximum surge motion 15% of water depth, for the catenary system at least 1/10 of the line must lie on the seabed	Column diameter, depth column, draft, platform radius, and unstretched mooring line length	FAST

Table 3.9: Optimisation overview.

3.6 Conclusion

Given the steady growth in global demand for energy and the need to tackle climate change, it is imperative to decarbonise the power grid through the advancement of alternative energy sources. Fixed offshore wind technology has already established its viability; however, with the majority of nearshore locations now extensively utilised, the pursuit of more remote deep water offshore sites has become indispensable to sustain and fulfill the increasing energy requirements. This has created a gap in the market for floating offshore wind. Since there is a greater, more consistent resource further offshore it creates potential for more efficient, cost-effective solutions. However, with new technology comes inherent risk and cost. Focusing on key areas which could benefit from cost reduction, could seek out a more competitive energy source in floating offshore wind. Honing in on the areas where cost reductions can be made is the key. Since CapEx makes up the majority of cost, at 70% overall, it is a cost which would benefit from a reduction. The offshore turbines and the floating platforms are the highest contributors to CapEx. The turbines have a high TRL, whereas the floating support structures are relatively novel with only three operational floating wind farms around the world. This highlights the platform as a key area for improvement and learning to reduce the cost.

This review has shown that an optimisation framework to find the most optimal platform could be a fundamental tool in exploring a wide design space to find the best solution since the industry lacks maturity. The reduction in cost related to the optimisation of the platform is hoped to make floating offshore wind more competitive with other energy sources and reduce reliance on finite energy sources.

The purpose of this chapter was to identify the understanding matured and the knowledge gaps yet to be addressed in the current literature on the area of optimisation of floating offshore wind turbine support platforms. By finding potential weaknesses in the current work it is hoped they can be improved to help find the cheapest platform for a given site, in the least computationally inexpensive way.

This review has highlighted that there has been relatively little amount of work done on the optimisation of floating offshore platforms. However, from the research

carried out a signification amount focused on Spar platform optimisation (48%), with several papers (32%) considering all three platform types, with a relatively simplified geometrical model. Focusing more work on the optimisation of floating offshore platforms with more detailed work on each individual platform is expected to find new competitive solutions in the future.

Although there is little literature in this area, one of the main findings from this review is there is no universal solution, the site characteristics will play a huge part in deciding which platform is 'best'. For this reason, this work proposes a solution in the form of a concept selection tool. Prefiltering before the optimisation to optimise only platforms which are appropriate for the site would be hoped to reduce computational time and give realistic solutions.

The developments in the fixed offshore wind industry as mentioned in this review have already well surpassed the common 5 MW turbine, with this in mind only 4% of current literature uses the IEA 15 MW turbine. For academia to make improvements it is important to keep up with industry trends, for this reason, the author's view is to consider turbines 15 MW and greater for future work in this area.

It has been made clear through this work that cost is the main driver, being considered as the objective in 82% of current literature. The remaining literature is expected to be indirectly linked to the cost since for example reducing platform response will reduce ultimate and fatigue loads, impacting the operations and maintenance cost positively. This is an important factor in most industries since one of the main objectives is to make the technology more cost competitive. The other objective which was consistently found in the literature was the platform response at 52%, again this was highlighted as also being linked to the cost of energy since the response will affect not only power production but the loading experienced by the platform.

Given the importance of finding the cost accurately, several areas of improvement and further research have been identified for the cost models used within the optimisation approaches reviewed. Improvements could be made to include welding, paint, forming, and other overhead costs, with little effect on the computational time. Furthermore, by more accurately comparing the cost of different platform typologies, it is

hoped that any bias created by the fact of considering all the costs proportional only to the mass of the material used could be removed. If, rather than CapEx, the focus is on optimising the LCoE or an equivalent, a better prediction of support structure geometry which will generate the most affordable energy could be found. It has been highlighted here that there is a need for a better AEP model as well to be developed and included, to find the cost of energy of each platform.

The most common constraint was on the platform response (93%) followed by the design variables of the floating platform (79%). The importance of platform response for the overall operation of the system has been highlighted as important, hoping to improve energy production, increase the life span and reduce maintenance costs. The inclusion of constraints on the design variable is expected to seek out solutions which are feasible, manufacturable, and transportable while reducing computational time.

Since the majority of work carried out has been related to straight sided columns to make up the floating platforms, exploring less traditional shapes could seek out a cheaper option, if the models were combined with better cost models. Similarly, including the scantling design would be interesting since this would also affect the cost of the platform.

Overall the potential future improvements found from this literature review are, the flexibility to include more than one turbine size, more detailed platform modelling, and a concept selection tool. This review has highlighted how useful optimisation could be in this field however gaps within the current research have been highlighted which could be improved on to further help find the best solution for a site, considering both cost and performance to help provide more competitive green energy sources to help decarbonise the grid.

Chapter 4

Model Development

The developed model and sub-models are presented in Figure 4.1, showing the inter-dependencies on each other. The subsequent sections detail each of these sub-models.

4.1 Geometrical Model

The goal of this work is to explore different geometries, including traditional straight-sided (SS) columns and non-traditional truncated cones (TC), allowing new geometries to be explored. For this reason, this work allows the geometry of each segment to vary to find the most optimal design. See Figure 4.2 for an example. The variables used to describe this geometry are overall length (L_o), the segments' radius (R_i), shell thickness (t_i) and length of individual segments (L_i).

The geometry presented in Figure 4.2 is used to describe all columns within this work, where bracings are present, they are expressed as cuboids shown in Figure 4.3.

The platforms considered in this study are a semi-submersible, a tension leg platform (TLP), and a spar. The spar is represented by a cylindrical column with a tapered upper section, reflecting geometries used in projects such as Hywind Tampen and Hywind Scotland. Semi-submersible designs vary considerably; however, there is increasing convergence towards a four-column configuration with a central column connected by bracings. The turbine is mounted on the central column, which provides structural stability and optimal load distribution. This central column arrangement has been

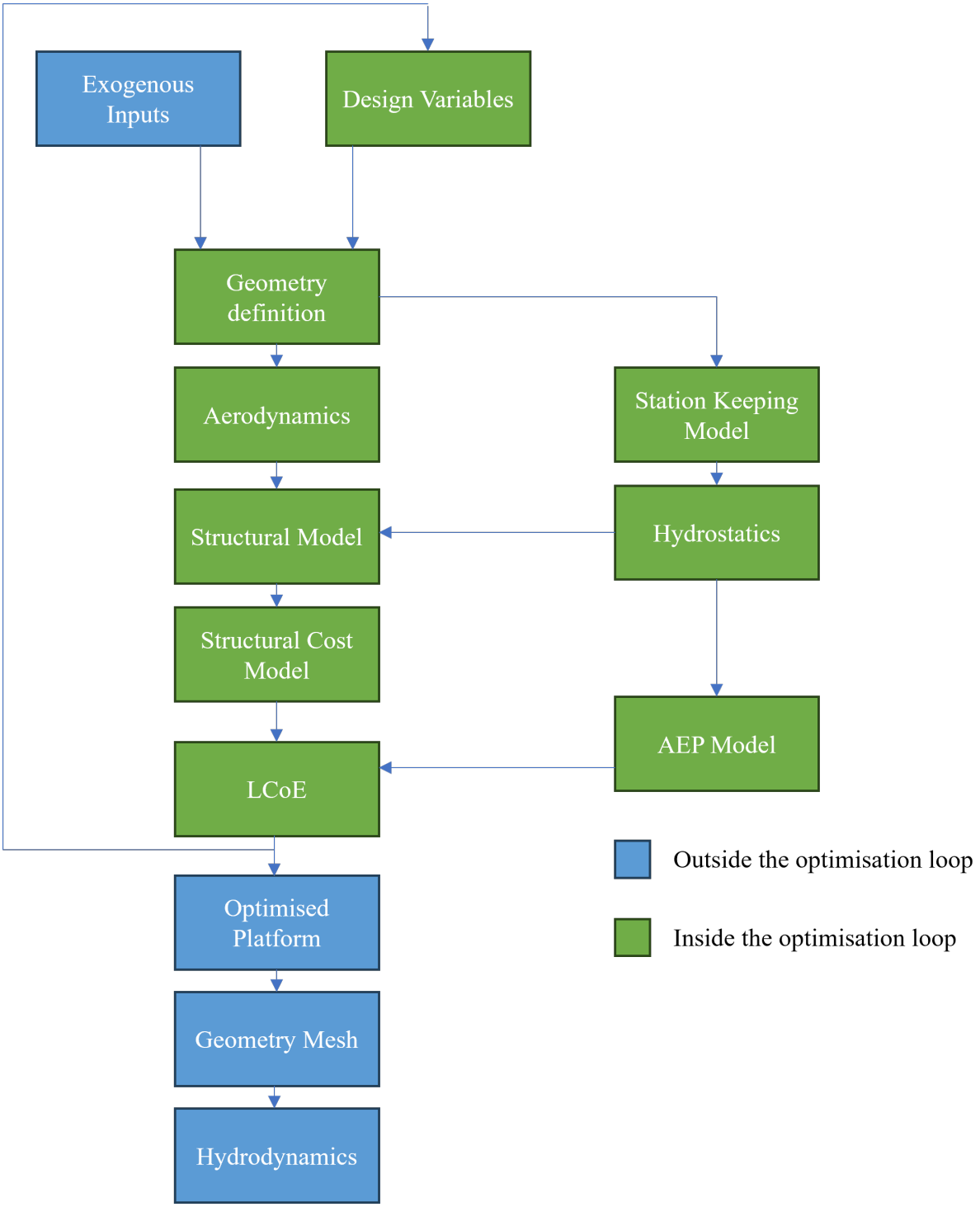

Figure 4.1: Model flow chart.

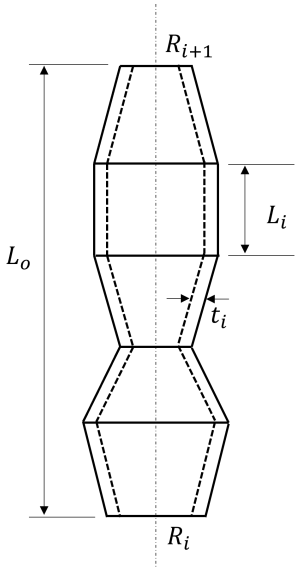

Figure 4.2: Column geometry example, where L_o is overall length, R_i is The segments radius, t_i is shell thickness and L_i is the length of individual segments

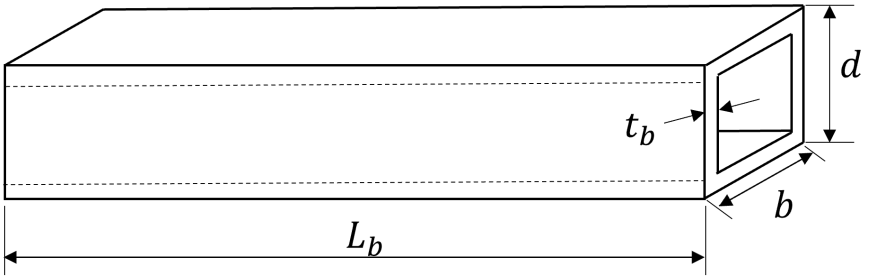

Figure 4.3: Bracing geometry example, where L_o is overall length, R_i is The segments radius, t_i is shell thickness and L_i is the length of individual segments

identified as the most suitable option for a 15MW turbine (175). This study highlights central column configurations offer superior performance for large floating offshore wind turbines. They simplify ballast distribution, reduce design complexity, and provide better overall stability compared to off-centred layouts. This arrangement also achieves key design metrics with significantly less hull steel mass, making it more efficient and cost-effective for scaling up to 15MW turbines and beyond. For this reason, the UMaine design has been selected as the reference for this study, owing to its configuration, frequent use in research, and the availability of detailed geometric data. Finally the TLP selected for the base line was the pelastar design, since it has been frequently used in literature with available dimensions.

4.2 Structural Model

The structural model implements a method to calculate the required scantling in a quick, yet efficient first estimate utilising DNV standards (176). Section 4.2.1 firstly presents the consideration for manufacturability. This is followed by shell thickness calculation in Section 4.2.2 and the stiffener sizing in Section 4.2.3.

4.2.1 Manufacturing Considerations

Manufacturability is a huge constraint within the industry, which is missing from current research. The first consideration was linking the number of segments to the available plate sizes, allowing for more realistic segments and a more accurate calculation of the manufacturing cost. Similarly, the number of plates which needed to be rolled to create one segment was considered. This information was found in (19; 20), and it was noted that the thickness of the plate used affects the maximum size available. See Table 4.1 for the values.

Thickness (mm)	Length x Width (mm)	Length x Width (mm)	Length x Width (mm)
6	12000 x 2000	12000 x 2500	12000 x 3050
8	12000 x 2000	12000 x 2500	12000 x 3050
10	12000 x 2000	12000 x 2500	12000 x 3050

12.5	12000 x 2000	12000 x 2500	12000 x 3050
15	12000 x 2000	12000 x 2500	12000 x 3050
20	12000 x 2000	12000 x 2500	12000 x 3050
25	12000 x 2000	12000 x 2500	12000 x 3050
30	12000 x 2000	12000 x 2500	12000 x 3050
35	12000 x 2000	12000 x 2500	12000 x 3050
40	12000 x 2000	12000 x 2500	12000 x 3050
45	12000 x 2000	12000 x 2500	12000 x 3050
50	12000 x 2000	12000 x 2500	12000 x 3050
55	12000 x 2000	12000 x 2500	12000 x 3050
60	12000 x 2000	12000 x 2500	12000 x 3050
65	12000 x 2000	12000 x 2500	12000 x 3050
70	12000 x 2000	12000 x 2500	12000 x 3050
75	12000 x 2000	12000 x 2500	12000 x 3050
80	12000 x 2000	12000 x 2500	12000 x 3050
85	12000 x 2000	12000 x 2500	12000 x 3050
90	12000 x 2000	12000 x 2500	12000 x 3050
95	12000 x 2000	12000 x 2500	12000 x 3050
100	5000 x 2000	5000 x 2500	7500 x 3050
110	5000 x 2000	5000 x 2500	5000 x 3050
120	5000 x 2000	5000 x 2500	5000 x 3050
130	5000 x 2000	5000 x 2500	
140	5000 x 2000	5000 x 2500	
150	5000 x 2000	5000 x 2500	
160	4000 x 2000		
170	4000 x 2000		
180	4000 x 2000		
190	4000 x 2000		
200	4000 x 2000		

Table 4.1: Plate sizes (19; 20).

The relationship between plate height, width, and thicknesses provided in Table 4.1 was also considered in the work, rather than values to decimal points which are not standard and cannot be manufactured at a cheap price. Unlike all other work in this area, there is the option to decide between four different stiffener geometries: tee, equal and unequal angle, flat, and box. This was considered to determine which was cheapest, it was found that for a given inertia the tee and angle stiffener was the cheapest, followed

by box and flat. See Table 4.2 for the standard dimensions.

Height (mm)	Width (mm)	Thickness (mm)
60	60	6
65	65	7
70	70	8
75	75	9
80	80	10
90	90	12
100	100	13
110	110	15
120	120	16
130	130	18
140	140	20
150	150	25
160	160	
180	180	
200	200	
250	250	
300	300	
350	350	
400	400	
450	450	

Table 4.2: Stiffener sizes (21; 22).

Similarly to the plate size, the same considerations were made for the stiffeners used, only utilising standardised sizes.

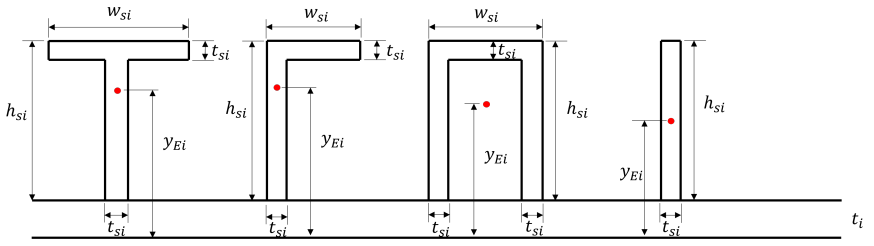

Figure 4.4: Different stiffener geometries in this work, where width is w_{si}, height is h_{si}, thickness is t_{si}, and y_{Ei} is the centre of mass.

By making these considerations it is hoped a more accurate and realistic representation of the manufacturing cost could be determined, and the values can be easily

altered to suit the manufacturing capabilities and avoid custom parts.

4.2.2 Shell Considerations

Firstly, the shell stress must be calculated for the cylindrical components. To find the stress DNV-RP-C202 was applied, similar to work (10; 168; 176) for a conical shell loaded by external pressure. This standard is applicable for a shell segment between two ring-stiffeners of radii R_i and R_{i+1}, and the buckling constraint is valid for circular cylindrical shells with equivalent radii.

The angle between the two radii can be found using Eq. 4.1.

$$\alpha = \tan^{-1}\left(\frac{R_{i+1} - R_i}{L_o}\right), \tag{4.1}$$

Where $i = 1, 2, ..., Nos$. Using α, the equivalent radius of each segment can be found.

$$R_{ei} = \frac{R_{i+1} + R_i}{2cos\alpha} \tag{4.2}$$

The equivalent thickness and length can be found Eq. 4.3 and 4.4.

$$t_{ei} = t_i cos\alpha \tag{4.3}$$

$$L_{ei} = \frac{L_i}{cos\alpha} \tag{4.4}$$

The normal stress due to external pressure and critical stress in each shell segment is presented in Eq. 4.5.

$$\sigma_i = \frac{\gamma_b p R_i}{t_{ei}} \leq \sigma_{crit} = \frac{f_y}{\sqrt{1 + \lambda_i^4}} \tag{4.5}$$

The variable p is the pressure, which is assumed to be the maximum hydrostatic pressure found at the maximum draft. The other variables in this formula can be calculated using Eq. 4.6-4.10.

$$\lambda_i = \sqrt{\frac{f_y}{\sigma_{Ei}}} \tag{4.6}$$

$$\sigma_{E_i} = \frac{C_i \pi^2 E}{12\left(1-\nu^2\right)} \left(\frac{t_{e_i}}{L_{E_i}}\right)^2 \tag{4.7}$$

$$C_i = 4\sqrt{1+\left(\frac{0.6\,\xi_i}{4}\right)^2} \tag{4.8}$$

$$\xi_i = 1.04\sqrt{Z_i} \tag{4.9}$$

$$Z_i = \frac{L_{Ei}^2}{R_{ei} t_{ei}} \sqrt{1-\upsilon^2} \tag{4.10}$$

In the case where bracings are required, for a TLP or Semi-submersible, the necessary thickness to meet the buckling constraint of the bracing will also be required. Considering the cross-section, as seen in Figure 4.5, the stress can easily be found:

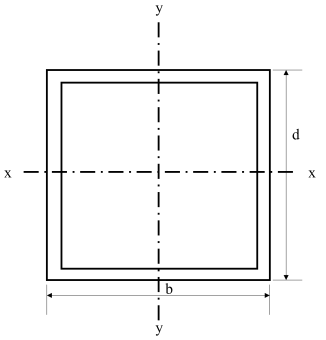

Figure 4.5: Cross section of the bracing.

$$\sigma_{yy} = \frac{M_{yy}}{I_{yy}} \tag{4.11}$$

The bending moment in a TLP's leg is caused by the tension applied at the connection point of the mooring line. In this case, the connection point is assumed to be at the end of the leg. This tension is a downward force that creates the bending moment in the leg. The second moment of inertia of the bracing can be found:

$$I_{b_{yy}} = \sum \left(\frac{db^3}{12} + A_i d_i^2\right) \tag{4.12}$$

The first component in the formula of inertia is the moment of inertia of the individual

segment about its own centroid axis. The second component is the parallel axis theorem which considers inertia in relation to the centre of the global system. The provided moment by the stiffener must be greater than the yield stress of the material, depending on the thickness, see Table 4.3 for the yield stress of S355 steel.

Thickness (mm)	Minimum Yield Stress (MPa)
3-16	355
16-40	345
40-63	335

Table 4.3: Yield stress of S355 for different thicknesses (23).

4.2.3 Stiffener Sizing

The other structural check which is required is to ensure the stiffener provides a large enough inertia (177). This is done by comparing the inertia of the stiffeners against the required inertia, see Eq. 4.13 (10).

$$I_{yy} \geq I_{\text{req},i} = \frac{\gamma_b p R_i R_{E_i}^2 L_{\text{ef},i}}{3E} \left[2 + \frac{3E y_{E_i} \cdot 0.005 R_i}{R_{E_i}^2 \left(\frac{f_y}{2-\sigma} \right)} \right] \tag{4.13}$$

$$L_{efi} = 1.56\sqrt{R_i t_i} \tag{4.14}$$

The methodology presented to determine the structural geometry of each platform has its limitations which are discussed in the following paragraphs:

Using DNV-RP-C202 as the sole basis for determining shell thickness in floating platforms constructed from conical shells under external hydrostatic pressure introduces several limitations. While the recommended practice provides guidance for buckling and strength under external pressure, it is primarily developed for cylindrical shells and does not fully capture the complex stress distribution and local instability phenomena in conical geometries. Conical shells experience non-uniform curvature and varying stiffness along their length, which can lead to stress concentrations and buckling modes that differ significantly from those assumed in the standard [Farkas and

Jármai, 2008; Farkas and Jármai, 2013; DNV, 2002]. Moreover, this approach considers only the maximum hydrostatic pressure and neglects other critical environmental loads such as wind, wave, and current-induced forces, as well as dynamic effects from turbine operation. These additional loads can significantly influence stress patterns and fatigue life, particularly at highly stressed regions like the tower base. Ignoring tower base fatigue during design can lead to underestimating long-term damage accumulation, compromising structural reliability and safety. Although stiffeners designed according to Eurocode 2005 can ensure sufficient inertia relative to required stiffness, the interaction between shell buckling and stiffener performance under combined loading remains highly sensitive to imperfections and load eccentricities. Without a full finite element analysis (FEA) and coupled hydro-aero-servo simulations, these interactions remain approximated, potentially resulting in conservative or unsafe designs. To achieve classification approval, a complete structural verification process is required. This typically includes:

Fully coupled dynamic analysis (hydro-aero-servo) to capture turbine, platform, and control system interactions under operational and extreme conditions. Global and local finite element modelling to assess stress distribution, buckling behaviour, and fatigue life under combined loads. Ultimate and accidental limit state checks for all relevant load cases, including environmental and operational scenarios. Fatigue analysis at critical points such as the tower base and connections, using long-term load histories. Compliance with classification society rules (e.g., DNV-ST-0119 for floating wind) and integration of design safety factors.

In summary, while DNV-RP-C202 and Eurocode provide useful baseline checks, they should be complemented by advanced numerical modelling, fatigue assessment, and full coupled analysis to meet classification requirements and ensure structural integrity for conical shell configurations in floating platforms.

4.3 Cost Model

The cost has been used within the objective function in the majority of work, and if not directly present it is indirectly linked to finding the optimal platform (94). Since current literature assumes the total platform cost is based on the material mass alone, sometimes utilising a higher density of steel or complexity factor to consider other manufacturing costs, a more accurate cost estimate is required. In the present work, a more detailed approach has been applied to determine if a bias has been created towards platform mass and to determine if non-traditional geometries are cheaper when the manufacturing cost is considered. In order to determine the manufacturing cost of the floating platform, (10; 131; 168) were used as a basis. The cost can be split into four main categories: material, forming, welding, and painting. The welding contribution can be further broken down into welding the segments from plates, welding the stiffeners from parts, welding the stiffeners to the shell, assembly of segments, and finally, welding each segment together to create the full structure. As an example, Figure 4.6 highlights the contribution of each to the overall cost of a steel column. This figure shows that using material mass alone leads to a large under-prediction of total cost. It is expected that by increasing the complexity, for example, Semi-submersible and TLP, this cost will be even less accurate.

Since the substructure costs are considered in isolation, a discount rate is typically not applied because there are no time-distributed cash flows to convert into present value. Discounting is relevant for full project-level financial models that include capital expenditure, operational expenditure, and revenues over multiple years, whereas substructure cost estimation is a static exercise focused on physical cost drivers such as materials and fabrication. Applying a discount rate without considering other components would introduce unnecessary financial assumptions and distort comparisons, as the discount rate reflects overall project risk and financing rather than individual component costs. Similarly, inflation has also been neglected, as this analysis does not account for time-based cost escalation and focuses solely on present-day cost estimates for comparative purposes. For the presented reasons, both discounting and inflation

are excluded from this model.

A key factor influencing substructure costs is the location of fabrication. Regional cost variations can arise due to differences in labour rates, material availability, supply chain maturity, and logistical constraints. For example, manufacturing in regions with established offshore wind infrastructure may reduce costs through economies of scale, while remote locations could incur higher expenses due to transport and limited facilities. While this is an important consideration, a detailed analysis of regional cost scenarios is outside the current scope of this work. However, it is recommended for future research to incorporate these variations to provide more accurate and region-specific cost estimates, which might change which platform is most suitable for a specific site.

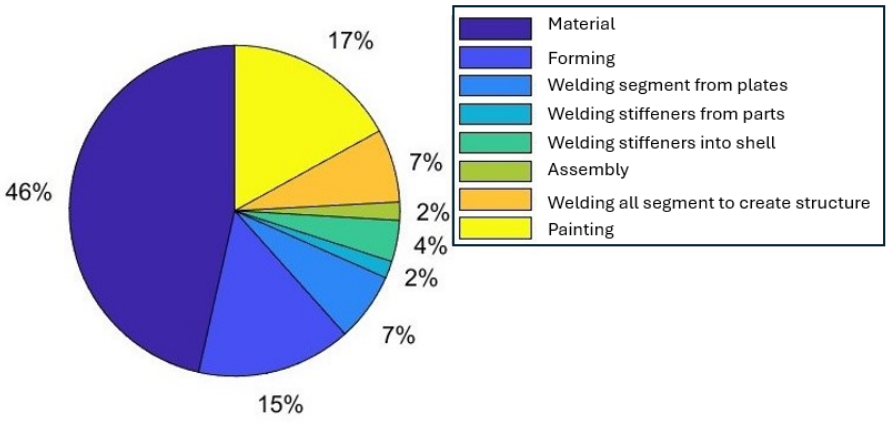

Figure 4.6: Cost breakdown of the tapered column presented in (10).

The fabrication process is used to methodically calculate the cost, see Figure 4.7. The red zig-zag lines represent the weld.

The total cost of the floating structure can then be determined by summing each of these cost components, see Eq. 4.15.

$$K_T = K_M + K_{F0} + K_{F1} + K_{F2} + K_{F3} + K_{F4} + K_P \tag{4.15}$$

The formula for each cost presented in Eq. 4.15 are explained in the subsequent sub-sections.

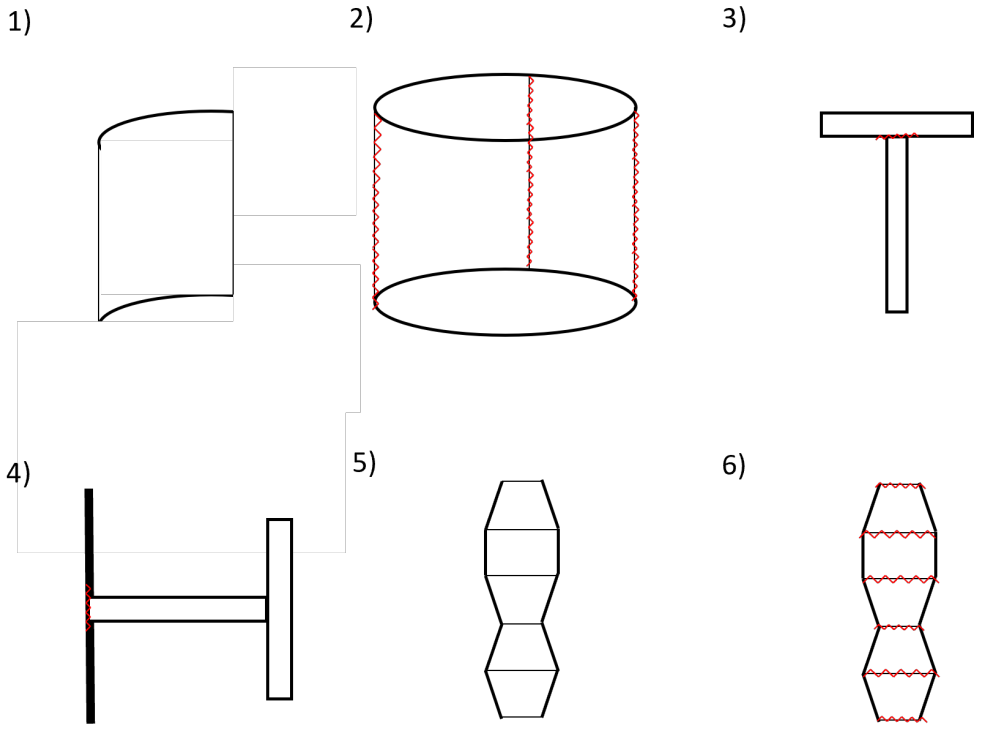

Figure 4.7: Fabrication process: 1) Forming 2) Welding formed plates to create a segment 3) Creating the stiffener from parts 4) Welding the stiffener into the shell 5) Assembling all segments 6) Welding segments together.

4.3.1 Material Cost

The material cost is one of the simplest to calculate; the total mass of the platform, considering the shell and stiffeners mass, is multiplied by the cost of the material per unit of mass, see Eq. 4.17. The cost of the ballast material can be calculated in a similar way.

$$K_M = k_m m_{total} \tag{4.16}$$

$$K_b = k_b m_b \tag{4.17}$$

4.3.2 Forming Cost

The forming cost (Eq. 4.18) considers (n_p), the number of parts, in this case plates being formed into curved shapes (10).

$$K_{F0i} = n_p k_f \Theta_f e^{\mu} \tag{4.18}$$

Where μ presented in Eq. 4.19 is the time for bending a 3m wide plate (10).

$$\mu = 6.8582513 - 4.527217 t_i^{-0.5} + 0.009541996(2R_{ei})^{0.5} \tag{4.19}$$

The same calculation can be done for forming the stiffener parts, since ring stiffeners are required the plates will have to be rolled to get the desired curvature. The total forming cost (Eq. 4.20) is then found by summing K_{F0i} for the formed plates and stiffener components for the number of segments, no_s (10).

$$K_{F0} = \sum_{i=1}^{no_s} K_{F0i} \tag{4.20}$$

4.3.3 Welding Cost

The welding cost, as mentioned before, can be broken down into a number of sections. Firstly welding n_p curved plates together to create shell segments using GMAW-C (Gas Metal Arc Welding with CO_2 butt welds) can be calculated using Eq. 4.21 (10).

$$K_{F1_i} = k_f \left[\Theta_c \sqrt{n_p \, \rho \, V_i} + 1.3 \cdot 0.152 \times 10^{-3} \cdot t_i^{1.9358} \, n_p \, L_{e_i} \, n_w\right] \tag{4.21}$$

Where n_w is the number of welds, where it is possible, two welds are carried out on the inner and outer surfaces. The reason for this is that it is cheaper to make two shallow welds in comparison to one very large weld due to the larger amount of material required. The only time one large weld would be carried out is when access is limited; however, in this case, the components are large, and this is not an issue. Θ_f is the manufacturing complexity factor. This is considered as 3 for all cases, which is in line with the cylindrical column in the work by Farkas et al. (10). This was not considered higher for semi-submersible or TLP because it is expected that the complexity of the weld will not change, the impacting factor here will be the number of welds, due to the increased parts The total cost of welding all plates together for each segment can be found in Eq. 4.22 (10).

$$K_{F1} = \sum_{i=1}^{no_s} K_{F1i} \tag{4.22}$$

The stiffeners can be welded together from their formed parts utilising GMAW-c fillet welds, see Eq. 4.23 (10).

$$K_{F2i} = k_f No_{stiff} [\Theta_f \sqrt{n_{ps} \rho V_{si}} + 1.3x0.3394x10^{-3} a_{wi}^2 n_w (R_{ei} - h_i) 2\pi] \tag{4.23}$$

n_{ps}, the number of parts to make up a stiffener, i.e a tee is constructed of two parts and a box stiffener, three parts. The difficulty parameter Θ_f within this calculation is assumed to be 3 for all cases, which is in line with (10). The cost related to each segment can be summed to find the total cost in Eq. 4.24 (10).

$$K_{F2} = \sum_{i=1}^{no_s} K_{F2i} \tag{4.24}$$

The stiffeners can then be welded into the shell, again using GMAW-c fillet welds

(Eq. 4.25 and 4.26) (10).

$$K_{F3i} = k_f No_{stiff}[\Theta_f \sqrt{n_{ps}\rho(V_{si}} + V_i) + 1.3x0.3394x10^{-3} a_{wi}^2 n_w R_i 2\pi] \tag{4.25}$$

$$K_{F3} = \sum_{i=1}^{no_s} K_{F3i} \tag{4.26}$$

The assembly denoted by 'A' and the welding denoted by 'W' of the fully stiffened shell structure from n_p can be found using Eq. 4.27 and 4.28 respectively (10).

$$K_{f4A} = k_f \Theta_f \sqrt{n_p \rho(V_{si} + V_i)} \tag{4.27}$$

$$K_{f4Wi} = 1.3 k_f 0.152 x 10^{-3} t_i^{1.9358} 2\pi R_i \tag{4.28}$$

Summing both costs together gives the total cost to assemble and weld the structure (Eq. 4.29) (10).

$$K_{F4} = \sum_{i=1}^{no_s} K_{F4Wi} + K_{f4A} \tag{4.29}$$

4.3.4 Paint Cost

The paint cost is related to the surface area of the inside and outside of the shell, and the stiffeners. The paint cost is expressed in Eq. 4.30 (10).

$$K_P = k_p A_{tot} \tag{4.30}$$

4.4 Hydrostatics

The hydrostatics analysis is used as a first check, if the geometry does not pass static requirements the design and analysis process is stopped, discarding the considered geometry. In order to carry out hydrostatic analysis a number of reference points have to be determined, for a set draft, the Centre of Buoyancy (CoB) and gravity (CoG) must be found. The CoB can be found by integrating the area from the still water level

to the draft of the platform (178; 179).

$$z_B = \frac{1}{V}\int_{-T}^{0} zA_z.dz \tag{4.31}$$

The CoG of each segment can be calculated using geometry and then the overall CoG of the system can be found, including the RNA and tower mass, and relative CoG (178; 179).

$$z_G = \frac{\sum m_{component} \cdot CoG_{component}}{m_{total}} \tag{4.32}$$

At this point, since the draft and platform mass are known, the required ballast mass can be found and the related cost can be calculated, where V is displaced water.

$$m_b = m_t - \rho_{sw}V \tag{4.33}$$

$$K_b = k_b m_b \tag{4.34}$$

The angle of inclination of the wind turbine is an important parameter as it will affect wind turbine power production and restoring stability. It has also been suggested that it has the potential to affect other systems, such as the mooring lines and equipment in the nacelle, although the latter was disproved by (148). The aerodynamic force acting on the turbine can be used to find the moment acting on the turbine, and then this can be used within Eq. 4.35 to find the pitch angle. The aerodynamic force is dependent on the load case under analysis in operational conditions, the aerodynamic thrust on the rotor and the drag on the nacelle and tower are considered, and in survival conditions, only the drag acting on the rotor, tower and nacelle is considered.

$$M_{R,y} = (\rho g I_{yy} + F_B z_B - mgz_G)sin(\theta) + C_{55moor}\theta \tag{4.35}$$

Eq. 4.35 considers all of the elements within the stability triangle, presented in Figure 4.8 (12). The first element in the equation represents the waterplane stabilised platforms, such as Barge and Semi-submersibles. These platforms are characterised by a shallow draft and a large second moment of waterplane area and the requirement for

mooring lines is mostly for position-keeping purposes. The second term is the ballast contribution, which is the stabilising mechanism used for Spar platforms. The last term is the mooring contribution, which provides stability for TLPs and other platforms with taut mooring lines.

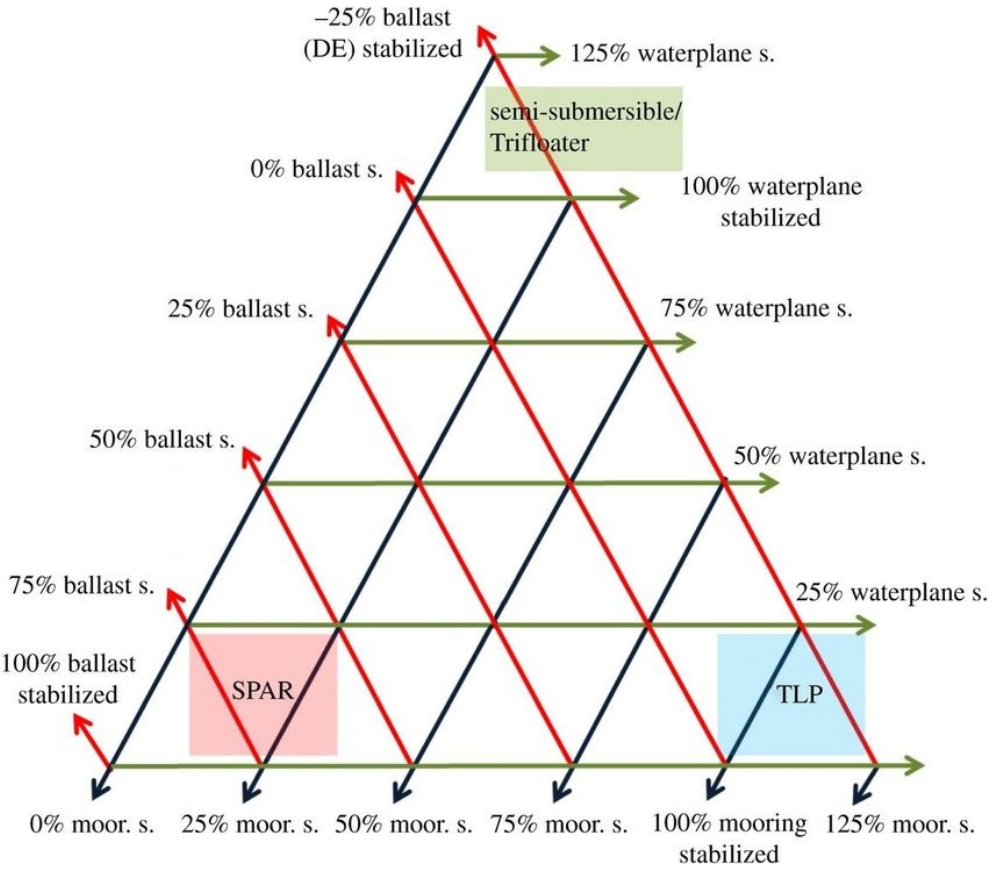

Figure 4.8: Stability triangle, this triangle can become destabilised or have a negative contribution to the restoring capabilities due to the Centre of Gravity position (11; 12)

4.5 Mooring line and Anchor System

4.5.1 Catenary Mooring Line Sizing

The station-keeping model is required to more accurately determine the stiffness contribution to the system. In this work, an inelastic, catenary equation mooring model was used to determine the mooring line stiffness in a quick and simple manner at the initial equilibrium. This work can consider 3 to 6 mooring lines depending on the user's

preference. However, all work was assumed to have a 3 line equivalent system. The pretension is an important starting point as this helps to determine the overall required size of the mooring lines, for this work it is assumed that the total tension between all mooring lines is equal to the thrust and drag acting on the tower and rotor in an extreme load case which still produced power (DLC 1.6), to avoid complicated analyses at this stage.

It was considered that the tension in each line should be 20% of the minimum breaking load (132). The MBL is correlated to the diameter, which can be found in (13). This information was used to create a graph and the equation of a line could be found, see Figure 4.9.

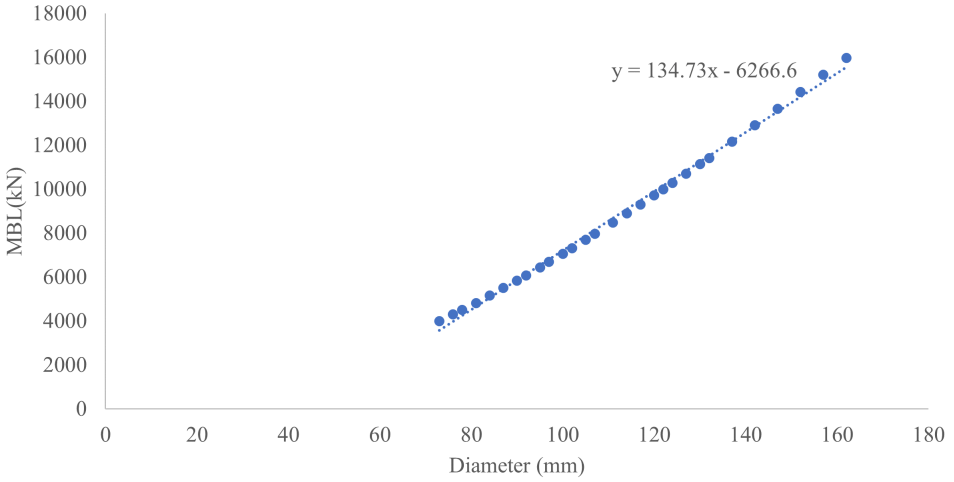

Figure 4.9: Mooring line diameter vs MBL for grade 3 steel (13).

.

The weight per meter of the studless catenary mooring line in water was then determined using the formula from (180).

$$w_{moor} = g(\rho_{moor} - \rho_{sw})\frac{\pi}{4}D_{moor}^2 \tag{4.36}$$

The hanging section of the catenary mooring line length can be found using the following formula (181).

$$l_s = \sqrt{h^2 + 2h\frac{T_{pre}}{w_{moor}}} \tag{4.37}$$

It has been estimated using the work by Pan et al. (182) that on average 71% of the catenary mooring line hangs whereas the remaining 29% lies on the seabed, for 185m water meter depth. Using this ratio allows the total length, L_{moor} to be calculated. This is expected to vary when the distance between the fairlead and seabed becomes smaller, like in the case of Hywind, but for this work, the assumption was considered (183).

Anchor radius, A_{rad}, can now be easily found using Pythagoras' theorem, the length and the distance from the fairlead coordinate to the seabed.

The vertical and horizontal components of the mooring line tension can be found using the following Eq. 4.38 and 4.39 (181).

$$T_v = w_{moor} L_{moor} \tag{4.38}$$

$$T_h = \sqrt{T_{pre}^2 - T_v} \tag{4.39}$$

4.5.2 Taut Mooring Line Sizing

The same approach is applied to the taut system, however, the mooring line length is considered to be equal to the distance between the seabed and the fairlead coordinate. The diameter, mass and stiffness can be calculated using the following equations, where α_m, β_m and c_m vary with mooring line type, these constants are shown in Table 4.4 (24).

$$D_{moor} = \sqrt{MBL/\alpha_m} \tag{4.40}$$

$$w_{moor} = \beta_m D_{moor}^2 \tag{4.41}$$

$$Stiffness_{moor} = c_m D_{moor}^2 \tag{4.42}$$

The total mass and the cost (K_{ML}) of the taut or catenary mooring lines can be

Mooring Line Material	α_m	β_m	c_m
Nylon	139357	0.6476	1.18x10^6
Polyester	170466	0.7978	1.09x10^6
Polypropylene	105990	0.4526	1.06x10^6
Wire rope	584175	3.6109	4.04x10^7

Table 4.4: Constant value for to determine taut mooring diameters and mass (24).

found by using the total length and the mass per length.

$$K_{ML} = m_{ml} k_{ml} \tag{4.43}$$

4.5.3 Mooring Stiffness

Catenary Mooring Lines

The static stiffness, c_{ii} provided by the catenary mooring line can be calculated analytically, where ii represents the DoF. The surge and sway stiffness are equal and calculated using Eq. 4.44 and 4.45 (14; 184).

$$k_{11} = \frac{1}{\frac{L_{\text{moor}}}{EA_{\text{moor}}} + \frac{1}{w_{\text{moor}}} \cdot \left(\frac{-T_v}{\sqrt{T_h^2+T_v^2}+\sin^{-1}\left(\frac{T_v}{T_h}\right)} \right)} \tag{4.44}$$

Where EA_{moor} is the Young modulus of the mooring line (185).

$$c_{11} = \frac{3}{2}\left(k_{11} + \frac{T_h}{A_{rad}}\right); \tag{4.45}$$

The coupled surge-pitch and sway-roll motions are also equal and can be found using Eq. 4.46 and 4.47 (184).

$$k_{12} = \frac{1}{\left(\frac{1}{w_{moor}}\right)\left(\frac{T_h}{\sqrt{T_h^2+T_v^2}-1}\right)} \tag{4.46}$$

$$c_{15} = -3\left(\frac{-R_{moor}}{2}k_{12} + \frac{z_M}{2}k_{11} + z_M\frac{T_h}{A_{rad}}\right) \tag{4.47}$$

The stiffness in the heave direction (c_{33}) is assumed to be zero for catenary systems

since the contribution is negligible in comparison to the hydrostatic stiffness created by the platform. The roll and pitch stiffness are also equal and can be found using Eq. 4.48 (184).

$$c_{44} = N_{Moor}\left(-z_M R_{moor} k_{12} + \frac{z_M^2}{2}k_{11} + \frac{R_{moor}^2}{2}k_{22} + z_M T_v + T_h\frac{R_{moor}}{2} + z_M^2\frac{T_h}{2A_{rad}}\right) \tag{4.48}$$

Where k_{22} can be found using Eq. 4.49 (184).

$$k_{22} = \frac{1}{(\sqrt{(T_h^2 + T_v^2)} + \frac{1}{EA_{moor}}\frac{T_v}{w_{moor}})} \tag{4.49}$$

The contribution from the yaw DoF can be calculated using Eq. 4.50 (184).

$$c_{66} = (3T_{pre}\frac{(R_{moor} + L_{delta}cos(\alpha))}{L_{upper}})(R_{moor} + (L_{delta} + L_{upper})cos(\alpha_i)); \tag{4.50}$$

Where L_{delta} and L_{upper} are the length of the delta line and the length of the upper segment of the line, respectively, which are taken as a ratio from (186). The variable α_i is the angle between the mooring line and the z-axis. Due to symmetries, the following matrix for total mooring line stiffness, C_{moor} is presented below, further details on this stiffness matrix are given in (12).

$$C_{moor} = \begin{bmatrix} c_{11} & 0 & 0 & 0 & c_{15} & 0 \\ 0 & c_{11} & 0 & -c_{15} & 0 & 0 \\ 0 & 0 & 0 & 0 & 0 & 0 \\ 0 & -c_{15} & 0 & c_{44} & 0 & 0 \\ c_{15} & 0 & 0 & 0 & c_{44} & 0 \\ 0 & 0 & 0 & 0 & 0 & c_{66} \end{bmatrix} \tag{4.51}$$

Taut Mooring Lines

The taut mooring line stiffness model utilises the same analytical approach presented in (187; 188).

$$C_{11} = T_T/L_{moor} \tag{4.52}$$

$$C_{15} = T_T T/L_{moor} \tag{4.53}$$

$$C_{33} = Stiffness_{moor} \tag{4.54}$$

$$C_{44} = C_{55} = \left(-T_T(abs(z_G) + abs(z_m))^2/L_{moor}\right) \tag{4.55}$$

4.5.4 Anchor sizing

The anchor type and size can be determined since the mooring line details are known. To determine the cheapest but most suitable option available, driven piles, gravity, suction piles and drag embed anchors were considered. The following, Table 4.5 details information about anchors used in the current literature, expressing the number of anchors, the type and their cost.

Reference	Platform Used	Mooring Type	Anchor Type	Anchor Cost	Number of Anchors	Anchor Mass (ton)	€/ton
(41)	Semi-submersible	Catenary	Plate anchor	€37800	6	3.14	1720
(41)	Spar	Catenary	Plate anchor	€18920	3	3.14	1720
(39)	Semi-submersible	Catenary	Drag embed	€49047	3	4.1	3429
(9)	Hywind Spar	Catenary	Stevshark Mk5	€342000	3	17	5767
(9)	WindFloat	Catenary	Stevshark Mk5	€456000	4	17	5767
(9)	TLWT	Catenary	Stevshark Mk6	€456000	3	3	15767
(29)	Semi-submersible	Catenary	Drag-embed	£91000	3	*N/A*	*N/A*
(44)	Semi-submersible	Catenary	Stevshark Mk5	€123000	1	*N/A*	*N/A*

(44)	Spar	Drag embed	Catenary	£291000	3	*N/A*	*N/A*
(41)	TLP	Taut	Plate anchor	€129600	8	8.1	1720
(9)	TLB B	Taut (angled)	Stevemanta VLA	€1042500	3	40	7471
(9)	TLB X3	Taut (angled)	Stevemanta VLA	€938400	3	36	7471
(9)	TLWT	Taut	Suction Pile	€15375000	3	50	8815
(9)	SWAY	Taut	Suction Pile	€1435000	1	140	8815
(29)	TLP	Taut	Driven Pile	€800000	5	*N/A*	*N/A*
(127)	TLP	Taut	Driven Pile	€3232910	5	53	10412

Table 4.5: Anchor and mooring line details.

Using Table 4.5, a price for each anchor type could be found and is presented in Table 4.6.

Anchor Type	Price per ton (£/ton)
Stevshark Mk5	5,767
Stevpris Mk6	15,766
Suction Pile	8,815
Driven Pile	10,412
Gravity Anchor	price/kg steel or concrete

Table 4.6: Price per ton of each anchor used in the current works model.

A parameter which helps determine the required size of the anchor is the Ultimate Holding Capacity (UHC). Ferri et al. (129) state that the UHC should be 1.5 times the maximum tension in the line. Considering the work published by the author (25) and which is presented in Chapter 6, Section it can be easily identified that soil condition and mooring line type affect which anchor is applicable, this was also considered in the present work (see Table 4.7).

Anchor type	Loading	Applicable mooring system type	Seabed type
Drag anchor	Horizontal	Catenary	Soft/Medium
Driven Pile	Vertical or Horizontal	Catenary or Taut	Soft/Medium/Hard

Suction pile	Vertical or Horizontal	Catenary or Taut	Soft/Medium
Gravity Anchor	Vertical or Horizontal	Catenary or Taut	Soft/Medium/Hard

Table 4.7: Details on anchor suitability for seabed types, adapted from (25).

In order to simplify this work, the same assumption was made as in Monfort et al. (14), this work considers that all soil types can be classed as either clay or sand, see Figure 4.10.

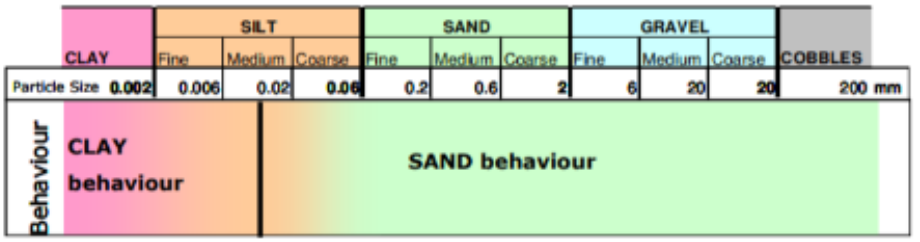

Figure 4.10: Soil classification (14).

The UHC for each anchor type can be found using the ABS design standard presented in (169). The equations used to find the dimensions and therefore mass for each anchor type are presented in Table 4.8. The equations presented below are for soft clay only, where the constant values change depending on soil type and can be found in (169).

Dimension	Driven Pile	Suction Bucket	MK5	MK6	Gravity
Length (m)	$1.01UHC^{0.311}$	$1.1161UHC^{0.3442}$	N/A	N/A	N/A
Diameter (m)	$0.076UHC^{0.38}$	$0.3095UHC^{0.2789}$	N/A	N/A	N/A
Thickness (m)	$\frac{1.0531UHC^{0.4042}}{1000}$	$\frac{2.058UHC^{0.2803}}{1000}$	N/A	N/A	N/A
Mass (ton)	Use density and geometry	Use density and geometry	$\frac{UHC}{392.28}^{\frac{1}{0.92}}$	$\frac{UHC}{509.96}^{\frac{1}{0.93}}$	$\frac{UHC}{9.81}$

Table 4.8: Details of the equations used to calculate anchor mass for each considered typology for soft clay.

Since ABS standards do not consider gravity anchors (14) was used. This work shows that the UHC of the gravity anchors' holding capability comes mainly from the weight and partially from the friction between the soil and the anchor. The friction coefficient for different soils is specific to each site, and since this work categorises the soil into groups, it is difficult to estimate this value accurately. Therefore, the current work bases the hold capacity purely on the weight of the anchor. With the weight of all anchor types, the cost can be found by combining the previously defined price per tonne and the mass.

$$K_A = m_a k_a \tag{4.56}$$

4.5.5 Complete Cost

The overall cost of the mooring, ballast and support structure can now be combined to give the overall cost.

$$COST_{overall} = K_T + K_{ML} + K_A + K_b \tag{4.57}$$

4.6 Hydrodynamics

The following section presents the methodology to predict the response of the floating platform in the frequency domain to wave loads. For this work, frequency domain analyses were carried out due to the considerations in Chapter 3 surrounding the trade-offs between time and frequency domains. To summarise here, the frequency domain was adopted since this is an early design phase, where the prioritisation is to cover the largest space in a short period of time. The trade-off here is accuracy; however, at this stage of design, the accuracy provided by the frequency domain is expected to be adequate.

To determine the response of the platform, the linear equations of motion must be solved (see Eq. 4.58 (132)).

$$F_e(\omega, \mu)\eta_a = [-(M + A(\omega))\omega^2 + B(\omega)i\omega + C]x(\omega) \tag{4.58}$$

Where F_e is the wave load per unit wave amplitude, η_a is the wave amplitude, M is the mass matrix, A is the added mass, B is a damping matrix, C is the stiffness matrix, and ω is the frequency. Rearranging this equation, the RAO for displacement can be found.

$$RAO_{x_j} = \frac{F_e(\omega, \mu)}{[-(M + A(\omega))\omega^2 + B(\omega)i\omega + C]} \tag{4.59}$$

In this equation, j refers to the degree of freedom, i.e for surge $j = 1$. To find the hydrodynamic properties of the system, the mass and stiffness matrix can be calculated analytically, but the added mass, damping and excitation force must be calculated by other means. In this work, NEMOH was used, which is a potential flow solver which uses the boundary element method to compute wave loads on offshore structures (189). The inputs for NEMOH are a mesh, which is automatically generated using CAD software SALOME and a Python script, the frequencies and wave direction, and the water depth.

The mass matrix can be easily constructed using information about the geometry of the platform, m is the total mass, and x_G, y_G and z_G are the coordinates of the centre of gravity, see Eq. 4.60.

$$M = \begin{bmatrix} m & 0 & 0 & 0 & mz_G & -my_G \\ 0 & m & 0 & -mz_G & 0 & mx_G \\ 0 & 0 & m & my_G & -mx_G & 0 \\ 0 & -mz_G & my_G & m_{44} & 0 & m_{46} \\ mz_G & 0 & -mx_G & 0 & m_{55} & 0 \\ -my_G & mx_G & 0 & m_{64} & 0 & m_{66} \end{bmatrix} \tag{4.60}$$

The terms m_{44}, m_{55} and m_{66} are the moment of inertia in the respective DoF. This can be calculated by finding the inertia of the object about its axis and combining this with the inertia about the global axis. This has to be done for each segment of the platform, RNA and tower, the latter two can be found in the literature (185; 190). In

some cases, certain terms within this matrix will be zero due to the symmetry of the platform, further simplifying the problem.

The stiffness matrix is constructed of three terms: gravitational, hydrostatic, and mooring. The gravitational stiffness matrix is presented in Eq. 4.61, this matrix represents the restoring which occurs when the platform is rolled or pitched.

$$C_{Gravity} = \begin{bmatrix} 0 & 0 & 0 & 0 & 0 & 0 \\ 0 & 0 & 0 & 0 & 0 & 0 \\ 0 & 0 & 0 & 0 & 0 & 0 \\ 0 & 0 & 0 & -mgz_G & 0 & 0 \\ 0 & 0 & 0 & 0 & -mgz_G & 0 \\ 0 & 0 & 0 & 0 & 0 & 0 \end{bmatrix} \tag{4.61}$$

The hydrostatic stiffness of the platform is due to the change in restoring moments of the waterplane area caused by the change in buoyancy. This change typically comes from a roll/pitch rotation or a change in hydrostatic load due to a small change in heave. Since this matrix is linear with the rotation/displacement, it is only valid for relatively small rotations/displacements. The matrix can be found using Eq. 4.62 (178).

$$C_{Hydrostatic} = \begin{bmatrix} 0 & 0 & 0 & 0 & 0 & 0 \\ 0 & 0 & 0 & 0 & 0 & 0 \\ 0 & 0 & \rho g A_{wp} & 0 & 0 & 0 \\ 0 & 0 & 0 & \rho g I_{xx} + \rho g V z_B & 0 & 0 \\ 0 & 0 & 0 & 0 & \rho g I_{yy} + \rho g V z_B & 0 \\ 0 & 0 & 0 & 0 & 0 & 0 \end{bmatrix} \tag{4.62}$$

Where A_{wp} is the waterplane area, V is the initial displaced volume, z_B is the centre of buoyancy and I_{xx} and I_{yy} are the second moment about the x and y-axis respectively. The mooring stiffness calculation is presented in Section 4.5.3

One additional consideration within the damping is a set value for viscous damping, this is assumed to be linked to the ratio of damping, mass and stiffness of the 5MW NREL turbine combined with the mass and stiffness of the new platform, the viscous damping of a specific platform can be found using Eq. 4.63. This is a limitation of this work and is purely an approximation. This can, however, be calculated more accurately; however, for this work, a large design space and quick computation is favoured since this is a method to determine initial designs.

$$B_v = \frac{B_{v_{5MW}}}{\sqrt{2M_{5mw}C_{5MW}}}\sqrt{2MC} \tag{4.63}$$

In order to obtain the velocity and acceleration RAOs they can be calculated by deriving the displacement RAO with respect to frequency, see Eq. 4.64 and 4.65.

$$RAO_{\dot{x}_j} = \omega RAO_{xj} \tag{4.64}$$

$$RAO_{\ddot{x}_j} = \omega^2 RAO_{xj} \tag{4.65}$$

In order to find the response spectrum of the platform, the RAOs must be combined with the sea spectrum. In this work, the JONSWAP spectrum (S_η) was used since the case studies are based in the North Sea and similar environments around the coast of Scotland. The velocity and acceleration response can be calculated in the same way as the displacement response spectrum in Eq. 4.66.

$$S_{pj} = RAO_{xj}^2 S_\eta \tag{4.66}$$

To determine the representative amplitude of the displacement, velocity, and acceleration in each DOF, the zeroth moment must be found, which is linked to the response spectrum. Eq. 4.67 details how this was calculated. The velocity and acceleration amplitudes can be found by replacing the displacement response with the relevant response spectrum.

$$\sigma_i = \sqrt{\int_0^\infty S_{pj}(\omega) d\omega} \tag{4.67}$$

The overall displacement of the platform is important and is typically used as a constraint within the optimisation process. This can be done by using the translational displacement amplitudes of each direction and the Pythagorean theorem. This only considers the displacement due to waves, so the effect due to wind must also be considered; this can be calculated using Eq. 4.68. Once calculated, these two values can be combined to get the overall displacement.

$$D_{wind} = \sqrt{(\frac{F_{tot}}{C_{moor1,1}})^2} \tag{4.68}$$

Where F_{tot} is the total force experienced, combining the drag experienced by the tower and RNA and the thrust on the hub. An important parameter is the nacelle acceleration, similar to the mean translational motion. It is used within the optimisation procedure as a constraint to ensure equipment within the nacelle is not damaged, etc, due to excessive accelerations. This can be found using Eq 4.69 (132).

$$Naccelle_{acc} = -\omega^2(RAO_{acc_{1,1}} + z_H(RAO_{acc_{5,5}}) \tag{4.69}$$

4.7 Aerodynamic model

To calculate the platform motions due to the wind turbine, a simplistic estimation was used to find the force generated by the wind. In the initial design stages, to ensure a quick estimation of the aerodynamic loads, a point load was considered. The aerodynamic load acting on the turbine due to the wind can be split into two different categories: generating power and parked. When the turbine experiences a wind speed between cut in and cut out wind speed it will be generating thrust, this thrust force can be calculated using Equation 4.70. Where the wind speed U is the wind speed taken at hub height. Where the wind data is not at hub height, it can be corrected for wind shear using the power law and a roughness value of 0.12 for open sea with waves (191).

$$F_T = \frac{1}{2}\rho_{air} C_T A_{rotor} U^2 \tag{4.70}$$

This point force is assumed to be acting on the centre of the hub. In both cases, power generation and parked, the tower drag force is present and can be calculated using Eq. 4.72. Where c_D is considered to be one.

$$dF_D = \frac{1}{2}\rho_{air} U^2 c_D D_{tower}(z) dz \tag{4.71}$$

When the turbine is parked, there will not only be drag on the tower but also on the blades, which can be calculated in the same way as the tower drag for each blade. The blade drag force is assumed to be acting at hub height, and the tower drag is assumed to act on the centre of the tower's frontal area.

$$dF_b = \frac{1}{2}\rho_{air} U^2 c_D D_{blade](z)dz} (4.72)$$

4.8 Design Load Case

In order to define the environment, there are a number of different DLCs which can be considered from the IEC 614000 standards. In this case, it is important to consider the worst-case scenario to identify an initial design geometry. The best-suited DLC is 6.1, which is an extreme environment. The environment can be described by wind conditions, waves, met ocean directionality, sea currents, water level and type of analysis.

In order to study the 50-year wave, 30 years of data for each site considered were used (192). This data consists of wind speed, wave height and period. Combining this data with the Weibull fit function, the shape and scale parameters for each site were found. The cumulative Weibull distribution combined with the newly calculated shape (k) and scale (η) factor can then be used to find the probability of each wave height occurring (see Eq. 4.73) (193).

$$P_{cl} = 1 - e^{\left(\frac{H}{k}\right)^{\eta}} \tag{4.73}$$

Rearranging the Eq. 4.73, giving Eq. 4.74. This can be identified as a straight line function where y is the left-hand side, γ is the gradient, x is $ln(H_S)$, and the intercept is $ln(\beta)$.

$$ln(ln[1 - P_{cl}(H_s)]^{-1} = \gamma[ln(H_s) - ln(\beta)] \tag{4.74}$$

Using this equation, the calculated probability and the corresponding significant wave height, the following plot can be created, see Figure 4.11. This graph can be used with the probability of a 50-year wave occurring to find the significant wave height. First, the probability of a 50-year wave occurring is found using Eq. 4.75.

$$P_{50} = 1 - \frac{3}{24 \cdot 365.25 \cdot 50} \tag{4.75}$$

The probability of a 50-year wave occurring can then be used to determine the y coordinate in the line function, which can then be traced onto the x-axis where the 50-year significant wave height can be calculated. With this significant wave height value, the most probable period can be found using the weather data to create a wave scatter diagram, detailed wave height and period, see Figure A.1, in the Appendix.

The information regarding significant wave height and period can be used to create a JONSWAP spectrum which can be used in the hydrodynamic analyses to obtain the platform's response amplitude. The wave condition should be multidirectional and misaligned with the wind speed. Since there are some elements of symmetry for different platforms, the number of directions which need to be studied does not include the full 360 degrees. For example, a Spar requires only one direction. Since the wind speed is considered as a point load within this work, it has only been considered in one direction, in alignment with the y-axis. Current is also not considered within this model, hence it could not be included.

This method was used in contrast to an environmental contour method, or extreme value approaches, because of the lack of data available, the probability of occurrence and the wave height itself were unknown, making it difficult to use any other methodology.

Finally, to determine the power output of the model, the 15 MW IEA power curve

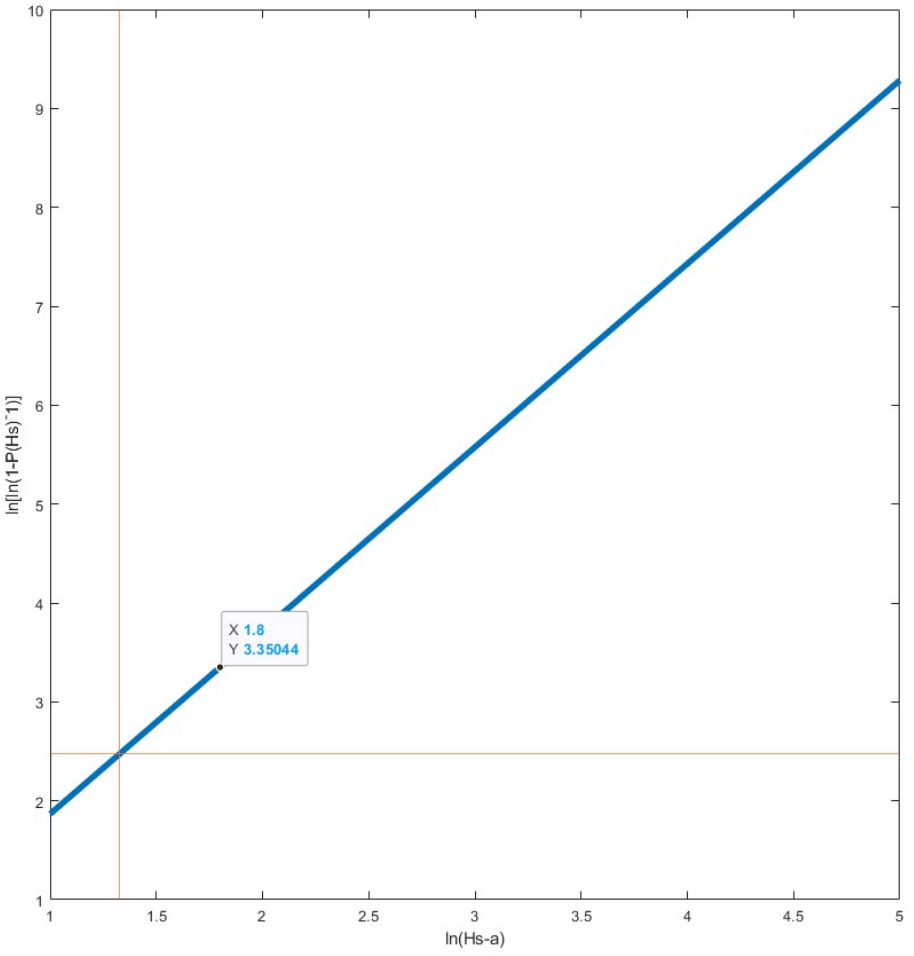

Figure 4.11: The Cumulative Probability Density Function on log scale for Scotwind site 14.

was used, as shown in Figure 4.12, and combined with the Weibull probability distribution for the wind speed at the site of interest. Consideration of all losses, such as electrical, availability, and wake effects, has been neglected. This decision was made because such losses can vary significantly depending on site conditions, technology choices, and operational strategies, and incorporating them would introduce additional uncertainty beyond the scope of this study. Furthermore, as the focus of this work is solely on substructure costs rather than full farm economics over the project lifetime, these factors were intentionally excluded.

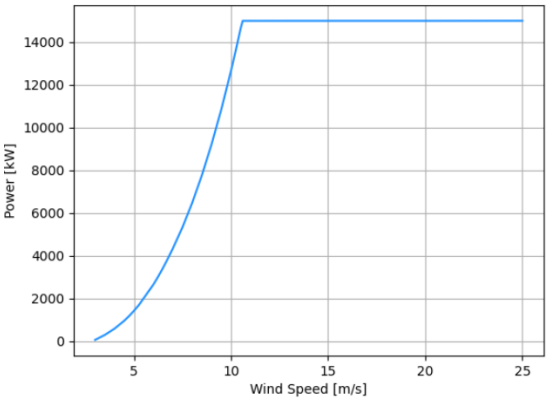

Figure 4.12: IEA 15MW turbine power curve.

Chapter 5

Methodology Validation

This Chapter is dedicated to the validation of the models used within this work, seeking an understanding of any differences when compared to existing work. The models which are validated within this Chapter are the cost, structural and hydrodynamic models.

5.1 Cost Model

The cost model validation is split into two sections. The first Section 5.1.1 covers the Spar platforms, and the latter Section 5.1.2 covers both TLP and Semi-submersible cost validation.

5.1.1 Spar

The validation of the current proposed cost model is difficult given the huge variations in the literature, however, information has been collected regarding optimised geometrical variables which could be processed through the model proposed in this work and the results compared, see Table 5.1.

Ref.	Draft (m)	Radius (m)	Length (m)	Fairlead Coordinate (m)	Platform Cost (M€)	Mooring Line Cost (M€)	Anchor Cost (M€)	Water Depth (m)	Turbine Size (MW)
(122)	43.4	8.91	48.4	-25	3.72	0.55	0.23	300	5
(122)	91.35	6.12	96.35	-25	4.81	0.59	0.26	300	5

(4)	82.91	7.375	88	0	7.43			120	5
(4)	106.14	7.955	111.17	0	10.36			120	10
(15)	87.28	6.875	93.48	0	7.37 (16.95 considering production costs)			120	5

Table 5.1: Optimised geometries found in the literature.

Some assumptions had to be made for this table; the work by Karimi et al. (122) did not present the length, but the work states the freeboard must be five meters. Combining this information with the draft allowed the length to be found. An assumption had to be made for the fairlead in both (4; 15) since they do not consider it in their work, for simplicity, 0 was used. The water depth for these also was not used in their work, hence 120m was used, since this was one of the base cases in (4).

The cost inputs for this work were considered the same as Hesgeth et al. (131) since their cost model is similar. The material cost was 2.7€/kg and the fabrication cost was 2.7€$/min$. The painting cost was considered as $26.31e^{-6}$€$/mm^2$ the same as Farkas et al. (10).

Combining the information about material, fabrication and painting cost with the information in Table 5.1 the following results are presented in Table 5.2

Reference	Platform cost (M€)	Mooring cost (M€)	Anchor cost (M€)	Angle of inclination (°)	Platform Cost (m€/MW)
(122)	4.163	0.3568	0.10596	4.51	0.8326
(122)	5.597	0.3568	0.10596	1.89	1.1194
(4)	6.965	0.225	0.10593	1.21	1.393
(4)	10.92	0.5245	0.1945	1.77	1.092
(15)	9.115	0.2253	0.10596	0.9448	1.823

Table 5.2: Cost estimated by model presented in this work.

Karimi et al. (122) have predicted a lower cost for the platform, which is expected to be due to only using the platform mass and 2.5$/kg, which is expected to include all manufacturing costs. The hull in (122) has a prescribed thickness, whereas the

current work finds the minimum thickness allowable to reduce the overall cost, if this was implemented in the work by (122) the cost might actually be lower.

In the work by Ghigo et al. (4) this cost is relatively similar compared to the current work, this is potentially due to the higher price per ton used and the consideration of higher-density steel to consider flanges and welds. The work by Bracco et al. (15) estimates the full production of the platform to cost 16.9 M€, which is high compared to other work. The material cost is 7.37 M€ in their work when compared to the current work the material cost is expected to be roughly 4 M€. The thickness of the steel used is not presented which may have led to a higher cost but in general, it is expected that the cost has been overestimated in their work.

Overall, when comparing the calculated values in m€/MW in Table 5.2 to the range in the literature, which is m€0.6141/MW at the minimum and m€1.2995/MW at the maximum, the results from the current model fall within this range.

The mooring line cost in (122) is slightly higher. This could be due to the different techniques used. Karimi et al. (122) use a price per meter kN, which is related to the maximum steady state tension in the line. The current work presented focuses on using the mass to find the price linked to the MBL and the diameter of the line. The anchoring cost in (132) is greater; however, this cost includes the installation, which could be the reason for the difference in cost, along with the method to determine the required anchor size. In general, it can be noticed that the mooring line cost is heavily related to the water depth and the turbine size. In particular, the turbine size determines the tension in the line. The anchoring cost like the mooring line is driven primarily by the turbine size. In terms of percentage, the cost of the mooring ranges from 2 - 9% and the anchoring from 1-3% of the combined cost of the mooring, anchor and platform. The higher mooring line costs are directly correlated with the water depth with (122) having the highest mooring line costs.

The overall cost breakdown of material, welding, forming and painting of (15) can be seen in Figure 5.1. The breakdown for the other work only differs by one of two percent and follows a similar cost breakdown to (10).

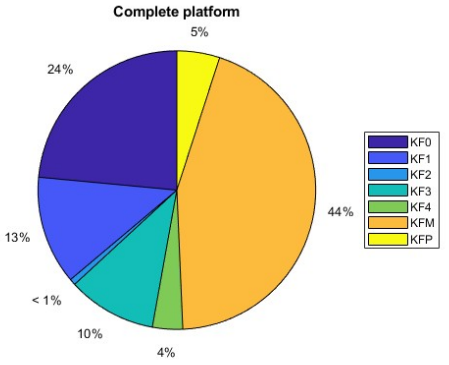

Figure 5.1: Cost Breakdown (15).

5.1.2 Semi-submersible and TLP

Validating the Spar cost against current literature is relatively simple, given its standard geometry and a large amount of research. However, another check to further validate the cost model is the comparison of both Semi-submersible and TLP costs. This is a lot more complex to compare given the huge variation in platform geometries, the lack of dimensions published and the little amount of work in this area. The WindFloat (Semi-submersible platform) from Principle Power and the Pelastar (TLP) were used for this process, see Figure 5.2. The estimated dimensions of each can be seen in Table 5.3

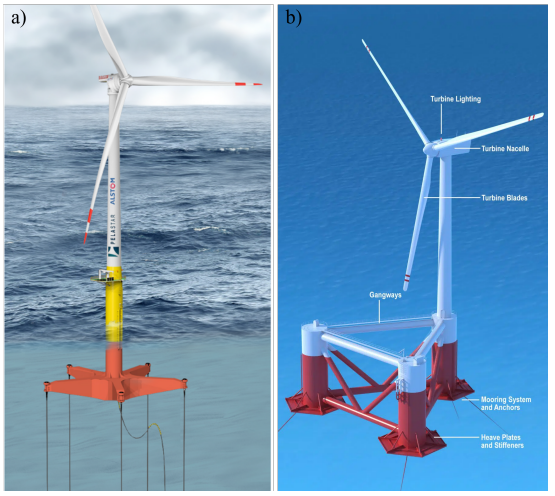

Figure 5.2: a) Pelastar TLP b) WindFloat Semi-submersible.

Parameter	Principle Power	Pelastar	Units
Diameter	10.5	6.18	m
Column Height	27.5	25	m
Pontoon length	50	25	m
Draft	18	25.03	m
Bracing Width	2	2	m
Bracing Depth	2	5	m

Table 5.3: The estimated dimensions of Principle Power and Pelastar Platform (15; 26; 27).

There were a number of references for the WindFloat platform. However, there was only one for the Pelastar. Table 3.3.8 details the cost found in the literature and the equivalent cost found for the current cost model presented in this work.

Reference	Platform cost M€	Mooring Cost M€	Anchor Cost M€	Platform cost M€/MW
WindFloat				
(101)	3.1	0.31	0.036	0.62
(41)	3.8	1.21	0.038	0.76
(29)	4.553	0.033		0.9106
(9; 45)	7.50	0.168	0.0456	1.5
Current model	2.94	0.24	0.152	0.588
Pelastar				
(15)	4.85 (Material) and 12.1 (Total Production)			0.97
Current model	2.1	0.0139	5.479	0.42

Table 5.4: The cost of Principle Power and Pelastar Platform.

It can be highlighted in Table 5.4 that the current model predicts a lower cost compared to the literature. A couple of assumptions were made in the model to estimate this cost. Firstly, the bracings are rectangular, not cylindrical and an equivalent thickness is used to consider that there would also be additional material for stiffeners.

This could lead to an underestimation in cost related to welding, forming, painting and material of the bracings. The WindFloat platform also has heave plates, which are excluded from the current model, leading to a potential reason for the lower cost estimate.

It is expected that the cost of material related to all of the literature will be an overestimation since they don't consider the required thickness based on structural considerations. The work by (41; 101) utilises the same model, considering a lot of additional costs such as: electricity consumption, water consumption, business and administration cost, amortisation of the machinery, and industrial profit, among others, which could explain the reasoning behind the higher cost estimate. Heidari et al. (29) includes a cost per ton for stiffened columns, truss members, heave plates and outfitting. The cost per tonne of steel varies a lot in the literature however a value of roughly 3€/kg is deemed acceptable. Averaging the €/kg in (29) for each of the listed costs is 4.65€/kg. This considers all of the manufacturing costs and is expected to be the reason for the overestimation. Both (9; 45) have the highest cost prediction of 7.5 M€. The cost calculation in this work is purely based on the mass and a complexity factor of 200% for WindFloat. Overall, it is thought that not only is the complexity factor too high, but also the material used appears to be an overestimate, given that the Spar is expected to be roughly half of the price and have 800 tonnes less mass than the WindFloat. In general, it is expected that the Spar would have a higher mass and cost compared to the Semi-submersible (94) despite the more simplistic geometry.

The estimated mooring cost for the WindFloat falls within the range of costs found in the literature. The current model, unlike the literature, finds the required length and diameter of the mooring line based on the tension experienced. The anchor cost for this model is, however, much higher than the cost calculated in the literature. This is potentially due to how the required anchor size was determined, with no literature explaining how this is calculated. Since the cost model presented in this work finds the UHC and then finds the cost based on this, it is expected to be a more accurate representation.

The work by (15) overall predicts a cost of 12.1M€ for the Pelastar which seems

high. Work by (15) uses a higher material density for steel to account for welding and flanges, it then also applies the same complexity factors which are in (9; 45). Since the complexity factor is expected to consider additional manufacturing costs it could be an overestimation to include this with the increased material density, which is potentially why it is much higher. The work by Bracco et al. (15) also considered ballast material for the TLP, which is not included in this work, also leading to the reduced cost estimate of the platform and the larger cost related to the station-keeping system. Myhr et al. (9) does not include the Pelastar, however, it also estimates the anchor cost to be greater than the platform cost.

A more generic comparison can be made by comparing the calculated €/MW value to the work carried out in (94), it is expressed that the minimum and maximum cost for the Semi-submersible in literature is 0.94 and 1.38 and the TLP is 0.47 and 1.0221. Both the TLP and Semi-submersible costs calculated by the current cost model are slightly less than this range, both roughly 0.4 €/MW. This is expected to be for the same reasoning as provided prior.

5.2 Structural Model

Validating the structural model is difficult since there is no real work done on the stiffeners required within the structure however, the thickness, and mass of the structure of the OC3 Spar are known and presented in (137). Using the dimensions of the OC3 Spars geometry, the thickness and mass can be calculated, see Table 5.5.

Characteristic	**Literature**	**Calculated Value**
Shell Thickness (m)	0.0314	0.04
Structural mass (kg)	8.066e6	8.23e6

Table 5.5: Comparison of the dimensions of the mooring line from literature and current model.

The required shell thickness is slightly larger but since this is an initial design phase, where only a few basic analyses are carried out this is a good starting point,

which could be further refined with more detailed analysis in further design stages. The overall mass is larger due to the thickness being greater and the addition of the mass of the stiffeners. It is expected that the greater thickness is the largest contributor to the difference since the stiffener mass accounts for roughly 0.2% of the overall mass and 1.43% of the structural mass.

5.3 Hydrodynamic Model

To validate the hydrodynamic model, the OC3 Spar with the 5 MW NREL turbine. The validation of the platform RAO is presented and compared to the literature in the following sections.

5.3.1 OC3 Spar

Utilising the model in Section 4.6 the RAO for the OC3 Spar was found and is presented below in Figure 5.3. This Figure shows the comparison of the current model, an in-house tool developed at the University of Strathclyde and the literature (16). It can be noted that the in-house solver is slightly different for the DoF covered, but only very minorly. The current model predicts a different RAO for heave, surge and pitch. The expected reason for this is the structural calculation considered within this work, the thickness of the shell and the stiffener size are predicted and consequently considered in the mass of the platform. The thickness of the shell is expected to be 40 mm using DNV-GL design rules, whereas the literature expects it to be roughly 30 mm. By combining the greater thickness and stiffener mass considerations, the overall mass of the platform is greater. The greater mass also leads to a slight change in the CoG contributing to the difference in RAO. To ensure the RAO model is correct a method to double-check this is to force the mass to be the same, which in turn will also create the same CoG as literature.

The RAO with the same platform mass is expressed in Figure 5.4, this shows the same trend in RAO as the in-house model.

As well as the listed differences above, the hydrodynamic coefficients can also lead

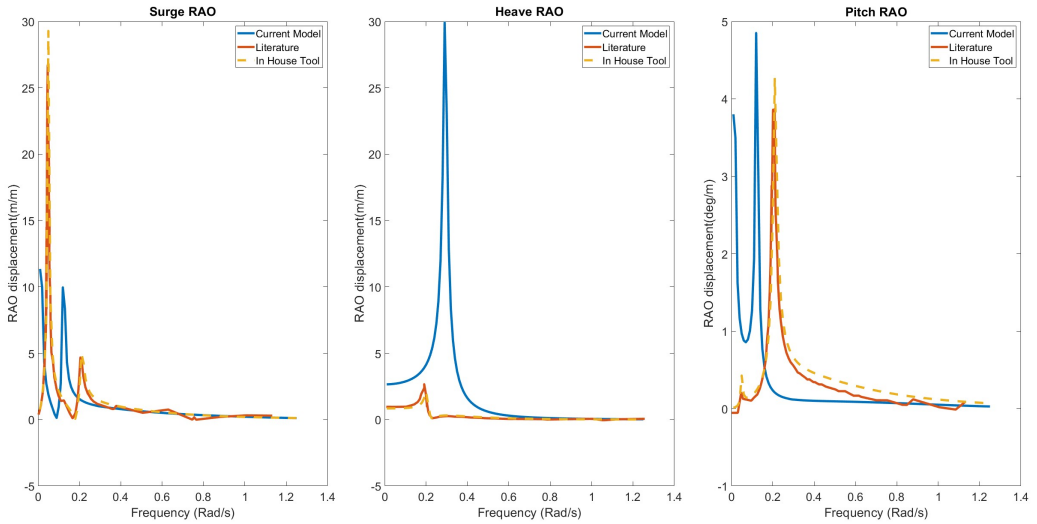

Figure 5.3: RAO for 5 MW NREL Turbine and OC3 Spar (16).

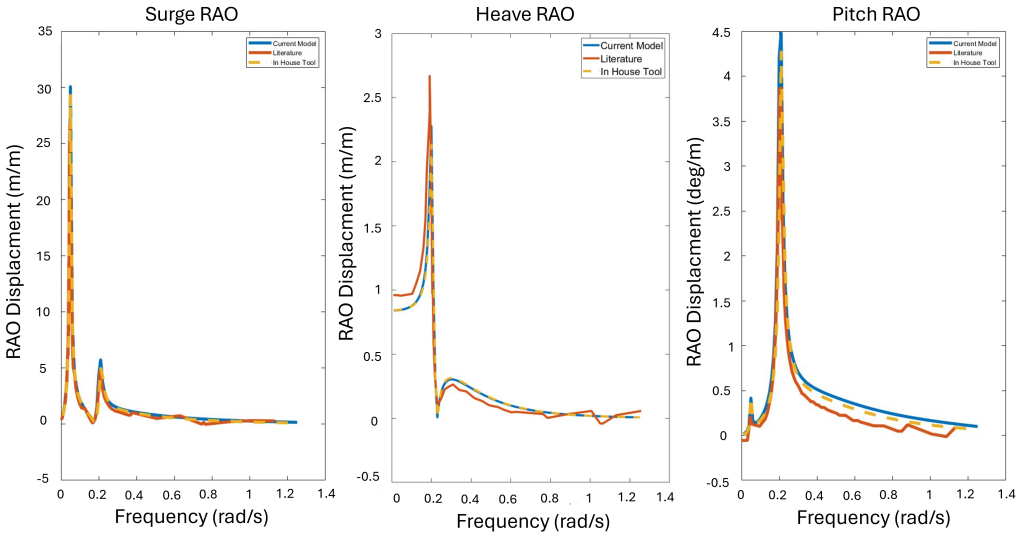

Figure 5.4: RAO for 5 MW NREL Turbine and OC3 Spar, with exact same mass as literature (16).

to differences. The excitation force calculated by NEMOH and compared to literature can be seen in Figure 5.5. This Figure shows a strong similarity to the literature.

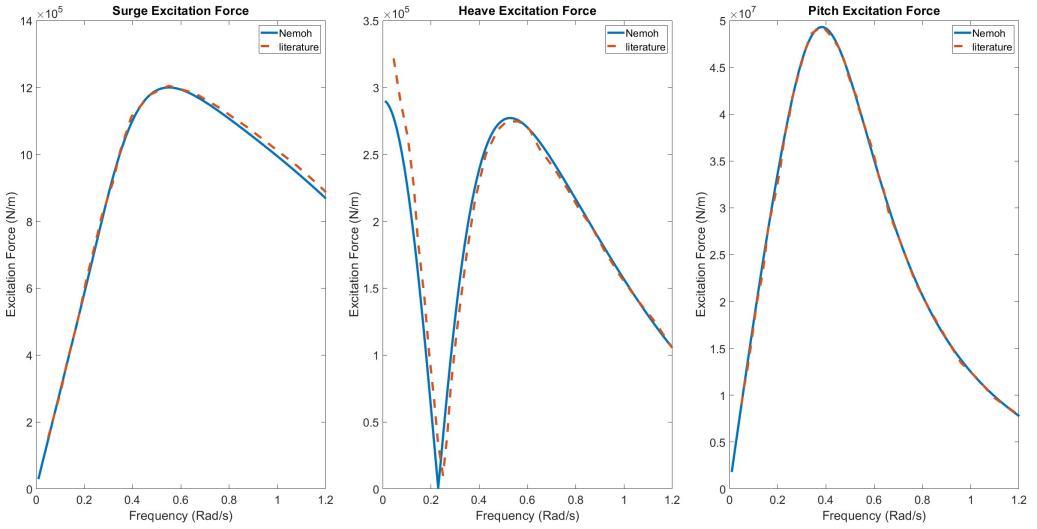

Figure 5.5: Comparison between excitation force found in literature and the current model for OC3 Spar (16).

Figure 5.6 shows the added mass calculated. For the added mass in the heave direction, the current work is very similar to the literature. The added mass in the surge and pitch direction follow the same shape however are shifted up on the y-axis leading to a difference of roughly 5% for both, potentially leading to the difference in RAO.

Finally, Figure 5.7, details the damping. The damping in the three DoFs is very similar to the literature. These small differences are expected to be the reason for the difference in the RAOs from literature, the in-house tool and the current model. The inaccuracy could also come from the literature using a finer mesh and/or a different method (WAMIT) to calculate the hydrodynamic coefficients. The author is however satisfied by the similarity in the results and deems them acceptable since increasing the mesh size would lead to a significant increase in computational time.

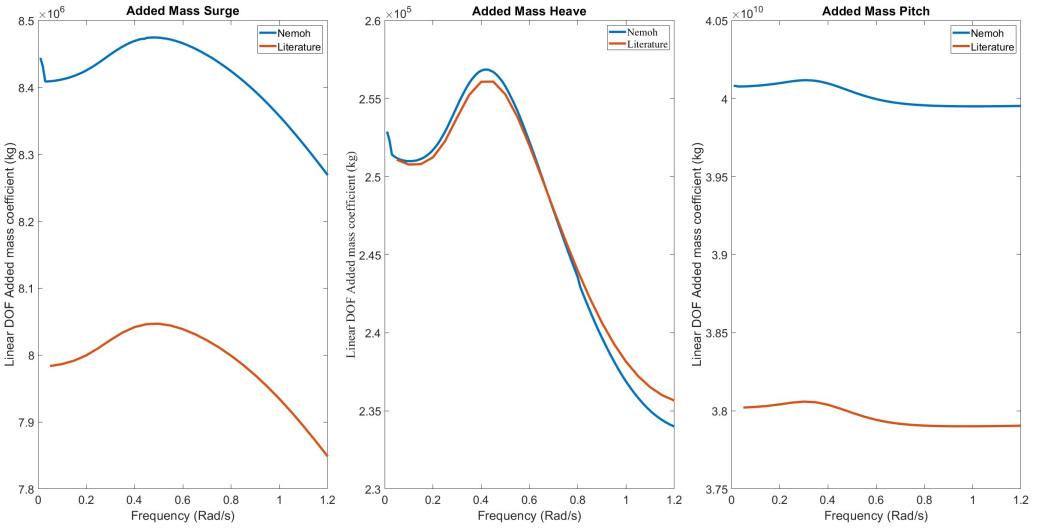

Figure 5.6: Comparison between added mass found in literature and the current model for OC3 Spar (16).

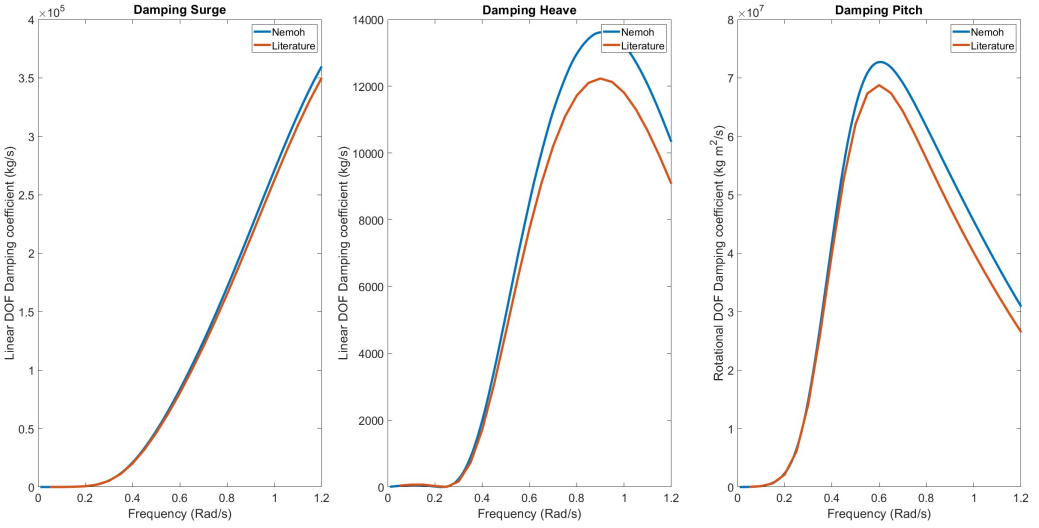

Figure 5.7: Comparison between damping found in literature and the current model for OC3 Spar (16).

Chapter 6

Floating Sub-structure Concept Preliminary Selection

The literature review in Chapter 3 highlights the potential of Multidisciplinary Design, Analysis, and Optimisation (MDAO) methods to reduce the Levelised Cost of Energy (LCoE). However, a major challenge in applying MDAO lies in developing a flexible and robust framework capable of accurately representing different platform typologies—namely waterplane-stabilised, ballast-stabilised, and mooring-stabilised configurations—while keeping computational demands manageable.

To address this challenge, this chapter introduces a preliminary platform selection method that ranks sub-structure concepts based on their suitability for a given site. The goal is to reduce the overall design space considered during the MDAO process, thereby allowing for a more detailed exploration of a narrowed subset without increasing computational cost.

The proposed method employs the Technique for Order of Preference by Similarity to Ideal Solution (TOPSIS), a Multi-Criteria Decision Analysis (MCDA) technique. This method is particularly well-suited to the task, as it effectively handles conflicting criteria, evaluates alternatives based on their proximity to both ideal and worst-case solutions, and integrates both expert judgement and quantitative data (11).

TOPSIS supports decision-making in scenarios where trade-offs exist—such as between cost and performance—by assigning user-defined weightings to each parameter.

These weightings reflect the relative importance of different criteria from the user's perspective. By combining the assigned weights with site-specific characteristics and the physical attributes of each platform type, the method produces a ranked list of platform concepts tailored to the site in question.

To demonstrate the applicability of the method, a case study is presented based on conditions associated with the ScotWind leasing round.

6.1 Platform Typology Classification Review

From reviewing each platform typology in Chapter 2, it is clear that there are common key parameters which can help identify which platform is appropriate for a given site. The parameters related to the site characteristics which affect platform choice were identified as: the seabed typology, water depth, wave height, and tidal range. It can be noted that the turbine itself will also have an impact on the platform performance however at this early design stage it cannot be considered but can be considered in the optimisation process itself. The following sections review each key parameter related to the site characteristics and are as follows: Section 6.1.1 details the seabed characteristics, Section 6.1.2 focuses on water depth, Section 6.1.3 details information of wave height and Section 6.1.4 considers the effects of tidal range. The remaining sections are related to the platform: Section 6.1.5 reviews the cost of each platform, Section 6.1.6 details Technology Readiness Level (TRL), and finally Section 6.1.7 compares the size of each platform.

6.1.1 Seabed Characteristics

The type of seabed the platform must be secured into plays a key role in determining which anchors and, hence, mooring arrangements are applicable. For a taut mooring system, it is required that the anchor can handle both horizontal and vertical loading (17; 194). For this reason, specialised anchors such as driven piles, suction piles, or gravity anchors are required. Driven pile anchors are harmful to the environment, since this process requires piling via a hammer for installation, a large amount of noise is

created, affecting surrounding life. The gravity anchor and the driven pile are challenging to remove upon decommissioning due to their weight and embedded characteristics, respectively. Suction piles offer a less intrusive, comparatively straightforward installation and decommissioning process (14). Catenary mooring systems can use simplistic drag-embedded anchors which are cheap, simple to install, and recoverable in the decommissioning phase (17; 194). The four main anchor types can be seen in Figure 6.1. Each anchor is compatible only with specific types of soils/seabeds, however, categoris-

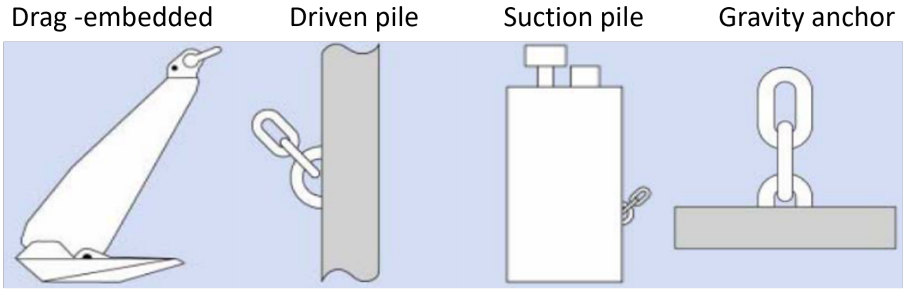

Figure 6.1: Anchor types (17).

ing soil is a complex problem. Monfort et al. (14) also state that this is difficult and in general, when selecting an anchor in situ tests will be required, but soil can be categorised as sand or clay. The reason for this is that other substrates, such as gravel and cobbles, have very similar behaviour to sand, and silt and clay can both be considered as clay due to their shared characteristics. Soil conditions can also be categorised by soft, medium, and hard, using the same description in (195). Soft soil consists of <30% hard material, medium material contains between 30 and 70% hard material, and hard soil consists of >70% hard material. Anything larger than gravel materials, such as rubble, cobbles, boulders, and bedrock, is classed as a 'hard' material, and mud, sand, and gravel are considered soft material (196). This classification scale was used to determine which would be best for each anchor type shown in Table 6.1.

The drag anchor is most suited to cohesive sediment, however, it cannot be too stiff or it will not be able to penetrate the seabed (17; 28; 29). For this reason, it is expected a 'soft' to 'medium' sea bed soil such as sand and clay would be most applicable. The driven pile is applicable to all types of seabeds; however, in conditions

where the seabed is 'hard', like bedrock, installation can become expensive. Due to the nature of suction pile anchors, they have difficulty holding in certain soft seabeds like sand and struggle to penetrate hard seabeds, but can hold in soft soil such as clay (17; 28; 30). Finally, the gravity anchor can be used in a range of seabeds, and it is expected that the holding capacity can change with time in soft soil since soils can be displaced (17; 28; 29; 194; 197; 198). On the other hand, it is expected that they may not be compatible with sloped seabeds, depending on the substrate. Gravity anchors can become unfeasible, when the vertical and horizontal loads become large making them technically still possible but economically unfeasible not only due to their cost but the impact on logistics for transporting and installing such large anchors.

Anchor type	**Loading**	**Applicable mooring system type**	**Seabed type**
Drag anchor	Horizontal	Catenary	Soft/Medium
Driven Pile	Vertical or Horizontal	Catenary or Taut	Soft/Medium/Hard
Suction pile	Vertical or Horizontal	Catenary or Taut	Soft/Medium
Gravity Anchor	Vertical or Horizontal	Catenary or Taut	Soft/Medium/Hard

Table 6.1: Details on anchor suitability for seabed types (17; 28; 29; 30).

Since the type of platform can help dictate the mooring system, the seabed of the sites can help determine the best platform (194). This is true for a TLP where taut lines are required, and typically, spar and semi-submersibles utilise catenary lines. However, there are cases which have explored a combination of taut and catenary lines, but this has never been implemented in a commercial site. Where there are a number of mooring and anchor systems that are suitable for the given seabed, the determining factors will be cost and installation of the different anchors and mooring lines.

6.1.2 Water Depth Characteristics

Water depth is a relatively simple parameter to help determine which platform is suitable or unsuitable. The Spar platform is restricted to deep water locations, due to its

large draft (17; 89; 194). On the other hand, TLPs are expected to be most appropriate for intermediate water depths due to their expensive station-keeping systems (89). The Semi-submersible is flexible since it can be used in a range of water depths (17; 89; 194). However, for shallow water deployment, fixed bottom turbines are also suitable. These have the advantage of being cheaper with a higher TRL compared to Semi-submersible designs. It has been expressed that there is a cut-off point for both fixed and floating platforms. Fixed platforms are expected to be appropriate up until 70m and the floating platform depth range starts from 30m (199). However, in the range between 30-70m, the cost and TRL will play a huge role in determining the most appropriate platform (199). Water depth can be categorised as shallow, intermediate, and deep. The cut-off for these categories is determined by the user in this work however, based on the mentioned points, shallow water is considered below 70m, intermediate water is from 70m to 150m, and deep water is greater than 150m.

6.1.3 Wave Height Characteristics

The wave height of the given site is not a particular issue for the Spar, as these can operate in high-sea states due to their small waterplane area and large draft. Similar to the Spar, a TLP can also operate in high sea states because of its high stability provided by the taut mooring lines (89). Since the Semi-submersible has a larger waterplane area, it is more susceptible to higher motions in larger sea states. The semi-submersible is, therefore, more suited to lower sea states compared to other typologies (89). This is, however, a very difficult way to categorise which platform is most suitable, given the huge variety in shape and size of each platform typology. It is expected that the only way to determine which platform has the best dynamic response accurately in a given sea state is to carry out hydrodynamic analysis, which should be done later in the optimisation stage instead. However, in this work, it is considered that TLP operates best followed by the Spar and semi-submersible, sticking to the generic shapes and respective dynamic response in different sea states. As a rule of thumb for this work the sea states can be classed as follows, a low sea state would have a significant wave height of 3m and less, and a high sea state would be 8m and greater, since there is no

literature on this classification the assumption is purely based on the authors knowledge and the Beaufort scale. Similar to the water depth categorisation, this categorisation of water depth is a user input which can be changed based on opinion. Since completing this work, the following was published (200). This work establishes threshold values to classify conditions as mild, moderate, or severe, corresponding to values of less than 7.5, between 7.5 and 11, and greater than 11, respectively. Compared to the present study, the thresholds proposed in (200) are notably less conservative. However, at the time this study was conducted, adopting a conservative approach was justified due to the limited availability of prior research in this area.

6.1.4 Tidal Range Characteristics

The tidal range is an important parameter for the TLP as it has a taut mooring system (89). The platform is designed to avoid a situation whereby one or more tendons are slack, since this would induce snap loads. For these reasons, the TLP needs to be positioned in an area which is exposed to little changes in mean water level due to the tide. Instead of specifying a fixed allowable tidal range, a more universally applicable approach is to use the ratio of water depth to tidal range as a site-specific criterion. This accounts for the natural variation in tidal range with water depth and proximity to shore. A reasonable upper bound for this ratio is approximately 5%, based on insights gathered through discussions with multiple industry experts.

6.1.5 Cost Breakdown

The wind turbine and its support structure are often shown in a cost breakdown, as roughly 30% of the CapEx each. The CapEx itself is the majority of the overall cost ranging from 53% to 77% (40; 41), OpEx is between 18% and 30% and DecEx cost found in the literature range from creating revenue to costing 5% of the overall cost. It can be highlighted that work should be done to reduce the CapEx since it is the largest percentage of the cost, however, there could potentially be a trade-off where increasing the CapEx slightly might reduce the OpEx a considerable amount by decreasing the probability of failure, or introducing more sensors allowing maintenance requirements

to be better predicted. Given the different platform typologies, it is clear that there is a cost variation depending on the platform. In order to compare platforms in terms of cost, information was collected from the presented work in Chapter 2 and is presented in Table 6.2 (4; 9; 29; 31; 32; 33; 34; 35; 36; 37; 38; 39; 40; 41; 42; 43; 44; 45; 46). Since the preliminary costs, turbine whole system, and transmission costs are considered constant for all platform types, they were not considered in the CapEx cost. Information on the cost of a barge was difficult to quantify due to a lack of relevant sources. For this reason, the mooring and installation costs were assumed to be the same as a Semi-submersible, given their similar size and the use of a similar mooring arrangement. This is a limitation of this work since no other information was available. It can also be noted that the costs have been considered separately within this work. The reason for this is that there is often a bias towards CapEx since it holds the largest share of the overall cost. Considering each separately will allow the impact of each to be considered when selecting a design.

	Spar			**Semi-submersible**			**Barge**			**TLP**			**Monopile**		
	Max	Min	Mean	Max	Min	Mean	Max	Min	Mean	Max	Min	Mean	Max	Min	Mean
Floating Sub-Structure (steel) (£M/MW)	1.49	0.545	0.957	1.64	0.664	0.891	0.984	0.398	0.534	1.2	0.326	0.796	0.5	0.225	0.367
Mooring and Anchor (£M/m)	0.335	0.017	0.192	3.2	0.107	0.710	3.2	0.107	0.710	1.053	0.017	0.481	N/A	N/A	N/A
Installation (£M/MW/km)	0.038	0.001	0.022	0.036	0.001	0.01	0.036	0.001	0.01	0.138	0.012	0.053	0.028	0.012	0.019
OpEx (£M/MW/km)	0.209	0.0007	0.046	0.208	0.0007	0.036	0.208	0.0007	0.036	0.21	0.0007	0.046	0.056	0.002	0.015
DecEx (£M/MW/km)	0.039	-0.001	0.012	0.039	-0.001	0.009	0.039	-0.001	0.009	0.042	0.001	0.025	0.015	0.005	0.011

Table 6.2: Cost breakdown for each geometry, highlighting minimum, means and maximum values found across the literature (4; 9; 29; 31; 32; 33; 34; 35; 36; 37; 38; 39; 40; 41; 42; 43; 44; 45; 46).

Cost is an important part of any project. Hence, CapEx, OpEx, and DecEx have been considered separately in this work, allowing the user to input which is most important or which are equally important to their work.

The mean cost for the support structure for the Spar is the greatest, as discovered in Chapter 2, which is correlated to the fact that the cost of the support structure is typically linked to its mass, with no consideration to the manufacturing cost. Since the Spar is large, in terms of size and mass, the steel required to construct it is high, leading to the cost being high. This is a limitation to using values from literature since the cost is often calculated in a fairly rudimentary way, with little known about the actual accuracy of the assumptions made. The Spar is followed by the semi-submersible, which can be expected as these platforms still have a relatively high mass but are expected to be lighter. Similarly to the discussion of the spar cost the manufacturing cost is often neglected which would expect to be higher for a semi-submersible since it is not a single cylindrical column, it is a number of components which need to be welded together, which takes up not only time, and resources but space to store and complete the full assembly. The TLP is expected to be one of the lightest floating platforms, and therefore the cheapest of the three.

Finally, the monopile is expected to be cheapest, however, it does have a mass which is very dependent on water depth. Since there is a limit to water depth on the current monopile technology, these are still typically lower in mass compared to

a spar. Monopiles also have a highly established supply chain and a large amount of learning behind them, which also helps to drive down the cost. The monopile is roughly half the cost of the TLP and Semi-submersible this is expected to be due to the standardisation and lower complexity in geometry and therefore lower manufacturing costs for the monopile. It can however, be noted that the barge is cheaper than all other floating platforms, the reason for this is expected to be due to the very little amount of research related to its cost and the research which has been carried out is very basic only considering material mass. The variation in cost is lowest for the monopile, which is likely to be related to the maturity of the technology. The Spar, Semi-submersible, and TLP have a similar range in cost, but the variation in barge cost is much lower, potentially related to the lack of research on it.

The cost of the station keeping is the same for the barge and the Semi-submersible since they were assumed to be the same due to the lack of literature surrounding the barge. It would be expected that the Spar would also be similar since the same mooring system is deployed, however, it is expected to be cheaper. A possible reason for this is that the Semi-submersible and barge have a larger waterplane area and hence experience greater effects due to wave load, requiring a station-keeping system to handle higher loads, which would be more expensive. Three pieces of research consider the Spar mooring and anchor (M&A) cost to be less (9; 29; 45).

The average installation cost (£/MW/km) is the lowest for the Semi-submersible and the barge due to their simplistic installation technique, inherent towing stability, and lack of specialised vessel requirements (201). The semi-submersible with the integrated turbine is towed to the site and then hooked up, avoiding turbine installation being carried out offshore, which is difficult with two dynamic systems and higher risk. The monopile is cheaper than the other floating options since they do not need floating cranes and AHVs, that are not readily available and are expensive. There is also a correlation with monopiles being used in much shallower sites due to their nature, which often is linked to a shorter distance to shore and therefore it is easier to get more favourable weather windows to carry out the installation due to the smaller window required for the installation (201). The Semi-submersible is found to be cheaper than

the monopile, this could potentially be due to the requirement of expensive vessels for the monopile installation such as a jack-up vessel, as well as the turbine integration occurring offshore which is takes a longer time compared to quay-side integration. It could, however, be argued that a monopile would be cheaper due to closer proximity to shore and therefore distance to travel, the lower sensitivity to weather window availability and industry standard practice having been developed over a number of years. This highlights, just as Chapter 2 did, the inaccuracies within the literature and sometimes optimised cost predictions for floating offshore wind. The Spar is expected to be the second most expensive, and the TLP is the most expensive. The Spar is likely to be second most expensive since it is large and quite difficult to manage from a logistics perspective, and where there is not a deep water port capabilities the turbine integration will have to be carried out offshore which is more costly in terms of vessels required and increases the length of time it takes to carry out the installation in comparison to quay-side integration. The TLP is the most expensive which comes at no surprise since the best method to carry out the installation is unknown, further research is being done on this area to try and gain a better understanding of the associated costs with different installation techniques. The TLP has the largest range in cost but this could be related to there being no commercially installed TLPs to compare to.

As expected, the OpEx (£/MW/km) for the monopile on average is cheaper, this is expected to be due to the environment a monopile operates in being less harsh and closer to shore, leading to lower failure rates. Moving further offshore, the distance to travel becomes greater and the weather and metocean conditions become much harsher, making it harder to access weather windows to carry out maintenance and a greater potential for higher failure rates since the environmental load is greater. The cost for the barge and Semi-submersible is expected to be the same since they are similar, however, there are typically more components and bracings related to a Semi-submersible which have the potential to increase failure rates, which presumably is not captured in the literature. Both the Spar and TLP OpEx are greater than the Semi-submersible and the barge, the TLP is potentially more expensive since it has a complex mooring system.

The DecEx cost for the monopile and floating wind considers the complete removal

of the wind farm. It can be noted that, reviewing the mean values, the Semi-submersible is the cheapest; this is potentially due to the ease of removal, compared to the Spar, TLP, and monopile. The reasons for each are large size, making it more difficult to handle, lack of stability, complex mooring system, and more complicated removal process, respectively. It can be seen that the monopile is more expensive on average than all of the floaters except the TLP. This is potentially due to the complex mooring related to the TLP and the fact that a decommissioning of a TLP for floating offshore wind has never happened. This reason is also expected to affect the cost estimates of the other floating platforms. This is expected to be the reason for the larger range in all costs for the floating wind compared to the monopile. Negative pricing can be seen in this for the decommissioning because (9; 45) consider that the cost-benefit from the scrap material is greater than the cost of the decommissioning process, creating a profit.

6.1.6 Technology Readiness Level

Technology Readiness Level (TRL) is a metric which is used to describe the maturity of a technology. This scale assists in assessing the readiness of evolving technologies before they are incorporated into larger systems or subsystems (202). The higher the TRL of the technology, the easier it is to implement immediately. Thus proving its feasibility and the existence of a supporting manufacturing supply chain. Table 6.3 details platform typologies and their TRL in 2015 and 2022 based on installation status, capacity, commercial status, and the number of operational years. The TRL rating is based on the Department of Energy scale (202).

		From 2015			Data as of 2023				
Platform Type	Classification	TRL	Full scale pro-type status	Pre-commercial array status	Full scale pro-type status	Pre-commercial array status	Commercial Array status	Reference	New TRL
WindFloat	Semi-submersible	4	2011	2018	2MW operational from 2011	25MW operational from 2020	50 MW operational 2021, with 4 more projects with operational dates through the next 5 years	(67; 203; 204)	8.5
IDEOL	Casisson/ Barge	3	2015	Undisclosed	2 and 3MW prototype operational since 2018	30MW operational by 2024	Multiple, multi-MW projects all over the world with no operational dates	(67; 204; 205; 206)	7
Saitec SATH	Barge				30kW operational since 2020 and 2MW operational since 2022	Underdevelopment multi-MW operational dates starting from 2025	Initial stages	(67; 207; 208; 209)	7
SeaReed	Semi-submersible	3	2018	2020	N/A	28.5MW project cancelled	N/A	(67; 210; 211)	6
Trifloater	Semi-submersible	4	TBC	TBC	Model Proven, via model testing	N/A	N/A	(67; 212; 213)	6
Spinfloat	Semi-submersible	3	TBC	TBC	6MW demonstrator, cancelled	N/A	N/A	(214)	4

Nautilis semi-sub	Semi-submersible	3	TBC	TBC	No model however was used for the LIFE50+ project funded by EU Horizon (2020 program)	N/A	N/A	(67; 215)	N/A
Nezzy SCD	Semi-submersible	2	TBC	TBC	Scale model operational 2020, and 16.6MW full scale operational from 2022	N/A	N/A	(67; 216; 217)	4
Eolink	Semi-submersible				Scaled prototype operational from 2018	5MW by 2024	Operational by 2026	(67; 204; 218)	4
Tetrafloat	Semi-submersible	3	TBC	TBC	Tank testing carried out 2021	N/A	N/A	(17; 219)	3
Cobra semi-Spar	Semi-submersible				Tank testing carried out	Was proposed for Kincardine offshore farm however was replaced by WindFloat	N/A	(67; 220)	7
OO-star	Semi-submersible				Tank testing 2018, Pre-construction phase 2022	N/A	N/A	(67; 221; 222)	4
Hexafloat	Semi-submersible				Full scale testing predicted 2023	N/A	N/A	(67)	4
vVolturnUS	Semi-submersible	3	2018	TBC	Scaled prototype 2013, 11MW under consent application	N/A	N/A	(67; 223)	7
V-Shaped Semi-sub	Semi-submersible	3	2015	TBC	Installed 2015	2 and 5 MW turbines decommissioned 2021	N/A	(67; 224)	5

Hywind	Spar	4	2009	2017	Installed 2009	Installed	30MW operational since 2017	(67; 225)	9
Sway	Spar	3	TBC	TBC	0.01MW prototype installed 2014 now decommissioned	N/A	N/A	(226; 227)	5
WindCrete	Spar	3	TBC	TBC	scale model testing 2022 and prototype development	N/A	N/A	(228; 229; 230)	4
Hybrid Spar	Spar	4	2013	TBC	Installed 2013	Installed 2016	N/A	(67; 231)	5
Advanced Spar	Spar	4	2013	TBC	Installed 2013	N/A	N/A	(67; 232)	5
SeaTwirl	Spar	3	TBC	TBC	First prototype test 2007 and installation 2015	N/A	2023 first commercial order	(67; 233)	4
DeepWind Spar	Spar	2	TBC	TBC	1kW prototype			(68)	4
PelaStar	TLP	3	TBC	TBC	N/A			(67)	N/A
Blue H TLP	TLP	3	2018	2020	Installed	N/A	N/A	(234)	6
GICON-SOF	TLP	3	2015	2017	Tank testing 2013	Pre-construction 2.3MW, 10MW consented	N/A	(67; 204)	4
Eco TLP	TLP	3	2018	TBC	2MW demonstrator cancelled 2016	N/A	N/A	(235; 236)	N/A
TLP Wind	TLP	3	TBC	TBC	Tank testing 2018	5MW 2019 project cancelled	N/A	(67; 237; 238)	4

Advanced Floating Turbine	TLP	2	TBC	TBC	Scale model created 2013	N/A	N/A	(239)	2
SBM TLP	TLP				8MW underdevelopment, subject to finance	N/A	N/A	(67; 240)	7
PivotBouy TLP	TLP				scale model and 6MW project completed	2022-2025 6MW development	15Mw+ underdevelopment expected earliest 2026	(67; 204; 241)	4

Table 6.3: TRL from 2015 updated for 2023.

This TRL information was then averaged to give Table 6.4.

Platform Type	TRL Average	Maximum TRL
Spar	5.14	9
Semi-submersible	5.5	9
TLP	5	7
Barge	7	7
Monopile	9	9

Table 6.4: TRL Average and maximum values.

6.1.7 Platform Size

The final consideration is the size of the platform, since the geometry of each platform varies, as will the ease of transport and port handling. This is a significant challenge, as it is unknown whether existing ports can handle some of these large platforms (242). This could potentially lead to certain platforms, such as the Spar, being taken out of consideration. Considering generic platform geometries, the size from largest to smallest volume is expected to be as follows: Spar, Semi-submersible and Barge, monopile, and TLP. To categorise each platform the waterplane area is considered along with the draft.

6.2 Methodology

In order to determine the most suitable platform for a specific site, the TOPSIS methodology has been implemented, utilising marking criteria and user ranking using the same approach as presented in (11). This method is advantageous because it creates a flexible framework with qualitative and quantitative criteria. The TOPSIS method is presented in Section 6.2.1 and the inputs used for the attributes and marking criteria are given in Section 6.2.2.

6.2.1 TOPSIS Methodology

The fundamental concept of TOPSIS is that the best solution should have the farthest distance from the Negative Ideal Solution (NIS) and be the closest to the Positive Ideal Solution (PIS), providing a ranking of the solutions. Overall, this process is computationally inexpensive and allows human judgment to be considered. Figure 6.2 shows the process followed for this work.

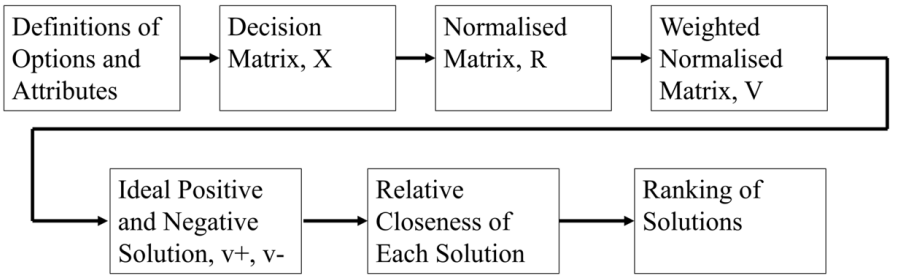

Figure 6.2: TOPSIS Methodology.

For complex decisions, such as platform selection, multi-criteria decision-making (MCDM) is required. This can be presented in matrix form, known as the decision matrix, as shown in Eq. 6.1. X_d is constructed of m alternatives and n criteria, where each element in the matrix expresses the mark for the j-th option.

$$X_d = \begin{array}{c} \\ A_1 \\ A_2 \\ \vdots \\ A_m \end{array} \begin{array}{c} \begin{array}{cccc} C_1 & C_2 & \cdots & C_n \end{array} \\ \begin{bmatrix} x_{11} & x_{12} & \cdots & x_{1n} \\ x_{21} & x_{22} & \cdots & x_{2n} \\ \vdots & \vdots & \ddots & \vdots \\ x_{m1} & x_{m2} & \cdots & x_{mn} \end{bmatrix} \end{array} \tag{6.1}$$

The vector C in Eq. 6.1 represents the criteria with respect to the A_{i-th} Alternatives. Vector A will be described in Section 6.2.2. From the initial matrix, X_d, a normalised matrix, R, will be derived to scale the results appropriately, making them comparable. This can be done by using the formula presented in Eq. 6.2 for each element of the

decision matrix.

$$r_{i,j} = \frac{x_{i,j}}{\sqrt{\sum_{i=1}^{m} x_{i,j}^2}} \tag{6.2}$$

Once matrix R is constructed using $r_{i,j}$, the weighted normalised matrix V can be defined. This matrix encompasses all potential $i-th$ solutions, characterised by the n marks for each criterion. This utilises a weight vector (w_j) as reported in Eq. 6.3. This vector is a user input and provides a level of importance for each attribute. The scale of importance can be, for example, 1-5 or 1-10, depending on the granularity required.

$$v_{i,j} = w_j \cdot R \tag{6.3}$$

This method considers Euclidean space, giving each solution in the V matrix a point in the n-dimensional Euclidean space. The J+ set presented in Eq. 6.4 describes the maximum mark for every positive marking criterion (for example the TRL is a positive criterion, where a higher value is better). The J-set for the PIS presents the lowest mark for every negative criterion, i.e. cost criteria. Combining this information together then gives the PIS. The NIS is the opposite, utilising the minimum for the J+ set and maximum values for the J-set. PIS, A+ formula is given in Eq. 6.4 and NIS, A- is given in Eq. 6.5

$$\begin{aligned} A^+ &= (v_1^+, \ldots, v_n^+), \\ v_j^+ &= \begin{cases} \min(v_{i,j}) & \text{if } j \in J^+ \\ \max(v_{i,j}) & \text{if } j \in J^- \end{cases} \end{aligned} \tag{6.4}$$

$$\begin{aligned} A^- &= (v_1^-, \ldots, v_n^-), \\ v_j^- &= \begin{cases} \max(v_{i,j}) & \text{if } j \in J^+ \\ \min(v_{i,j}) & \text{if } j \in J^- \end{cases} \end{aligned} \tag{6.5}$$

To determine the ranking of candidates (platforms), the relative distance of each solution to the ideal solution must be found. In order to do so, Eq. 6.6 and 6.7 are used, where S_i^+ is the distance of the i-th solution to the PIS and S_i^- for the NIS, respectively.

$$S_i^+ = \sum_{j=1}^{n} (v_j^+ - v_{i,j})^2 \tag{6.6}$$

$$S_i^- = \sum_{j=1}^{n} (v_j^- - v_{i,j})^2 \tag{6.7}$$

The relative closeness of each potential solution to the PIS will be indicated through the closeness index, C_i, shown in Eq. 6.8, where the solution closest to 1 is the most favourable.

$$C_i = \frac{s_i^-}{s_i^+ + s_i^-} \tag{6.8}$$

6.2.2 Marking criteria and attributes

For this work, there are a total of nine key attributes to consider in identifying the most appropriate platform. The first five are related solely to the platform and are quantifiable parameters: CapEx, OpEx, DecEx, TRL, and size. The remaining four are linked to the platform's compatibility with the site. These considerations involve assessing the platform and station-keeping system with the water depth and wave height, and the tidal range and soil conditions, respectively. These attributes are more difficult to quantify numerically. Therefore, compatibility of zero and one was applied for each platform type, where zero represents incompatibility and one represents compatibility between the platform or mooring system and the site.

Using the information in Section 6.1.2, the water depth which is suitable for each platform can be defined. For example, a Spar would be compatible above the minimum allowable water depth of $120m$, where this is the case for a specific site the water depth compatibility will be prescribed a value of one and for sites where water depth is below $120m$ it will be zero. Similarly, a monopile would only be compatible below the maximum allowable water depth ($60m$). Both the soil condition and tidal range can be assessed using the information in Section 6.1.1 and 6.1.4, respectively. In the case where the tidal range to depth ratio is greater than the allowable ratio (5%) the site is not compatible with the TLP but is compatible with the other platform types. The soil condition can be easily categorised in terms of compatibility using the anchor type and

the suitable mooring lines. The sensitivity to wave height for each platform is slightly more difficult to define since, as the wave height increases, the performance, in general, will worsen for all platforms. As discussed in Section 6.1.3, Spar and TLP platforms are expected to perform better in higher sea states compared to Semi-submersibles. By evaluating the site's maximum significant wave height alongside the platform's expected operational range (low and high significant wave height thresholds), the compatibility between the site and platform can be assessed. These combined attributes form the A vector, as introduced in Section 6.2.1.

To account for different stakeholders' point of view, the user defines a weighted vector by prescribing an importance value to each attribute, this information is then used to create the weighted matrix. The importance ranking can be organised in many different ways; however, for this specific work, the criteria are ranked from one to five, five being very important and one being very unimportant. The different options highlighted with vector C are the possible support structures. Both vectors A and C are highlighted in Table 6.5:

Attributes (vector C)	**Support structures (vector A)**
Soil condition compatibility	Spar
Tidal range compatibility	Semi-submersible
Water depth compatibility	Barge
Wave height compatibility	TLP
CapEx	Monopile
OpEx	
DecEx	
TRL	
Size	

Table 6.5: Attributed and potential support structure options.

A pre-filtering criterion was set to remove unfeasible platforms for the sites from the TOPSIS ranking process. This was applied to water depth compatibility since it is a physical constraint. The same was applied to the tidal range compatibility, removing the TLP platform where the tidal range to depth ratio was greater than 5%.

6.3 Case Study: Scotwind

An area of interest for floating offshore wind has been the Scotwind sites awarded in 2022. Table 6.6 and Figure 6.3 highlight the details of each site, along with the four site parameters related to determining the most appropriate platform. The project developer and proposed installed capacity were easily found on (18). The water depth and maximum significant wave height were found using bathymetry charts and downloadable data from (192). The tidal range and soil type were identified from maps on (243). Based on the sea bed configuration the category the soil came under was easily identifiable.

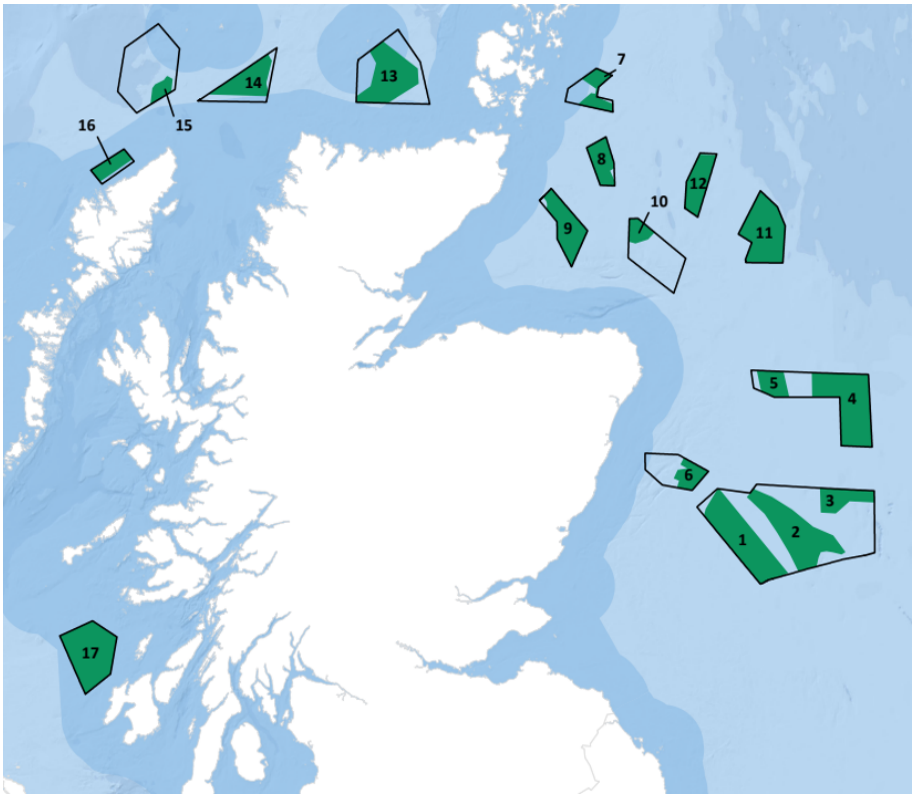

Figure 6.3: Recent Scotwind sites up for leasing (18).

Number on Figure	Developers	Capacity (MW)	Water Depth (m)	Water Depth Category	Maximum Significant Wave Height (m)	Tidal Range (m)	Soil Type	Soil Category
2	SSE Renewables, CIP and Marubeni	2610	100	Intermediate	9.29	3	Sand and muddy sand	Soft
3	Falck Renewables and BlueFloat Energy	1200	100	Intermediate	9.29	2	Sand and muddy sand	Soft
4	Shell and Scottish-Power Renewables	2000	100	Intermediate	10.24	2	Sand (major), rock and sediment, gravelly sand	Soft
5	Vattenfall and Fred Olsen Renewables	798	100	Intermediate	10.24	1	Rock and sediment, gravelly sand	Medium
7	DEME, Aspiravi and Qair	1008	100	Intermediate	8.87	3	Sandy gravel, rock and sediment, gravelly sand	Medium
8	Falck Renewables, Orsted and BlueFloat Energy	1000	100	Intermediate	8.5	3	Sandy gravel, rock and sediment, gravelly sand and sand	Medium
10	Falck Renewables and BlueFloat Energy	500	100	Intermediate	8.83	3	Sand	Soft
11	Shell and Scottish Power Renewables	3000	100-250	Deep	9.82	2	Muddy sand, sandy mud	Medium
12	Floating wind Allyance (Baywa r.e., Elicio and BW Ideol)	960	100-250	Deep	9.07	2	Muddy sand, sandy mud	Medium
14	Northland Power	1500	100-250	Deep	11.91	4	Sand, gravel, rock and sediment, sandy gravel, gravely sand	Medium

15	Magnora ASA and Technip UK	495	100-250	Deep	12.08	3	Sand, gravel, rock and sediment, sandy gravel, gravely sand	Medium

Table 6.6: Details of Scotwind sites.

For this case study, the following inputs found in Table 6.7 were determined by carrying out a survey at the Future Wind and Marine Conference 2023. This survey was anonymous and was accessed via a poster at the conference to avoid bias. The weighting parameters from this survey were then combined to find the average. The average found was in agreement with the opinion of the author. The survey can be found here (244). Water depth is important since certain platforms are limited by depth; hence, it was given a weighting of three. The reason for this was that it is a physical barrier in some cases, such as the spar. The water depth which is most suitable for each platform is also correlated to the lowest cost of that platform. Similarly, the soil condition was also given an importance of three since a secure anchoring system is needed. Certain mooring systems require different anchorage, but most platforms and catenary systems can be made suitable for the environment, but come at a cost, hence the rating. The tidal range can heavily affect the mooring system, adding extra loading, particularly when a taut system is used. Since a large tidal range can have serious consequences, such as a snapped mooring line, leading to the risk of drifting, shutting down the turbine or potentially asset loss, a rating of four was considered. The wave height can affect the performance of the turbine, with higher wave height and motions leading to a reduction in power and hence a knock-on effect on LCoE. The other effect could potentially be an increase in fatigue, which will increase the OM cots. For these reasons, it was given a weighting of four. The CapEx was given a weighting

of five since it accounts for the majority of the overall cost and ultimately is a driver for any project which hopes to be profitable. The OpEx has been weighted at three since this contributes to 25-30% of the overall cost. Finally, the DecEx was weighted at two since it makes up a very small portion of the cost and, in the experts' opinion, is less important than CapEx. A higher TRL was attractive because the industry would have already learnt useful lessons for manufacturing, installation, and operation. The size of the platform is of relatively high importance since ports around Scotland have a limited capacity, therefore, it was given an importance ranking of four.

Criteria Limits	**Value**
Maximum allowable water depth for a monopile	60m
Minimum allowable water depth for a Spar	120m
Allowable ratio of tidal range to water depth	5%
Low significant wave height cut off	3m
High significant wave height cut off	8m
Weighting vector inputs	**Value**
Soil condition compatibility	3
Tidal range compatibility	4
Water depth compatibility	3
Wave height compatibility	4
CapEx	5
OpEx	3
DecEx	2
TRL	3
Size	4

Table 6.7: Inputs for the criteria limits and the weighting vector

Using the platform-selecting code and input data from the user the results can be found and presented in Table 6.8. It comes as no surprise that there is no support structure which fits all sites. The results highlighted in red are not applicable.

Rank	Site 2	Site 3	Site 4	Site 5	Site 7	Site 8	Site 10	Site 11	Site 12	Site 14	Site 15
1	Barge (0.5925)	Barge (0.5925)	Barge (0.5925)	TLP (0.5744)	TLP (0.5744)	TLP (0.5744)	Barge (0.5925)	Barge (0.5680)	Barge (0.5680)	Spar(0.5863)	Spar(0.5863)
2	Semi-submersible (0.5799)	Semi-submersible (0.5799)	Semi-submersible (0.5799)	Barge (0.5680)	Barge (0.5680)	Barge (0.5680)	Semi-submersible (0.5799)	Semi-submersible (0.5568)	Semi-submersible (0.5568)	Semi-submersible (0.4609)	Semi-submersible (0.4609)
3	TLP (0.5324)	TLP (0.5324)	TLP (0.5324)	Semi-submersible (0.5568)	Semi-submersible (0.5568)	Semi-submersible (0.5568)	TLP (0.5324)	Spar(0.5027)	Spar(0.5027)	Barge (0.4608)	Barge (0.4608)
4	Monopile	Monopile	Monopile	Monopile	Monopile	Monopile	Monopile	TLP (0.4772)	TLP (0.4772)	TLP	TLP
5	Spar	Spar	Spar	Spar	Spar	Spar	Spar	Monopile	Monopile	Monopile	Monopile
Proposed platform	N/A	Concrete Semi-submersible	Steel and concrete Semi-submersible	Semi-submersible	TLP	Concrete Semi-submersibles	Concrete Semi-submersible	Steel and concrete Semi-submersible	Ideol damping pool foundation	N/A But states Deeper water capabilities, potentially a Spar	N/A but possibly a Concrete Semi-submersible

Table 6.8: The most platforms ranked in order of best to worst for each site.

6.4 Discussion

The results yielded from this work are generally mixed in comparison to the proposed platform by the developers, with only two of the sites being correctly predicted. It can be noted that the developers' choice for site 2 is unknown and therefore cannot be compared. A main contributing factor to the differences in the proposed platform is expected to be the user inputs, which can vary heavily from person to person and in this case developer to developer. The reasons for these variations are expressed in the following paragraphs. It can be seen that sites 3, 4, 10, 11, and 12 present the developers' choice as the second-best platform, with the barge marginally outranking the Semi-submersible. This is expected to be the case since the most important parameter in the weighting vector was CapEx, therefore this is the main consideration in the ranking. This is one of the reasons the barge outranks the Semi-submersible for all sites. This comes back to a highlighted issue in Section 6.1.5, which states that there is little cost research carried out on the barge platform. Literature suggests a barge would be cheaper because of expensive manufacturing related to the more complex Semi-submersible, however, it is possible the barges higher material mass could contribute to it being more expensive, but there is a lack of literature surrounding this. When considering the closeness value, it can be seen that these two platforms are very

similar, only separated by a hundredth. Another key factor in the barge ranking higher is the lack of dynamic response considered in this work. Comparing a Semi-submersible and a barge, the barge tends to have a larger response, which is unfavourable. It was noted by the author that by reducing the weighting of the CapEx importance, the Semi-submersible was higher ranked than the barge, meaning seven of the ten sites which have proposed developer platforms are predicted correctly, see Table 6.9. Overall, it can be seen that this code is relatively effective in comparison to the developers' choice of platforms and can allow the user to make a better-informed decision based on the user's preference, as well as rule out platforms which are not appropriate for the characteristics of the site. It can be noted that the three sites which are not correctly predicted are likely to have had different opinions on what was important for their work.

Site 5 developers propose a Semi-submersible, whereas the TOPSIS ranking suggests a TLP would be a more effective platform. The reason for the TLP ranking highest is due to the low tidal changes, larger wave heights and medium hardness soil at the site. The TLP is suited for a smaller variation in tidal range but can cope with larger wave heights (89; 245). Similar to the tidal range, the taut mooring system of a TLP requires relatively firm soil to place the anchor system. Since the site characteristics match a suitable environment for a TLP, it was proposed to be best for the specific weighting. The Semi-submersible is considered second best due to the larger waterplane area. Since the wave height is larger on this site, the platform response will be larger.

Site 8, similarly to site 5, the developer has proposed a Semi-submersible, but the TOPSIS suggested a TLP. This is expected to be due to the soil condition being medium and the water depth being intermediate. The developer in both cases may have been more interested in the ease of installation, which would affect the platform choice since a TLP is expected to be more difficult to install due to its more complex mooring system. Another factor which could have led to site 5 and 8 developers choosing a Semi-submersible over a TLP is low TRL since there are no operational TLPs at a commercial scale [1].

[1] At the time of the survey.

The developers of site 15 are going to use a Semi-submersible for their site, rather than a Spar, this could be related to the much easier installation and handling. The size of the Spar would be practically impossible to handle given the current infrastructure in Scotland. For site 15 the developers suggest they will use a concrete Semi-submersible, however, this site has the largest maximum significant wave height which could make it difficult to operate it. For this reason, a Spar is proposed as the best solution.

Rank	Site 2	Site 3	Site 4	Site 5	Site 7	Site 8	Site 10	Site 11	Site 12	Site 14	Site 15
1	Semi-submersible (0.6607)	Semi-submersible (0.6607)	Semi-submersible (0.6607)	TLP (0.6407)	TLP (0.6407)	TLP (0.6407)	Semi-submersible (0.6607)	Semi-submersible (0.6407)	Semi-submersible (0.6407)	Spar(0.6194)	Spar (0.6194)
2	Barge (0.6449)	Barge (0.6449)	Barge (0.6449)	Semi-submersible (0.6407)	Semi-submersible (0.6407)	Semi-submersible (0.6407)	Barge (0.6449)	Barge (0.6245)	Barge (0.6245)	Semi-submersible (0.5001)	Semi-submersible (0.5001)
3	TLP (0.5837)	TLP (0.5837)	TLP (0.5837)	Barge (0.6245)	Barge (0.6245)	Barge (0.6245)	TLP (0.5837)	Spar(0.5480)	Spar(0.5480)	Barge (0.4945)	Barge (0.4945)
4	Monopile	Monopile	Monopile	Monopile	Monopile	Monopile	Monopile	Monopile	Monopile	TLP	TLP
5	Spar	Spar	Spar	Spar	Spar	Spar	Spar	TLP	TLP	Monopile	Monopile
Proposed platform	N/A	Concrete Semi-submersible	Steel and concrete Semi-submersible	Semi-submersible	TLP	Concrete Semi-submersibles	Concrete Semi-submersible	Steel and concrete Semi-submersible	Ideol damping pool foundation	N/A But states deeper water capabilities, potentially a Spar	N/A bu possibly a con crete Sem submersibl

Table 6.9: The platforms ranked in order of best to worst for each site, with a CapEx importance ranking of three rather than five.

Site 2 did not have a proposed platform, but based on this work, a barge or a Semi-submersible would be best, and a TLP would also be possible but would potentially be more expensive.

Sites 2, 3, 4, 10, 11, and 12 have similar characteristics, causing them to have the same ranked order for platforms. The most suitable platform for these sites is a Semi-submersible, followed closely by a barge. Neither the monopile nor the Spar is applicable for these sites due to the water depth. In general, the Semi-submersible and barge are the most generic platforms, due to being able to be deployed under a wide range of conditions. However, it is recommended that further inspection of the hydrodynamic performance would be required. The Semi-submersible and barge rank higher than the TLP due to the weighting placed on the TRL and CapEx.

Similarly, sites 5, 7, and 8 have similar characteristics where Spar and Monopile platforms are not applicable due to water depth. TLP is expected to be the best choice for these sites due to the seabed and the importance of the inputs used for the TOPSIS. It can however be noted for sites 5 and 8 the Semi-submersible has the same closeness value, making it equally as good an option as the TLP.

Finally, sites 14 and 15 have the same ranking. The Spar is considered the best here due to the deep water since water depth importance is high. It can, however, be noted that the Semi-submersible and barge are potential options, but since the Spar has a higher TRL, and is better in higher sea states, it ranks first based on the weighting

parameters. Semi-submersibles have been proven to operate in high wave heights like these sites experience, however, analysis of the specific geometry would be required to draw proper conclusions (225; 246; 247; 248; 249). However, in general terms, it is intuitive to assume that a Spar would perform better than a Semi-submersible or a barge since it has a smaller waterplane area. It can be noted that further hydrodynamic analysis would need to be carried out for a complete assessment. The monopile and TLP are not applicable here due to the water depth.

Since one of the key benefits of a TOPSIS is the ability to consider different weighting vectors, a number of weighting matrices were generated from the benchmark presented in the previous section. Each weighting attribute was altered individually by doubling and halving it to create 18 new weighting matrices. The percentage of each platform ranking highest for each site was found and is presented in Table 6.10 and 6.11.

Site Number	2	3	4	5	7	8	10	11	12	14	15
Spar	0%	0%	0%	0%	0%	0%	0%	0%	0%	22%	0%
Semi-submersible	78%	78%	78%	33%	33%	33%	78%	89%	89%	78%	100%
TLP	11%	11%	11%	67%	67%	67%	11%	0%	0%	0%	0%
Barge	11%	11%	11%	0%	0%	0%	11%	11%	11%	0%	0%
Monopile	0%	0%	0%	0%	0%	0%	0%	0%	0%	0%	0%

Table 6.10: The percentage of each platform which ranked best for the weighting matrices with each attribute doubled.

Site Number	2	3	4	5	7	8	10	11	12	14	15
Spar	0%	0%	0%	0%	0%	0%	0%	0%	0%	0%	0%
Semi-submersible	89%	89%	89%	22%	22%	22%	89%	89%	89%	100%	100%
TLP	0%	0%	0%	67%	67%	67%	0%	0%	0%	0%	0%
Barge	11%	11%	11%	11%	11%	11%	11%	11%	11%	0%	0%
Monopile	0%	0%	0%	0%	0%	0%	0%	0%	0%	0%	0%

Table 6.11: The percentage of each platform which ranked best for the weighting matrices with each attribute halved.

Table 6.10 and 6.11 confirm the findings for sites 2 through 12 the platform choice is well predicted with each platform for the site being found as the best solution for 67% and greater for the different weighting matrices. It can be noted, however, that sites 14 and 15 find that a Semi-submersible would, in general, be the best solution when varying the weighted matrix, which is in agreement with the developer's choice. Overall, this work highlights the Semi-submersible as being a very good solution, which confirms why the majority of developers have opted for this platform.

6.5 Conclusion

The aim of this work was to create a tool which would help rule out and rank support structures for floating offshore wind turbines in a systematic manner, considering a number of constraints and user inputs, to help reduce computational times related to the optimisation of floating offshore wind platforms. This process will reduce computational time and allow a more realistic optimisation to be carried out considering a specific site and its characteristics. The TOPSIS methodology proposed was used to carry out a case study on the recent Scotwind sites, confirming the validity of the work, and showing that 70% of sites were accurately predicted compared to the developers' choice of platform. This work does, however, highlight some disagreements with the developers' choice of floating platform for sites 5, 8, and 14. The main reason for disagreement is likely to

be linked to the weighting provided by the survey. This technique could be useful not only to help developers make quick and informed decisions but primarily to help reduce computational time for optimisations by ruling out platforms which are not appropriate for a site. This work also finds that overall, the most commonly found best solution is a semi-submersible due to its adaptability for each site.

There are a number of limitations to this work, which could pose as potential future work. Considering specific platforms rather than general substructures would greatly improve this analysis; however, this requires a lot of data for each technology. Allowing for considerations in terms of ease of installation, dynamic response, more accurate cost predictions, logistics, space requirements, and the installation campaign would improve the overall ranking of the platforms studied in this research.

Chapter 7

Optimisation Problem

This chapter provides a structured overview of the optimisation problem, beginning with its formal definition in Section 7.1. The following sections elaborate on the key components: the objective function (Section 7.2), the design variables (Section 7.3), the associated bounds (Section 7.4), and the constraints (Section 7.5) relevant to the different geometry types. Finally, Section 7.6 presents the optimisation technique employed in this study.

7.1 Optimisation Definition

The optimisation problem is formulated as the task of identifying a set of design variables $\hat{x}$ that minimises a given objective function $J(x)$:

$$\hat{x} = [x_1, x_2, \ldots, x_k] \tag{7.1}$$

This optimisation is subject to both equality and inequality constraints:

$$h_i(x) = 0, \quad i = 1, \ldots, m \tag{7.2}$$

$$g_j(x) \leq 0, \quad j = 1, \ldots, p \tag{7.3}$$

Here, $\hat{x}$ is a k-dimensional design vector, where each variable x_k may be bounded by upper and lower limits, i.e., $x_k^{\min} \leq x_k \leq x_k^{\max}$.

As this study focuses on a single-objective problem, the objective function $J(x)$ is scalar-valued. The model architecture used in the optimisation process is illustrated in Figure 4.1. To reduce computational expense, the hydrodynamic analysis component is excluded from the optimisation loop and treated as a pre-processed input.

7.2 Objective

The primary objective, consistently emphasised in the literature and discussed in Chapter 3, is cost minimisation, and this work follows the same approach. The objective function of the current research is the summation of the platform, anchor and mooring line cost, see Eq. 4.57 in Chapter 4.

$$J(x) = COST_{overall} \tag{7.4}$$

7.3 Design Variables

This section details the design variables used to describe the different platform geometries.

7.3.1 Spar

The Spar platform is shown in Figure 7.1. The platform can be easily uniquely defined with the following variables:

- Vector of inner column radii , R_1;
- Draft, T;
- Fairlead coordinate, z_m;

Since the platform is constructed of a number of segments, a vector or radii is required, which allows not only straight-sided cylinders to be considered but also truncated cones. The overall platform length can be found by using the draft and the required freeboard. Finally, the vertical coordinate of the fairlead is considered, which is highlighted with the orange circle in Figure 7.1.

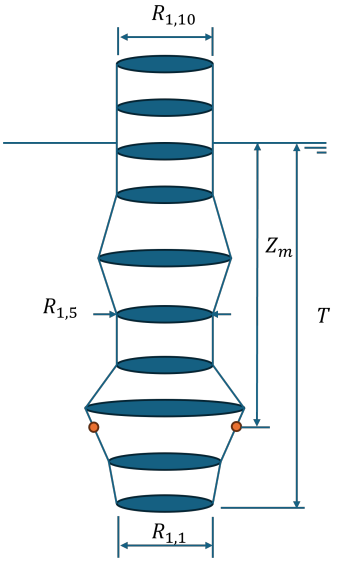

Figure 7.1: The Spar platform geometry

.

7.3.2 TLP

The TLP, shown in Figure 7.2, can be described in the same way. However, further design variables are required for the bracings. The design variable for the bracing length is considered to the centre of the column. When used in the calculations, the cylinder volume, which intersects the bracing, is subtracted from the leg.

- Vector of inner column radii, R_1;
- Draft, T;
- Fairlead coordinate, z_m;
- Bracing depth, b_d;
- Bracing width, b_w;
- Bracing length, b_l.

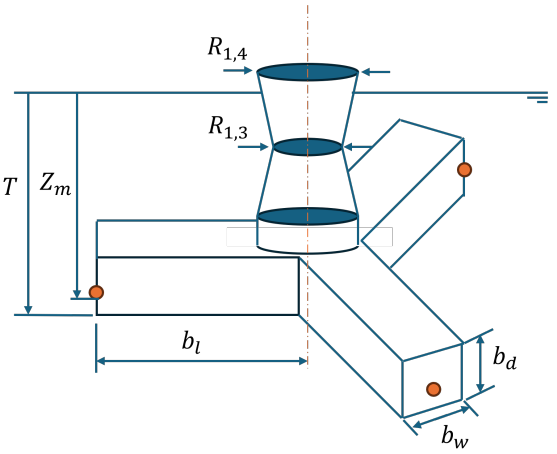

Figure 7.2: The TLP geometry.

7.3.3 Semi-submersible

The Semi-submersible shown in Figure 7.3 highlights the requirement for an extra radii vector to describe the outer columns. The length of the inner and outer columns is assumed to be the same.

- Vector of inner column radii, R_1;
- Vector of outer column radii, R_2;
- Draft, T;
- Fairlead coordinate, z_m;
- Bracing depth, b_d;
- Bracing width, b_w;
- Bracing length, b_l.

7.4 Bounds

In order to create a design space, the design variables must have boundaries, which are presented in Table 7.1. It is important to implement realistic bounds to ensure

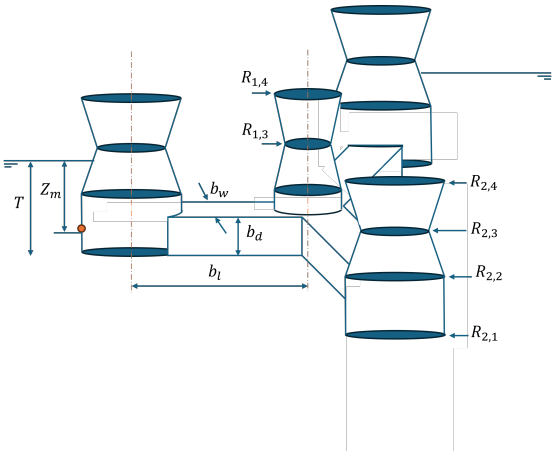

Figure 7.3: The Semi-submersible platform geometry.

the design space is wide enough, but not so wide that it will explore unfeasible or uneconomical designs.

The radius bounds were set to be between 1 and 10, the lower bound is set to 1 to ensure sufficient space to carry out welding and painting inside the section. The upper limit has been set for logistical reasons, if the radius starts to become larger than 10, it would take a huge space to manufacture and store the components of the platform. The draft bounds were set based on what was seen in the literature for each platform type. Similar to the radius the upper bounds were set as a limit to the size which could be handled or realistically would be. For example, a spar with a draft greater than 140m would result in a length of over 155m. The spar is already difficult enough due to its size, so this constraint was added. The mooring line vertical coordinate was decided by running prior optimisations with a constraint on the maximum value equal to the draft, and it was found that the most common values lay between these bounds. The bracing width and depth bounds were set to be the same as the radius, the size logic came from the UMaine platform sizing, with the width being equal to the radius of the outer columns and the depth being 7m. Finally, the bracing length was also based on the main platform, which is 51.25m. The TLP geometry bounds were further justified by the pelastar design presented in Table 5.3, and for the spar, Table 5.1 was used.

Design variable	R_1	R_2	T	z_m	b_d	b_w	b_l
Spar							
Lower bound	1	N/A	60	-70	N/A	N/A	N/A
Upper bound	10	N/A	140	0	N/A	N/A	N/A
TLP							
Lower bound	1	N/A	15	-20	1	1	10
Upper bound	10	N/A	55	0	10	10	60
Semi-submersible							
Lower bound	1	1	15	-20	1	1	10
Upper bound	10	10	55	0	10	10	60

Table 7.1: Design variable bounds.

7.5 Constraints

Constraints are used to ensure feasible designs are explored. These constraints can be split into equality and inequality constraints, these differ slightly for each platform, but the following constraints are used in all cases:

$$h_1(x) = 0 \text{ where } h_1(x) = R_1(No_s + 1) - R_{tower} \tag{7.5}$$

$$g_1(x) \leq 0 \text{ where } g_1(x) = z_m + T \tag{7.6}$$

$$g_2(x) \leq 0 \text{ where } g_2(x) = -m_{ballast} \tag{7.7}$$

$$g_3(x) \leq 0 \text{ where } g_3(x) = -c_{55} \tag{7.8}$$

$$g_4(x) \leq 0 \text{ where } g_4(x) = \theta - \theta_{max} \tag{7.9}$$

The equality constraint ensures the final radius value is equal to the tower radius for

the connection. The inequality constraints which are used are, firstly, that the fairlead connection must be between the water line and the keel of the substructure (g_1). The ballast mass must be positive, and the mooring line stiffness in the pitch DOF must be positive g_2 and g_3 respectively. The former is to avoid the optimisation finding infeasible solutions, and the latter is linked to ensuring the platform can restore to its equilibrium when exposed to external forces. An important parameter is the static pitch of the turbine, which is considered in the final constraint (g_4). The DNV rules state that the maximum static angle is 5°, hence this was considered in this work (250).

The Semi-submersible has additional constraints regarding the geometry, shown in Eq. 7.10 and 7.11. The TLP platform requires this constraint along with constraints presented in Eq. 7.12

$$g_5(x) \leq 0 \text{ where } g_5(x) = b_d - T \tag{7.10}$$

$$h_2(x) = 0 \text{ where } h_2(x) = R_1 - R_2 \tag{7.11}$$

$$g_6(x) \leq 0 \text{ where } g_6(x) = z_m - T + b_d \tag{7.12}$$

The purpose of these constraints ensure the bracings are kept below the water line and the fairlead coordinate is on the bracing. This also helps with the mesh generation, for example, if the bracing legs intersect with the still water level, it changes the number of faces required, leading to issues in the automated meshing code. Eq. 7.11 is for manufacturability purposes since it will be easier to connect the bracings to a straight-sided cylinder.

Constraints such as port and yard capabilities were not considered in the current modelling but should be addressed in future work. Yard capacity limitations can significantly influence the feasibility and cost of floating offshore wind projects. Factors such as available fabrication space, crane lifting capacity, dry dock size, and storage areas determine whether large platforms can be constructed and assembled locally or require fabrication elsewhere with subsequent transport to site. These limitations are critical because they affect not only cost but also schedule, logistics, and regional content opportunities. Incorporating yard and port capability constraints into optimisation models would provide a more realistic assessment of feasible solutions and help identify

strategies that balance cost-effectiveness with practical implementation.

Another important consideration that has been omitted from this model is the treatment of mooring behaviour, particularly slack in tension leg platform (TLP) mooring lines. Since the hydrodynamic analysis is carried out outside the optimisation loop, the dynamic interaction between platform motions and mooring tension is not fully captured. This omission is significant because slack in TLP mooring lines can lead to severe consequences: when slack occurs cyclically, the sudden re-tensioning of lines introduces high impact loads, accelerates fatigue damage, and increases the risk of structural failure. These effects are amplified under harsh environmental conditions and during operational transients, making mooring integrity a critical aspect of TLP design. Neglecting this phenomenon means the current model does not account for one of the primary failure drivers in TLP systems. In practice, classification approval would require detailed coupled analysis of platform motions and mooring dynamics, including non-linear behaviour under extreme and fatigue load cases. Without this, the optimisation results may underestimate both cost and risk, leading to designs that appear feasible on paper but fail under real-world conditions.

7.6 Optimisation Technique

In this case, since the goal is to quickly identify geometries, a pattern search technique was used combined with the multi-start approach. Since the model has been developed within MATLAB the built-in function was utilised.

For this research, both a genetic algorithm (GA) and a pattern search were implemented; the former could not find a solution, which led to the latter being used within this work. The expected reasons for the GAs struggle can be linked firstly to the the methods in which both algorithms work, the GA relies on randomness to explore the search space, this can make it difficult to fine tune and find convergence in a large design space, which is what the particular problem has due to the number of variables and the broad bounds. Pattern search, on the other hand, is systematic and tests the next solution based on the prior to determine if it is better. As mentioned, this can lead to a local minimum rather than a global one. A method to counteract this is

applying the multi-start, which creates the randomness from a GA without the high computational time.

Chapter 8

Case Studies

This Chapter firstly presents inputs for the optimisation and is then split into three main sections, which discuss the optimisation results of Spar, Semi-submersible and TLP for both straight-sided (SS) and truncated cone (TC) models.

The aim of this chapter is to present the different optimisations carried out, and a detailed analysis of the results to find which platforms are best and where the advantages and disadvantages of each design lie.

8.1 Inputs

The inputs required for the optimisations carried out can be seen in Table 8.1. The inputs below vary from values which are set due to material type, such as steel density, Young's modulus and Poission's ratio, or parameters which are linked to the chosen 15 MW turbine (thrust coefficient). Other parameters such as ballast density, minimum freeboard, safety factor, stiffener type, plate height and width, maximum and costs were based on associated literature and the author's judgment. The ballast density reflects current literature and the use of concrete as the ballast (4). The stiffener type was selected based on a study carried out in Chapter 4, which found the Tee stiffener to be the cheapest option.

A key challenge and limitation of this work is the lack of real-world data, which makes it difficult to accurately compare results or quantify the uncertainty in the current

Parameter	Value	Units	Reference
Ballast Density	2500	kg/m^3	(4; 15; 131)
Minimum Freeboard	15	m	(190)
Thrust Coefficient	0.804	n/a	(251)
Force acting on the hub	2.87e6	N	Calculated for 50m/s wind speed in DLC 6.1
Force acting on the tower	1.414e6	N	Calculated for 50m/s wind speed in DLC 6.1
Safety Factor Structures	1.5	n/a	(10)
Steel Density	7850	kg/m^3	(15)
Youngs Modulus of Steel	2.15e5	MPa	(23)
Possions Ratio Steel	0.3	n/a	(10)
Stiffener Type	Tee	n/a	n/a
Maximum Plate Height	12	m	(19; 20)
Maximum Plate Width	3	m	(19; 20)
Paint Cost	28.8e-6	$\$/mm^2$	(10)
Fabrication Cost	2.96	$\$/min$	(10)
Ballast Cost	78.51	$\$/ton$	(4)
Material Cost	2960	$\$/ton$	(131)

Table 8.1: Inputs for the optimisations.

analysis.

8.2 Site 14: SS Spar vs TC Spar

This section carried out an optimisation for the SS and TC Spar for site 14 from the leased ScotWind sites (seen in Figure 6.3). The overall objective for all optimisations carried out is to minimise the cost, which is done utilising a pattern search optimisation technique with a multi-start approach, to find the global maximum. The constraints and bounds used for this optimisation are presented in the previous Chapter 7. The only difference between the optimisation for TC and SS is that the SS uses only one radius to represent the Spar's main body.

8.2.1 Static Stability

In order to assess the static stability Eq. 8.1 for restoring moment is useful. The main stability contributor for a Spar is the ballast component, which is identified as the second component of this equation; for this reason, the mass distribution, centre of

buoyancy and gravity are important.

$$M_{R,y} = (\rho g I_{yy} + F_B z_B - mgz_G)sin(\theta) + C_{55moor}\theta \tag{8.1}$$

As mentioned, the Spar is known for being a ballast stabilised platform where the lower vertical positioning of the CoG ballast mass helps to create the restoring moment to counteract the inclining moment of the wind. This can be realised with the above equation, if ballast mass is placed at the bottom of the column, it lowers the overall centre of gravity, creating a greater distance between CoB and CoG, helping to increase the overall stability contribution. The two optimal geometries predicted for this site can be seen in Figure 8.1.

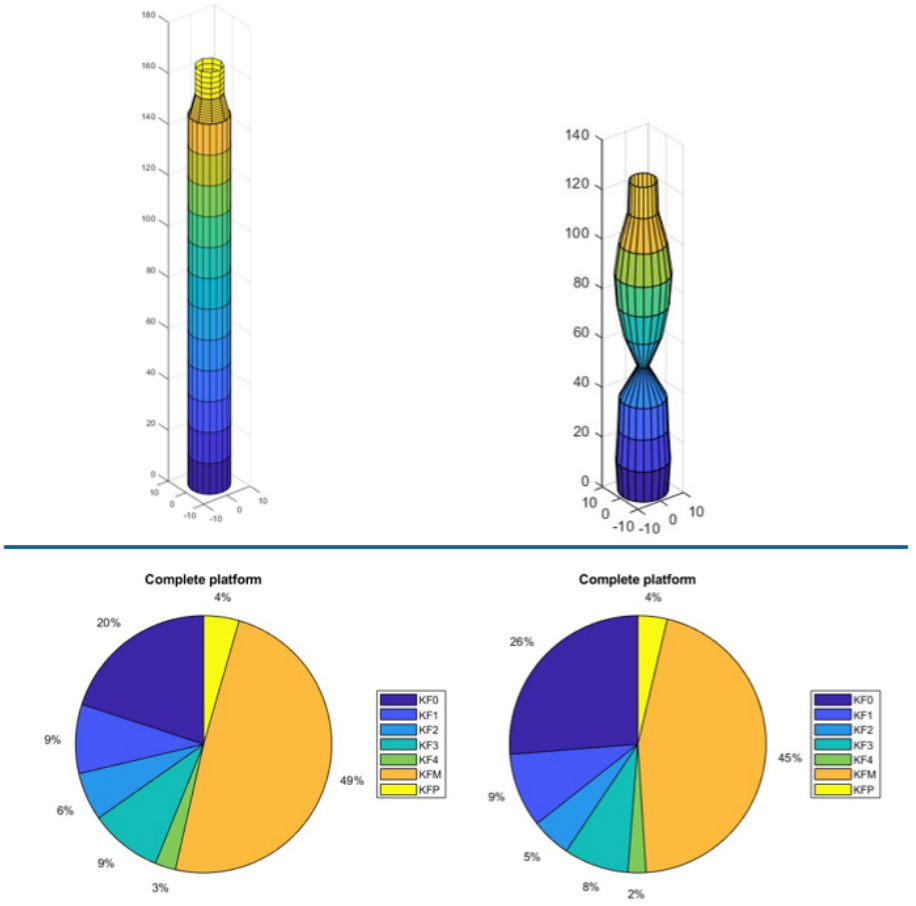

Figure 8.1: Comparison between the optimised solutions for SS1 Spar and TC1 Spar geometry and cost breakdown.

It can be noted firstly that the SS model has a much longer, slender body. The reason for this, from a static stability point of view, is that by increasing the length, the centre of gravity and ballast mass are lower. By lowering this mass, it creates a larger restoring force, meeting the maximum pitch angle constraint of 5°. In the TC case, the platform benefits from the variability in radius, leading to a much shorter design. The reason for this is that the lower segment of geometry can be wider, allowing the required ballast mass to be lower within the structure, leading to lower CoG and the required restoring force.

Varying Maximum Allowable Angle of Inclination

Stability is of the utmost importance for the survivability of the turbine and its subsystems. However, since floating offshore wind is a relatively new commodity how relaxed certain parameters can be is still unknown. An example of this is the maximum allowable pitch angle. Currently, this is restricted to a static pitch of 5° and a maximum of 10° within DNV-RP-0286 (252). To assess the affect on cost five optimisations were carried out varying the pitch angle constraint. For this case study, no freeboard was set and the only consideration was draft must be less than length, to reduce computational time.

Analysing Figure 8.2, as expected, the total mass and cost increase with the decreasing maximum allowable pitch angle. It can be noted that this optimisation favours increasing the ballast mass as the allowable pitch angle reduces. The reason for this is that ballast material has a lower cost compared to steel. Looking in detail at the TC geometries shown in Figure 8.2, it can be seen that the ballast mass required shows an exponential increase with the maximum angle of pitch. This is expected since increasing the mass of the lower segment will lower the overall CoG, creating a greater distance between the CoG and CoB, creating a greater restoring force, and reducing the angle of inclination of the platform. This helps understand the geometry found by the optimiser. In general, the upper section of the Spar is relatively similar; however, as the maximum allowable angle decreases, the radius and therefore the volume of the lower section increase.

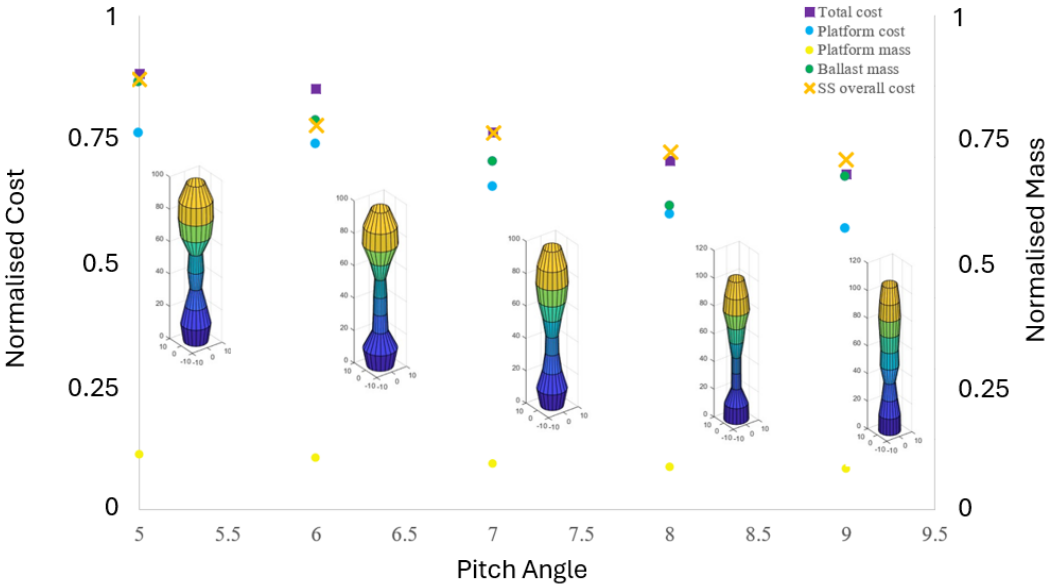

Figure 8.2: Optimisation results for TC varying maximum angle of inclination.

The difference in terms of percentage between the main design variables and cost can be seen in Table 8.2. This highlights again the increase in length and reduction in radius for the platform with the 5° constraint compared to the 9° constrained platform. Overall, this led to a cost saving for the less constrained platform.

Parameter	Difference
Average Radius	32% less for 9° constraint platform
Length	124% more for 9° constraint platform
Cost	20% less for 9° constraint platform

Table 8.2: Design variable comparison between 5° and 9° constrained platform.

The difference between the cost of 5 and 9° platforms is 20%. A total saving of $2.84M per platform could be made by relaxing the maximum angle. The effect on power, however, considering a 15MW turbine, neglecting all other losses and, only considering the platform cost would have to be considered. The impact of the angle of inclination on the power is unknown however it is expected to have some effect size the

turbine is not in the perfect operating condition where the rotor is perpendicular to the incoming wind. The choice of controller could limit this impact, more work would have to be done to consider this. Another element to consider with the relaxation of the maximum inclination angle is the novelty of floating offshore wind. Safety is important, and it is unknown if allowing a turbine to operate at 9 degrees is safe. Considering the operational life of the platform is also important, with a larger pitch displacement, the accelerations in the nacelle could potentially be unfavourable for carrying out maintenance. The oscillations could also lead to a higher failure rate of the platform, mooring lines or anchors. It is, however, expected by (148) that the equipment inside the nacelle would be unaffected; further research in this area would be necessary to confirm this.

8.2.2 Cost Comparison

In order to find the cheapest overall TC, the optimal number of segments had to be found. In order to find this out, the SS optimisation was run first to gain an understanding of a reasonable number of segments, which was found to be 12. The TC optimisations were then run with 9, 10, 11 and 12 segments, and the results were assessed. The optimal number of segments for the TC was found to be 10. Firstly, using 10 segments is cheaper than the 11 and 12 segments platforms since the TC overall has a shorter length, based on this, a lower number of segments can be used to make up the platform with the fixed plate height of 12 m.

Considering the 9-segment optimisation for the TC, it was found to be more expensive since the length of the individual segments is longer than the set plate height (12 m). When this happens, the model splits the segments into smaller segments to consider manufacturability until the segment height is less than the plate height. The impact is a higher manufacturing cost since the number of welds which need to be carried out is increased. It is obvious that in a real-world situation, potentially only one more segment would be required, lowering the segment height desired by the designer. However, in this model, it is impossible to do this since the number of design variables cannot be altered during the optimisation, making this a limitation of the model, and

requiring the segment number to be tuned manually.

From this analysis, the SS platform was found to be the cheapest, despite having a higher mass, the more simplistic geometry benefits from lower manufacturing costs. The two optimal designs TC1 and SS1 designs are presented in Figure 8.3. The 10-segment design, TC1, is only slightly more expensive than the 12-segment SS1 model. The main reason TC1 is more expensive is the manufacturing cost, however this is limited since the platform is a lot shorter and has fewer segment minimising the weld cost required, and overall being only slightly more expensive than SS1.

The second 'best' solutions found from the optimisations are SS2 and TC2. It was noted that SS2 had 10 segments and was 6.5% more expensive than TC1. The reasons for this are due to SS2 having a much larger radius and overall length to get the desired stability. Whereas TC1 benefits from the wider base and pinched centre, and SS1 is longer but much more slender, which is highly linked to the manufacturing costs, particularly forming and welding. These geometries can be seen in Figure 8.3

This work has found that the cost of the SS geometry is lower by roughly 1.78%. The optimal SS1 geometry is cheaper, however, it is extremely large. The OC3 Spar for the 5 MW turbine is 135 m long, whereas this platform for a 15 MW turbine is, as expected, longer at just over 145 m in length. This huge size makes it more difficult to store, handle, and ultimately transport to the site. For this reason, the slightly more expensive TC might be more suitable. The following subsections compare the cost of each part in detail between the two optimal geometries.

Material

Comparing the overall material cost for both platforms, it has been highlighted that SS1 is 6.4% lower. However, interestingly in Figure 8.1 shows the material cost contributes to 49% of the SS1 and only 45% of the TC1, highlighting the expected mass saving for non-traditional geometries. The material cost can be broken down further into three parts, shell, stiffener and ballast, which are explained in the subsequent paragraphs.

The cost of material related to the shell is very similar, with TC1 being marginally cheaper by 0.8%, showing there is a very small benefit in material reduction for the non-

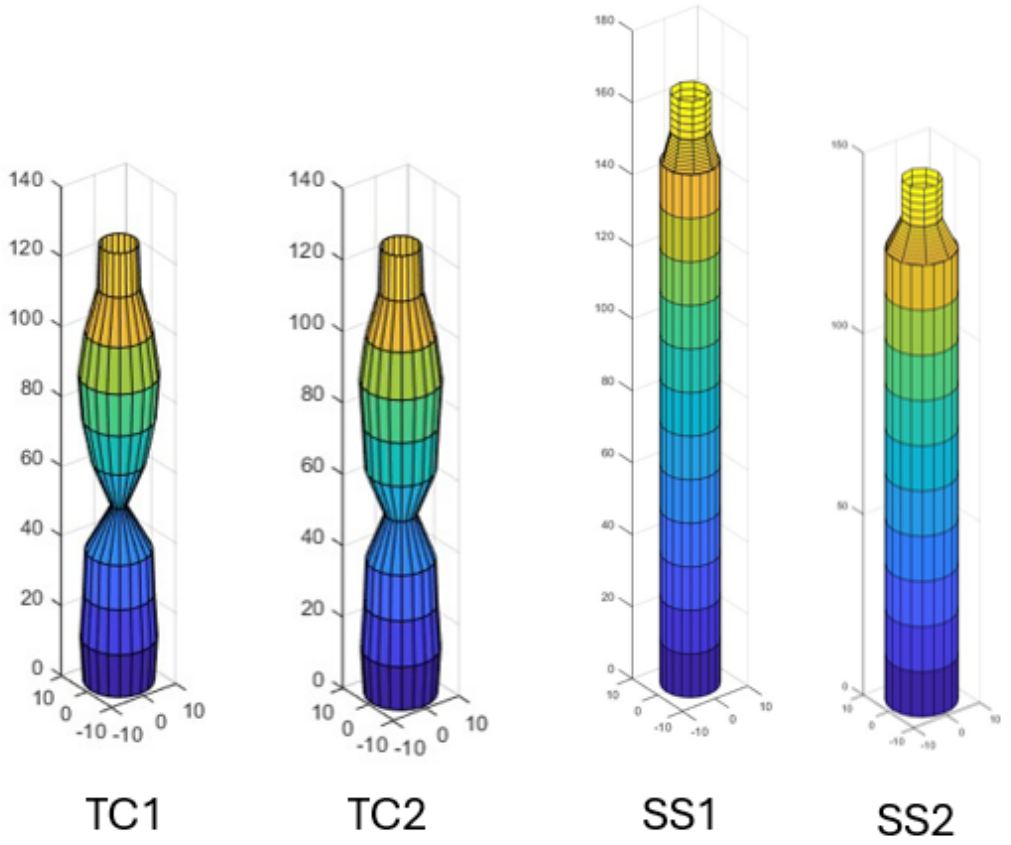

Figure 8.3: Optimisation results for Spar.

traditional geometry. However, they are very similar, and the reason for the similarity is the thicker shell required (50 mm) and smaller size of TC1 compared to the 45 mm thickness and longer geometry for SS1. The thickness is greater because the stress acting on the shell is larger due to the average radius of TC1 being greater. The reduction in thickness is clearly a benefit for SS1, however the longer length inherently increases the material required which leads to this almost complete cancellation of the thinner shell benefit.

The stiffener material cost is considerably lower for the SS1. Similar to the shell, the thickness required for the stiffeners for TC1 is 30mm compared to 8mm for SS1. One disadvantage of the SS1 is that due to the longer length of the platform, 13 more stiffeners are required. The reduction in thickness however is more impactful meaning SS1 stiffener material is cheaper.

Finally, the largest contributor to the difference is ballast material. Both mass and cost for TC1 are greater by 13%, which is linked to the platform being shorter and requiring a greater ballast mass to create the desired restoring force.

Forming

The total forming cost is slightly cheaper for TC1 by 12%. The forming of the shell is more expensive for SS1 by 1.96% , despite on average TC1 having a larger radius and thicker shell, making the plates harder and more expensive to roll. The reason for SS1 having a higher cost is the overall longer length, number of segments (12 compared to 10) and therefore the number of plates which have to be rolled.

The cost difference for forming the stiffeners is, however, almost double for TC1. The difference is not expected to come from the number of stiffeners since TC1 requires a total of 71 stiffeners, whereas SS1 requires 84. The cost difference is linked to the thickness of the stiffeners, where TC1 is more than triple that of the SS1, which increases the forming cost.

Welding

The total welding cost is very close, with TC1 being 1.41% cheaper. The welding cost consists of: welding the shell segments from plates, welding stiffeners from parts, welding stiffeners into the shell, assembling and welding segments. Looking at the cost breakdown, welding curved plates together to create the segments has a lower cost for SS1 (by 10.82%). This is expected to be cheaper firstly because of the reduction in the thickness of the shell and the average radius being lower. Since the segments are made up of a number of plates, which are 3m in width, the radius has a large effect on the number of plates required to make the segment.

Welding the plates together for the stiffeners is, on the other hand, cheaper for TC1 (by 6.4%), which is linked to the longer platform length and extra stiffeners required for SS1.

When it comes to welding the stiffeners in the shell it is less related to the thickness of the shell and stiffener, but the height of the stiffener itself which is used to determine the weld size. Since the stiffener height is the same for both SS1 and TC1, the platform radius and volume are important. The radius of TC1 as mentioned, is on average ever so slightly larger, however, the overall volume of the structure is less, leading to roughly 10% reduction.

Finally, assembling and welding the segments together is lower for TC1 by 5.8 and 3.6% respectively. The assembly cost, similar to welding the stiffeners into the shell, has a strong correlation to the volume, hence the lower cost for TC1. Welding the segments together is linked to a number of segments, thickness and radius. This means that the higher cost is linked to the lower number of segments since TC1 has a greater thickness and radius.

Painting

The painting cost of the TC1 is cheaper for both the shell (inside and out) and the stiffeners (6.5%). Considering the shell first, the surface area of the structure is lower for TC1 due to the length being significantly shorter. The length and height of the stiffeners are the same, and the thickness has little impact on the surface area to be

painted. The difference comes from the 13 extra stiffeners required for SS1.

For the complete cost breakdown and optimised design variables for the optimised Spar geometries see Appendix A.1 and A.3 respectively.

Further Cost Breakdown Analysis

To try and better understand which part of the cost leads to the difference between the two solutions, further investigations were carried out. Firstly, in order to do this, the percentage difference in cost was found between the SS and TC (SS-TC/TC), where a negative percentage represents the TC being more expensive and vice versa for a positive percentage. This was then combined with the cost percentage of each component in relation to the total platform cost. Combining this information with the expected difference between SS and TC provides the weighted cost difference seen in Figure 8.4. To complement this figure the cost percentage difference for each sub cost and the corresponding percentage of each in relation to the total substructure cost is presented in Figure 8.5. To help identify the main contributor to the higher cost for TC, the blue points were added, which show the average percentage of each category compared to the overall cost. These Figures denote the stiffeners with an 's' and the ballast with a 'b'.

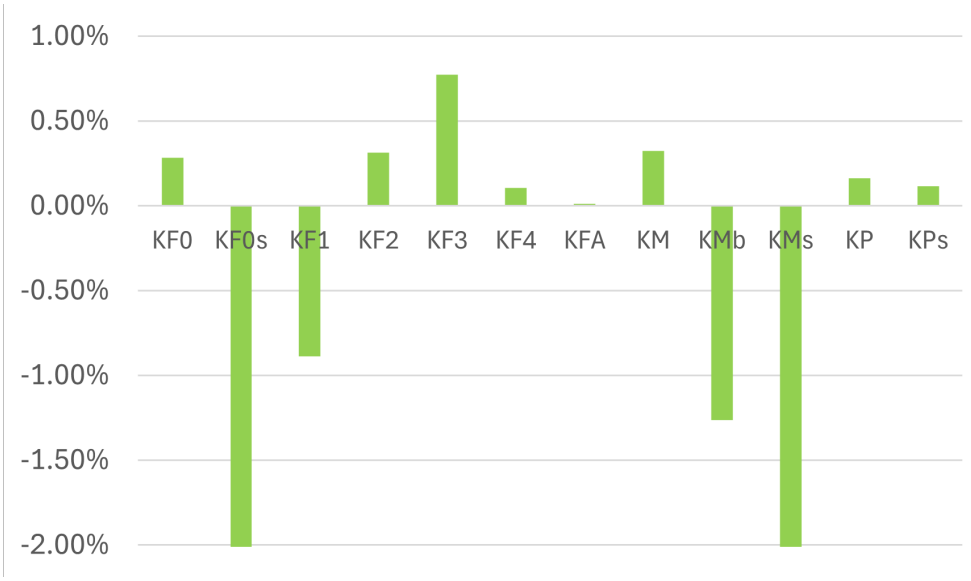

Figure 8.4: Weighted cost difference between SS1 and TC1.[1]

This highlighted that overall the TC substructure alone was more expensive by 4.7%, which can firmly be attributed to KF0s, KF1, KMb, and KMs as seen in Figure 8.4.

The forming of the stiffeners is 46% more for the TC and accounts for roughly 5% of the overall cost. When considering the weighted average in Figure 8.4, it highlights that this is one of the main contributors in making the TC more expensive. The difference in forming the shell is lower (2%) but accounts for 15% of the overall cost, therefore, it has a lower impact on the cost compared to forming the stiffeners.

Using Figure 8.5 and 8.4, it was noted that welding the plates to create segments and welding stiffeners into the shell are roughly 10% different between the two solutions and contribute a notable amount to the overall cost. The welding to create the shell segments (KF1), leads to an increased cost in the TC where as the welding of stiffeners into the shell (KF3) increases the SS cost.

The material cost of the shell (KM) is relatively similar, but the stiffener cost is significantly different, accounting for 3.5% of the overall cost, which is one of the lead caused for the TC cost to be higher, along with the stiffener forming (KF0s). The ballast material cost is 13% more for TC and accounts for 10% of the cost, the reason for the higher cost is linked to the optimisation algorithm driving a mass reduction in the platform, and in order to gain the desired freeboard and therefore draft, ballast mass has to be added to the platform. The optimisation converges to this solution since the ballast mass is a lot cheaper per ton than steel. This, however, is one of the reasons the TC is more expensive. The other welding costs have a relatively low difference and smaller overall contributions to the cost.

The paint cost difference between TC and SS is roughly 6.5% for stiffeners and 9% for the shell. However, they contribute 0.09% and 3.5% to the overall cost, as seen in Figure 8.4, they have little impact, and are higher for the SS since it has larger surface areas to be painted.

[1]KF0 (forming of shell), KFOs (forming of stiffeners), KF1 (welding shells plates into segments), KF2 (welding stiffeners from parts), KF3 (welding into shell), KF4 (assembling and welding shell segments), KM (material for shell), KMb (material for ballast), KMs (material for stiffeners), KP (painting inside and outside of the shell), KPs (painting stiffeners).

[1]KF0 (forming of shell), KFOs (forming of stiffeners), KF1 (welding shells plates into segments), KF2

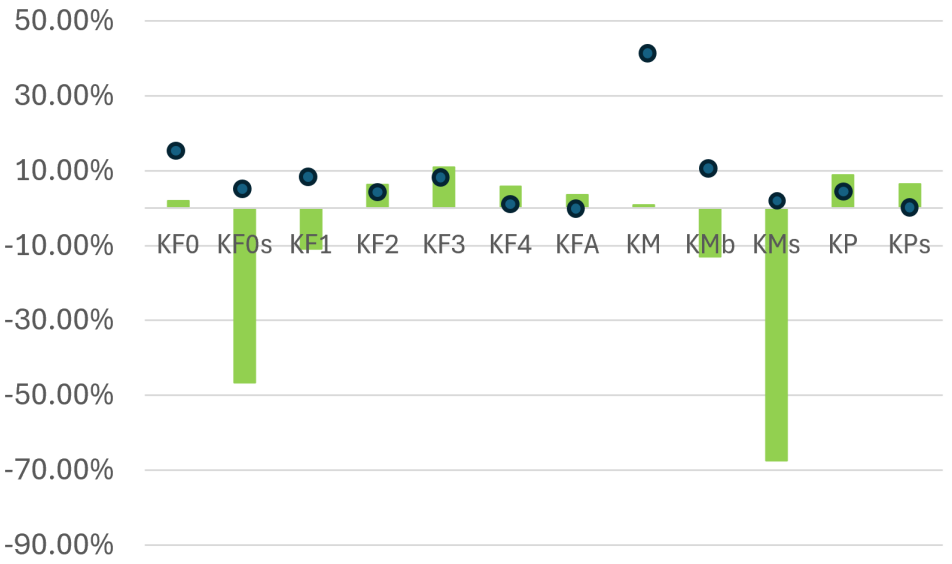

Figure 8.5: Difference in percentage of each cost between SS1 and TC1.[1]

Based on this new understand of which cost parameters drive the difference between TC and SS, to further understand the drivers, a number of additional optimisations were carried out and the results are presented in Figure 8.6, 8.7 and Table 8.3 shows the full cost breakdown. The optimisations carried out were:

- No KF0 costs considered (SSF1 and TCF1 optimal platforms);
- No KMb cost considered (SSB1 and TCB1 optimal platforms);
- No manufacturing costs considered (SSM1 and TCM1 optimal platforms);
- No KF1 and KF3 costs (SSF13 and TCF13 optimal platforms);

Before running the optimisations the corresponding cost was set to zero and the optimal results for SS and TC could then be compared, it was noted that the only scenario where the TC is cheaper is when all manufacturing costs are set to zero and only the shell mass is considered, see Figure 8.6.

(welding stiffeners from parts), KF3 (welding into shell), KF4 (assembling and welding shell segments), KM (material for shell), KMb (material for ballast), KMs (material for stiffeners), KP (painting inside and outside of the shell), KPs (painting stiffeners)

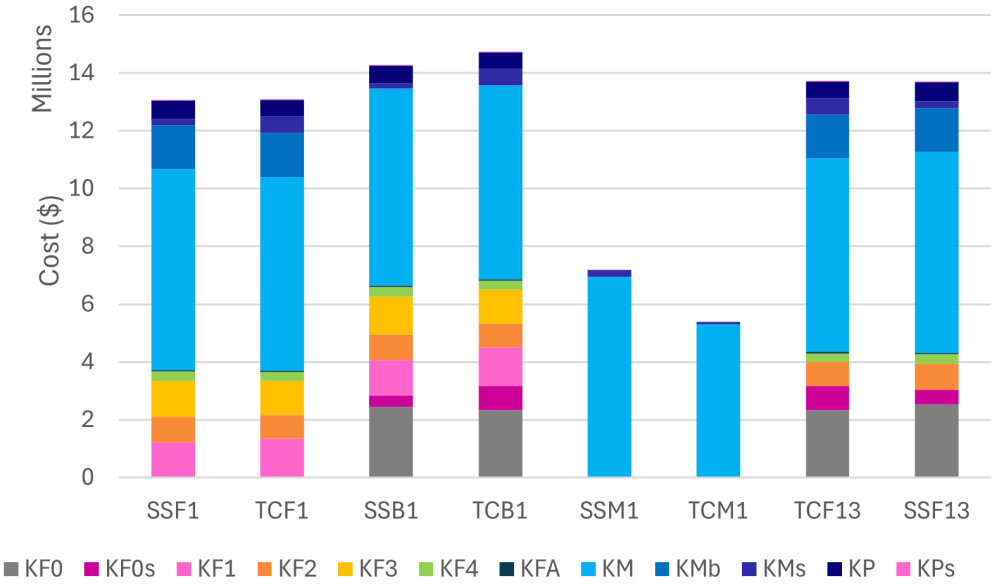

Figure 8.6: Further optimisations.

Neglecting the forming cost from the optimisation, the SSF1 solution is found to be 0.004% cheaper than TCF1, which highlights that the forming cost has a large impact on the cost. The optimal geometries without the forming cost can be seen in Figure 8.7.

Removing KF1 and KF3 from the optimisation, the most cost-effective solution is the truncated cone model (TCF13), which is cheaper by 0.02%. Figure 8.7 shows these two geometries, SSF13 and TCF13.

Setting the ballast cost equal to zero, the optimal solutions find the straight-sided platform to still be cheaper, but by 3% compared to the 4% in the original case with all costs. This highlights that the forming cost has a greater effect. The optimal solutions with no ballast cost can be seen in Figure 8.7, SSB1 and TCB1. It has been noted that the optimisation without ballast cost leads to a longer SS platform (SSB1). Since the ballast cost contributes roughly 10% to the total cost. SSB1 can increase its length and still remain cheaper than TCB1, due to its higher manufacturing costs.

Finally, removing all manufacturing costs and ballast cost, carrying the optimisation with only material mass results in platform SSM1 and TCM1 seen in Figure 8.7. This optimisation finds the TC model to be 25% cheaper, which is expected based on the

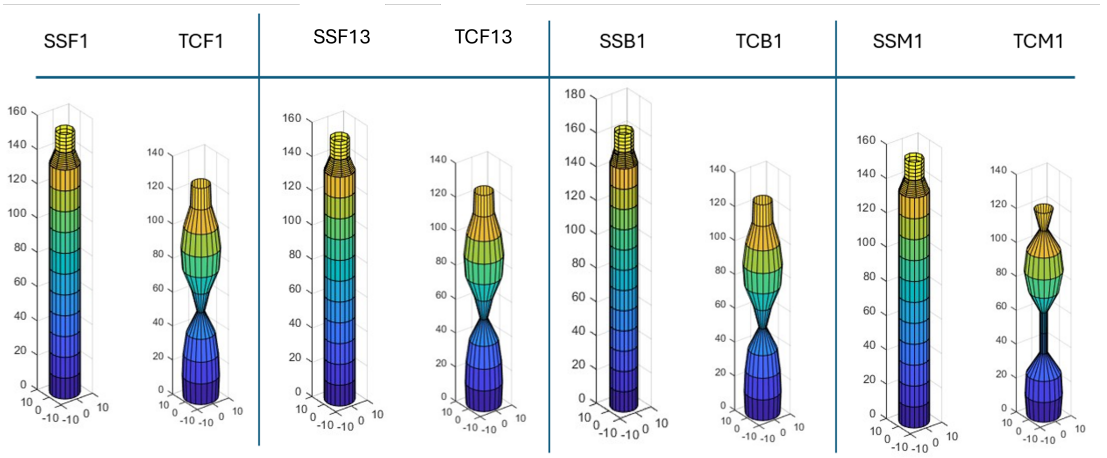

Figure 8.7: Further optimisations.

prior analysis, which finds the only case in which TC is cheaper is when there are no manufacturing costs considered and contribute a sizeable amount to the cost of the platform. The cost can be seen in Table 8.3, denoted by TCM1 and SSM1. The reason this is much lower is the benefit of TC using varying radii, by having an hourglass shape to create the desired stability. This proves that neglecting manufacturing costs is not acceptable, considering that it ultimately changes which solution is cheaper. TCM1 has the benefit of using smaller radii, driving down the mass of the platform. In order to reduce the radii values, the platform is slightly longer than the other optimal TC solutions. The reason other solutions are shorter is linked to increased manufacturing costs.

Cost	SSF1	TCF1	SSF13	TCF13	SSB1	TCB1	SSM1	TCM1
KF0 ($)	0	0	2.52E+06	2.33E+06	2.44E+06	2.33E+06	0	0
KF0s ($)	0	0	5.18E+05	8.52E+05	4.05E+05	8.44E+05	0	0
KF1 ($)	1.22E+06	1.35E+06	0	0	1.23E+06	1.35E+06	0	0
KF2 ($)	8.71E+05	8.17E+05	8.89E+05	8.17E+05	8.69E+05	8.11E+05	0	0
KF3 ($)	1.24E+06	1.19E+06	0	0	1.32E+06	1.18E+06	0	0
KF4 ($)	3.30E+05	3.01E+05	3.30E+05	3.01E+05	3.25E+05	3.02E+05	0	0
KFA ($)	5.00E+04	4.92E+04	5.00E+04	4.92E+04	5.12E+04	4.92E+04	0	0
KM ($)	6.96E+06	6.70E+06	6.96E+06	6.70E+06	6.84E+06	6.71E+06	6.95E+06	5.31E+06
KMb ($)	1.50E+06	1.52E+06	1.50E+06	1.52E+06	0	0	0	0
KMs ($)	2.38E+05	5.75E+05	2.38E+05	5.75E+05	1.66E+05	5.76E+05	2.36E+05	7.07E+04
KP ($)	6.24E+05	5.76E+05	6.57E+05	5.76E+05	6.22E+05	5.78E+05	0	0

KPs ($)	1.73E+04	1.54E+04	1.82E+04	1.54E+04	1.66E+04	1.54E+04	0	0
Total ($)	13061048	13085488	13693136	13731007	14279782	14740025	5377030	7188200
KML ($)	7.95E+05	7.71E+05	8.11E+05	7.71E+05	8.11E+05	7.71E+05	0	0
Anchor Cost ($)	2.43E+04	2.43E+04	2.43E+04	2.43E+04	2.43E+04	2.43E+04	0	0
Overall Cost ($)	13880040	13880576	14528347	14526098	15114983	15534896	5377030	7188200

Table 8.3: Spar cost comparison for different cost inclusions within the optimisation.

8.2.3 Dynamics

To determine the dynamic response of each platform the model presented in Chapter 4 was used. This analysis utilised the frequency domain. The hydrodynamics were found for DLC 6.1 and 1.6 as presented in Section 4.8, the former is a survivability load case where the turbine is turned off, and the latter is operating in an extreme condition. The site under investigation is site 14, now known as Havbredey, off the north-west coast of Scotland. The water depth, wind and wave data for this site were found in (192).

The dynamic response of the SS1 and TC1 was computed, and the results can be compared in Table 8.4.

		RMS Acceleration (m/s^2)			RMS Displacement (m)& (°)					
	Cost ($m)	Surge	Heave	Pitch	Surge	Heave	Pitch	Nacelle Accel-eration	Translational Motion Wind	Translational Motion Wave
TC1	17.64	1.22	0.03	0.72	2.89	0.07	6.7	0.65	0.07	2.89
SS1	17.33	0.82	0.12	0.41	2.03	0.32	5.99	0.50	0.08	2.05
Difference between TC1 and SS1, (TC1 - SS1) / SS1	2%	48%	-72%	76%	43%	-77%	12%	30%	-12%	41%

Table 8.4: Spar Dynamics comparison in percentage between SS1 and TC1 fo DLC 6.1 (negative % highlights SS being worse.)

It has been identified that TC1 has a lower displacement in heave but is larger in both surge and pitch, which is expected due to their strong coupling. The TC1 has a higher added mass and lower damping in the heave direction, the opposite is true for the surge and pitch direction. These results can be seen in Figures 8.8 and 8.9 (Figure 8.10 presents the damping coefficient normalised using critical damping for each DOF). The expected reason for a better heave response is the larger contribution from the added mass, which can be linked to the bottom area of the geometry. TC1 has a larger radius at the bottom, creating a larger area, therefore accelerating the water around it, creating additional inertia since the water moves with the structure. This means the larger the added mass, the more force is required to move the platform.

The surge and pitch are expected to be better for SS1. The former is linked to the frontal area of the platform, which is larger for SS1 due to the increased overall length. Similar to the heave motion, the larger the frontal area for surge DOF, the greater volume of water is accelerated and therefore increases added mass, making it more difficult to accelerate. For the pitch DoF it is a combination of both the previously explained reason for surge and the location of the CoG. Since SS1 has a lower CoG and when considering equation 8.2 it is clear that a lower CoG increases the restoring moment and capability of the platform. The acceleration follows a similar trend due to its correlation with displacement.

The damping follows the opposite trend from added mass, since it is correlated to

the radiated waves and the energy lost to the surrounding environment. In the heave DoF a larger waterplane area leads to stronger wave radiation, increasing radiation damping. For surge the frontal area and the wetted surface length, the wider cylinder radiates more waves in surge, increasing potential damping. Finally, for pitch, the moment of inertia of the waterplane area influences radiation damping; increasing the radius of the cylinder increases the damping.

$$M_{R,y} = (\rho g I_{yy} + F_B z_B - mgz_G)sin(\theta) + C_{55moor}\theta \tag{8.2}$$

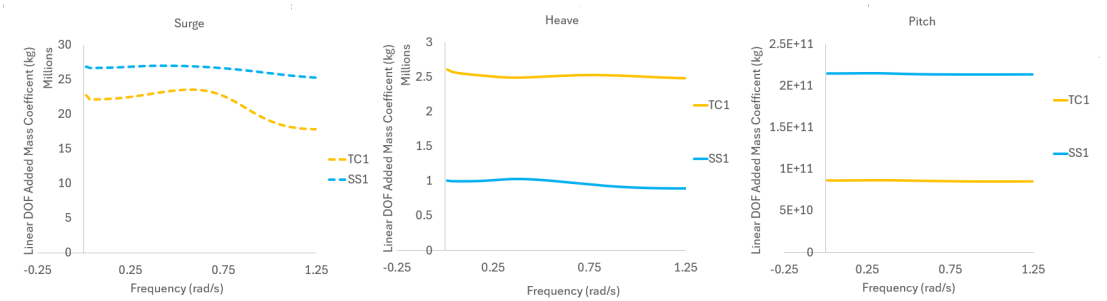

Figure 8.8: Added mass of the optimised Spar results.

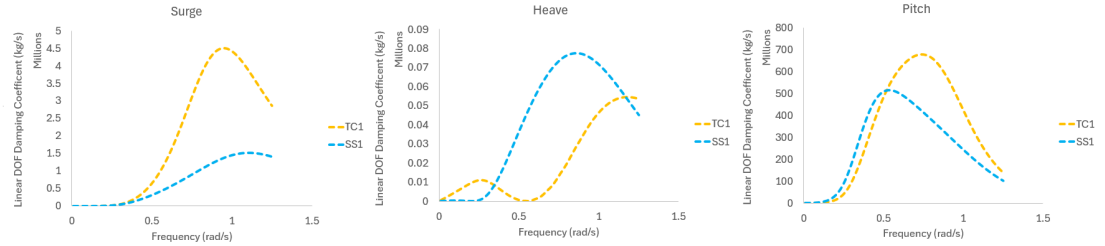

Figure 8.9: Damping of the optimised Spar results.

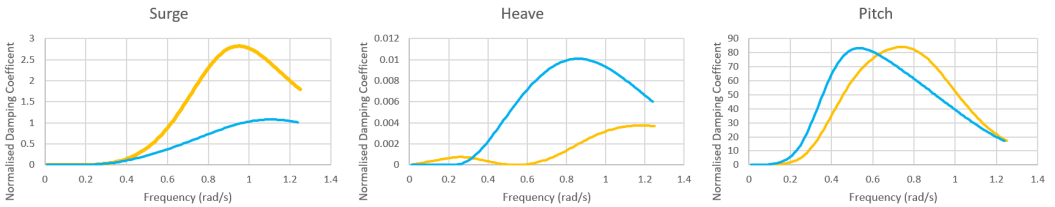

Figure 8.10: Damping coefficient normalised with the critical damping of the optimised Spar results.

The translational motion due to wind is lower for the TC model, which is linked directly to the mooring stiffness, which is greater for the TC model. This is expected to be linked to the mooring line fairlead coordinate, since the diameter of the mooring line is the same for each case, the location of the fairlead is 20m lower for TC1, requiring shorter mooring lines and increasing the stiffness in roll and pitch DOF.

The motion due to waves combines the RMS displacement values to get an overall displacement. Since both pitch and surge are smaller for SS1, it has a lower translational motion.

The nacelle acceleration of SS1 is lower due to the lower CoG providing the stability and the strong correlation between surge and pitch.

It can be noted, however, that nacelle acceleration for all platforms found within this work was below the $1.96m/s^2$ constraint commonly used in literature (136; 137; 138; 141; 142). Similarly, the translational motion was well within the 20% of water depth constraint considered in (136; 141).

The combined hydrostatic stiffness of TC1 is 9% higher due to its larger WPA. The gravitational stiffness is higher for SS1, it has a slightly lower mass overall but the CoG is lower leading to a higher stiffness. Since the mass is higher for TC1 it leads to a larger mass matrix.

Finally, the displacement RAOs can be seen in Figure 8.11.

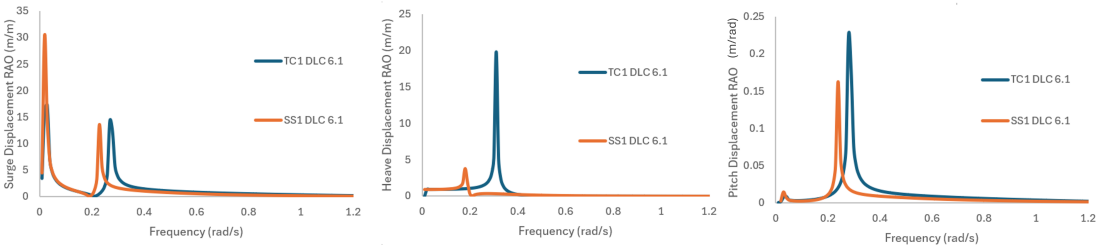

Figure 8.11: Displacement RAOs of the optimised Spar results.

In the surge direction, Figure 8.11 shows TC1 to experience a lower amplitude initial peak but a similar secondary peak which is offset to the right compared to SS1. The first peak is linked to the mooring system, while the second one is due to the strong coupling to the pitch DOF. The heave RAO, TC1 has a greater amplitude and is shifted to the right. The pitch direction has two peaks aligning with the peaks in

surge, with the same differences due to the coupled relationship. The common shift to the right-hand side for the secondary peak in surge, pitch, and the heave peak is linked to the TC1 having a higher stiffness in all DOF, therefore leading to the peak occurring at a higher frequency.

The reason for the shift along the x-axis for all of the DOF for TC1 is the greater stiffness overall of this platform due to the larger waterplane area (Hydrostatic stiffness), and additionally, its higher mooring line stiffness contribution for all DOFs. A sensitivity study was carried out to determine which parameter affected the mooring line stiffness. The fairlead coordinate and radius were varied to determine the underlying cause for increased stiffness. Figure 8.12 shows how the stiffness and mooring line dimensions are affected by changing these variables. It can be noted that the fairlead location has the largest impact on the stiffness, and the radius has little impact. The latter is expected to have little effect since changing them has little to no impact on the dimensions of the mooring line. When the fairlead coordinate changes, it does not change the mooring line diameter; however, it impacts the length of the line and the anchor radius, having a knock-on effect on the stiffness. The increases in peak amplitude are linked to higher added mass and lower damping, which were previously explained and can be seen in Figure 8.8 and 8.9 respectively. The final contributing factor is the mass matrix of TC1, which is larger, leading to both an amplitude increase and a shift along the x-axis.

From a Hydrodynamic point of view, both platforms are acceptable. However, SS1 does have a slight advantage in the surge and pitch direction, leading to an overall lower nacelle acceleration and translational motion. Lower motions are beneficial for a number of reasons, particularly from a fatigue perspective. Another area expected to benefit from lower motions is O&M, which will, generally speaking, increase accessibility, reduce downtime and lead to O&M cost benefits (253). In general, it would be much better from a health and safety point of view to carry out the transfer of technicians from the vessel to the turbine. Further analysis would have to be carried out to assess in detail how each platform would respond in a time simulation, which can capture non-linear effects and consider a coupled system (aero-hydro-servo-elastic)

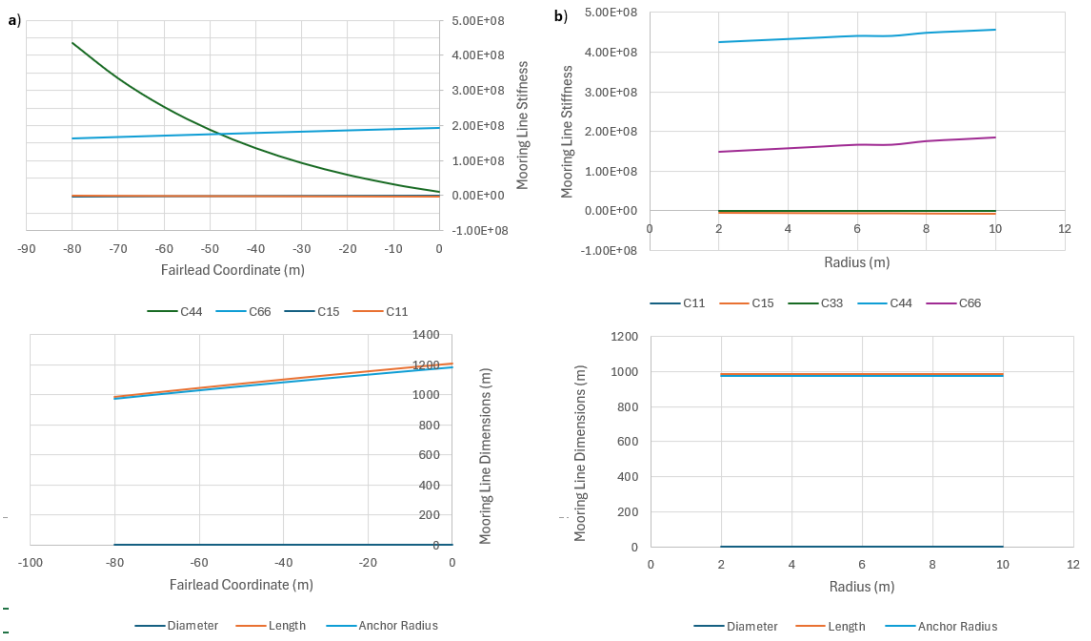

Figure 8.12: Mooring stiffness sensitivity a) Fairlead b) Radius

in a range of different environmental conditions.

8.3 SS Semi-submersible vs TC Semi-submersible

Similar to the Spar, a number of optimal solutions were found and ranked from cheapest to most expensive. The design variables for all optimisations for SS and TC are plotted in Figure 8.13 and 8.14.

In some cases, trends have been identified in the design variables for the TC and SS results across the two suitable sites (8 and 14). The design variables have fairly linearly gathered points. The bracing length average of the cluster is where the design variables for the optimal solution lie. Whereas the fairlead coordinates the lower point at -20 m, the optimal solution is found. As for the rest there is more of an inclined path towards the optimal point the bracing length and width are increasing towards the best solution for SS, however TC the bracing width variable is relatively constant. The draft is decreasing towards the best solution.

The best solutions have on average a lower radius and draft, and increased bracing lengths (larger waterplane areas). Both the depth and width of the bracing stay rel-

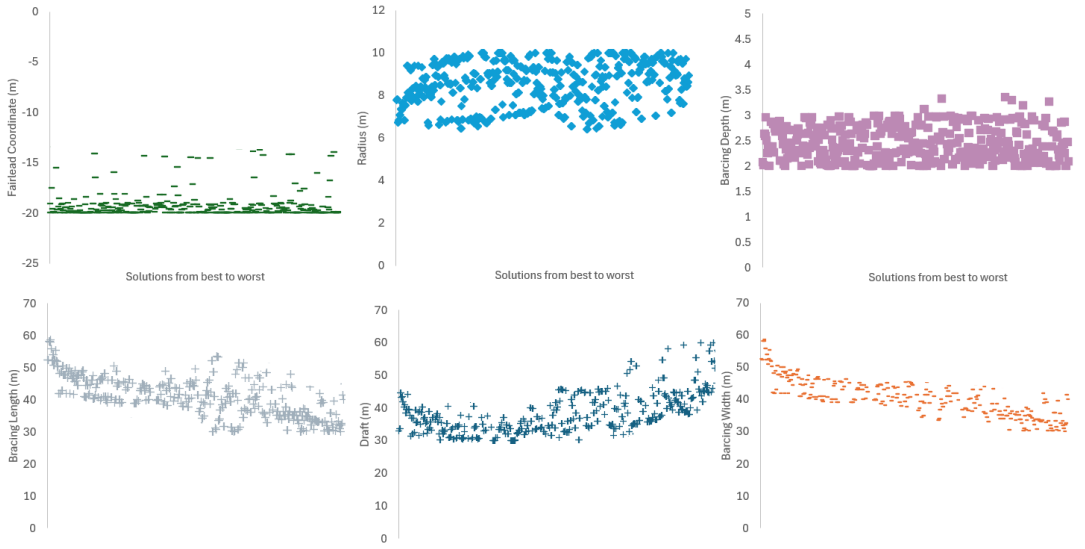

Figure 8.13: Design variables from all of the optimisations carried out from most optimal (right hand side, to the least left hand side) for the SS semi-submersible.

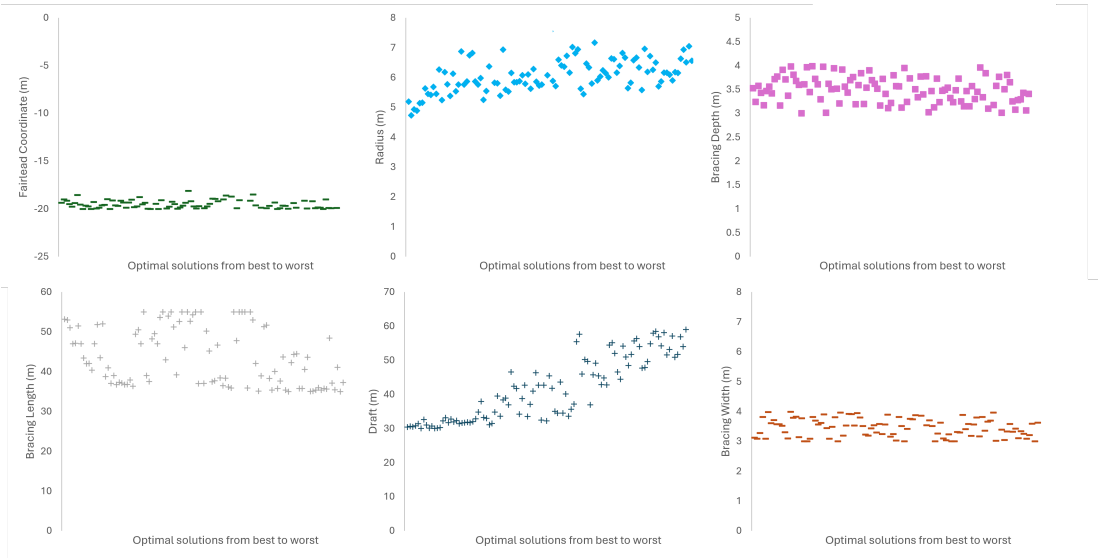

Figure 8.14: Design variables from all of the optimisations carried out from most optimal (right hand side, to the least left hand side) for the TC semi-submersible.

atively similar. Finally, the fairlead coordinate for the optimal designs moving away from the waterline, however the spread is revelative close. To find the desired stability, the optimal solution favours a longer bracing length, which in turn creates a larger second moment of waterplane area, which is the main method of stability for a Semi-submersible.

Initially, the optimal number of segments for the columns was explored. Since the draft bounds are between 15 and 55 m, three segments were run first, followed by four. It was found that there is actually a cost-benefit to having four segments due to the standard sizes of the plates. By using 3 segments within the optimisation, the standard plate is not large enough; therefore, each segment has to be split in half, creating 6 segments, which will lead to a higher manufacturing cost related to assembly and welding. The four segment overall is 4% cheaper than the three. To explore further, increasing the segments to five was also tested; this led to a more expensive optimal solution than the four-segment optimal solution, due to the higher manufacturing cost, similar to the issue with the three-segment optimal solution.

8.3.1 Site 14

The optimal solutions for the SS and TC optimisation can be seen in Figure 8.15.

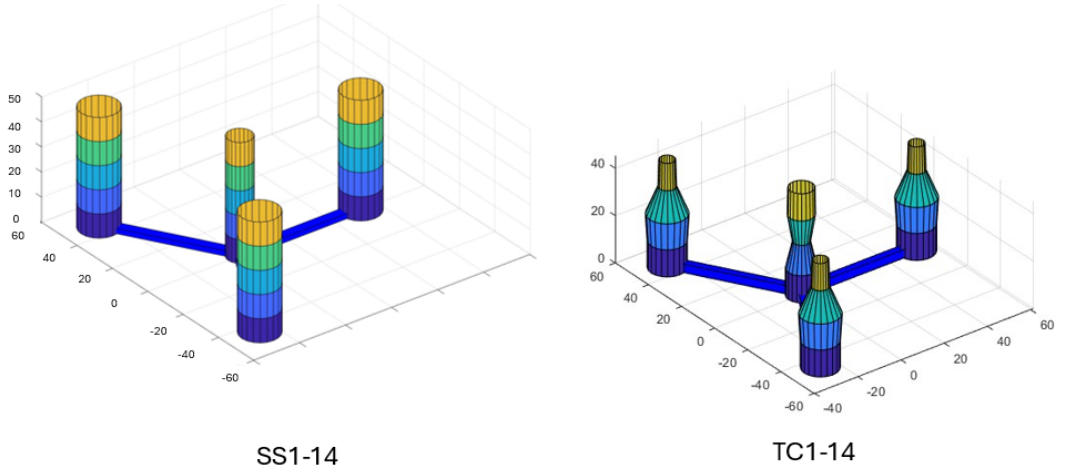

Figure 8.15: The most optimal Semi-submersible solutions for site 14.

Comparing the two geometries, the TC model has a smaller draft by 3 m. Since the

SS is longer, it requires one more segment, due to the longer length and the requirement for the plate height to be no greater than the stated maximum value of 12 m. On average, the inner radius is smaller by 0.1 m, and the outer column radius is 2.2 m smaller. The geometry of the bracings varies very little with the length and depth being 0.5 m larger for the TC and the width being 0.7 m larger for the TC.

By carrying out a number of multistarts, there were also a number of sub-optimal solutions found, a few of these are shown in Figure 8.16 and 8.17, for SS and TC Semi-submersible platforms.

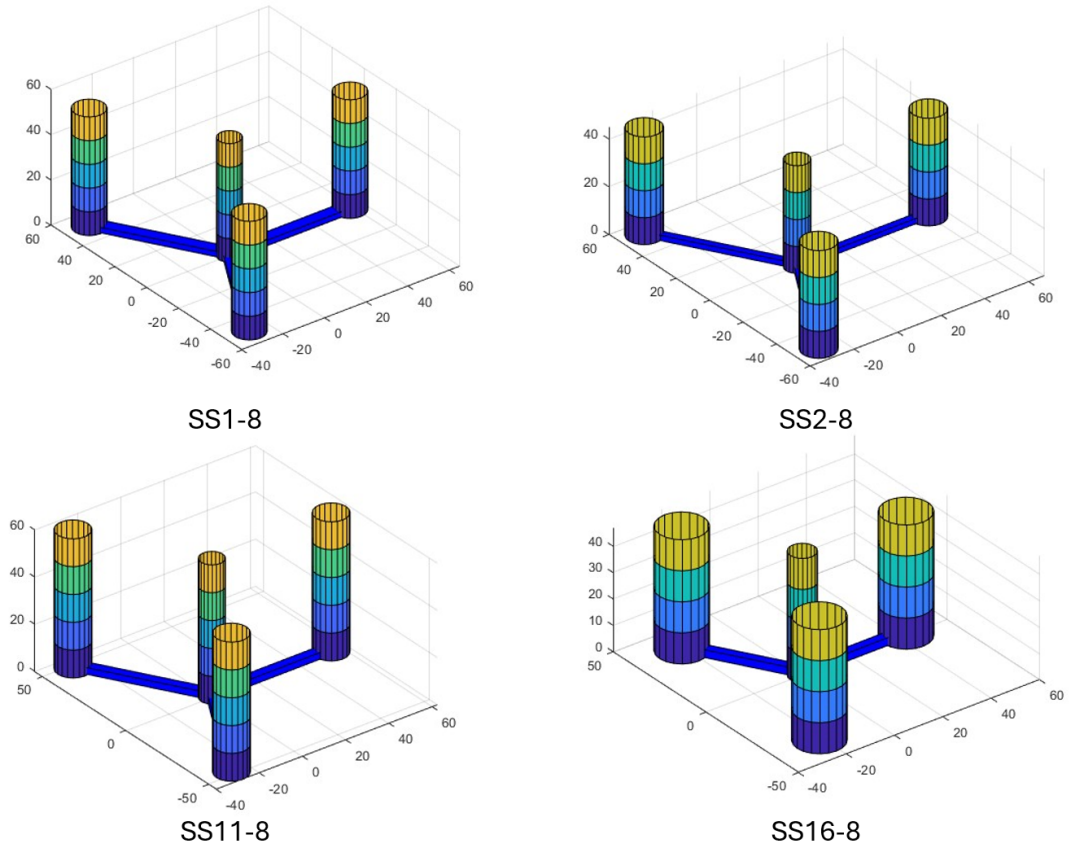

Figure 8.16: Sub-optimal Semi-submersible solutions for site 14.

These two figures show the evolution of the design variables to find the best geometry to meet the stability requirements while minimising cost. The overall height of the platform columns is reducing, while the bracing length is increasing, creating the required second moment of waterplane area. The platform has also evolved to have a

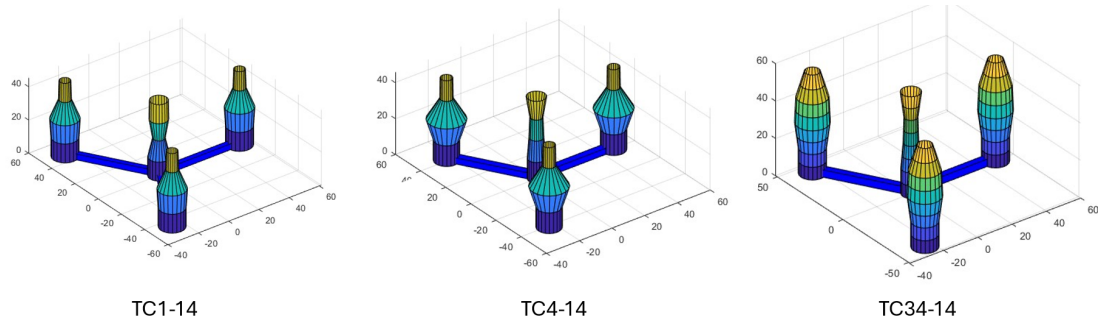

Figure 8.17: Sub-optimal Semi-submersible solutions for site 14.

larger radius at the base of the column tapering up, lowering the CoG, providing better stability and acting like a heave plate. The design variables for each platform presented can be found in Appendix Table A.2.

It can be noted that the optimised geometries for both TC and SS bracings are more similar to the principal power design rather than the Umaine Semi-submersible, which has much wider bracings.

Cost

The cost breakdown of each platform is shown in Figure 8.18 and the total cost breakdown can be found in Appendix Table A.5.

Interestingly, compared to the Spar platform, the TC solution is cheaper for the semi-submersible. Considering all of the costs, it has been found that the TC model is cheaper by 12%.

Allowing the columns' radius to vary leads to a substantial reduction in material mass and cost. The inner column, which hosts the turbine, has a relatively similar radius when comparing the two solutions and therefore has a similar thickness. The average lower radius and length lead to a 6% reduction in shell material cost. However, since the TC on average has a lower radius and the required inertia is linked to the radius, the stiffener height required is lower for the TC by 60 mm. The inner columns also required 6 fewer stiffeners due to the reduction in column length. These reasons lead to the stiffener material cost for the inner column being lower by 30%.

The outer column, as mentioned, has a 2.2 m lower radius on average for the TC,

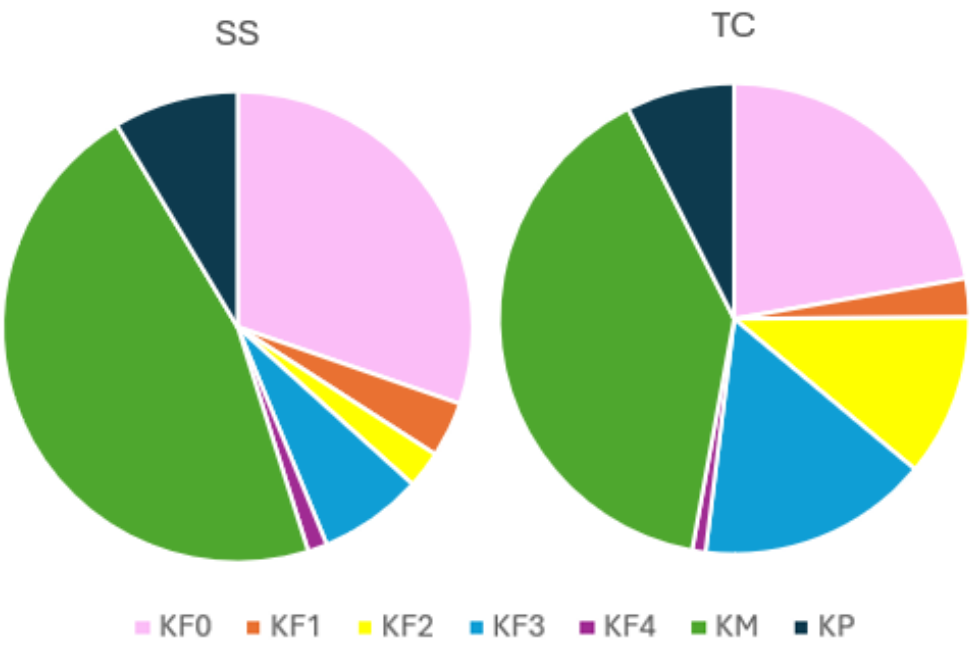

Figure 8.18: The cost breakdown of the optimal solutions for site 14.

which in turn requires a lower shell thickness of 15 mm compared to 20 mm for the SS. This leads to a really significant cost reduction of 45% for the TC. The stiffener size required for the outer column is, however, larger; this only affects the height of the stiffener, increasing from 120 to 400 mm for the TC. This is expected to be due to the TC having some radii sections larger than the SS. The outer column also requires more stiffeners, which at first is hard to understand given the inner column has fewer stiffeners and is the same length. However, the required spacing between the stiffeners is linked directly to the thickness and radius of the shell. The radius has a larger impact due to it being much greater than the thickness, however, the TC model's outer columns have a lower thickness in comparison to SS, which will cause the stiffeners to be closer and require more. The same can be said for the radius.

The ballast material cost is lower for the TC due to the benefit of the wider lower sections, lowering the CoG much more effectively than the SS model. The cost-benefit here is roughly 8%.

The forming cost for the inner and outer column shell plates is lower by 15% and 50%, respectively. Since the inner column is relatively similar in radius, the main benefit is the shorter length. The outer columns have a much greater cost benefit, and this is due to the much lower radius on average, and importantly, the shell, which is 5mm thinner, making it much easier to roll and therefore cheaper. The inner and the outer column plates, which make up the stiffeners, are also cheap by 10 and 12%. This is due to there being fewer stiffeners and the average radius being lower for the TC, and the thickness of the plates being the same.

The cost for welding the plates together to get the segments KF1 is lower for the TC inner and outer columns but higher for the bracings. The inner column is cheaper by 4% since the radius is similar and the number of plates required to create a segment is the same. The outer columns benefit from a 50% cost reduction, linked to the thickness of the shell which is less and the number of plates required to make each segment being lower. The bracing is 31% more expensive for the TC due to the size of the bracing being in general larger, with longer welds to be carried out. The thickness does not affect this since they both require the same plate thickness based on the bending stress present.

Welding the stiffeners from part (KF2) and welding the stiffeners into the shell (KF3) as expected are both lower for the inner column of the TC model. Both costs are lower for TC since the average radius is 30% smaller than SS. Whereas the outer column cost is significantly higher for the TC, since the radius follows the opposite trend and is larger for the outer column, and there are three columns, unlike the inner column, which is only one, hence the outer column cost in general has a more significant impact. The KF2 cost is strongly influenced by the height of the stiffener and KF3 by the volume of the stiffener and the shell.

Assembling and welding the segments together (KF4), overall, is very similar in both cases. Breaking it down into each part, welding the inner column segments together is lower by 15% firstly due to the lower number of segments, and the lower radius, meaning fewer and shorter welds are required. Welding the outer column segments together is 64% cheaper for the TC due to the lower thickness and average radius.

Welding the bracings onto the structure is 10% more for the TC since the bracing width and depth combined are greater and will require a longer weld. Finally assembling the full structure together is 13% cheaper for TC because it has one less segment for each column.

The paint cost overall is 2% less for TC. The reduction mainly comes from the inner and outer columns (7% and 36% less). Painting the TC stiffeners in the inner column is less since the height of the stiffeners is 60 mm shorter. As explained before, the outer columns' stiffeners are larger in height and, therefore, have a larger surface area and almost double their related painting cost. The bracings are larger for the TC to create a large surface area and stability, hence the paint cost is 11% higher for the TC models' bracings.

Mooring and anchorage costs are the same for both TC and SS since the site is the exact same and the fairlead coordinates are within 1% of each other.

Dynamics

To determine the dynamic response of each platform, the model presented in Chapter 4 was used. This analysis utilised the frequency domain. The hydrodynamics were found for DLC 6.1 and 1.6 as presented in Section 4.8, the former is a survivability load case where the turbine is turned off, and the latter is operating in an extreme condition. The site under investigation is site 14, now known as Havbredey off the north-west coast of Scotland. The water depth, wind and wave data for this site was found in (192).

The dynamic response of the SS1-14 and TC1-14 was computed, and the results can be compared in Table 8.5.

	RMS Acceleration (m/s^2)			RMS Displacement (m)&(°)					
	Surge	Heave	Pitch	Surge	Heave	Pitch	Nacelle Accel-eration	Translational Motion Wind	Translational Motion Wave
TC1-14	0.004	0.331	0.133	0.847	1.530	5.567	0.352	0.066	1.749
SS1-14	0.019	0.507	0.067	0.950	2.257	5.255	0.322	0.066	2.449
Difference between TC1 and SS1, (TC1 - SS1) / SS1	48%	-72%	76%	43%	-77%	72%	30%	-12%	41%

Table 8.5: Semi-submersible Dynamics comparison in percentage between SS1-14 and TC1-14.

Inherently, all of the optimal results have a static pitch inclination angle of 5 degrees. The reason for this is that the optimisation seeks the platform geometries which are closest to the maximum inclination angle constraint. By doing so, the cost minimum can be found since as soon as this constraint is relaxed, the cost is reduced further, as shown in Section 8.2.1. The rationale behind this is to improve the stability of the platform in the case of a semi-submersible by increasing the water plane area to increase the second moment of WPA. The larger the platform, the larger the mass and components, and therefore the material and manufacturing cost. To gain a better understanding the hydrodynamics for both platforms have been calculated and compared, starting with the displacements and accelerations. In all directions apart from pitch, the TC model has better performance. The pitch acceleration is expected to be higher at $0.352 m/s^2$ compared to $0.322 m/s^2$ for the SS. The overall translational motion due to the wind is expected to be the same since this is linked to the mooring system, which is very similar. The overall oscillatory amplitude from the waves, however, is 29% lower for the TC model. The better performance is likely linked to the wider base of the columns, which should act in a similar manner to a heave plate, reducing the response in heave and pitch. The larger WPA is the main contributor to the improved stability.

The natural frequencies of both platforms are within 4-9% of each other, with the TC having higher natural frequencies, but still avoiding problematic frequencies.

Varying Number of Columns

Varying the number of columns to determine if there are any benefits, with the optimal solution for each presented in Figure 8.19.

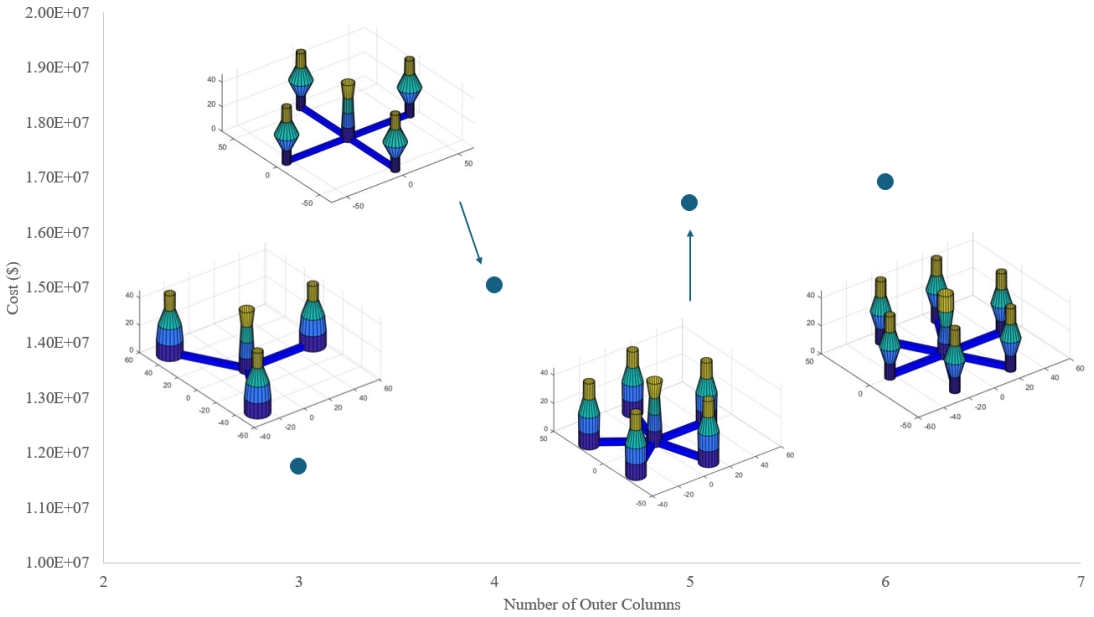

Figure 8.19: The optimal solutions costs for varying number of outer columns.

This figure highlights as expected a cost increase when the number of columns is increased. All costs from material to manufacturing are increased with the increasing outer columns. The dimensions of the geometry are all very similar, apart from bracing length and radius, which are both decreasing with the increase in the number of columns. This size reduction is expected to be linked to the larger waterplane area due to the additional columns, allowing the bracing length and radius to be reduced. Since stability is linked directly to the second moment of the WPA, an increased area but reduced length of bracing will still be able to provide the necessary restoring force. Figure 8.20 shows the overall cost of the platform, mooring and anchor cost and shows how the latter two increase very linearly. Again, this is expected since there will be more mooring lines and anchors required with this work.

The current work assumes a mooring line for each outer column however, for 6 outer columns there may only be 3/4 lines rather than 6. To understand the impact on cost

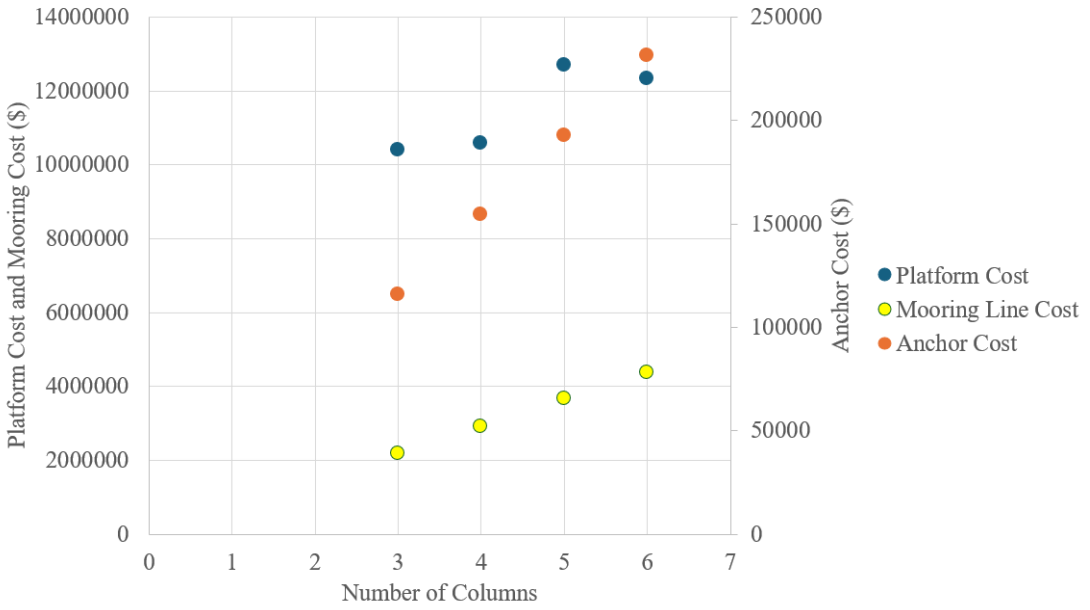

Figure 8.20: The cost of the platform, mooring and anchor cost when varying the number of outer columns.

	6 Lines vs 4 Lines
Mooring Line Cost	-33%
Anchor Cost	-33%
Total Cost	-19%

Table 8.6: Difference between the cost for 4 and 6 mooring lines for the 6 columns Semi-submersible (the percentage is calculated as $(4_{lines} - 6_{lines})/6_{lines}$).

and performance, 4 vs 6 lines were compared for the Semi-submersible with 6 outer columns. The cost comparison can be seen in Table 8.6, showing a reduction of around $4 million for the 4-line configuration.

This is a substantial cost reduction, and for this to be viable, the performance has to be considered. Overall, the accelerations and translational displacements are only marginally higher by roughly 0.000275%, which is so small it can be ignored. It is clear that implementing 4 lines rather than 6 would be the sensible solution, which not only reduces initial cost but will reduce installation and decommissioning costs since, in theory, it should take less time to install.

Spar vs Semi-submersible

The first difference which can be noted between the two different optimal platform solutions is the size. Both SS and TC optimal Spar solutions have drafts of 118 and 110 m, respectively. In contrast, the Semi-submersible has a draft of 33 and 30 m for TC and SS. The other dimension which is important is the size of the waterplane, which can be compared with radius, both Spar options are around 8 m and the semi-submersible around 53 m. Clearly, the Spar is much longer, which in comparison to the Semi-submersible could be difficult to handle in ports and might not be suitable for some ports due to the large draft. Despite the Semi-submersible having a larger waterplane area, its lower draft would make it much easier to handle in a wide range of ports and could be more easily stored or moored at the port location. The size difference also becomes very important when considering the ability to manufacture such large parts and the number of facilities and their location to the activity which have the capacity.

The cost of the Spar is higher, which is linked primarily to material cost, as expected. The full cost breakdown is shown in Table 8.7. This table shows the cost percentage difference between the Spar and Semi-submersible TC and SS platforms. The percentage difference calculation subtracts the Spar cost from the Semi-submersible cost and divides by the Spar cost. Where the percentage is negative, this means the spar is more expensive, and where positive, the spar is cheaper. In some cases, the percentage is over 100%, if this were 200%, it indicates the cost is double.

Looking at the cost breakdown in Table 8.7, it can be highlighted that firstly, the mooring lines for the Semi-submersible are slightly different. One expected reason is the mooring line length, the Spar benefits from its large draft, allowing the fairlead coordinate to be much lower compared to the Semi-submersible. The anchor cost, on the other hand, is linked to the required UHC, which is derived from the thrust acting on the turbine, which is the same for both cases.

Assessing the cost breakdown of the platform, it is noted that there is a different trend when comparing the TC models and the SS models. Firstly, the TC models find KF2, KF3 and KP to be more expensive for the Semi-submersible. KF2 and KF3 are

Cost Category	TC	SS
Platform Cost	-43%	-28%
Total Anchor Cost	0%	0%
Mooring Line Cost	189%	173%
KF0	-35%	21%
KF1	-81%	-62%
KF2	30%	-65%
KF3	31%	-34%
KF4	-63%	21%
KM	-59%	-93%
KP	16%	54%
Overall Cost	-39%	-20%

Table 8.7: Cost comparison between the Semi-submersible and Spar TC and SS (calculated (semisubmersible-spar)/spar, where negative shows the spar is more expensive).

linked to the number of stiffeners, which is 106 in total for the Semi-submersible and 70 for the Spar; therefore, this makes sense to be more expensive. Since the Semi-submersible is made up of a larger number of parts and more stiffeners, the overall inner and outer surface area is larger, leading to a higher paint cost. On the other hand, the SS finds only KF0 and KP to be more expensive, the latter being explained already. The forming is expected to be higher for the semi-submersible since there are 4, 48m columns, which overall are around double the length of the Spar. The costs, which are higher for the Spar, are expected to be linked to the thicker shell and its overall very large size. The difference between the TC and SS models will be linked to the benefits which we can seek using truncated cones within the model, which have been explained in previous sections.

Installation is expected to be around 13% of the CapEx for floating offshore wind and will differ depending on platform type. The difference in cost comes from the different strategies required for each platform type. A Semi-submersible can be fully assembled at the port side and then, when a given weather window becomes available, towed to its site and moored. In comparison, a Spar can either be towed to the site, upended, connected to pre-installed mooring lines and the turbine installed offshore, or, if the water depth permits, towed in a similar manner as the semi-submersible to the site. The former involves a lot more offshore activities which have a higher

	Acceleration			Translational Motion	
	Surge	Heave	Pitch	Wind	Wave
TC	-78%	755%	-78%	-97%	-11%
SS	-62%	361%	-82%	-16%	73%

Table 8.8: TC and SS Spar vs Semi-submersible (calculated (semisubmersible-spar)/spar, where negative shows the spar is worse).

associated risk and cost. There are, however, cases such as Hywind Scotland where the water is deep enough to carry out the same activities as a Semi-submersible, but this is expected to be fewer locations. When more varied activities have to be carried out offshore, typically, the vessel requirement increases. For example, installing a turbine offshore in deep waters would require a floating crane or specialised crane such as WindSpider, which is expensive and achieving a hire is difficult due to high demand and low numbers. Similarly, with more intricate activities carried out offshore, the weather plays a very important role, achieving the desired weather windows to carry out the activities, which will not only take longer but also cost more.

Since the inclination angle is a constraint, and the objective is to minimise cost, all optimal platforms have a static pitch angle of 5 deg. One thing which can determine which is better is the dynamic response. Comparing the overall motion due to wind and wave, it was noted that the SS Spar had the overall lowest motions due to waves, because of its large mass, small WPA and low CoG. Table 8.8 indicates the difference in RMS acceleration and translational motions between SS Spar and Semi-submersible and TC Spar and Semi-submersible. The percentage values which are negative indicated the spar, and where a percentage is greater than 100% such as 200% this indicated the acceleration or motion is double. When comparing accelerations, for each degree of freedom, the larger the area moving in that direction, the lower the acceleration. With this said, the accelerations and displacements are all within an acceptable limit prescribed by DNV-ST-0286.

Overall, each platform has benefits, the semi-submersible is slightly cheaper and smaller draft making it easier to handle however, the Spar provided the lowest displacement, so overall the selection would depend on the situation and what the op-

erator/investor prefers. A huge factor which would also affect the choice is the local supply chain and the proximity to manufacturing sites, as this will affect the overall cost. Further research would also have to be carried out on the O&M impact, one of the platforms might be more susceptible to issues, or the motions generated could cause premature issues with other systems, such as the turbine, mooring lines, etc.

8.3.2 Site 8

The optimal Semi-submersible geometries for site 8 can be seen in Figure 8.21

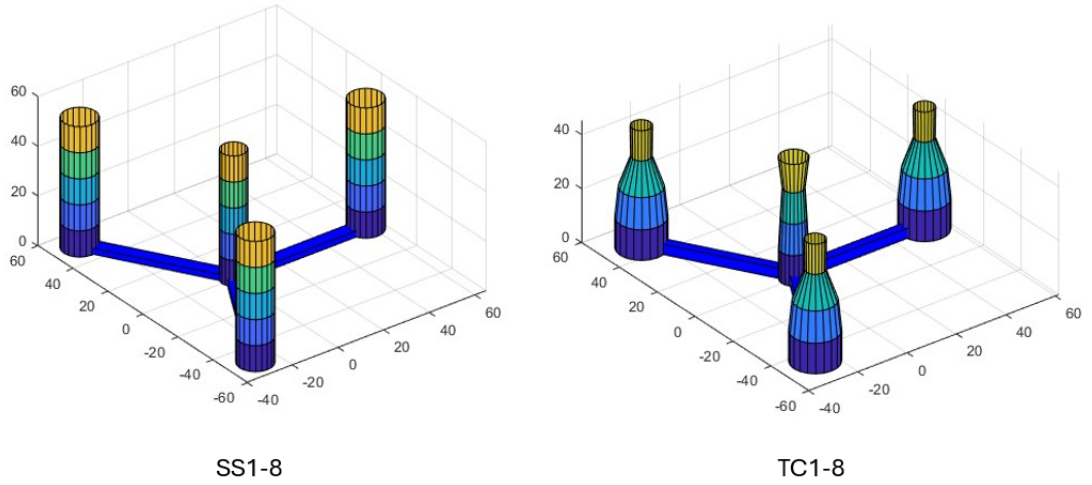

Figure 8.21: The most optimal TC and SS Semi-submersible geometries for site 8.

These solutions are relatively similar to those for site 14. The main difference between the two is the water depth of 100 m rather than 300 m for site 14 and a slightly different seabed, which leads to a decrease in mooring line cost and an increase in anchor cost for site 8. The increased anchor is linked to soil compatibility, site 14 can use a driven pile whereas site 8 requires a Drag Embed Anchor (Stevpris MK5) which is more expensive. The mooring line cost is more for site 14 since the mooring line length is almost double. The cost increase is linked to the mass of the mooring line, which is linked to the water depth increase.

Cost

In terms of thicknesses, size of stiffeners, and number of segments, the optimal solutions for site 8 follow the exact same trends. The only difference comes from the number of stiffeners in the outer column. This can be seen in Figure 8.22 where the ratio between TC and SS are plotted for each site. The similarity in design led to the TC being cheaper for similar reasons as site 14.

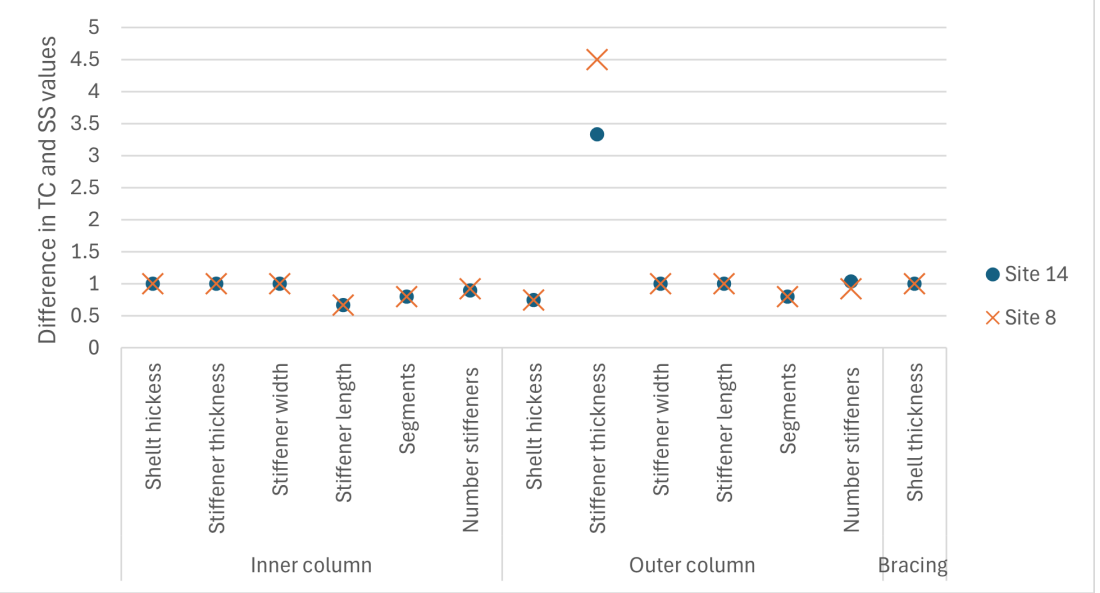

Figure 8.22: Geometry dimension ratio between SS and TC Semi-submersible for each site.

There are fewer stiffeners in the outer column because the difference in the radius ratio between the two sites is greater for site 8, which, as discussed before, leads to a larger spacing between the stiffeners and hence fewer stiffeners.

Comparing the main cost category ratio between TC and SS for each site, in Figure 8.23. Where both values are greater than 1 this shows that TC cost was greater and where it is less than 1 TC was cheaper. It can be noted in this figure that both sites follow the same trend in terms of the difference between TC and SS values.

Overall, this shows that each platform geometry found for site 8 and site 14 could be used in either case, and the main difference between the two is the mooring and anchor cost. These costs are mostly affected by the fairlead coordinate and the overall

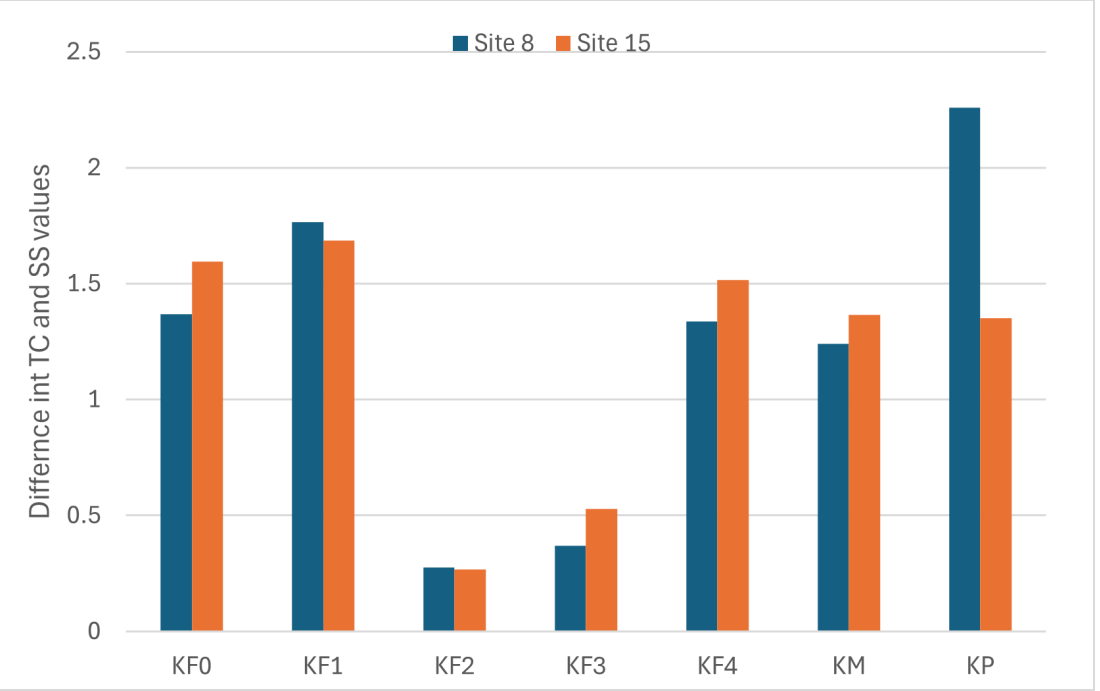

Figure 8.23: Cost ratio between SS and TC Semi-submersible for each site.

width of the platform, which is mostly influenced by the bracing length.

8.4 SS TLP vs TC TLP

This Section reviews the optimisation of the TLP for TC and SS, varying the number of bracings, and finally drawing a comparison to the optimised Semi-submersible for site 8.

8.5 Site 8

The top three geometries found for both TC and SS can be seen in Figure 8.24 and 8.25, respectively. Three are shown to show the evolution of the platform shape to find the cheapest, optimal solution. Moving from left to right presents increasing cost geometries. Both Figures show a trend for a larger internal column and shorter bracings for the most optimal (left-hand) platform. The optimised design variables for each platform can be found in Table A.3 Appendix.

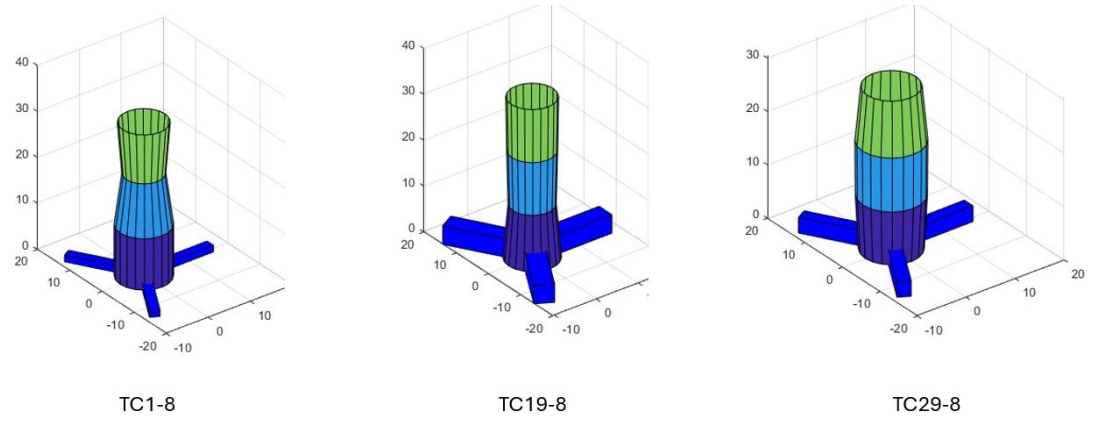

Figure 8.24: Optimised TC TLPs for site 8.

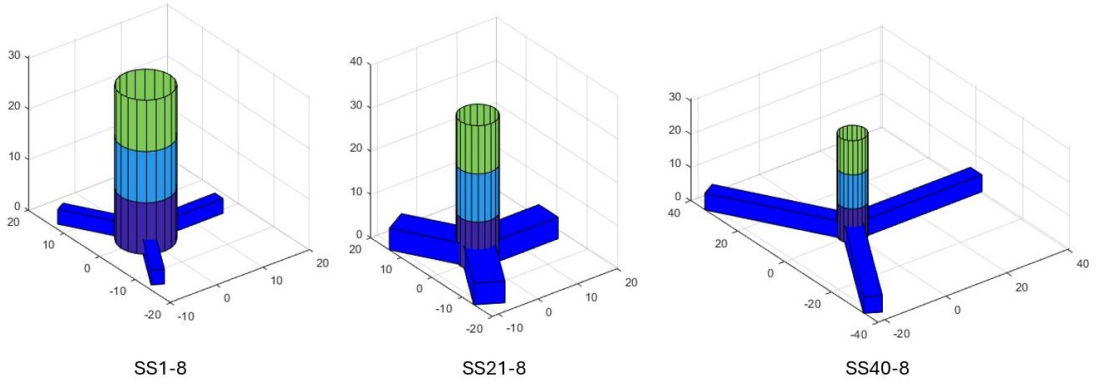

Figure 8.25: Optimised SS TLPs for site 8.

8.5.1 Cost

The most optimal TC and SS TLP cost breakdowns can be seen in Figure 8.26. Overall similarly to the Semi-submersible, the TC is cheaper but only by roughly 1%. The full cost breakdown can be found in Appendix A.8.

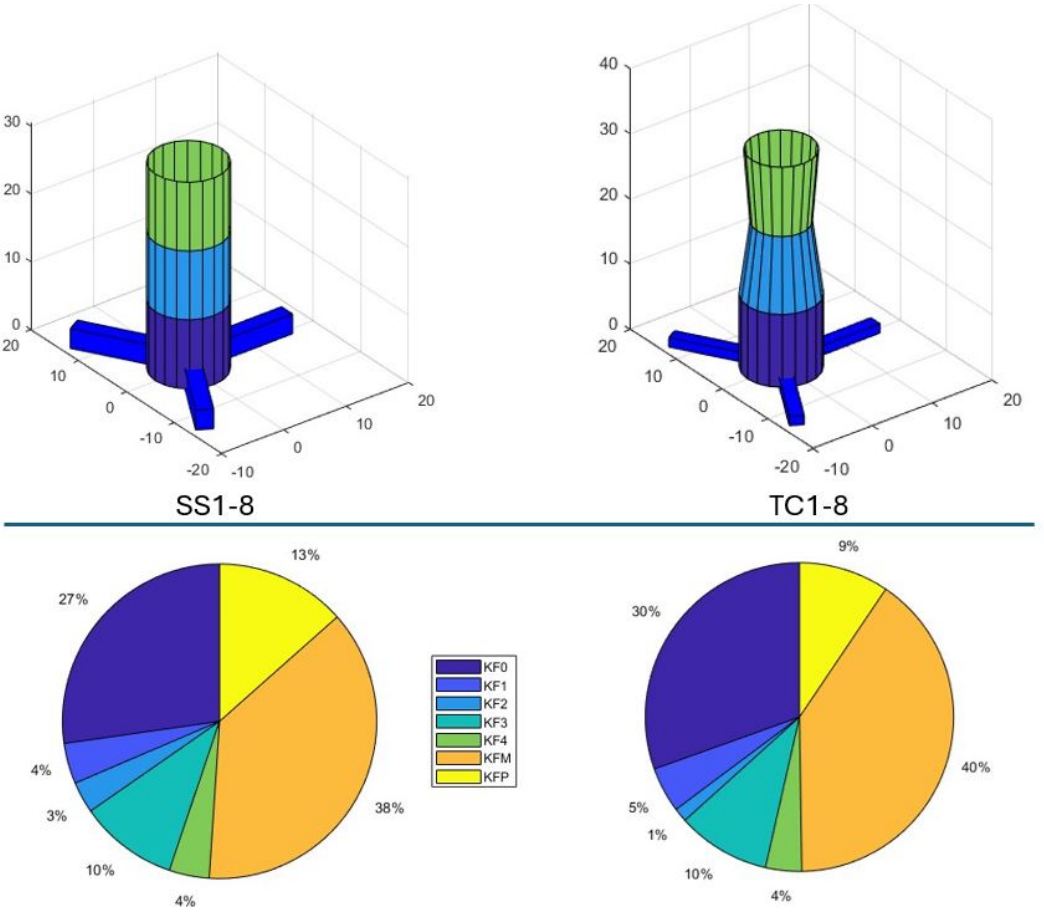

Figure 8.26: Most optimal TC and SS TLPs for site 8.

Comparing the geometry it can be noted that the TC has an 8 m larger draft and on average a radius 1 m larger. However, the bracings for the TC are significantly smaller, which is where the majority of the cost benefit comes from. Since the SS inner cylinder is shorter, it requires 4 fewer stiffeners; the short length also leads to a cost benefit. The number of segments required for both TC and SS is 3. The other parameters regarding stiffener size and thicknesses are the same, apart from the height of the stiffeners, which is 65 mm for TC vs 150 mm for SS. The expected reason is

the relationship between stiffener inertia and shell stress. The stress is greater for the TC due to its geometry, and considering eq. 8.3, the higher the stress, the lower the required inertia of the stiffener, since the second component of this equation will be negative. The higher stress leads to a lower required inertia for the TC and therefore a smaller stiffener size.

$$I_{yy} \geq I_{reqi} = \frac{\gamma_b p R_i R_{Ei}^2 L_{efi}}{3E}[2 + \frac{3Ey_{Ei}0.005R_i}{R_{Ei}^2(\frac{f_y}{2-\sigma})}] \tag{8.3}$$

Looking in detail, the cost benefit from the TC can be assessed. The forming cost is higher for the TC TLP. This is expected since the central column is greater in both dimensions and has a larger number of stiffeners, which also need to be rolled.

The welding cost overall is lower for the SS model. Welding the segments from plates for the central column is lower for SS but welding the bracings from parts is more expensive for SS due to their larger size. Welding the stiffeners together from parts is cheaper for the TC, which is counter-intuitive given there are more stiffeners, but this is linked to the smaller stiffener height required. However, welding the stiffeners into the shell is more expensive for the TC due to the 4 extra stiffeners and the on average larger radius, leading to a longer weld. The full assembly and welding of the segments together is greater for TC for similar reasons; a greater radius leads to a longer weld and therefore is more expensive. The TC does have the benefit of the bracing being smaller and therefore a lower weld cost associated, but this benefit is not enough to make it cheaper.

Both material and paint costs are highly correlated since they are both linked to the size of the platform. For this reason, the central column material and painting cost are lower for the SS. The bracing and stiffener material and painting costs are lower for the TC.

8.5.2 Dynamics

Overall, it has been noted that both platforms have relatively similar dynamic performance. The comparison can be seen in Table 8.9. Greater than 100% indicates SS has

a higher value and vice versa.

	RMS Acceleration (m/s^2)			RMS Displacement (m)&(°)					
	Surge	Heave	Pitch	Surge	Heave	Pitch	Nacelle Acceleration	Translational Motion Wind	Translational Motion Wave
TC1	4.5E-41	5.7E-42	2.9E-42	1.1E-41	1.4E-42	1.6E-44	0.755	0.007	1.14E-41
SS1	4.5E-41	7.7E-43	2.4E-42	1.1E-41	1.9E-43	1.4E-43	0.709	0.006	1.12975E-41
Difference between TC1 and SS1, (TC1 - SS1) / SS1	100%	742%	117%	100%	742%	117%	108%	108%	101%

Table 8.9: TLP dynamics comparison in percentage between SS and TC.

The main difference is the heave acceleration and displacement which is significantly higher for the TC model, however, it can be noted that the acceleration is so small for both that they are negligible. This is due to the stiffness provided by the mooring system. The directions which have lower accelerations are directly correlated with the higher mooring stiffness in the DoF.

The added mass and damping follow the same trends, both TC and SS can be seen in Figure 8.27. The added mass in the surge direction is greater for the TC since the frontal area is greater due to the larger central column. The opposite can be said for the added mass in heave and pitch, this is greater for SS since the bracings are much larger. The same trends can be noted for the excitation force shown in Figure 8.28. The lower added mass and higher damping will lead to a lower response of the platform.

The TC benefits from a lower mass and lower CoG in comparison to the SS, mainly due to the ability of the platform to seek a larger radius at the base and a smaller radius at the top of the central column. This helps aid the response of the platform within waves, however the main stability contributor is the mooring lines.

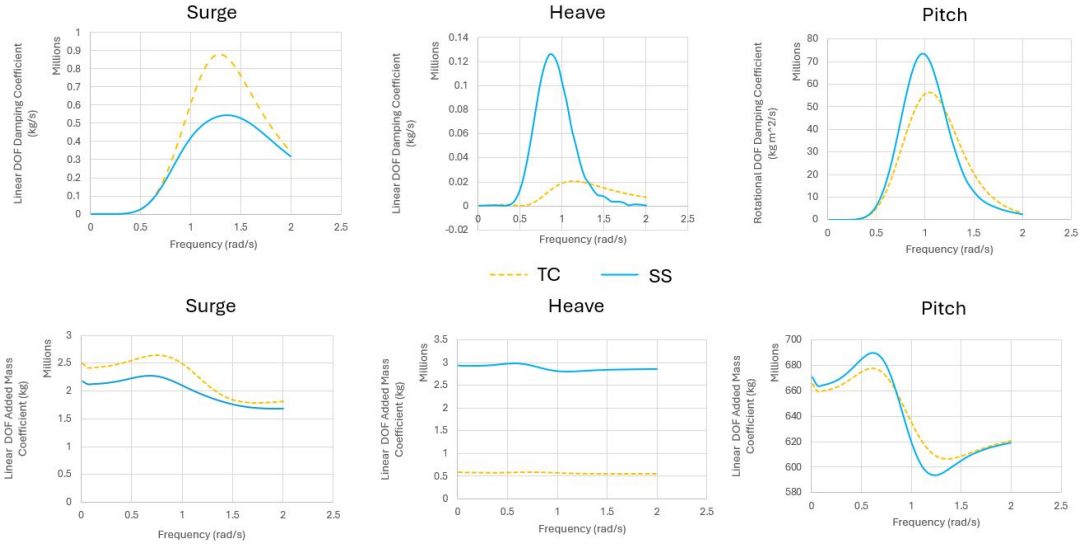

Figure 8.27: Added mass and damping for TC and SS TLP at site 8.

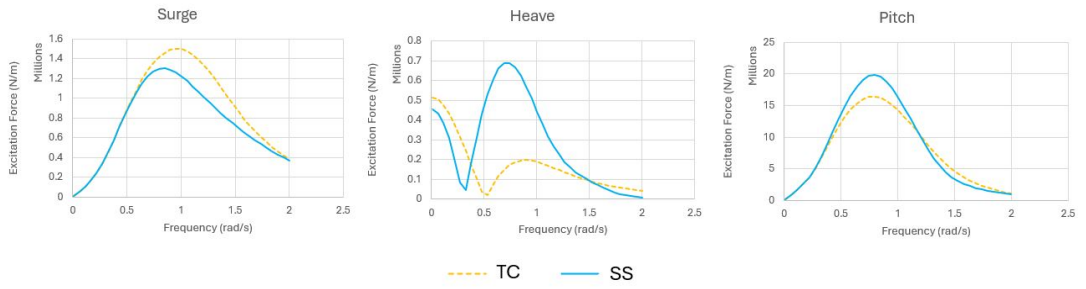

Figure 8.28: Excitation force for TC and SS TLP at site 8.

8.5.3 Varying Number of Legs

Similarly to the Semi-submersible, the number of legs was varied in the optimisation to identify the cheapest configuration and if there are any trends. Figure 8.29 shows the cost of TLPs with 3-6 legs, highlighting the 5-leg configuration to be the cheapest. The reason for this being the cheapest option is the trade-off between the length of the inner column and the radius. Compared to other options, it is slightly shorter but has a slightly higher radius. The bracing size is the second shortest with the lowest width but highest depth. The main cost benefit from the platform manufacturing comes from the forming of plates, since the radius is relatively similar, but overall, the inner column is 3 m shorter. Table 8.10 shows the cost of each platform divided by the cost of the 5-bracing TLP, where it is less than one, the 5-bracing TLP is more expensive and vice versa. The only substructure which is cheaper overall is the 4-bracing configuration, which has bracings 5 m shorter than the 5-bracing TLP, and overall lower mass, leading to lower material costs. It can also be noted that the stiffeners required for the 4-bracing TLP are smaller due to the geometry. However, the overall benefit of the 5-leg platform is the lower mooring and anchor cost. The expected reason is the lower required tension due to the buoyancy and weight of the platform. In general, this makes sense since a number of concepts which have been proposed have 5 bracings, such as hexafloat and pelastar (4; 15).

There was no real trend identified in Figure 8.29, this can some times be an indicator that the global minimum was not found. However, to overcome this problem, 10,000 optimisations were carried out for each case, and these were the cheapest platforms

Cost	3v5	4v5	6v5
Platform Cost	1.20	0.95	3.06
Anchor Cost	1.17	1.09	1.4
Mooring Line Cost	1.8	1.36	1.2

Table 8.10: Cost difference between 3, 4 and 6 compared to 5 bracing TLP found.

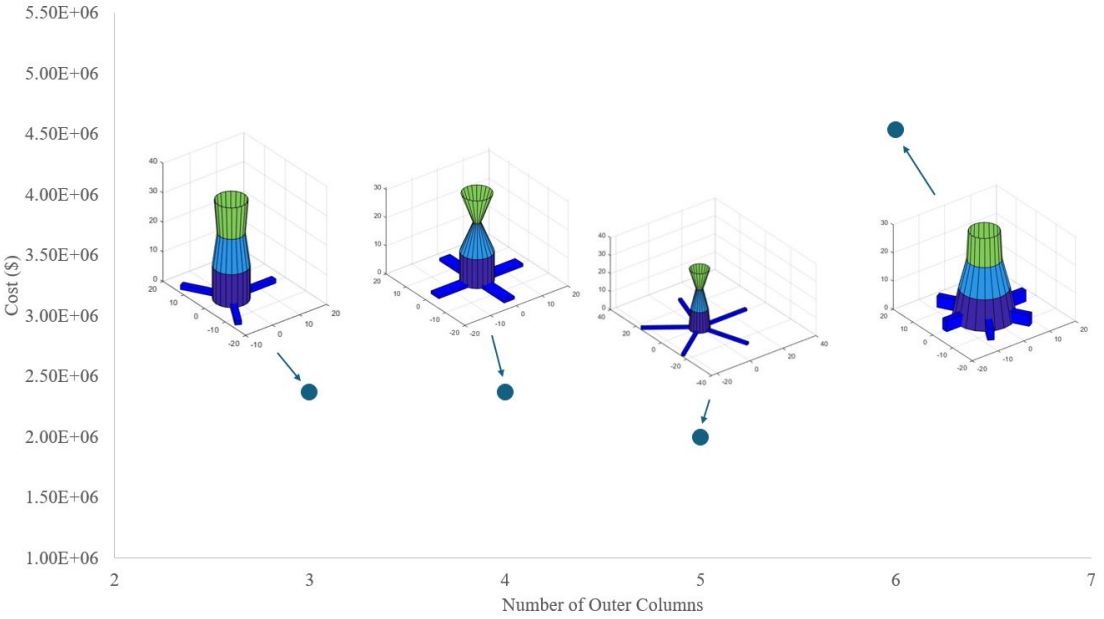

Figure 8.29: Cost for different number of bracings for a TLP.

8.5.4 TLP vs Semi-submersible

The main difference between the Semi-submersible and the TLP is cost. The TLP is roughly $10 million cheaper, which is substantial, particularly when you consider a 10 million dollar saving per platform over a complete farm. The reason for the huge difference in cost is that the TLP is much smaller, therefore requiring less material, has a smaller surface area and has fewer parts to form and weld. The savings in cost of the platform still outweigh the expensive anchor costs, where the cost of the semi-submersible anchors is only 10% of the TLPs. There is a mooring line benefit also for the TLP, which comes from the much shorter lines required compared to the catenary

system. This smaller size also helps with handling, it would be much easier to transport and handle within a non-specialised port. In terms of dynamics, the TLP is also better due to the taut mooring lines minimising the movement to something similar to a fixed platform.

With these benefits in mind, it would seem to be a more favourable solution. TLPs do, however, come with their own drawbacks. Firstly, the installation cost is expected to be higher due to their lack of stability without mooring lines, unlike a Semi-submersible. For this reason, other specialised vessels will be required, and it is expected that the installation process will be longer due to the taut mooring lines. The use of taut mooring lines is under constant tension, which might make them more susceptible to snapping, which could lead to the potential loss of the full asset. Another potential drawback from this is increased O&M activities, where lines may need to be replaced which will lead to an increased cost. To avoid this, an element of over-engineering might need to be applied, which inevitably will increase the cost. Overall, the Semi-submersible is a proven technology which puts more confidence in developers to utilise it.

8.6 Findings Summary

The subsequent sections summarise the main findings of the case studies carried out for Spar, Semi-submersible and TLP.

8.6.1 Spar

Geometry and Stability

This section summarises the findings from the studies carried out on the SS and TC Spar stability. The main findings are listed:

- The TC favours a shorter, wider geometry with a pinched segment to ensure the CoG is lower to create the required stability.
- The SS, on the other hand, is best when longer and narrower, lowering the CoG by increasing the lever for the restoring moment.

- Relaxing the maximum inclination constraint from 5 to 9 degrees reduces the cost by 20%, and the geometry becomes narrower and slightly longer to achieve this.
- The surge and pitch are lower for SS due to the higher added mass in these DOF, since the frontal area is larger.
- The heave is lower for TC because it has a higher added mass in heave, due to the larger area at the base.
- The nacelle acceleration for SS is lower due to the lower CoG.

Cost

After conducting numerous analyses, the most optimal SS had 12 segments and the TC had 10. Overall, the SS is cheaper than TC Spar the overall reasons are summarised in Table 8.11.

Category	Cheaper Platform	Reasons	Driving Geometry Parameters
Material	SS1	SS1 thinner shell and stiffener thickness due to lower average radius; SS1 lower ballast mass due to longer platform length.	Radius and platform length
Forming	TC1	TC1 shorter and therefore has fewer segments and plates to roll.	platform length
Welding	TC1	TC1 is cheaper since the platform is shorter and has fewer stiffeners; TC1 has lower volume, reducing the cost to weld stiffeners into the shell and the assembly and weld cost.	Average radius and platform length
Painting	TC1	The overall shell area is lower and the lower number of stiffeners.	Platform length

Table 8.11: Cost difference reasons and drivers for the Spar platforms.

At first glance, the opposite of what is expected is true. The material costs are lower for SS1, and the manufacturing costs are higher for TC1. The material cost is lower for SS1 not due to the shell but the stiffener and ballast mass being lower. So, considering other works, the basic material cost, otherwise known as shell, is cheaper for TC1.

The material cost is cheapest for platforms with a small radius and longer length, since this has the largest share in cost, it is the major platform geometry shape driver. Conversely, the forming cost is lowest for shorter length platforms, the other things which impact this, although less so, are the thickness of the materials and the radius of the plate which is being rolled. Evidently a smaller radius and thickness is beneficial, however small radius and short length do not go hand in hand. Both forming and welding require the platform to have a small radius and a shorter length. However, these cannot both be small, as one is small, the other is larger to create the desired stability. Similarly, there is a trade-off with the radius and thickness; the larger the average radius of the TC, the more susceptible it is to higher stress due to the changing geometry, which increases the shell and stiffener thickness. The number of stiffeners also affects welding. On the other hand, the forming is more impacted by the thickness, the welding less so. Finally, the paint cost seeks smaller areas and a lower number of stiffeners, so similar to welding and forming, the length and radius are more important, with length being more impactful to the paint cost here, since this also impacts the number of stiffeners.

Overall, it is clear that the material cost is in conflict with the manufacturing costs, the former wants a tall slender geometry to meet the stability constraints and the latter seeks in general a platform which is smaller in both dimensions but since this is unachievable a shorter platform with a larger average radius. The material cost wins this battle in the bid to find the cheapest platform since it accounts for roughly 50% of the overall cost.

8.6.2 Semi-submersible

Geometry and Stability

The general findings of the optimal geometry and the rationale are presented below:

- In general, the best solutions have on average a lower radius, draft, and increased bracing lengths (larger waterplane areas), depth and width of the bracing stay relatively similar with a slight increase for the optimal solutions. The fairlead coordinate is lower for the optimal designs, moving away from the waterline.

- The TC favours a tapered column shape getting narrower at the top.
- The TC has a lower column length, the inner column radius is very similar however the outer column is significantly lower compared to SS. The bracing geometry is relatively unchanged between the two designs.
- The pitch displacement is better for SS because of the lower CoG.
- The surge and heave displacement is better for TC since because of the wider base and larger WPA.
- The nacelle acceleration lower for SS, since its linked to pitch DOF and the platform has a lower COG.

Cost

The optimal TC design had 4 segments and the SS 5. The cheapest solution was the TC model, by 12%. The reasons are listed below:

- The main driver is the material cost reduction, which is mainly attributed to the outer column's smaller average radius and the short column lengths; overall, there is a material cost saving of 19%.
- TC requires less ballast mass since the lower section radius is larger resulting in 8% cost reduction.
- Forming costs are also significantly lower for TC, for the inner column, this is due to the short length and for the outer columns, both the length and the lower radius play a major role.
- Welding cost is higher for TC due to the bracings being larger, requiring longer welds to be carried out in order to assemble the segments.
- Paint cost is very similar, the TC is cheaper due to its small size as mentioned before.

- The difference between the results found for sites 8 and 14 is minimal, meaning the platforms are interchangeable between sites; the main difference comes from the station-keeping system. The mooring line cost is higher for site 14, due to the increased water depth, and the anchor cost is lower since a driven pile can be used in the site's soil, unlike site 8, which requires a DEA, which is more expensive.

- Overall, the TC benefits from having shorter columns, smaller average radius for both inner and outer columns, and a thinner outer column shell. The benefits outweigh the larger bracings for the TC design. The Semi-submersible benefits from having a number of 'parts' which can be made smaller but still maintain the desired stability.

Varying the number of columns also had an impact on cost, with 3 being the cheapest, increasing logarithmically with column number. This is linked to all elements: materials, manufacturing, mooring and anchors.

Comparing the Spar to the Semi-submersible for the same site, the Spar is more expensive, this is linked to the material cost and generally higher manufacturing cost linked to its large size. The mooring line cost, on the other hand, was found to be more expensive for the Semi-submersible since the fairlead connection point is higher and requires longer mooring lines.

8.6.3 TLP

Geometry and Stability

The most optimal TLP TC and SS geometries favour a taller, slender central column with small bracings in all dimensions. When comparing the two designs, however, the TC is longer by 9 m but has an average radius 1 m lower. In general, the stability of the TLP designs was excellent, with almost negligible motions presented for the DLCs considered. This stability can be attributed to the mooring system, which had a high stiffness, allowing the platform to act similarly to a fixed-bottom design.

Cost

In a similar trend to the Semi-submersible the cheapest TLP design is the TC but in this case only by 1%, this is due to the lower number of 'parts' of the platform which for the semi-submersible can be made smaller in order to reduce material and manufacturing cost while still maintaining stability. The costs are presented and difference explained below:

- Forming is more expensive for TC, because of the larger radius and more stiffeners. For the same reason, the welding of plates to create segments is also higher for TC.
- Welding the bracings together from plates is lower for TC since the bracing size is lower.
- Welding stiffeners together for TC is cheaper because the stiffeners required are smaller.
- Welding stiffener into the shell is more for TC since the number of stiffeners is higher.
- Material cost is higher for TC, this is linked to the longer column length and higher average radius.
- Paint cost, on the other hand, is lower for TC since the surface area is smaller, which is linked primarily to the bracing's size.

The number of legs was varied for the TLP, finding the 5-leg platform to be the cheapest since it benefits from long, narrow bracings and a slim but short central column, and smaller anchors and mooring line diameters can be used.

The optimised platforms for sites 8 and 15 are similarly interchangeable for the semi-submersible case because they are so similar. The TLP and the Semi-submersible can both be compared for site 8. The TLP is cheaper, this is because of the smaller size, lower mass and manufacturing cost. These benefits still outweigh the much more expensive anchors required for the TLP.

The expected $/kg for each platform was also calculated and is presented in Figure 8.30. This figure shows the cost variations that arise depending on whether TC of SS segments are included, and it also highlights the higher costs associated with more complex platforms. A comparison of the $/kg values calculated in this work demonstrates that the $/kg assumptions commonly used in the literature, as discussed in Chapter 2, are too low.

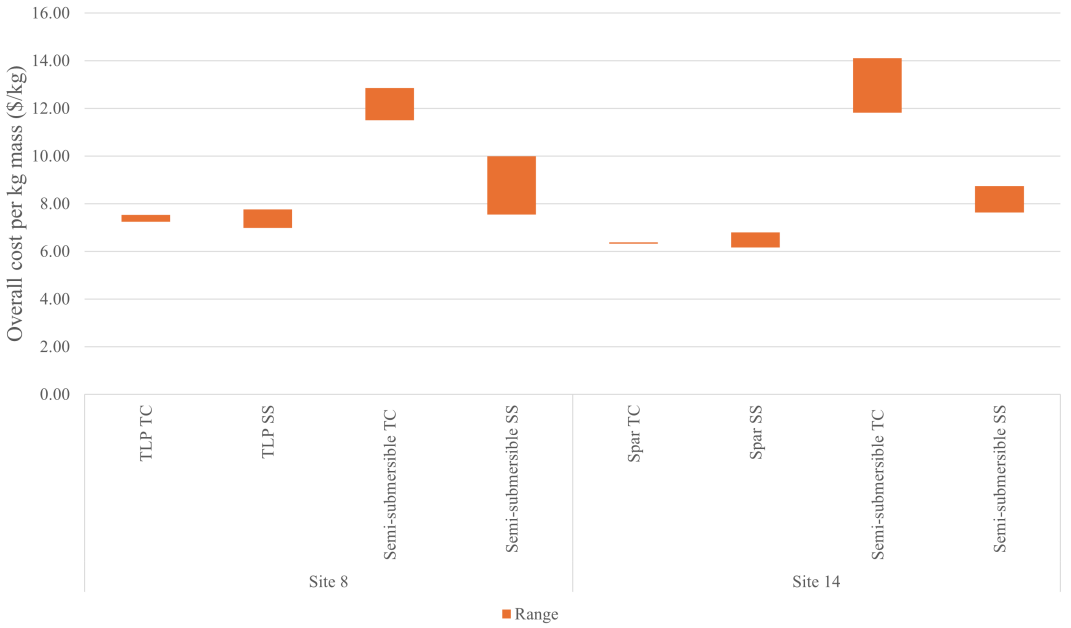

Figure 8.30: Cost per kg for each platform type at the specific sites.

Chapter 9

Conclusions

Offshore wind is essential to decarbonise the grid and help meet net-zero goals around the globe. As the capacity build-out increases and near-shore sites are utilised, developers are being pushed into deeper waters where current fixed-bottom technology is no longer either technically or economically feasible. This challenge can be addressed by using floating substructures, allowing capacity to further develop and meet government targets. The UK government have made strong commitments for both fixed and floating technology with a target of 5 GW of floating offshore wind by 2030. The support of the government is key to aiding the development and growth of this industry.

The introduction of floating offshore wind may address the deeper water challenges, but it does, however, have its own difficulties. The major challenge for floating offshore wind is the cost, with it expected to be double that of fixed-bottom offshore wind. Several factors cause this, the sites are typically further from shore, in deeper waters and using technology which is nascent and lacking adequate supply chains and infrastructure to handle the large component sizes. One key contributor is a lack of maturity, which drives up cost, standardisation of floating substructures is nowhere near its fixed bottom counterpart, with over 80 designs being presented across literature and industry. This does not allow cost reductions from learning and mass manufacturing. Research is therefore required across the cost life cycle of floating wind platforms to determine what the optimal platform are/is.

To understand the research carried out in this field, a review was carried out for

both the cost modelling for floating offshore wind and the optimisation of the floating substructure. Starting with the former, this allowed the author to highlight the major gaps, such as the lack of detail, assumptions and uncertainty within cost models and little consideration for manufacturing cost and manufacturability. By carrying out this review, the author has collected and presented all of the information surrounding the topic into detailed tables, making it much easier to quickly determine the cost and the range across the literature. The cost model literature review presented a number of areas which could improve the accuracy of cost estimates, including the charter type, fuel costs, weather windows, losses due to downtime, improved AEP models, and the manufacturing costs for the platform to more accurately assess the cost and draw comparisons. Furthermore, combining the best parts of current models into a new model is expected to improve the accuracy.

The optimisation literature review finds the majority of current work to have a strong focus on the Spar optimisation (48%), with roughly only 32% considering multiple types. However, the main takeaway from this review is that the most common objective is cost at 82%. The lack of accuracy was echoed through substructure optimisation models, which leads to the substructure being optimised to reduce material mass and therefore cost, with no consideration for manufacturing costs, which can result in non-traditional geometries being the optimal solution, since the complex manufacturing costs are disregarded.

A general challenge is determining the different platform typologies' site suitability, with cost models and optimisation frameworks focusing typically on generic sites. A number of platforms are considered for the same site, rather than using specific sites and determining what platforms suit the site characteristics and why. This can be a time-consuming exercise, particularly when optimising a platform for a site which it typically would not be used for due to the site and the platform's characteristics not being compatible. Another challenge is the turbine size considered, with the majority of literature using a 5MW NREL turbine, which is outdated, and it is expected that the 15MW turbine will be the standard size from 2030.

Therefore, based on these challenges, the overall aim of this work was to success-

fully develop a flexible optimisation framework for a variety of floating offshore wind substructures, which is quick and efficient. This work was broken down into five main sections of work:

- Firstly, the literature review, as mentioned, assessed both floating offshore wind cost and floating substructure optimisation, highlighting the drawbacks and gaps which needed further research.

- Work package two developed a preliminary selection tool by implementing a TOPSIS methodology to rank the main platform stability classes for the Scotwind sites. The methodology used allows a number of criteria and information regarding the site and the platform to be considered.

- The third work package focused on developing a flexible multi-disciplinary model which includes the main floating typologies, Spar, Semi-submersible and TLP. Considering structural design, hydrostatics, a detailed manufacturing cost model, quasi-static mooring line model, and anchor sizing.

- In work package 4, an optimisation framework was developed leveraging the model in work packages 2 and 3. Firstly, to determine which platforms to optimise for which site, the model from package 3 was used with a pattern search algorithm and a multi-start approach to find the global minimum. The objective was to minimise the overall cost considering material, manufacturing, anchor and mooring line cost while meeting a number of performance and geometry constraints.

- Finally, the hydrodynamics of the optimal platforms were assessed using a frequency domain approach. This was to ensure the optimal platforms presented passed DNV operational standards.

The main overall findings of this EngD research are summarised in the following paragraphs.

An issue highlighted in the review section was the length of time associated with an optimisation simulation. By implementing the pre-filtering concept selection presented in Chapter 6, it has proven helpful in tackling this challenge, reducing the number of

different geometries to only the most suitable for each site in a quick yet systematic manner. This tool not only helped to rank the platforms from 'best' to 'worst' for various sites, but after carrying out a sensitivity study, proved how versatile a Semi-submersible could be for a range of different sites and conditions.

The optimisation of Semi-submersible and TLP were both carried out at two different sites, the result was platforms which were almost identical in geometry for each platform typology. Showing that a standard optimised geometry for each platform typology could be found and implemented across industry to drive standardisation and develop supply chains and enhanced manufacturing techniques to reduce the cost.

Comparing platforms in general, the Spar is most expensive, followed by the semi-submersible, and the TLP is the cheapest. The Spar cost is high due to the high mass and the large number of panels required to create the structure. The TLP benefits from being small and lightweight and having fewer parts to assemble and weld compared to a Semi-submersible.

Ultimately, to get the cheapest platform, the smallest it can possibly be to provide the required stability is best. For a Spar, this means long, thin platforms are best to find the minimum cost since radius and length are inversely connected to create desired stability. The Semi-submersible seeks a small radius and column length but long, narrow bracings for the optimal geometry to create the second moment of WPA for stability. Lastly, the TLP short narrow cylinders with small bracing are the optimal shape since the stability is provided by the mooring lines.

For the Spar geometry, the TC is more expensive, despite TC having lower mass, the manufacturing costs outweigh the benefit. Therefore, traditional geometries are best for the Spar platform design. The opposite is true for TLP, but more say the Semi-submersible. Since the Semi-submersible has more 'parts', it has more flexibility in the geometry shape to get the desired stability, allowing the components to be relatively small, reducing the material and manufacturing cost of the TC designs. The TLP lies between the two, with only a central column and bracings. It then relies more heavily on the size of the components to achieve stability, but this is less of an impact compared to the Spar, since the main stability is provided by the mooring lines. Interestingly,

the Semi-submersible and TLP are cheaper using non-traditional geometries.

The main parameters which affect cost the most for each manufacturing cost are as follows: the forming cost is most influenced by the number of parts, radius and thickness. Welding costs are linked to the thickness and length of the weld, where there are larger plates or more parts, the weld cost is higher. The size of the weld is linked to the size and, therefore, volume of the parts being welded. For example, the cost of stiffeners being welded into the shell is mostly linked to their height. Painting is mostly influenced by the surface area of the platform and the stiffeners, therefore, a large geometry leads to a higher cost

All of the platforms presented in this work had good stability characteristics since this was a constraint on the optimisation. The use of optimisation to quickly and efficiently determine suitable geometries with desired characteristics could be much more useful to designers than iterative methods, which are used traditionally. The process itself could be used as a starting point to highlight some very effective solutions from which these could be further enhanced by carrying out an iterative detailed design process.

Overall, this research was successful in developing a flexible optimisation framework for a variety of floating offshore wind substructures, which is quick and efficient. Carrying out optimisations for a range of platform typologies for different sites. Highlighting manufacturing cost is not something to be disregarded when comparing traditional and non-traditional geometries, as well as platform types, to understand the true cost. Material costs were highlighted as the majority share (40%) of the cost. However, the remainder of the cost is made up of forming, welding and painting of the structure from all of the steel components required. Given these findings, this research has been successful in meeting the aims and objectives and contributing to the existing knowledge to help improve the understanding of the floating support structure and the associated costs.

Chapter 10

Future work

In order to improve on the current work, explore further issues, a number of areas are proposed for this research field.

Improved input data for the concept selection tool would allow more nuanced results. It could be enhanced further by including more detailed cost estimates for specific typologies for each stability class to get a more accurate assessment. Carrying out this approach could help highlight a specific platform and its characteristics, which would work across a variety of sites and help with the lack of standardisation across the industry.

Including more comprehensive cost models, including the full lifecycle of a wind farm, such as installation, O&M and decommissioning. This inclusion stems from the extremely low manufacturing cost of the TLP, which, in theory, makes it the best option where suitable. However, it has its drawbacks, such as an expected higher installation cost due to a more complicated installation campaign and potentially higher failure rates or redundancy required for the mooring system. Including consideration of the manufacturing location within an installation model would greatly improve the ability to identify the most suitable solution. This would determine whether manufacturing can be carried out locally or must be completed in another country with subsequent transport to site, particularly where platform size limits construction options and transport feasibility. Building on this, incorporating port capabilities as constraints within the optimisation model would allow identification of the best solution for a region, not

purely based on cost but also on what can realistically be built, while accounting for potential local content and added value. Similarly, for O&M, the selected strategy depends on the platform type and the expected maintenance port. By combining all of this information, the true optimal solution can be found in a holistic approach. Finally, further validation of the cost model would be useful, the current work was validated using literature however having data from the industry would have helped improve this model further.

To account for uncertainty and variation in cost inputs, it is recommended that future work adopts a probabilistic modelling approach to assess the implications of cost ranges and identify the most probable values. Such a methodology would also enable analysis of the influence of external shock factors on costs, such as fluctuations in steel prices. This methodology would help to overcome the challenges of lack of real-world data.

Future research should aim to validate cost estimates against actual fabrication yard capabilities to improve the accuracy and practicality of the modelling. This would involve assessing whether yards can accommodate platform size, infrastructure requirements, and associated costs. However, obtaining such data is challenging because yard-specific cost information and operational constraints are often commercially sensitive and not publicly available. While general cost structures are understood, access to verifiable yard data was not feasible for this study. Incorporating these real-world constraints in future work would significantly enhance the robustness of cost modelling and provide more realistic insights for deployment planning.

In addition, the feasibility of local manufacturing, such as in Scotland, is an important consideration. Local fabrication could provide significant benefits, including reduced transport costs, shorter lead times, and increased local content, which supports regional economic development. However, this requires a detailed feasibility study to assess whether existing ports and yards have the capacity to handle large floating platforms, considering factors such as crane capabilities, dry dock size, and storage space. Furthermore, supply chain constraints—such as the availability of specialised equipment, skilled labour, and material sourcing—must also be evaluated, as these fac-

tors can significantly influence cost, schedule, and overall feasibility. These constraints should be integrated into optimisation models to ensure that solutions are not only cost-effective but also practically achievable within regional infrastructure and supply chain limits.

Exploring alternative materials, such as concrete, could offer potential benefits compared to steel, including lower fabrication costs and opportunities for increased local content. Assessing the advantages of concrete-based solutions would require consideration of port capabilities, potential cost savings, and the trade-off between higher mass and reduced fabrication complexity. Future work should also evaluate the logistical implications of using heavier materials, such as transport feasibility and installation requirements, alongside their impact on overall project economics. Incorporating these factors into the optimisation framework would provide a more comprehensive understanding of material selection and its influence on cost, feasibility, and regional value creation.

Since both TC and SS optimised platforms share the same objective and constraints for hydrostatic performance, each site has the same expected static performance, with slightly different dynamic performance. Development of a 'next phase' optimisation would be useful, this could include the utilisation of a genetic algorithm and the turbine coupled with the platform, rather than just a point load. The current work could be a baseline or an initial search for such optimisation using several optimal platforms as a starting point to speed up the process. Another option which would be beneficial in terms of computational time is the development and implementation of a surrogate model to quickly predict the dynamics, so as not to slow the optimisation process. By doing so, the dynamics can be considered in the optimisation loop to compare the different results and assess whether it is worth including in the optimisation. It would be valuable to explore if the geometry changes and, if so, by how much for the TC, and if there is a potential cost benefit. Having considered the dynamics within the optimisation, the impact of the motions on the AEP would be beneficial to further investigate the difference between different platform typologies and the TC and SS geometries. The next step would be to validate non-traditional geometries through a fully coupled

analysis that accounts for turbine, platform, and controller interactions (hydro-aero-servo coupling). This should be complemented by a full finite element (FEM) validation of the structural design, which can then be integrated into the optimisation model to provide a comprehensive assessment of platform characteristics.

More work on the maximum allowable static and dynamic pitch angle of the platform is required to determine if this could be relaxed without negatively impacting fatigue and structural integrity. The impact on the energy yield could also be considered to create the full comparison and find if there is an optimal operating point where the platform cost is lower due to a relaxed constraint, but it doesn't negatively impact potential O&M costs.

Bibliography

[1] Global Wind Energy Council, GLOBAL OFFSHORE WIND REPORT 2021, https://gwec.net/wp-content/uploads/2021/09/GWEC-Global-Offshore-Wind-Report-2021.pdf, online; accessed 28 January 2022.

[2] A. Arapogianni, A.-B. Genachte, J. Moccia, The offshore wind market deployment: forecasts for 2020, 2030 and impacts on the european supply chain development, Energy Procedia 24 (2012) 2–10.

[3] M. Hannon, E. Topham, J. Dixon, D. McMillan, M. Collu, Offshore wind, ready to float? global and uk trends in the floating offshore wind market, Renewable and Sustainable Energy Reviews (2019).

[4] A. Ghigo, L. Cottura, R. Caradonna, G. Bracco, G. Mattiazzo, Platform optimization and cost analysis in a floating offshore wind farm, Journal of Marine Science and Engineering 8 (11) (2020) 835.

[5] BVGA, Lcoe – weighted average cost of capital (wacc).
URL https://bvgassociates.com/lcoe-weighted-average-cost-capital-wacc/

[6] V. Benifla, F. Adam, Development of a genetic algorithm code for the design of cylindrical buoyancy bodies for floating offshore wind turbine substructures, Energies 15 (3) (2022) 1181.

[7] L. Birk, G. n. F. Clauss, Optimization of offshore structures based on linear analysis of wave-body interaction, in: International Conference on Offshore Mechanics and Arctic Engineering, Vol. 48234, 2008, pp. 275–289.

[8] A. Myhr, T. A. Nygaard, Load reductions and optimizations on tension-leg-buoy offshore wind turbine platforms, in: The Twenty-second International Offshore and Polar Engineering Conference, OnePetro, 2012.

[9] A. Myhr, C. Bjerkseter, A. Ågotnes, T. A. Nygaard, Levelised cost of energy for offshore floating wind turbines in a life cycle perspective, Renewable energy 66 (2014) 714–728.

[10] J. Farkas, K. Jármai, F. Orbán, Cost minimization of a ring-stiffened conical shell loaded by external pressure, Welding in the World 52 (2008) 110–115.

[11] A. Kolios, M. Collu, A. Chahardehi, F. Brennan, M. Patel, A multi-criteria decision making method to compare support structures for offshore wind turbines, in: European wind energy conference, Warsaw, 2010.

[12] M. Borg, M. Collu, A comparison between the dynamics of horizontal and vertical axis offshore floating wind turbines, Philosophical Transactions of the Royal Society A: Mathematical, Physical and Engineering Sciences 373 (2035) (2015) 20140076.

[13] L. Qingdao Anchor Chain Co., Data sheets of offshore mooring chain.
URL `qd-anchor-chain.com/product/50.html`

[14] D. T. Monfort, Design optimization of the mooring system for a floating offshore wind turbine foundation, Instituto Superior Técnico (2017).

[15] G. BRACCO, L. OBERTI, Cost analysis and design optimization for floating offshore wind platforms.

[16] J. Jonkman, Definition of the floating system for phase iv of oc3, Tech. rep., National Renewable Energy Lab.(NREL), Golden, CO (United States) (2010).

[17] J. Rhodri, M. C. Ros, Floating offshore wind: Market and technology review prepared for the scottish government, Carbon trust report (2015).

[18] Offshore Wind Scotland, Scotwind round 1 bid results, (accessed: 13.04.2022) (2021).
URL https://www.offshorewindscotland.org.uk/news-events/2022/january/scotwind-1-results/

[19] SPS, Offshore plate.
URL https://www.murraysteelproducts.com/offers/plate

[20] Murray Steel Products, Plate.
URL https://sps-bmsteel.co.uk/products-and-services/offshore-and-structural-grades/offshore-plate#panel-a1

[21] Montanstahl speacil profiles in steel, Steel channels.
URL https://www.montanstahl.com/products/stainless-steel-structurals-bright-bars/stainless-steel-channels/

[22] Ozkan Steel, Reaching the uk government's target of 40gw of offshore wind by 2030 will require almost £50bn in investment.
URL https://www.ozkansteel.com/en/products/shipbuilding-oil-gas-profiles/products

[23] V. Igwemezie, A. Mehmanparast, A. Kolios, Materials selection for xl wind turbine support structures: A corrosion-fatigue perspective, Marine Structures 61 (2018) 381–397.

[24] ORCA FLEX, Ropewire:axial and bending stiffness.
URL https://www.orcina.com/webhelp/OrcaFlex/Content/html/Ropewire,Axialandbendingstiffness.htm

[25] V. Sykes, M. Collu, A. Coraddu, Topsis methodology applied to floating offshore wind to rank platform designs for the scotwind sites, Ocean Engineering 310 (2024) 118634.

[26] K. R. Hussein, A. W. Hussein, E. Hegazy, A. A. Amin, Structural design of a

floating foundation for offshore wind turbines in red sea, Analysis and Design of Marine Structures (2013) 575–583.

[27] Department of Energy, Windfloat pacific project.
URL https://www.boem.gov/sites/default/files/about-boem/BOEM-Regions/Pacific-Region/Renewable-Energy/11-Kevin-Bannister---BOEM-Workshop.pdf

[28] ABS, Offshore anchor data for preliminary design of anchors of floating offshore wind turbines, https://www.osti.gov/servlets/purl/1178273, accessed on: 03.10.2023 (2023).

[29] S. Heidari, Economic modelling of floating offshore wind power: Calculation of levelized cost of energy (2017).

[30] J. C. Nordstrom, Innovative offshore wind plant design study (2014).

[31] S. Alsubal, W. S. Alaloul, E. L. Shawn, M. Liew, P. Palaniappan, M. A. Musarat, Life cycle cost assessment of offshore wind farm: Kudat malaysia case, Sustainability 13 (14) (2021) 7943.

[32] ORE Catapult, Wind farm costs, (accessed: 19.09.2023) (2023).
URL https://guidetoanoffshorewindfarm.com/wind-farm-costs

[33] D. Westwood, Offshore wind assessment for norway, Oslo: The Research Council of Norway. North Sea Energy (2010).

[34] A. G. Gonzalez-Rodriguez, Review of offshore wind farm cost components, Energy for Sustainable Development 37 (2017) 10–19.

[35] I. Slengesol, W. P. De Miranda, N. Birch, J. Liebst, A. van der Herm, Offshore wind experiences: a bottom-up review of 16 projects, Tec Rep, OceanWind (2010).

[36] M. J. Kaiser, B. F. Snyder, Modelling offshore wind installation costs on the us outer continental shelf, Renewable energy 50 (2013) 676–691.

[37] J. Jacquemin, D. Butterworth, C. Garret, N. Baldock, A. Henderson, Inventory of location specific wind energy cost, Garrad Hassan & Partners Ltd for WIND-SPEED WP2 Report D 2 (2009).

[38] ODE, Study of the costs of offshore wind generation (2007).

[39] L. Castro-Santos, E. Martins, C. Guedes Soares, Methodology to calculate the costs of a floating offshore renewable energy farm, Energies 9 (5) (2016) 324.

[40] C.-S. Laura, D.-C. Vicente, Life-cycle cost analysis of floating offshore wind farms, Renewable Energy 66 (2014) 41–48.

[41] C. Maienza, A. Avossa, F. Ricciardelli, D. Coiro, G. Troise, C. T. Georgakis, A life cycle cost model for floating offshore wind farms, Applied Energy 266 (2020) 114716.

[42] T. Stehly, P. Beiter, P. Duffy, 2019 cost of wind energy review, Tech. rep., National Renewable Energy Lab.(NREL), Golden, CO (United States) (2020).

[43] A. Martinez, G. Iglesias, Mapping of the levelised cost of energy for floating offshore wind in the european atlantic, Renewable and Sustainable Energy Reviews 154 (2022) 111889.

[44] A. Martinez, G. Iglesias, Multi-parameter analysis and mapping of the levelised cost of energy from floating offshore wind in the mediterranean sea, Energy Conversion and Management 243 (2021) 114416.

[45] C. Bjerkseter, A. Ågotnes, Levelised costs of energy for offshore floating wind turbine concepts, Master's thesis, Norwegian University of Life Sciences, Ås (2013).

[46] M. Lerch, M. De-Prada-Gil, C. Molins, G. Benveniste, Sensitivity analysis on the levelized cost of energy for floating offshore wind farms, Sustainable Energy Technologies and Assessments 30 (2018) 77–90.

[47] The Guardian, Timeline: The history of wind power.
URL `https://www.theguardian.com/environment/2008/oct/17/wind-power-renewable-energy`

[48] Orsted, 1991-2001 the first offshore wind farms.
URL https://orsted.com/en/about-us/whitepapers/making-green-energy-affordable/1991-to-2001-the-first-offshore-wind-farms

[49] Siemens Gamesa, 30 years of powerful performance.
URL https://www.siemensgamesa.com/en-int/products-and-services/offshore

[50] United Nations, The paris agreement.
URL https://www.un.org/en/climatechange/paris-agreement

[51] R. Norris.

[52] Energy Voice, Uk renewable energy capacity set to double by 2026, when offshore wind will overtake onshore.
URL https://www.energyvoice.com/renewables-energy-transition/wind/uk-wind/274960/uk-renewable-energy-capacity-double-2026/

[53] AURORA energy research, Reaching the uk government's target of 40gw of offshore wind by 2030 will require almost £50bn in investment.
URL https://auroraer.com/media/reaching-40gw-offshore-wind/

[54] BBC News, World's first floating wind farm starts generating electricity.
URL https://www.bbc.co.uk/news/uk-scotland-41652707#:~:text=The%20world%E2%80%99s%20first%20floating%20wind,officially%20opened%20by%20Nicola%20Sturgeon

[55] S. Sánchez, J.-S. López-Gutiérrez, V. Negro, M. D. Esteban, Foundations in offshore wind farms: Evolution, characteristics and range of use. analysis of main dimensional parameters in monopile foundations, Journal of Marine Science and Engineering 7 (12) (2019) 441.

[56] Z. D. Eric Paya, The frontier between fixed and floating foundations in offshore wind.

URL https://www.empireengineering.co.uk/the-frontier-between-fixed-and-floating-foundations-in-offshore-wind/

[57] nataional geographic, Continental shelf.
URL https://education.nationalgeographic.org/resource/continental-shelf

[58] ABPmer, Sectoral marine plan for offshore wind energy.
URL https://www.gov.scot/publications/draft-sectoral-marine-plan-sustainability-appraisal/documents/

[59] Y. Liu, S. Li, Q. Yi, D. Chen, Developments in semi-submersible floating foundations supporting wind turbines: A comprehensive review, Renewable and Sustainable Energy Reviews 60 (2016) 433–449.

[60] A. Z. D. Eric Paya, The frontier between fixed and floating foundations in offshore wind.
URL https://www.empireengineering.co.uk/the-frontier-between-fixed-and-floating-foundations-in-offshore-wind/#:~:text=What%20determines%20the%20frontier,case%2Dby%2Dcase%20basis.

[61] S. Lefebvre, M. Collu, Preliminary design of a floating support structure for a 5 mw offshore wind turbine, Ocean engineering 40 (2012) 15–26.

[62] C. Trust, Floating wind joint industry project – phase 2 summary report, https://www.carbontrust.com/our-work-and-impact/guides-reports-and-tools/floating-wind-joint-industry-project-phase-2-summary, online; accessed: 11.05.2023.

[63] K. Tong, Technical and economic aspects of a floating offshore wind farm, Journal of Wind Engineering and Industrial Aerodynamics 74 (1998) 399–410.

[64] J. Carroll, A. McDonald, D. McMillan, Failure rate, repair time and unscheduled o&m cost analysis of offshore wind turbines, Wind Energy 19 (6) (2016) 1107–1119.

[65] M. D. P. Gil, J. L. Domínguez-García, F. Díaz-González, M. Aragüés-Peñalba, O. Gomis-Bellmunt, Feasibility analysis of offshore wind power plants with dc collection grid, Renewable Energy 78 (2015) 467–477.

[66] ORE Catapult, The financials of floating wind.
URL https://ore.catapult.org.uk/blog/financialsfloatingwind/#:~:text=Mating,of%20expensive%20jack%2Dup%20vessels.

[67] ABS, Floating offshore wind turbine development assessment, (accessed: 13.06.2022) (2021).
URL https://www.boem.gov/sites/default/files/documents/renewable-energy/studies/Study-Number-Deliverable-4-Final-Report-Technical-Summary.pdf

[68] EU, Future deep sea wind turbine technologies, (accessed: 13.06.2022) (2014).
URL https://cordis.europa.eu/project/id/256769/reporting

[69] ofgem, How ofgem is responding to the energy crisis.
URL https://www.ofgem.gov.uk/news-and-views/blog/how-ofgem-responding-energy-crisis

[70] M. Kausche, F. Adam, F. Dahlhaus, J. Großmann, Floating offshore wind-economic and ecological challenges of a tlp solution, Renewable Energy 126 (2018) 270–280.

[71] ORE Catapult, Floating offshore wind: Cost reduction pathways to subsidy free, ORE CATAPULT report (2022).

[72] T. Tanmay, Multi-disciplinary optimization of rotor nacelle assemblies for offshore wind farms: An agile systems engineering approach (2018).

[73] A. Shires, Design optimisation of an offshore vertical axis wind turbine, Proceedings of the Institution of Civil Engineers-Energy 166 (1) (2013) 7–18.

[74] D. Lovell, J. Doherty, Aerodynamic design of aerofoils and wings using a constrained optimisation method, in: ICAS PROCEEDINGS, Vol. 19, AMERICAN INST OF AERONAUTICS AND ASTRONAUTICS, 1994, pp. 14–14.

[75] M. Jureczko, M. Pawlak, A. Mężyk, Optimisation of wind turbine blades, Journal of materials processing technology 167 (2-3) (2005) 463–471.

[76] A. Shourangiz-Haghighi, M. A. Haghnegahdar, L. Wang, M. Mussetta, A. Kolios, M. Lander, State of the art in the optimisation of wind turbine performance using cfd, Archives of Computational Methods in Engineering 27 (2020) 413–431.

[77] R. Barnes, E. Morozov, Structural optimisation of composite wind turbine blade structures with variations of internal geometry configuration, Composite Structures 152 (2016) 158–167.

[78] D. Medici, Experimental studies of wind turbine wakes: power optimisation and meandering, Ph.D. thesis, KTH (2005).

[79] L. Wang, A. Kolios, T. Nishino, P.-L. Delafin, T. Bird, Structural optimisation of vertical-axis wind turbine composite blades based on finite element analysis and genetic algorithm, Composite Structures 153 (2016) 123–138.

[80] E. M. Fagan, O. De La Torre, S. B. Leen, J. Goggins, Validation of the multi-objective structural optimisation of a composite wind turbine blade, Composite structures 204 (2018) 567–577.

[81] Z. Chen, K. Stol, B. Mace, Wind turbine blade optimisation with individual pitch and trailing edge flap control, Renewable energy 103 (2017) 750–765.

[82] G. Collecutt, R. Flay, The economic optimisation of horizontal axis wind turbine design, Journal of wind engineering and industrial aerodynamics 61 (1) (1996) 87–97.

[83] N. A. Cencelli, Aerodynamic optimisation of a small-scale wind turbine blade for low windspeed conditions, Ph.D. thesis, Stellenbosch: Stellenbosch University (2006).

[84] M. Muskulus, S. Schafhirt, Design optimization of wind turbine support structures-a review, Journal of Ocean and Wind Energy 1 (1) (2014) 12–22.

[85] E. Uzunoglu, D. Karmakar, C. Guedes Soares, Floating offshore wind platforms, Floating offshore wind farms (2016) 53–76.

[86] C. Pike-Burke, Multi-objective optimization (2019).

[87] G. Venter, Review of optimization techniques (2010).

[88] Offshore energy, Offshore drilling: History and overview.
URL https://www.offshore-energy.biz/offshore-drilling-history-and-overview/.

[89] M. Leimeister, A. Kolios, M. Collu, Critical review of floating support structures for offshore wind farm deployment, in: Journal of Physics: Conference Series, Vol. 1104, IOP Publishing, 2018, p. 012007.

[90] Aaron Du, Semi-submersible, spar and tlp – how to select floating wind foundation types?, (accessed: 21.10.2024) (2021).
URL https://www.empireengineering.co.uk/semi-submersible-spar-and-tlp-floating-wind-foundations/

[91] Equinor, Hywind scotland.
URL https://www.equinor.com/energy/hywind-scotland

[92] A. Durakovic, World's largest floating offshore wind farm fully operational.
URL https://www.offshorewind.biz/2021/10/19/worlds-largest-floating-offshore-wind-farm-fully-operational/

[93] principle power, Kincardine offshore wind farm.
URL https://www.principlepower.com/projects/kincardine-offshore-wind-farm

[94] V. Sykes, M. Collu, A. Coraddu, A review and analysis of the uncertainty within cost models for floating offshore wind farms, Renewable and Sustainable Energy Reviews 186 (2023) 113634.

[95] J. Carroll, A. McDonald, I. Dinwoodie, D. McMillan, M. Revie, I. Lazakis, Availability, operation and maintenance costs of offshore wind turbines with different drive train configurations, Wind Energy 20 (2) (2017) 361–378.

[96] F. Dinmohammadi, M. Shafiee, A fuzzy-fmea risk assessment approach for offshore wind turbines, International Journal of Prognostics and Health Management 4 (13) (2013) 59–68.

[97] A. Ioannou, A. Angus, F. Brennan, Stochastic prediction of offshore wind farm lcoe through an integrated cost model, Energy Procedia 107 (2017) 383–389.

[98] D. Lim, K. Kim, G.-L. Yoon, A probabilistic model of the lcoe for korean offshore windfarms, Applied Economics Letters (2021) 1–6.

[99] B. Yeter, Y. Garbatov, C. G. Soares, Risk-based life-cycle assessment of offshore wind turbine support structures accounting for economic constraints, Structural Safety 81 (2019) 101867.

[100] J. Aldersey-Williams, I. D. Broadbent, P. A. Strachan, Better estimates of lcoe from audited accounts–a new methodology with examples from united kingdom offshore wind and ccgt, Energy policy 128 (2019) 25–35.

[101] L. Castro-Santos, E. Martins, C. G. Soares, Cost assessment methodology for combined wind and wave floating offshore renewable energy systems, Renewable Energy 97 (2016) 866–880.

[102] L. Castro-Santos, A. Filgueira-Vizoso, I. Lamas-Galdo, L. Carral-Couce, Methodology to calculate the installation costs of offshore wind farms located in deep waters, Journal of Cleaner Production 170 (2018) 1124–1135.

[103] L. Castro-Santos, D. Silva, A. R. Bento, N. Salvacao, C. G. Soares, Economic feasibility of floating offshore wind farms in portugal, Ocean Engineering 207 (2020) 107393.

[104] L. Castro-Santos, A. R. Bento, D. Silva, N. Salvação, C. Guedes Soares, Economic

feasibility of floating offshore wind farms in the north of spain, Journal of Marine Science and Engineering 8 (1) (2020) 58.

[105] EU, Life 50 plus project.
URL https://lifes50plus.eu/

[106] G. Benveniste, M. Lerch, M. de Prada, M. Kretschmer, J. Berque, A. López, G. Pérez-Morán, Lcoe tool description, technical and environmental impact evaluation procedure, LIFES50+ Deliv 2 (2) (2016).

[107] J. Bosch, I. Staffell, A. D. Hawkes, Global levelised cost of electricity from offshore wind, Energy 189 (2019) 116357.

[108] B. R. Sarker, T. I. Faiz, Minimizing transportation and installation costs for turbines in offshore wind farms, Renewable Energy 101 (2017) 667–679.

[109] F. Judge, F. D. McAuliffe, I. B. Sperstad, R. Chester, B. Flannery, K. Lynch, J. Murphy, A lifecycle financial analysis model for offshore wind farms, Renewable and Sustainable Energy Reviews 103 (2019) 370–383.

[110] T. Adedipe, M. Shafiee, An economic assessment framework for decommissioning of offshore wind farms using a cost breakdown structure, The International Journal of Life Cycle Assessment 26 (2) (2021) 344–370.

[111] C. Milne, S. Jalili, A. Maheri, Decommissioning cost modelling for offshore wind farms: A bottom-up approach, Sustainable Energy Technologies and Assessments 48 (2021) 101628.

[112] A. Ioannou, Y. Liang, M. Jalón, F. Brennan, A preliminary parametric techno-economic study of offshore wind floater concepts, Ocean Engineering 197 (2020) 106937.

[113] B. Johnston, A. Foley, J. Doran, T. Littler, Levelised cost of energy, a challenge for offshore wind, Renewable Energy 160 (2020) 876–885.

[114] F. Duan, Wind energy cost analysis: Coe for offshore wind and lcoe financial modeling (2017).

[115] IMO, Imo 2020 – cutting sulphur oxide emissions.
URL https://www.imo.org/en/MediaCentre/HotTopics/Pages/Sulphur-2020.aspx

[116] M. Collu, A. Maggi, P. Gualeni, C. M. Rizzo, F. Brennan, Stability requirements for floating offshore wind turbine (fowt) during assembly and temporary phases: Overview and application, Ocean engineering 84 (2014) 164–175.

[117] ORE Catapult, Approaching a critical review: an assessment of real world crew transfer vessel capabilities at gwynt y môr.
URL https://ore.catapult.org.uk/app/uploads/2017/12/Approaching-a-critical-review.-An-assessment-of-real-world-crew-transfer-vessel-capabilities-at-Gwynt-y-M%C3%B4r.pdf

[118] K.-t. Ma, Y. Wu, S. F. Stolen, L. Bello, M. ver der Horst, Y. Luo, Mooring designs for floating offshore wind turbines leveraging experience from the oil & gas industry, in: International Conference on Offshore Mechanics and Arctic Engineering, Vol. 85116, American Society of Mechanical Engineers, 2021, p. V001T01A031.

[119] J. Salas, Planet's largest wind turbine record broken again at 26-mw.
URL https://newatlas.com/energy/world-record-offshore-wind-turbine-dongfang-26-mw/#:~:text=China%2C%20the%20undisputed%20global%20leader,the%20longest%20US%20aircraft%20carrier.

[120] Construction News, Chinese yard to make scottish caissons.
URL https://www.theconstructionindex.co.uk/news/view/chinese-yard-to-make-scottish-caissons

[121] V. Sykes, M. Collu, A. Coraddu, A review and analysis of optimisation techniques applied to floating offshore wind platforms, Ocean Engineering 285 (2023) 115247.

[122] M. Karimi, M. Hall, B. Buckham, C. Crawford, A multi-objective design optimization approach for floating offshore wind turbine support structures, Journal of Ocean Engineering and Marine Energy 3 (1) (2017) 69–87.

[123] G. Clauss, L. Birk, Hydrodynamic shape optimization of large offshore structures, Applied Ocean Research 18 (4) (1996) 157–171.

[124] E. N. Wayman, Coupled dynamics and economic analysis of floating wind turbine systems, Ph.D. thesis, Massachusetts Institute of Technology (2006).

[125] P. Sclavounos, C. Tracy, S. Lee, Floating offshore wind turbines: Responses in a seastate pareto optimal designs and economic assessment, in: International Conference on Offshore Mechanics and Arctic Engineering, Vol. 48234, 2008, pp. 31–41.

[126] I. Fylling, P. A. Berthelsen, Windopt: an optimization tool for floating support structures for deep water wind turbines, in: International Conference on Offshore Mechanics and Arctic Engineering, Vol. 44373, 2011, pp. 767–776.

[127] C. J. Nordstrom, B. J. Morrison, W. L. J. Hurley, Innovative offshore wind plant design study, `https://www.osti.gov/servlets/purl/1327306`, online; accessed 25 January 2023.

[128] G. Ferri, E. Marino, N. Bruschi, C. Borri, Platform and mooring system optimization of a 10 mw semisubmersible offshore wind turbine, Renewable Energy 182 (2022) 1152–1170.

[129] G. Ferri, E. Marino, Site-specific optimizations of a 10 mw floating offshore wind turbine for the mediterranean sea, Renewable Energy (2022).

[130] F. Sandner, D. Schlipf, D. Matha, P. W. Cheng, Integrated optimization of floating wind turbine systems, in: International Conference on Offshore Mechanics and Arctic Engineering, Vol. 45547, American Society of Mechanical Engineers, 2014, p. V09BT09A030.

[131] J. M. Hegseth, E. E. Bachynski, J. R. Martins, Integrated design optimization of spar floating wind turbines, Marine Structures 72 (2020) 102771.

[132] M. Hall, B. Buckham, C. Crawford, Evolving offshore wind: A genetic algorithm-based support structure optimization framework for floating wind turbines, in: 2013 MTS/IEEE OCEANS-Bergen, IEEE, 2013, pp. 1–10.

[133] M. Hall, B. Buckham, C. Crawford, Hydrodynamics-based floating wind turbine support platform optimization: A basis function approach, Renewable Energy 66 (2014) 559–569.

[134] J.-C. Gilloteaux, P. Bozonnet, Parametric analysis of a cylinder-like shape floating platform dedicated to multi-megawatt wind turbine, in: The Twenty-fourth International Ocean and Polar Engineering Conference, OnePetro, 2014.

[135] F. Lemmer, W. Yu, K. Müller, P. W. Cheng, Semi-submersible wind turbine hull shape design for a favorable system response behavior, Marine Structures 71 (2020) 102725.

[136] M. Leimeister, A. Kolios, M. Collu, P. Thomas, Larger mw-class floater designs without upscaling?: A direct optimization approach, in: International Conference on Offshore Mechanics and Arctic Engineering, Vol. 58769, American Society of Mechanical Engineers, 2019, p. V001T01A032.

[137] M. Leimeister, A. Kolios, M. Collu, P. Thomas, Design optimization of the oc3 phase iv floating spar-buoy, based on global limit states, Ocean Engineering 202 (2020) 107186.

[138] M. Leimeister, A. Kolios, M. Collu, Development of a framework for wind turbine design and optimization, Modelling 2 (1) (2021) 105–128.

[139] S. Dou, A. Pegalajar-Jurado, S. Wang, H. Bredmose, M. Stolpe, Optimization of floating wind turbine support structures using frequency-domain analysis and analytical gradients, in: Journal of Physics: Conference Series, Vol. 1618, IOP Publishing, 2020, p. 042028.

[140] J. M. Hegseth, E. E. Bachynski, B. J. Leira, Effect of environmental modelling and

inspection strategy on the optimal design of floating wind turbines, Reliability Engineering & System Safety 214 (2021) 107706.

[141] M. Leimeister, A. Kolios, Reliability-based design optimization of a spar-type floating offshore wind turbine support structure, Reliability Engineering & System Safety 213 (2021) 107666.

[142] N. Pollini, A. Pegalajar-Jurado, S. Dou, H. Bredmose, M. Stolpe, Gradient-based optimization of a 15 mw wind turbine spar floater, in: Journal of Physics: Conference Series, Vol. 2018, IOP Publishing, 2021, p. 012032.

[143] F. Lemmer, K. Müller, W. Yu, D. Schlipf, P. W. Cheng, Optimization of floating offshore wind turbine platforms with a self-tuning controller, in: International Conference on Offshore Mechanics and Arctic Engineering, Vol. 57786, American Society of Mechanical Engineers, 2017, p. V010T09A080.

[144] A. C. Pillai, P. R. Thies, L. Johanning, Comparing frequency and time domain simulations for geometry optimization of a floating offshore wind turbine mooring system, in: International Conference on Offshore Mechanics and Arctic Engineering, Vol. 51975, American Society of Mechanical Engineers, 2018, p. V001T01A016.

[145] S. Zhou, K. Müller, C. Li, Y. Xiao, P. W. Cheng, Global sensitivity study on the semisubmersible substructure of a floating wind turbine: Manufacturing cost, structural properties and hydrodynamics, Ocean Engineering 221 (2021) 108585.

[146] M. Brommundt, L. Krause, K. Merz, M. Muskulus, Mooring system optimization for floating wind turbines using frequency domain analysis, Energy Procedia 24 (2012) 289–296.

[147] DNV, Dnv-rp-0286: Coupled analysis of floating wind turbines, Det Norske Veritas (2019).

[148] A. R. Nejad, E. E. Bachynski, T. Moan, Effect of axial acceleration on drivetrain

responses in a spar-type floating wind turbine, Journal of Offshore Mechanics and Arctic Engineering 141 (3) (2019).

[149] A. Younis, Z. Dong, Trends, features, and tests of common and recently introduced global optimization methods, Engineering Optimization 42 (8) (2010) 691–718.

[150] M. Mitchell, An introduction to genetic algorithms, MIT press, 1998.

[151] S. Katoch, S. S. Chauhan, V. Kumar, A review on genetic algorithm: past, present, and future, Multimedia tools and applications 80 (2021) 8091–8126.

[152] X.-S. Yang, Chapter 6 - genetic algorithms, in: X.-S. Yang (Ed.), Nature-Inspired Optimization Algorithms (Second Edition), second edition Edition, Academic Press, 2021, pp. 91–100. doi:https://doi.org/10.1016/B978-0-12-821986-7.00013-5.
URL https://www.sciencedirect.com/science/article/pii/B9780128219867000135

[153] K. Deb, A. Pratap, S. Agarwal, T. Meyarivan, A fast and elitist multiobjective genetic algorithm: Nsga-ii, IEEE transactions on evolutionary computation 6 (2) (2002) 182–197.

[154] V. De Buck, C. A. M. López, P. Nimmegeers, I. Hashem, J. Van Impe, Multi-objective optimisation of chemical processes via improved genetic algorithms: A novel trade-off and termination criterion, in: Computer Aided Chemical Engineering, Vol. 46, Elsevier, 2019, pp. 613–618.

[155] P. Wilson, H. A. Mantooth, Model-based optimization techniques, Model-based engineering for complex electronic systems 2013 (2013) 347–367.

[156] F. Neri, S. Rostami, Generalised pattern search based on covariance matrix diagonalisation, SN Computer Science 2 (3) (2021) 171.

[157] C. Bogani, M. Gasparo, A. Papini, Generalized pattern search methods for a class

of nonsmooth optimization problems with structure, Journal of Computational and Applied Mathematics 229 (1) (2009) 283–293.

[158] R. Martí, Multi-start methods, Handbook of metaheuristics (2003) 355–368.

[159] P. M. Zadeh, M. A. S. Shirazi, 5—multidisciplinary design and optimization methods, Metaheuristic applications in structures and infrastructures (2013) 103–127.

[160] J. Nocedal, S. J. Wright, Numerical optimization, Springer, 1999.

[161] P. E. Gill, W. Murray, M. A. Saunders, Snopt: An sqp algorithm for large-scale constrained optimization, SIAM review 47 (1) (2005) 99–131.

[162] T. Edition, Introduction to optimum design.

[163] K. Schittkowski, Nlpql: A fortran subroutine solving constrained nonlinear programming problems, Annals of operations research 5 (1986) 485–500.

[164] M. J. Powell, et al., The bobyqa algorithm for bound constrained optimization without derivatives, Cambridge NA Report NA2009/06, University of Cambridge, Cambridge 26 (2009).

[165] A. Pegalajar-Jurado, M. Borg, H. Bredmose, An efficient frequency-domain model for quick load analysis of floating offshore wind turbines, Wind Energy Science 3 (2) (2018) 693–712.

[166] K. Larsen, P. C. Sandvik, Efficient methods for the calculation of dynamic mooring line tension, in: The First ISOPE European Offshore Mechanics Symposium, OnePetro, 1990.

[167] A. Otter, J. Murphy, V. Pakrashi, A. Robertson, C. Desmond, A review of modelling techniques for floating offshore wind turbines, Wind Energy 25 (5) (2022) 831–857.

[168] J. Farkas, K. Jármai, Optimum design of steel structures, Springer, 2013.

[169] ABS, Offshore anchor data for preliminary design of anchors of floating offshore wind turbines.
URL https://www.osti.gov/servlets/purl/1178273

[170] CPR Subsea, Renewables cable buoyancy.
URL https://www.crpsubsea.com/products/product-families/buoyancy-floats/distributed-buoyancy/renewables-cable-buoyancy/

[171] Deep Water Buoyancy, Floating offshore wind cable buoyancy.
URL https://deepwaterbuoyancy.com/product/floating-offshore-wind-cable-buoyancy/

[172] J. M. Jonkman, D. Matha, Dynamics of offshore floating wind turbines—analysis of three concepts, Wind Energy 14 (4) (2011) 557–569.

[173] DNV, Dnv-st-0119: Floating wind turbine structures (2021).

[174] R. Amaral, K. Laugesen, M. Masciola, D. von Terzi, P. Deglaire, A. Viré, A frequency-time domain method for annual energy production estimation in floating wind turbines, in: Journal of Physics: Conference Series, Vol. 2265, IOP Publishing, 2022, p. 042025.

[175] C. A. R. Castillo, M. Collu, F. Brennan, Comparative design space exploration of centred and off-centred semisubmersible configurations for floating offshore wind turbines, Ocean Engineering 324 (2025) 120740.

[176] DNV, Buckling strength of shells, Recommended practice RP-C202. Høvik, Norway (2002).

[177] European standard, EuroCode 3 design of steel structures, https://www.phd.eng.br/wp-content/uploads/2015/12/en.1993.1.1.2005.pdf, online; accessed 21 February 2023.

[178] J. N. Newman, Marine hydrodynamics, The MIT press, 2018.

[179] J. A. Myers, Handbook of equations for mass and area properties of various geometrical shapes, Vol. 7827, US Naval Ordnance Test Station China Lake, CA, 1962.

[180] O. FLEX, Chain: Mechanical properties.
URL https://www.orcina.com/webhelp/OrcaFlex/Content/html/Chain,Mechanicalproperties.htm

[181] O. Faltinsen, Sea loads on ships and offshore structures, Vol. 1, Cambridge university press, 1993.

[182] Q. Pan, M. Y. Mahfouz, F. Lemmer, Assessment of mooring configurations for the iea 15mw floating offshore wind turbine, in: Journal of Physics: Conference Series, Vol. 2018, IOP Publishing, 2021, p. 012030.

[183] O. Vold, G. Hakon, T. Guttormsen, L. Delp, Hywind scotland pilot park project plan for construction activities 2017 (2017).

[184] M. Karimirad.

[185] J. Jonkman, S. Butterfield, W. Musial, G. Scott, Definition of a 5-mw reference wind turbine for offshore system development, Tech. rep., National Renewable Energy Lab.(NREL), Golden, CO (United States) (2009).

[186] M. Karimirad, T. Moan, Wave-and wind-induced dynamic response of a spar-type offshore wind turbine, Journal of waterway, port, coastal, and ocean engineering 138 (1) (2012) 9–20.

[187] M. K. Al-Solihat, M. Nahon, Stiffness of slack and taut moorings, Ships and Offshore Structures 11 (8) (2016) 890–904.

[188] M. Collu, Lecture notes in advanced mechanical engineering (January 2018).

[189] R. Kurnia, G. Ducrozet, Nemoh v3.0 user manual (12 2022). doi:10.13140/RG.2.2.12752.28162.

[190] C. Allen, A. Viscelli, H. Dagher, A. Goupee, E. Gaertner, N. Abbas, M. Hall, G. Barter, Definition of the umaine volturnus-s reference platform developed for the iea wind 15-megawatt offshore reference wind turbine, Tech. rep., National Renewable Energy Lab.(NREL), Golden, CO (United States); Univ. of ... (2020).

[191] DNV-GL, Dnvglrpc205, environmental conditions and environmental loads, Tech. rep. (2019).

[192] Lautec Esox, Offshore wind resource map, https://esox.lautec.com/map/, (accessed: 13.04.2022) (2022).

[193] M. H. Patel, Dynamics of offshore structures, Butterworth-Heinemann, 2013.

[194] N. Salvação, C. Guedes Soares, Resource assessment methods in the offshore wind energy sector, in: Floating Offshore Wind Farms, Springer, 2016, pp. 121–141.

[195] J. Li, M. Tran, J. Siwabessy, Selecting optimal random forest predictive models: a case study on predicting the spatial distribution of seabed hardness, PloS one 11 (2) (2016) e0149089.

[196] B. N. Tissot, M. A. Hixon, W. Barss, D. L. Stein, Fish-habitat associations on a deep reef at the edge of the oregon continental shelf (1992).

[197] M. Ikhennicheu, M. Lynch, S. Doole, F. Borisade, D. Matha, J. Dominguez, R. Vicente, T. Habekost, L. Ramirez, S. Potestio, et al., Review of the state of the art of mooring and anchoring designs, technical challenges and identification of relevant dlcs (2021).

[198] Cribbs, G. and Karrsten, G. and Laud, M. and Fiand, K. and Broadbent, S., Overview of Anchoring Solutions and Smart Installation Methods for Offshore Floating Wind, online; accessed 25 January 2023.

[199] E. Paya, A. Z. Du, The frontier between fixed and floating foundations in offshore wind, https://www.empireengineering.co.uk/the-frontier-between-fixed-and-floating-foundations-in-offshore-wind/, (accessed: 12.07.2022) (2020).

[200] M. Biglu, M. Hall, E. Lozon, S. Housner, Reference site conditions for floating wind arrays in the united states, Tech. rep., National Renewable Energy Laboratory (NREL), Golden, CO (United States) (2024).

[201] Z. Jiang, Installation of offshore wind turbines: A technical review, Renewable and Sustainable Energy Reviews 139 (2021) 110576.

[202] Department of Energy, Technology readiness assessment guide, (accessed: 13.06.2022) (2011).
URL https://www2.lbl.gov/dir/assets/docs/TRL%20guide.pdf

[203] Principle Power, Projects, (accessed: 20.09.2023) (2023).
URL https://www.principlepower.com/projects

[204] Carbon Trust, Floating wind joint industry programme phase iv summary report (2022).

[205] BW-Ideol, Our assets, our projects, (accessed: 20.09.2023) (2022).
URL https://bw-ideol.com/en/our-projects

[206] BW-Ideol, France's first offshore wind turbine and bw ideol's first demonstrator, (accessed: 13.06.2022) (2022).
URL https://www.bw-ideol.com/en/floatgen-demonstrator

[207] RWE Renewables, Demosath floating unit launched into water, (accessed: 20.09.2023) (2022).
URL https://www.rwe.com/en/press/rwe-renewables/2022-07-20-demosath/

[208] Saitec, Bluesath: Saitec's first offshore wind deployment in spain, (accessed: 20.09.2023) (2023).
URL https://www.saitec.es/en/news.html?BlueSATH-Saitec-first-offshore-wind-deployment-in-Spain

[209] Saitec, Our projects, (accessed: 20.09.2023) (2023).
URL https://saitec-offshore.com/en/projects/

[210] BW-Ideol, Ideol in partnership with atlantis in the uk to bring the offshore wind industry to the next era seeking to establish a 1.5 gw floating offshore wind projects pipeline, (accessed: 13.06.2022) (2022).
URL https://www.bw-ideol.com/en/actualites/ideol-partnership-atlantis-uk-bring-offshore-wind-industry-next-era-seeking-establish-15

[211] A. Durakovic, Shell and partners cancel floating wind project offshore france, (accessed: 20.09.2023) (2022).
URL https://www.offshorewind.biz/2022/11/16/shell-and-partners-cancel-floating-wind-project-offshore-france/

[212] OER, Completion verification and assessment of tri-floater, (accessed: 13.06.2022) (2021).
URL https://ocean-energyresources.com/2021/12/03/completion-verification-and-assessment-of-tri-floater/"

[213] NOV, Model tests confirm gustomsc tri-floater performance in harsh environment, (accessed: 13.06.2022) (2022).
URL https://www.nov.com/about/news/model-tests-confirm-gustomsc-tri-floater-performance-in-harsh-environment

[214] 4coffshore, Wind farm france spinfloat demonstrator, (accessed: 13.06.2022) (2021).
URL https://www.4coffshore.com/windfarms/france/spinfloat-demonstrator-france-fr66.html

[215] Life50+, Innovative floating offshore wind energy, (accessed: 20.09.2023) (2015).
URL https://lifes50plus.eu/

[216] Wind Power Monthly, Exclusive: Radical 16.6mw nezzy² twin floating offshore wind platform takes shape in china, (accessed: 20.09.2023) (2022).
URL https://www.windpowermonthly.com/article/1797699/exclusive-radical-166mw-nezzy%C2%B2-twin-floating-offshore-wind-platform-takes-shape-china

[217] EnBW company, Enbw - aerodyn research project: Floating wind turbine "nezzy²" passes its second test in the baltic sea, (accessed: 20.09.2023) (2020).
URL https://www.enbw.com/company/press/nezzy-passes-test-in-the-baltic-sea.html

[218] Eolink, Technology scaling up, (accessed: 20.09.2023) (2023).
URL http://eolink.fr/en/

[219] J. Serrano González, M. Burgos Payán, J. M. Riquelme Santos, Á. G. González Rodríguez, Optimal micro-siting of weather vaning floating wind turbines, Energies 14 (4) (2021) 886.

[220] KOWL, Section 36c variation environmental statement kincardine offshore windfarm project, (accessed: 13.04.2022) (2016).
URL https://marine.gov.scot/sites/default/files/00528219.pdf

[221] 4coffshore, Flagship - metcentre floating wind farm, (accessed: 20.09.2023) (2023).
URL https://www.4coffshore.com/windfarms/norway/flagship---metcentre-norway-no63.html

[222] Flagship, What is flagship?, (accessed: 13.06.2022) (2022).
URL https://flagships.eu/

[223] 4coffshore, New england aqua ventus floating wind farm, (accessed: 20.09.2023) (2023).
URL https://www.4coffshore.com/windfarms/united-states/new-england-aqua-ventus-united-states-us3z.html

[224] 4coffshore, Fukushima forward - phase 2 floating wind farm, (accessed: 20.09.2023) (2023).
URL https://www.4coffshore.com/windfarms/japan/fukushima-forward---phase-2-japan-jp13.html

[225] Equinor, Here's why floating wind power is the future — and how offshore expertise from norway is making it possible, (accessed: 13.06.2022) (2020).
URL https://www.equinor.com/about-us/why-floating-wind-power-is-the-future

[226] Inocean, Sway offshore wind turbine, (accessed: 13.06.2022) (2021).
URL https://www.inocean.no/projects/sway-offshore-wind-turbine/#:~:text=The%20SWAY%C2%AE%20system%20is,leg%20moorings%20and%20slack%20moorings.

[227] New Atlas, World's biggest wind turbine to take a spin in norway, (accessed: 13.06.2022) (2010).
URL https://newatlas.com/worlds-biggest-wind-turbine/14215/

[228] Windcrete, Concrete floating platform for wind turbines, (accessed: 13.06.2022) (2020).
URL https://www.windcrete.com/

[229] Windcrete, Windcrete participated at the congreso eólico marino in bilbao, (accessed: 13.06.2022) (2023).
URL https://www.windcrete.com/windcrete-participated-at-the-congreso-eolico-marino-in-bilbao/

[230] Windcrete, Concrete floating platform for wind turbines, (accessed: 13.06.2022) (2023).
URL https://www.windcrete.com/

[231] T. Harada, Hybrid spar, (accessed: 13.06.2022) (2016).
URL https://www.offshorewindscotland.org.uk/media/12667/td-uk-md0002r4_op_deepwind-cluster-fow-20210401.pdf

[232] K. Freeman, G. Hundleby, C. Nordstrom, A. Roberts, B. Valpy, C. Willow, P. Torato, M. Ayuso, F. Boshell, Floating foundations: A game changer for offshore wind power, in: Innovation Outlook: Offshore Wind (IRENA, 2016), International Renewable Energy Agency, 2016.

[233] A. Memija, Swedish firm receives first commercial order for vertical axis wind turbine, (accessed: 20.9.2023) (2023).
URL https://www.offshorewind.biz/2023/07/05/swedish-firm-receives-first-commercial-order-for-vertical-axis-wind-turbine/

[234] Blue h engineering, The blue h historical technology development, (accessed: 13.06.2022) (2014).
URL http://www.bluehengineering.com/historical-development.html

[235] 4coffshore, Eco-tlp (dfowdc) floating wind farm, (accessed: 13.06.2022) (2016).
URL https://www.4coffshore.com/windfarms/united-kingdom/eco-tlp---(dfowdc)-united-kingdom-uk2p.html

[236] 4coffshore, Eco tlp - (dfowdc) floating wind farm, (accessed: 20.09.2023) (2023).
URL https://www.4coffshore.com/windfarms/united-kingdom/eco-tlp---(dfowdc)-united-kingdom-uk2p.html

[237] ORE Catapult, Tlp wind, (accessed: 20.09.2023) (2022).
URL https://ore.catapult.org.uk/stories/tlp-wind/

[238] 4coffshore, Tlpwind uk floating wind farm, (accessed: 20.09.2023) (2023).
URL https://www.4coffshore.com/windfarms/united-kingdom/tlpwind-uk-united-kingdom-uk2v.html

[239] 4coffshore, Nautica windpower- advanced floating turbine (aft), (accessed: 20.09.2023) (2023).
URL https://www.4coffshore.com/windfarms/united-states/nautica-windpower--advanced-floating-turbine-(aft)-united-states-us4u.html

[240] SBM offshore, Floating wind solutions, next step towards cost-effective floating wind energy (2020).

[241] X1wind, Projects, (accessed: 20.09.2023) (2023).
URL https://www.x1wind.com/projects/

[242] Crown Estate, Ports for offshore wind, /https://www.crownestatescotland.com/resources/docume for-offshore-wind-a-review-of-the-net-zero-opportunity-for-ports-in-scotland, (accessed: 13.06.2022) (2020).

[243] Marine Scotland, Maps nmpi part of scotlands environment, (accessed: 13.04.2022) (2022).
URL https://marinescotland.atkinsgeospatial.com/nmpi/

[244] V. Sykes, Floating substructure concept ranking.
URL https://forms.gle/4TjUrXcsGPuj5VW59

[245] E. C. Edwards, A. Holcombe, S. Brown, E. Ransley, M. Hann, D. Greaves, Evolution of floating offshore wind platforms: A review of at-sea devices, Renewable and Sustainable Energy Reviews 183 (2023) 113416.

[246] Wind Power Monthly, Ideol pilot doubles power yield and is 'ready for deployment', (accessed: 13.06.2022) (2020).
URL https://www.windpowermonthly.com/article/1671567/ideol-pilot-doubles-power-yield-ready-deployment

[247] Statoil, Hywind scotland demo, (accessed: 13.06.2022) (2017).
URL https://www.sintef.no/globalassets/project/eera-deepwind2017/presentasjoner/opening_hywind-eera-deepwind-2017-b-johansen.pdf

[248] A. E. Onstad, M. Stokke, L. Sætran, Site assessment of the floating wind turbine hywind demo, Energy Procedia 94 (2016) 409–416.

[249] Principle Power, Wind float 1, (accessed: 13.06.2022) (2020).
URL https://www.principlepower.com/projects/windfloat1

[250] J. Jonkman, Dnv gl joint industry project on coupled analysis of floating wind turbines, Tech. rep., National Renewable Energy Lab.(NREL), Golden, CO (United States) (2019).

[251] E. Gaertner, J. Rinker, L. Sethuraman, F. Zahle, B. Anderson, G. E. Barter, N. J. Abbas, F. Meng, P. Bortolotti, W. Skrzypinski, et al., Iea wind tcp task

37: definition of the iea 15-megawatt offshore reference wind turbine, Tech. rep., National Renewable Energy Lab.(NREL), Golden, CO (United States) (2020).

[252] DNVGL, Dnvgl-rp-0286: Coupled analysis of floating wind turbines, Recommend Practice DNVGL-RP-0286; DNV GL: Oslo, Norway (2019).

[253] K. Saeed, J. McMorland, M. Collu, A. Coraddu, J. Carroll, D. McMillan, Adaptations of offshore wind operation and maintenance models for floating wind, in: Journal of Physics: Conference Series, Vol. 2362, IOP Publishing, 2022, p. 012036.

Appendix A

Appendix

A.1 Wave scatter diagram

Tp \ Hs	0.5	1	1.5	2	2.5	3	3.5	4	4.5	5	5.5	6	6.5	7	7.5	8	8.5	9	9.5	10
1	0	0	0	0	0	0	0	0	0	0	0	0	0	0	0	0	0	0	0	0
2	0	0	0	0	0	0	0	0	0	0	0	0	0	0	0	0	0	0	0	0
3	0.00111	0.000441	0	0	0	0	0	0	0	0	0	0	0	0	0	0	0	0	0	0
4	0.008206	0.025669	0.001563	0	0	0	0	0	0	0	0	0	0	0	0	0	0	0	0	0
5	0.008883	0.055585	0.046276	0.00475	0.000122	0	0	0	0	0	0	0	0	0	0	0	0	0	0	0
6	0.004373	0.036822	0.068339	0.064008	0.015264	0.001224	4.94E-05	0	0	0	0	0	0	0	0	0	0	0	0	0
7	0.002381	0.027631	0.034647	0.03953	0.048747	0.026992	0.004993	0.000259	1.14E-05	0	0	0	0	0	0	0	0	0	0	0
8	0.001316	0.013823	0.027509	0.02387	0.019755	0.02368	0.02133	0.009906	0.002183	0.000278	3.80E-06	0	0	0	0	0	0	0	0	0
9	0.002571	0.016512	0.021539	0.020295	0.014542	0.011207	0.009994	0.008199	0.006381	0.003027	0.001129	0.000236	2.66E-05	0	0	0	0	0	0	0
10	0.001833	0.014237	0.017744	0.011899	0.008933	0.008024	0.00678	0.006354	0.005411	0.003126	0.001631	0.001069	0.000304	0.000133	4.56E-05	1.14E-05	0	0	0	0
11	0.00062	0.00913	0.016135	0.011043	0.006012	0.003738	0.002913	0.002795	0.002046	0.002658	0.001658	0.001278	0.000468	0.00024	8.37E-05	1.52E-05	1.14E-05	3.80E-06	0	0
12	0.000167	0.003632	0.007944	0.010104	0.005149	0.002274	0.001297	0.000711	0.000643	0.000472	0.000407	0.000502	0.000574	0.00024	0.000137	3.42E-05	3.80E-06	0	0	0
13	0.00011	0.001567	0.00316	0.004833	0.004012	0.002263	0.000913	0.000502	0.000308	0.000133	0.00011	9.13E-05	7.23E-05	6.08E-05	2.28E-05	5.32E-05	1.52E-05	3.80E-06	7.61E-06	0
14	4.94E-05	0.000597	0.001437	0.001301	0.001947	0.001418	0.000521	0.000232	0.000118	6.84E-05	8.75E-05	5.70E-05	1.90E-05	1.14E-05	1.52E-05	2.66E-05	7.61E-06	7.61E-06	7.61E-06	0
15	7.99E-05	0.000247	0.000601	0.000487	0.000665	0.000434	0.000236	6.08E-05	8.75E-05	2.66E-05	1.52E-05	3.80E-05	1.14E-05	5.32E-05	3.80E-05	0	0	0	0	0
16	1.90E-05	4.94E-05	0.000114	6.84E-05	0.000133	0.000106	3.42E-05	4.18E-05	4.56E-05	0	0	0	0	0	0	0	0	0	0	0
17	7.61E-06	1.14E-05	7.61E-06	1.90E-05	3.80E-05	3.80E-05	7.61E-06	4.94E-05	2.66E-05	0	0	0	0	0	0	0	0	0	0	0
18	0	0	0	3.80E-05	3.04E-05	3.80E-06	0	0	0	0	0	0	0	0	0	0	0	0	0	0
19	0	0	0	3.80E-06	3.80E-06	0	0	0	0	0	0	0	0	0	0	0	0	0	0	0
20	0	0	0	0	0	0	0	0	0	0	0	0	0	0	0	0	0	0	0	0
21	0	0	0	0	0	0	0	0	0	0	0	0	0	0	0	0	0	0	0	0
22	0	0	0	0	0	0	0	0	0	0	0	0	0	0	0	0	0	0	0	0

Figure A.1: Wave scatter diagrams for scotwind site 14

A.2 Design Variables for Spar platforms

Platform Number	Fairlead Coordinate (m)	Draft (m)	Length (m)	Radius (m)										Average Radius (m)
TC1	-24.26	110	125	8.91	9.64	8.92	8.48	2.00	9.24	10.15	8.54	5.35	5.00	7.62
TC2	-23.90	110	125	8.89	9.61	8.90	8.47	3.92	9.22	10.00	8.51	5.35	5.00	7.79
TC3	-28.82	110	125	9.01	9.62	9.02	8.57	5.50	9.33	10.17	8.61	5.35	5.00	8.02
TC4	-30.32	110	125	9.07	9.56	9.07	8.62	6.02	9.41	10.21	8.67	5.35	5.00	8.10
SS1	-5.65	130	145	7.34	N/A	N/A	N/A	N/A	N/A	N/A	N/A	N/A	N/A	7.34
SS2	-5.25	110	125	8.85	N/A	N/A	N/A	N/A	N/A	N/A	N/A	N/A	N/A	8.85
SS3	-4.97	118	133	7.99	N/A	N/A	N/A	N/A	N/A	N/A	N/A	N/A	N/A	7.99

Table A.1: Spar optimisation design variables.

Appendix A. Appendix

A.3 Cost breakdown for Spar platforms

	TC1	TC2	TC3	TC4	SS1	SS2	SS3
Shell Thickness	50	50	50	50	45	45	45
Stiffener width	450	400	450	450	450	450	450
Stiffener height	450	450	450	450	450	450	450
Stifferner thickness	30	30	30	30	8	10	15
Number of segments	10	10	10	10	12	11	10
Number of stiffeners	71	72	70	70	84	77	70
Platform mass (kg)	2.89E+06	2.77E+06	2.67E+06	2.86E+06	2.68E+06	2.64E+06	2.85E+06
Ballast mass (kg)	2.37E+07	2.18E+07	2.04E+07	2.32E+07	1.92E+07	1.78E+07	2.21E+07
Platform cost	16850000	17643000	1.81E+07	18361000	1.65E+07	1.68E+07	1.80E+07
Overall cost per kg ($/kg)	6.35	6.38	6.32	6.34	6.17	6.80	5.89
Total cost	17643971	18437621	1.89E+07	19144171	1.73E+07	1.76E+07	1.88E+07
Forming Shell	2413500	2549200	2.63E+06	2676900	2.46E+06	2.53E+06	2.76E+06
Forming stiffeners	851830	890330	8.77E+05	881620	4.55E+05	5.19E+05	6.54E+05
Welding Shell Segments from Plates	1389200	1.44E+06	1.46E+06	1.48E+06	1.24E+06	1.21E+06	1.28E+06
Welding Stiffeners from Parts	831290	882050	8.80E+05	887200	8.84E+05	8.92E+05	9.17E+05
Welding Stiffeners into Shell	1202000	1269400	1.26E+06	1264900	1.33E+06	1.31E+06	1.31E+06
Welding Segments	310250	323070	3.33E+05	336050	3.28E+05	3.32E+05	3.39E+05
Assembling Segments	49972	50723	5.14E+04	51595	5.18E+04	The reas	4.94E+04
Material Cost Shell	6919500	7233700	7.47E+06	7542700	6.97E+06	6.96E+06	7.25E+06
Material Cost Ballast	1600000	1710000	1.82E+06	1859000	1.39E+06	1.51E+06	1.73E+06
Material Cost Stiffeners	587620	571760	6.22E+05	627280	1.91E+05	2.39E+05	3.61E+05
Painting Stiffeners	15425	14582	1.54E+04	15425	1.68E+04	1.83E+04	2.03E+04
Painting Shell	597330	623590	6.46E+05	653360	6.36E+05	6.59E+05	7.09E+05

A.4 Design Variables for Semi-submersible platforms

	Columns			Bracing			Outer Column						Inner Column					
Platform Number	Fairlead Coordinate (m)	Draft (m)	Length (m)	Depth (m)	Width (m)	Length (m)	Radius (m)					Average Radius (m)	Radius (m)					Average Radius (m)
Site 14																		
TC1-14	-19.36	30.41	45.41	3.53	3.13	53.21	7.39	7.39	8.06	3.45	3.12	5.50	5.92	5.92	3.38	5.22	5.00	4.88
TC4-15	-19.51	30.84	45.84	3.43	3.83	47.06	6.43	6.43	10.00	3.26	3.11	5.70	4.46	4.46	3.63	3.22	5.00	4.08
TC34-14	-20.00	39.52	54.52	3.92	3.53	49.57	6.61	6.61	8.35	7.77	3.76	6.62	4.73	4.73	3.64	3.27	5.00	4.14
SS1-14	-19.05	33.08	48.08	2.08	3.95	52.52	7.78	7.78	7.78	7.78	7.78	7.78	5.00	5.00	5.00	5.00	5.00	5.00
SS4-14	-17.56	44.60	59.60	2.64	3.73	58.17	6.72	6.72	6.72	6.72	6.72	6.72	5.00	5.00	5.00	5.00	5.00	5.00
SS34	-20.00	32.67	47.67	2.73	3.88	42.94	9.20	9.20	9.20	9.20	9.20	9.20	5.00	5.00	5.00	5.00	5.00	5.00
Site 8																		
TC1-8	-19.62	30.18	45.18	3.77	3.43	53.00	8.59	8.59	7.46	3.48	3.64	5.79	4.87	4.87	4.30	3.70	5.00	4.33
TC14-8	-19.79	31.83	46.83	3.80	3.44	37.00	10.00	10.00	10.00	3.34	3.57	6.73	5.43	5.43	3.24	5.70	5.00	4.65
TC20-8	-20.00	40.44	55.44	3.58	3.45	54.00	4.00	4.00	8.09	7.38	4.11	5.89	5.10	5.10	3.96	3.32	5.00	4.09
SS1-8	-11.56	37.30	52.30	2.38	5.35	58.01	6.86	6.86	6.86	6.86	6.86	6.86	5.00	5.00	5.00	5.00	5.00	5.00
SS2-8	-19.90	30.10	45.10	2.20	3.04	60.00	7.08	7.08	7.08	7.08	7.08	7.08	5.00	5.00	5.00	5.00	5.00	5.00
SS11-8	-20.00	44.06	59.06	2.80	3.93	55.26	7.00	7.00	7.00	7.00	7.00	7.00	5.00	5.00	5.00	5.00	5.00	5.00
SS16-8	-19.08	32.10	47.10	2.96	3.34	42.93	9.18	9.18	9.18	9.18	9.18	9.18	5.00	5.00	5.00	5.00	5.00	5.00

Table A.2: Design variables of optimised Semi-submersible platforms.

Appendix A. Appendix

A.5 Cost breakdown for Semi-submersible platforms site 14

Cost	TC1-14	TC4-14	TC34-14	SS1-14	SS4-14	SS34-14
Shell Thickness Inner Column (mm) (mm)	20	25	20	20	25	25
Stiffener width Inner Column (mm)	6	6	6	6	6	6
Stiffener height Inner Column (mm)	60	60	60	60	60	60
Stiffener thickness Inner Column (mm)	120	200	250	180	250	90
Shell Thickness Outer Columns (mm)	15	15	20	20	25	25
Stiffener width Outer Columns (mm)	400	450	450	120	60	60
Stiffener height Outer Columns (mm)	60	350	60	60	60	60
Stiffener thickness Outer Columns (mm)	6	6	6	6	6	6
Bracing Thickness (mm)	6	6	6	6	6	6
Number Segments Inner Column ($)	4	4	8	5	5	4
Number of Segments Outer Columns ($)	4	4	8	5	5	4
Number of Stiffeners Inner Column ($)	54	64	77	60	75	60
Number of Stiffeners Outer Columns ($)	52	51	59	50	65	44
Platform mass (kg)	9.24E+05	9.62E+05	1.45E+06	1.39E+06	1.91E+06	1.96E+06
Ballast mass (kg)	1.76E+07	1.66E+07	2.11E+07	1.91E+07	2.00E+07	2.56E+07
Platform Cost ($)	1.04E+07	1.13E+07	1.72E+07	1.22E+07	1.43E+07	1.50E+07
Overall cost per kg ($/kg)	13.74	14.10	11.81	8.73	8.74	7.63
Total Cost ($)	1.27E+07	1.36E+07	1.72E+07	1.22E+07	1.67E+07	1.50E+07
Forming Shell Inner Column ($)	3.38E+05	2.66E+05	5.01E+05	3.99E+05	4.44E+05	3.55E+05
Forming stiffeners Inner Column ($)	1.87E+05	2.00E+05	2.43E+05	2.07E+05	2.59E+05	2.07E+05
Forming Shell Outer Columns ($)	1.21E+06	1.33E+06	3.38E+06	2.42E+06	2.17E+06	2.84E+06
Forming stiffeners Outer Columns ($)	5.80E+05	5.77E+05	7.29E+05	6.57E+05	7.84E+05	6.41E+05
Welding Shell Segments from Plates Inner Column ($)	7.60E+04	8.34E+04	8.15E+04	7.91E+04	1.31E+05	1.05E+05
Welding Shell Segments from Plates Outer Columns ($)	1.90E+05	2.09E+05	4.23E+05	3.78E+05	5.46E+05	5.93E+05
Welding Shell Segments from Plates Bracings ($)	9.43E+03	8.75E+03	9.60E+03	7.18E+03	8.52E+03	7.46E+03
Welding Stiffeners from Parts Inner Column ($)	4.70E+04	9.38E+04	1.57E+05	8.92E+04	1.91E+05	3.74E+04
Welding Stiffeners from Parts Outer Columns ($)	1.11E+06	1.41E+06	1.79E+06	2.20E+05	1.46E+05	1.13E+05
Welding Stiffeners into Shell Inner Column ($)	1.90E+05	2.64E+05	2.99E+05	2.33E+05	4.20E+05	2.22E+05
Welding Stiffeners into Shell Outer Columns ($)	1.46E+06	1.77E+06	2.24E+06	6.38E+05	8.10E+05	6.45E+05
Welding Segments Inner Column ($)	1.61E+04	2.03E+04	2.40E+04	1.90E+04	2.93E+04	2.44E+04
Welding Segments Outer Columns ($)	3.20E+04	3.19E+04	1.16E+05	8.88E+04	1.18E+05	1.35E+05
Welding Segments Bracings ($)	1.57E+03	1.71E+03	1.75E+03	1.42E+03	1.50E+03	1.56E+03
Assembling Segments ($)	4.34E+04	4.52E+04	5.87E+04	5.04E+04	5.97E+04	5.59E+04
Welding Columns and Bracings ($)	2.67E+03	2.22E+03	2.33E+03	2.49E+03	2.32E+03	2.79E+03
Assembling Columns and Bracings ($)	0.00E+00	0.00E+00	0.00E+00	0.00E+00	0.00E+00	0.00E+00
Material Cost Inner Column Shell ($)	6.61E+05	6.69E+05	6.55E+05	7.01E+05	1.08E+06	8.68E+05
Material Cost Inner Column Stiffeners ($)	1.11E+04	1.29E+04	2.11E+04	1.59E+04	2.38E+04	9.20E+03
Material Cost Outer Columns Shell ($)	1.80E+06	1.84E+06	3.33E+06	3.27E+06	4.37E+06	4.80E+06
Material Cost Outer Columns Stiffeners ($)	1.08E+05	1.90E+05	1.37E+05	4.69E+04	3.20E+04	2.96E+04
Material Cost Bracings ($)	1.57E+05	1.35E+05	1.62E+05	9.08E+04	1.28E+05	9.78E+04
Material Cost of Ballast ($)	1.39E+06	1.31E+06	1.66E+06	1.50E+06	1.58E+06	2.02E+06
Painting Shell Inner Column ($)	1.31E+05	9.84E+04	1.40E+05	1.41E+05	1.62E+05	1.31E+05
Painting Cost Stiffeners Inner Column ($)	4.74E+03	5.94E+03	4.69E+03	5.28E+03	8.50E+03	4.15E+03
Painting Cost Bracings ($)	9.27E+04	9.18E+04	9.97E+04	8.34E+04	1.03E+05	6.66E+04
Painting Shell Outer Columns ($)	5.15E+05	5.42E+05	8.81E+05	7.99E+05	7.26E+05	9.34E+05
Painting Cost Stiffeners Outer Columns ($)	2.97E+04	5.00E+04	2.21E+04	1.55E+04	1.17E+04	1.35E+04

Appendix A. Appendix

A.6 Cost breakdown for Semi-submersible site 8

	TC1-8	TC14-8	TC20-8	SS1	SS2	SS11	SS16
Shell Thickness Inner Column (mm)	25	25	20	25	25	25	25
Stiffener width Inner Column (mm)	6	6	6	6	6	6	6
Stiffener height Inner Column (mm)	60	60	60	60	60	60	60
Stiffener thickness Inner Column (mm)	100	60	250	150	60	250	90
Shell Thickness Outer Columns (mm)	15	15	20	20	20	25	25
Stiffener width Outer Columns (mm)	450	450	450	100	450	60	60
Stiffener height Outer Columns (mm)	60	400	60	60	400	60	60
Stiffener thickness Outer Columns (mm)	6	6	6	6	15	6	6
Bracing Thickness (mm)	6	6	6	6	6	6	6
Number Segments Inner Column ()	4	4	8	5	4	5	4
Number of Segments Outer Column ()	4	4	8	5	4	5	4
Number of Stiffeners Inner Column ()	60	56	75	65	56	75	60
Number of Stiffeners Outer Columns ()	51	51	64	55	48	65	44
Platform mass (kg)	9.90E+05	1.18E+06	1.31E+06	1.44E+06	1.42E+06	1.95E+06	1.94E+06
Ballast mass (kg)	2.03E+07	3.03E+07	1.56E+07	1.78E+07	1.41E+07	2.13E+07	2.50E+07
Platform Cost ($)	1.16E+07	1.43E+07	1.50E+07	1.18E+07	1.42E+07	1.47E+07	1.48E+07
Overall cost per kg ($/kg)	12.86	12.14	11.50	8.17	9.99	7.54	7.65
Total Cost ($)	1.27E+07	1.43E+07	1.50E+07	1.18E+07	1.42E+07	1.47E+07	1.48E+07
Forming Shell Inner Column ($)	3.04E+05	3.55E+05	5.59E+05	4.44E+05	3.55E+05	4.44E+05	3.55E+05
Forming stiffeners Inner Column ($)	1.97E+05	1.93E+05	2.43E+05	2.25E+05	1.94E+05	2.59E+05	2.07E+05
Forming Shell Outer Columns ($)	1.33E+06	1.81E+06	2.65E+06	1.97E+06	1.72E+06	2.22E+06	2.84E+06
Forming stiffeners Outer Columns ($)	5.87E+05	6.41E+05	7.13E+05	6.72E+05	1.18E+06	8.03E+05	6.40E+05
Welding Shell Segments from Plates Inner Column ($)	8.99E+04	1.04E+05	8.93E+04	1.17E+05	9.97E+04	1.30E+05	1.03E+05
Welding Shell Segments from Plates Outer Columns ($)	1.99E+05	2.50E+05	3.62E+05	3.54E+05	3.21E+05	5.45E+05	5.87E+05
Welding Shell Segments from Plates Bracings ($)	9.74E+03	8.17E+03	9.58E+03	8.08E+03	7.91E+03	8.56E+03	7.76E+03
Welding Stiffeners from Parts Inner Column ($)	3.80E+04	2.34E+04	1.61E+05	7.39E+04	2.36E+04	1.90E+05	3.70E+04
Welding Stiffeners from Parts Outer Columns ($)	1.41E+06	1.70E+06	1.60E+06	1.86E+05	1.70E+06	1.47E+05	1.13E+05
Welding Stiffeners into Shell Inner Column ($)	2.07E+05	1.96E+05	3.05E+05	2.59E+05	1.93E+05	4.18E+05	2.21E+05
Welding Stiffeners into Shell Outer Columns($)	1.78E+06	2.08E+06	2.06E+06	6.40E+05	2.05E+06	8.24E+05	6.41E+05
Welding Segments Inner Column ($)	2.22E+04	2.42E+04	2.53E+04	2.93E+04	2.44E+04	2.93E+04	2.44E+04
Welding Segments Outer Columns ($)	3.46E+04	4.02E+04	9.72E+04	7.83E+04	6.74E+04	1.23E+05	1.34E+05
Welding Segments Bracings ($)	1.70E+03	1.71E+03	1.66E+03	1.82E+03	1.23E+03	1.58E+03	1.48E+03
Assembling Segments ($)	4.50E+04	4.93E+04	5.71E+04	5.33E+04	5.31E+04	6.01E+04	5.56E+04
Welding Columns and Bracings ($)	2.71E+03	3.08E+03	1.89E+03	2.33E+03	2.36E+03	2.38E+03	2.80E+03
Assembling Columns and Bracings ($)	0.00E+00	0.00E+00	0.00E+00	3.50E+01	0.00E+00	0.00E+00	0.00E+00
Material Cost Inner Column Shell ($)	7.32E+05	8.35E+05	7.04E+05	9.52E+05	8.21E+05	1.08E+06	8.57E+05
Material Cost Inner Column Stiffeners ($)	8.36E+03	6.62E+03	2.21E+04	1.39E+04	6.69E+03	2.27E+04	8.78E+03
Material Cost Outer Columns Shell ($)	1.90E+06	2.31E+06	2.85E+06	3.14E+06	2.79E+06	4.52E+06	4.73E+06
Material Cost Outer Columns Stiffeners ($)	1.22E+05	2.26E+05	1.27E+05	4.13E+04	4.79E+05	3.16E+04	2.95E+04
Material Cost Bracings ($)	1.67E+05	1.17E+05	1.62E+05	1.15E+05	1.10E+05	1.29E+05	1.06E+05
Material Cost of Ballast ($)	1.60E+06	2.39E+06	1.23E+06	1.40E+06	1.11E+06	1.68E+06	1.97E+06
Painting Shell Inner Column ($)	1.10E+05	1.29E+05	1.53E+05	1.48E+05	1.26E+05	1.61E+05	1.30E+05
Painting Cost Stiffeners Inner Column ($)	3.62E+03	3.34E+03	4.70E+03	5.01E+03	3.12E+03	8.50E+03	4.15E+03
Painting Cost Bracings ($)	9.95E+04	5.51E+04	1.10E+05	1.24E+05	8.74E+04	1.01E+05	6.34E+04
Painting Shell Outer Columns ($)	5.67E+05	7.46E+05	7.00E+05	6.95E+05	6.18E+05	7.65E+05	9.25E+05
Painting Cost Stiffeners Outer Columns ($)	3.37E+04	5.76E+04	2.26E+04	1.34E+04	7.91E+04	1.21E+04	1.35E+04

A.7 Design Variables for TLPs

	Columns	Bracing			Inner Column			
Platform Number	Draft (m)	Depth (m)	Width (m)	Length (m)	Radius (m)			
TC1	28.38	2	1.42	15.79	5.63	5.63	4.15	5
TC19	30.03	4	4	17.49	5.56	4.56	4.83	5
TC29	25.45	2.33	2.92	15.84	5.37	5.87	5.94	5
SS1	20.64	6.72	5.24	20.15	4.01	4.01	4.01	4.01
SS21	28.51	6.35	5.00	17.90	4.38	4.38	4.38	4.38
SS40	25.76 5	5.03	40.62	4.08	4.08	4.08	4.08	4.08

Table A.3: Optimised TLP design variables for site 8.

Appendix A. Appendix

A.8 Cost breakdown of the optimised TLPs.

Cost Break Down	TC1	TC19	TC29	SS1	SS21	SS40
Shell Thickness Inner Column (mm)	20	20	20	20	25	25
Stiffener width Inner Column (mm)	6	6	6	6	6	6
Stiffener height Inner Column (mm)	60	60	60	60	60	60
Stiffener thickness Inner Column (mm)	65	130	90	150	150	160
Bracing Thickness (mm)	6	6	6	6	6	6
Number Segments Inner Column ()	3	3	3	3	3	3
Number of Stiffeners Inner Column ()	40	42	36	36	45	45
Platform mass (kg)	1.74E+05	1.59E+05	1.85E+05	1.33E+05	2.09E+05	2.15E+05
Platform Cost ($)	1.26E+06	1.19E+06	1.36E+06	1.03E+06	1.47E+06	1.50E+06
Overall cost per kg ($/kg)	7.25	7.53	7.33	7.76	7.06	6.99
Total Cost ($)	2.37E+06	2.39E+06	2.58E+06	1.03E+06	1.03E+06	1.03E+06
Forming Shell Inner Column ($)	2.50E+05	1.76E+05	2.97E+05	1.73E+05	2.25E+05	1.94E+05
Forming stiffeners Inner Column ($)	1.39E+05	1.32E+05	1.32E+05	1.13E+05	1.46E+05	1.42E+05
Welding Shell Segments from Plates Inner Column ($)	5.51E+04	4.31E+04	5.76E+04	3.45E+04	6.65E+04	5.54E+04
Welding Shell Segments from Plates Bracings ($)	3.26E+03	6.85E+03	4.68E+03	7.08E+03	6.52E+03	9.85E+03
Welding Stiffeners from Parts Inner Column ($)	1.85E+04	3.41E+04	2.37E+04	3.39E+04	4.69E+04	4.79E+04
Welding Stiffeners into Shell Inner Column ($)	1.25E+05	1.32E+05	1.20E+05	1.06E+05	1.70E+05	1.62E+05
Welding Segments Inner Column ($)	1.29E+04	1.07E+04	1.41E+04	1.02E+04	1.71E+04	1.59E+04
Welding Segments Bracings ($)	8.06E+02	1.52E+03	1.24E+03	2.82E+03	2.67E+03	2.36E+03
Assembling Segments ($)	1.70E+04	1.65E+04	1.76E+04	1.49E+04	1.86E+04	1.89E+04
Welding Columns and Bracings ($)	5.62E+02	5.35E+02	5.82E+02	5.25E+02	5.52E+02	5.25E+02
Assembling Columns and Bracings ($)	0.00E+00	0.00E+00	0.00E+00	7.72E+01	7.36E+01	7.40E+01
Material Cost Inner Column Shell ($)	4.89E+05	3.80E+05	5.03E+05	2.99E+05	5.34E+05	4.56E+05
Material Cost Inner Column Stiffeners ($)	5.70E+03	7.11E+03	6.76E+03	6.69E+03	8.46E+03	7.88E+03
Material Cost Bracings ($)	1.86E+04	8.25E+04	3.85E+04	8.83E+04	7.48E+04	1.71E+05
Painting Shell Inner Column ($)	9.89E+04	7.66E+04	1.07E+05	6.02E+04	8.06E+04	6.92E+04
Painting Cost Stiffeners Inner Column ($)	9.34E+03	1.19E+04	1.13E+04	1.11E+04	1.52E+04	1.48E+04
Painting Cost Bracings ($)	1.23E+04	7.97E+04	1.96E+04	6.97E+04	5.58E+04	1.29E+05

Appendix A. Appendix